



HAL
open science

Natural antimicrobials encapsulated by complex coacervation : understanding of molecular mechanisms

Wei Liao

► **To cite this version:**

Wei Liao. Natural antimicrobials encapsulated by complex coacervation : understanding of molecular mechanisms. Food engineering. Université Claude Bernard - Lyon I, 2022. English. NNT : 2022LYO10024 . tel-04050364

HAL Id: tel-04050364

<https://theses.hal.science/tel-04050364>

Submitted on 29 Mar 2023

HAL is a multi-disciplinary open access archive for the deposit and dissemination of scientific research documents, whether they are published or not. The documents may come from teaching and research institutions in France or abroad, or from public or private research centers.

L'archive ouverte pluridisciplinaire **HAL**, est destinée au dépôt et à la diffusion de documents scientifiques de niveau recherche, publiés ou non, émanant des établissements d'enseignement et de recherche français ou étrangers, des laboratoires publics ou privés.



**THESE de DOCTORAT
DE L'UNIVERSITE CLAUDE BERNARD LYON 1**

**Ecole Doctorale N°205
(Interdisciplinaire Sciences-Santé(EDISS))**

Discipline : Sciences des aliments

Soutenue publiquement le 26/09/2022, par :

Wei LIAO

**Natural antimicrobials encapsulated by
complex coacervation : understanding
of molecular mechanisms**

Devant le jury composé de :

CAPRON, Isabelle , Directrice de Recherche INRAE Nantes	Examinatrice
DUMAS, Emilie , MCF, Université Lyon 1	Examinatrice
ELAISSARI, Abdelhamid , Directeur de Recherche CNRS Lyon	Co-Directeur de thèse
GHARSALLAOUI, Adem , MCF, Université Lyon 1	Directeur de thèse
JADA, Amane , Chargé de Recherche CNRS Mulhouse	Rapporteur
MAILLARD, Marie-Noëlle , Professeure, AgroParisTech	Présidente
SANCHEZ GONZALEZ, Laura , MCF, Université de Lorraine	Rapporteuse
VITON, Christophe , Professeur, Université Lyon 1	Examineur

This research was developed at Laboratoire d'Automatique, de Génie des Procédés et de Génie Pharmaceutique (LAGEPP) et l'Ecole Doctorale Interdisciplinaire Sciences-Santé (EDISS)- ED 205 of the University Claude Bernard Lyon 1, with the financial support of a PhD fellowship (No. 201807565014) attributed by the China Scholarship Council (CSC).

This dissertation contains results that were published (or submitted) in international scientific journals.

PUBLICATIONS AND COMMUNICATIONS

Articles in international scientific journals

1. **Liao, W.**, Gharsallaoui, A., Dumas, E., & Elaissari, A. (2022). Understanding of the key factors influencing the properties of emulsions stabilized by sodium caseinate. *Comprehensive Reviews in Food Science and Food Safety*.
2. **Liao, W.**, Badri, W., Dumas, E., Ghnimi, S., Elaissari, A., Saurel, R., & Gharsallaoui, A. (2021). Nanoencapsulation of essential oils as natural food antimicrobial agents: an overview. *Applied Sciences*, 11(13), 5778.
3. **Liao, W.**, Dumas, E., Ghnimi, S., Elaissari, A., & Gharsallaoui, A. (2021). Effect of emulsifier and droplet size on the antibacterial properties of emulsions and emulsion-based films containing essential oil compounds. *Journal of Food Processing and Preservation*, 45(12).
4. **Liao, W.**, Gharsallaoui, A., Dumas, E., Ghnimi, S., & Elaissari, A. (2021). Effect of carrier oil on the properties of sodium caseinate stabilized O/W nanoemulsions containing Trans-cinnamaldehyde. *LWT-Food Science and Technology*, 146, 111655.
5. **Liao, W.**, Elaissari, A., Ghnimi, S., Dumas, E., & Gharsallaoui, A. Effect of pectin on the properties of nanoemulsions stabilized by sodium caseinate at neutral pH. *International Journal of Biological Macromolecules*, 2022.
6. **Liao W.**, Elaissari, A., Dumas, E., & Gharsallaoui, A. Pectin-sodium caseinate based nanoemulsions: effect of pH and ratio on oil-water interfacial behavior and colloidal stability. (Submitted to *Journal of Food Engineering*)
7. **Liao W.**, Elaissari, A., Dumas, E., & Gharsallaoui, A. (2023). Effect of trans-Cinnamaldehyde or citral on sodium caseinate: Interfacial rheology and fluorescence quenching properties. *Food Chemistry*, 400: 134044.
8. **Liao W.**, Elaissari, A., Dumas, E., & Gharsallaoui, A. (2023). The formation mechanism of multilayer emulsions studied by isothermal titration calorimetry and dynamic light scattering. *Food Hydrocolloids*, 136, 108275.

Oral/Poster communications in international conferences

1. **Wei Liao**, Abdelhamid Elaissari, Sami Ghnimi, Emilie Dumas and Adem Gharsallaoui. Pectin addition to nanoemulsions stabilized by sodium caseinate at neutral pH: effect on stability and lipid oxidation. *10th Edition of the International Euro-Aliment Symposium*, Romania 7th – 8th of October 2021. (Oral presentation)
2. Adem Gharsallaoui and **Wei Liao**. Free and encapsulated essential oil as natural food preservatives. *10th Edition of the International Euro-Aliment Symposium*, Romania 7th – 8th of October 2021.
3. **Wei Liao**, Abdelhamid Elaissari, Emilie Dumas and Adem Gharsallaoui. Pectin-sodium caseinate based nanoemulsions: effect of pH and ratio on oil-water interfacial behavior and colloidal stability. *11th International Colloids Conference*, Portugal, 12th – 16th of June 2022. (Poster)

Book Chapter

Liao, W., Badri, W., Alhibshi, A. H., Dumas, E., Ghnimi, S., Gharsallaoui, A., ... & Elaissari, A. (2021). Food Applications of Nigella sativa Essential Oil. In *Black cumin* (Nigella sativa) seeds: Chemistry, Technology, Functionality, and Applications (pp. 433-455). Springer, Cham.

ACKNOWLEDGEMENTS

First of all, I would like to thank China Scholarship Council for its financial support. Throughout the completion of this thesis, I have received a great deal of support and assistance. I wish to take this chance to thank those who have supported me during this time.

I would like to express my sincere gratitude to my supervisor Dr. Adem Gharsallaoui, for his continuous support, encouragement and fundamental advice during the entire project, for his patience, motivation, and immense knowledge. Of course, the success of this project would have been impossible without his well guidance. It was a great experience to work with him.

I would also like to express my sincere and deepest thanks to my co-supervisor, Dr. Abdelhamid Elaissari, whose immense knowledge, plentiful experience and passion for science and his friendship have encouraged me in all the time of my academic research and daily life. It was really a pleasure to work with him.

My sincere thanks to Dr. Emilie Dumas and Dr. Sami Ghnimi for reviewing my papers during my Ph.D. and giving me so many helpful suggestions. I would like to take this chance to thank the members of my thesis committee, Dr. Isabelle Capron, Dr. Amane Jada, Prof. Marie-Noëlle Maillard, Dr. Laura Sanchez Gonzalez and Prof. Christophe Viton who accepted to be part of the jury members and added a valuable asset for the validation of this research project. My sincere thanks also go to Dr. Nicole Jaffrezic-Renault for teaching me French. I would also like to thank Géraldine Agusti and Marie Hangouet for their teaching and guidance on a range of equipment.

A special acknowledgement goes to Dr. Jian Wang for his kind support in my research and my life in France. He helped me quickly integrate into the laboratory and provided technical assistance. A sincere appreciation to my colleges during my Ph.D. period, especially Fatemeh Baghi, Mohamad Tarhini, Eslam Elkalla, Rosso Annalisa, and Ghita Benkirane for all their special kindness.

Thanks to all my friends who enriched my life in France, especially Jin Tan, Yulong

He, Qian Chen, Bomin Fu, Weidong Zhang, Kangwei Li, Zexian Wang, Dandan Li, Cuirong Chen, Fengfeng mei, Zhiliang Hei, Meijian Zhang and Lingfeng Wu.

Tennis is a part of my life that brings lots of joy to me. Thanks to those who play with me regularly, especially Smail Benabderrazik, Zhiyu Sun, Yann Beaugrand and Didier Beaugrand.

A big thanks to my wife Tian Jiang, for being my best friend whom I can share everything, for always being there for me when I need her, for all the comprehension and love. Also, a special thanks to my kitty for always sitting next to me while I work.

Finally, I am highly indebted to my parents for their unconditional understanding and support for my long journey, allowing my studies to go the extra mile.

ABSTRACT

Protein based oil in water (O/W) emulsion systems have been widely used in the food industry due to their good amphiphilic properties, healthy, nutritious, and commercial availability. However, their application remains challenging under certain environmental conditions, such as acidic pH, high ionic strength, and high storage temperature. The first four sections of this thesis focused on the preparation of stable nanoemulsions by using different biopolymers in combination with natural food antimicrobial agents, to attain the target antibacterial activity. The effects of droplet size and carrier oil nature on the stability and antibacterial activity of nanoemulsions were investigated. In the second part, the effect of adding low methoxyl pectin (LMP) on the physicochemical stability of sodium caseinate (CAS)-stabilized nanoemulsions under certain conditions (high ionic concentration, acidic pH, freeze-thaw cycles, high temperatures, accelerated oxidation) was evaluated. Meanwhile, the effect of pH on the adsorption kinetics and interfacial dilatational rheology of CAS/LMP complexes at the oil-water interface was studied. In the next section, to understand the molecular mechanisms involved in the functionalities of our encapsulated system, the interactions between CAS and two used aldehydes, citral and trans-cinnamaldehyde (TCA), was carried out by interfacial properties and fluorescence quenching measurements. The quenching of CAS induced by TCA was further analyzed by the Stern-Volmer equation and the Van't Hoff equation to obtain the binding constant and the thermodynamic parameters of binding. In the final section, the mechanism of the formation of multilayer emulsions was investigated and compared by isothermal titration calorimetry and dynamic light scattering. Overall, this research work would improve the control of O/W protein-based emulsified products.

Keywords: Sodium caseinate; Low methoxyl pectin; Emulsion stability; Antimicrobials; Interfacial properties; Multilayered interfaces.

Les systèmes émulsionnés de type huile dans eau (H/E) à base de protéines sont largement utilisés en industrie alimentaire en raison de leurs bonnes propriétés amphiphiles, fonctionnelles, nutritionnelles ainsi que leur disponibilité dans le commerce. Cependant, leur application reste difficile dans certaines conditions environnementales, telles qu'un pH acide, une force ionique élevée et une température de stockage élevée. Les quatre premières parties de cette thèse se sont concentrées sur la préparation de nanoémulsions stables en utilisant différents biopolymères en combinaison avec des agents antimicrobiens alimentaires et naturels, pour atteindre l'activité antibactérienne cible. L'effet de la taille des gouttelettes d'huile sur la stabilité et l'activité antibactérienne des nanoémulsions a été tout d'abord étudié. Dans la deuxième partie, l'effet de l'ajout de la pectine faiblement méthylée (LMP) sur la stabilité physicochimique des nanoémulsions stabilisées par le caséinate de sodium (CAS) sous certaines conditions (force ionique élevée, pH acide, cycles de gel-dégel, températures élevées et oxydation accélérée) a été évalué. Parallèlement, l'effet du pH sur la cinétique d'adsorption et la rhéologie interfaciale des complexes CAS/LMP à l'interface huile-eau a été étudié. Pour comprendre les mécanismes moléculaires impliqués dans les fonctionnalités de nos systèmes d'encapsulation, les interactions entre le CAS et les deux aldéhydes utilisés, le citral et le *trans*-cinnamaldéhyde (TCA), ont été évaluées *via* l'étude des propriétés interfaciales et des mesures d'extinction de la fluorescence. L'extinction de la fluorescence du CAS induite par le TCA a été analysée par l'équation de Stern-Volmer et l'équation de Van't Hoff pour obtenir la constante d'interaction ainsi que les paramètres thermodynamiques de ces interactions. Dans la dernière partie, le mécanisme de formation des émulsions multicouches a été étudié par calorimétrie à titrage isotherme et par diffusion dynamique de la lumière. Dans l'ensemble, ce travail de recherche ouvrirait plus de possibilités pour l'élaboration d'émulsions H/E à base de protéines.

Mots clés : Caséinate de sodium ; Pectine faiblement méthylée ; Stabilité de l'émulsion ; Antimicrobiens ; Propriétés interfaciales; Interfaces multicouches.

CONTENT

LIST OF ABBREVIATIONS.....	1
INTRODUCTION.....	2
Organization of the thesis.....	5
Chapter I.....	6
Literature review I.....	7
Summary of literature review I.....	8
Abstract.....	9
1. Introduction	9
2. Sodium caseinate and its emulsifying ability	10
3. The major instability mechanisms in CAS-stabilized oil-in-water emulsions	11
3.1. Flocculation.....	12
3.2. Coalescence.....	13
3.3. Gravitational seperation	13
3.4. Ostwald ripening	13
4. Main factors determining the stability of CAS-stabilized emulsions.....	14
4.1. Effect of pH.....	14
4.2. Effect of ionic strength.....	14
4.3. Effect of emulsifier concentration.....	15
4.4. Effect of homogenization process.....	16
4.5. Effect of heating process.....	17
4.6. Effect of oxidation	17
5. General technologies for detecting and evaluating the emulsion stability	18
5.1. Visual observation.....	18
5.2. Microscopy observation.....	18
5.3. Particle size analysis	21
5.4. Surface charge.....	23
5.5. Rheological properties	24

6. Strategies to improve the stability of CAS stabilized emulsions	24
6.1. Optimizing emulsion formulation.....	24
6.2. Noncovalent bond	28
6.3. Covalent bond (Conjugation).....	29
7. Conclusion.....	30
References.....	31
Literature review II	36
Summary of literature review II	37
Abstract.....	38
1. Introduction	38
2. Synthetic and natural food antimicrobial agents	39
2.1. Traditional synthetic agents	39
2.2. Natural antimicrobial agents	40
3. Essential oils as food antimicrobial agents: current status and challenges ...	41
3.1. Advances in research on EOs as antibacterial agent.....	41
3.2. Challenges in the research of EOs as a food antibacterial	42
4. Nanoencapsulation versus Microencapsulation	43
5. Strategies for nanoencapsulation of essential oils	45
5.1. Lipid-based nanoencapsulation.....	46
5.2. Biopolymer-based nanoencapsulation	48
5.3. Equipment-based nanoencapsulation.....	50
6. Effect of nanoencapsulation on antibacterial activity of essential oils	51
7. Applications of nanoencapsulated natural antimicrobial agents	54
7.1. Aqueous food systems	54
7.2. Solid food system.....	54
7.3. Food packaging	55
8. Conclusion.....	55
References.....	56

Chapter II.....	62
Summary of Chapter II.....	63
Abstract.....	64
1. Introduction	64
2. Materials and methods	65
2.1. Materials	65
2.2. Preparation of nanoemulsions containing essential oils (EOs).....	65
2.3. Preparation of films containing EOs.....	66
2.4. Hydrodynamic particle size and size distribution.....	66
2.5. Zeta potential measurement	66
2.6. Antibacterial activity of emulsions	66
2.7. Antibacterial activity of films	67
2.8. Effect of emulsion size.....	67
2.9. Statistics	67
3. Results and discussion	67
3.1. Particle size distribution and ζ -potential of nanoemulsions.....	67
3.2. Antibacterial activity on nanoemulsions and films.....	67
3.3. Effect of emulsion size.....	69
3.4. Antibacterial activity of emulsions and their films.....	70
4. Conclusion.....	71
References.....	72
Chapter III.....	74
Summary of Chapter III	75
Abstract.....	76
1. Introduction.....	76
2. Materials and methods	77
2.1. Materials	77
2.2. Preparation of nanoemulsions.....	77

2.3. Effect of carrier oil concentration	77
2.4. Droplet hydrodynamic size and size distribution.....	77
2.5. Zeta potential (ζ)	77
2.6. Nanoemulsion stability to environmental stress	77
2.7. Viscosity.....	78
2.8. Interfacial tension.....	78
2.9. Antibacterial activity of nanoemulsions.....	78
2.10. Statistical analysis.....	78
3. Results and discussion.....	78
3.1. Effect of carrier oil content on the properties of TCA nanoemulsions	78
3.2. Physical stability of nanoemulsions against environmental stress	80
3.3. Antibacterial activity of nanoemulsions.....	83
4. Conclusion	84
Reference	85
Chapter IV	87
Summary of Chapter IV	88
Abstract.....	89
1. Introduction	89
2. Materials and methods	90
2.1. Materials	90
2.2. Preparation of oil-in-water (O/W) nanoemulsions	90
2.3. Droplet hydrodynamic size and size distribution.....	90
2.4. Zeta potential (ζ)	90
2.5. Creaming stability measurement.....	90
2.6. Viscosity measurements.....	91
2.7. Nanoemulsion stability to environmental stress	91
2.8. Lipid and protein oxidation measurements.....	91
2.9. Statistical analysis.....	92

3. Results and discussion	92
3.1. Effect of pectin concentration on the properties of nanoemulsions.....	93
3.2. Effect of pectin concentration on the ageing stability and environmental stress resistance of nanoemulsions	93
3.3. Effect of pectin addition on the oxidation of emulsified lipid and protein.....	95
4. Conclusion.....	96
References.....	97
Chapter V	98
Summary of Chapter V	99
Abstract.....	100
1. Introduction	101
2. Materials and methods	103
2.1. Materials	103
2.2. Sample preparation	104
2.3. Preparation of CAS/LMP mixtures and turbidity measurement.....	104
2.4. Interfacial properties of CAS-LMP complexes	104
2.5. Stability of CAS or CAS/LMP based nanoemulsions	105
2.6. Statistical analysis.....	107
3. Results and discussion	108
3.1. Turbidity kinetic of the CAS/LMP coacervates.....	108
3.2. Dynamic interfacial pressure and Dilatational rheological properties.....	110
3.3. CAS or CAS/LMP based nanoemulsions	114
4. Conclusion.....	123
References.....	124
Chapter VI	128
Summary of Chapter VI	129
Abstract.....	130

1. Introduction	130
2. Material and methods.....	131
2.1. Materials	131
2.2. Interfacial properties	131
2.3. Binding properties.....	131
2.4. Statistical analysis.....	132
3. Results and discussion	132
3.1. Impact of aldehydes on the interfacial behavior	132
3.2. Dilatational viscoelastic properties	133
3.3. Ultraviolet Spectroscopy.....	133
3.4. Fluorescence spectra	134
4. Conclusion.....	136
References.....	137
Chapter VII	138
Summary of Chapter VII	139
Abstract.....	140
1. Introduction	140
2. Materials and methods.....	141
2.1. Materials	141
2.2. Sample preparation	141
2.3. Preparation of primary emulsions and multilayer emulsions	141
2.4. Isothermal titration calorimetry (ITC)	141
2.5. Intrinsic fluorescence	142
2.6. Zeta potential (ζ potential)	142
2.7. Mean particle size	142
2.8. Microscopic image.....	142
2.9. Statistical analysis.....	142
3. Results and discussions.....	142

3.1. Mechanism of preparing multilayer emulsions.....	142
3.2. Effect of titration or mixing on the multilayer emulsions: analysis of droplet size and flocculation	145
4. Conclusion.....	146
References.....	149
GENERAL DISCUSSION, CONCLUSION AND PERSPECTIVES	151

LIST OF ABBREVIATIONS

All the abbreviations are indicated in the text

This list includes the most relevant

DLS	Dynamic light scattering
ITC	Isothermal titration calorimetry
O/W	Oil-in-water
CAS	Sodium caseinate
LMP	Low methoxyl pectin
TCA/TC	<i>trans</i> -Cinnamaldehyde
LCT	Long chain triglycerides
MCT	Medium-chain triglyceride
PDI	Polydispersity index
EO/EOs	Essential oils
HCl	Hydrochloric acid
NaOH	Sodium hydroxide
NaCl	Sodium chloride
pI	Isoelectric point

INTRODUCTION

Over the last decade, many efforts have been devoted to the incorporation of bioactive compounds into food formulations to provide products with additional functional benefits like antibacterial, antioxidant, anticancer, antiallergic, and anti-inflammatory molecules. However, certain compounds with great health benefits, such as essential oils (EOs), carotenoids, phytosterols, and vitamins, are lipophilic components that are difficult to introduce in food products or have limited effects when used directly. Indeed, there are several issues, such as low water solubility, chemical instability, and sensitivity to oxidative degradation, that should be overcome for further application of these fat-soluble compounds in food industries. Nowadays, the development of systems based on oil-in-water (O/W) emulsions could address these deficiencies to some extent. On the other hand, with increasing consumer awareness, there has been in recent years a strong interest in replacing synthetic emulsifiers with natural emulsifiers.

Different sources of proteins have been widely studied as natural emulsifiers for food encapsulation systems due to their good amphiphilic, healthy, and nutritional properties, as well as their commercial availability. Particularly, caseins from milk are the most common natural commercial emulsifiers in the food industry, which are generally produced and sold in the form of sodium caseinate (CAS). Protein-based emulsions have been shown to meet current industrial requirements for food emulsion stability, but under certain conditions (acidic pH range, high ionic strengths, and high storage temperatures), their instability still limits their further applications. In this consideration, many researchers have focused on improving the adaptability of emulsions to environmental conditions by using a combination of other emulsifiers rather than a single emulsifier. On the other hand, the addition of polysaccharides to protein emulsifiers could combine the advantages of the two biopolymers, allowing to obtain hybrid protein/polysaccharide interfaces able to surround oil droplets, thereby improving emulsifying performance against environmental stresses.

Proteins adsorbed at O/W interfaces can form interfacial layers which may exhibit viscoelastic or even elastic behavior. The properties of these interfacial layers such as interfacial tension, interfacial elasticity, and viscosity, have been regarded as key parameters to determine the physical stability of emulsions. These characteristics are generally performed using Langmuir troughs or drop tensiometers. In addition, the presence of polysaccharides at different pH values greatly affects the structural properties of proteins, which in turn affects the interfacial and functional properties of protein-coated droplets.

Besides, some EOs contain aldehyde compounds, which have chemically reactive functional groups that interact with protein molecules. These chemical interactions between oil phase components and emulsifiers will further affect the formation and stability of the emulsion-based delivery systems. Therefore, it would be very important to study the interfacial properties and molecular interactions of the oil-water interfaces for obtaining more information about evaluating or predicting the stability of emulsions.

In this thesis, two biopolymers, sodium caseinate (CAS) and low methoxyl pectin (LMP), and two natural antibacterial molecules, citral and *trans*-cinnamaldehyde (TCA), were used to prepare nanoemulsions. The antibacterial activity and physicochemical properties of these nanoemulsions were systematically investigated under different conditions. In addition, the interfacial properties of the O/W interfaces formed by CAS/LMP, the interactions between the different components in the emulsion system, and the mechanism of forming the multilayer interfaces were also investigated. In detail, food-grade emulsifiers and natural antibacterial molecules were firstly selected according to their antimicrobial activity and their physicochemical properties. The physical stability of the nanoemulsions based on selected materials (CAS and TCA) was then further optimized by adding carrier oil to the oil phase to avoid Ostwald ripening. To improve the stability of emulsions to environmental conditions, emulsions prepared from CAS-LMP complexes at different pH values were studied. Meanwhile, the effects of LMP concentration on the interfacial dilatational

rheology of the complexes at O/W interfaces were carried out under different pH values. Thereafter, for better understanding the molecular mechanisms involved in the formation of the developed encapsulated systems, the interactions between CAS and the two used aldehydes were investigated by interfacial properties and fluorescence quenching measurements. Finally, the mechanism of the formation of multilayered interfaces was studied by both isothermal titration calorimetry and dynamic light scattering.

Organization of the thesis

The purpose of this thesis is to prepare nanoemulsions containing antibacterial molecules by food-grade emulsifiers (sodium caseinate and lecithin), to study the stability of nanoemulsions under certain application conditions, and to investigate the molecular interactions between different components in the emulsion system. **Chapter 1** is a literature review, including two parts. The first part discusses the key factors affecting the performance of sodium caseinate (CAS) stabilized emulsions. Part II summarized the state of the art concerning nanoencapsulation of essential oils (EO) as natural food antimicrobial agents. **Chapters 2 to 7** present the main results achieved in this thesis, based on 6 articles that have been published or will be submitted to international journals. In details, **Chapter 2** describes the preparation of stable nanoemulsions by using different biopolymers in combination with natural food antimicrobial agents, to attain the target antibacterial activity, **Chapter 3** presents the effect of carrier oil on stability of CAS stabilized nanoemulsions containing EO, **Chapter 4** focuses on the effect of adding low methoxyl pectin (LMP) on lipid oxidation and physical stability of CAS based nanoemulsions at neutral pH, **Chapter 5** investigates the effects of pH and LMP concentration on the interfacial dilatational rheology of CAS/LMP complexes at O/W interfaces and the stability of CAS/LMP based nanoemulsions, **Chapter 6** studies the interactions between CAS and two used aldehydes (citral and *trans*-cinnamaldehyde (TCA)) by interfacial properties and fluorescence quenching measurements, and finally, **Chapter 7** explores the mechanisms of the formation of multilayer emulsions by isothermal titration calorimetry and dynamic light scattering.

In the final chapter, a general discussion, conclusion, and perspectives will be presented.

Chapter I

LITERATURE REVIEWS

Literature review I

Understanding of the key factors influencing the properties of emulsions
stabilized by sodium caseinate

**Published in: Comprehensive Reviews in Food Science and Food
Safety**

Summary of literature review I

Sodium caseinate (CAS) provides comparable emulsifying properties that allow it to meet current consumer demands for the stabilization of food emulsions, but instability on some specific conditions limits their application. Therefore, there is an urgent need to better understand the effects of different environmental and processing conditions on emulsion stability, and how to improve the stability of CAS-formed food emulsions. The objective of this literature review was to introduce the general factors affecting the stability of sodium caseinate (CAS) - stabilized O/W emulsions, such as environmental stress and process conditions, and the relative importance of the various instability mechanisms of CAS-based emulsions as well as their relationships. The commonly used methods for detecting emulsion stability are also introduced. In addition, the state-of-the-art strategies to combine CAS and polysaccharides via complexation or conjugation methods to improve emulsion stability are presented and summarized. This part is expected to provide theoretical basis for the application of CAS in food emulsification in the future. In summary, this review is expected to provide a template for researchers to understand the fundamental properties of CAS-stabilized emulsions and study their stabilization methods.

Understanding of the key factors influencing the properties of emulsions stabilized by sodium caseinate

Wei Liao¹ | Adem Gharsallaoui¹  | Emilie Dumas¹ | Abdelhamid Elaissari² 

¹Univ. Lyon, University Claude Bernard Lyon 1, CNRS, LAGEPP UMR 5007, Villeurbanne, France

²Univ Lyon, University Claude Bernard Lyon 1, CNRS, ISA-UMR 5280, Villeurbanne, France

Correspondence

Adem Gharsallaoui, Univ. Lyon, University Claude Bernard Lyon 1, CNRS, LAGEPP UMR 5007, 43 Bd 11 Novembre 1918, 69622 Villeurbanne, France.
Email: adem.gharsallaoui@univ-lyon1.fr

Funding information

Scholarship Council for support (No. 201807565014).

Abstract

Emulsions can be easily destabilized under various conditions during preparation and storage. Therefore, it is necessary to understand the factors that influence the stability of emulsions, which is essential for their subsequent studies. Sodium caseinate (CAS) is a well-used nutritional and functional ingredient in emulsion preparation due to its good solubility and emulsifying properties. CAS-stabilized emulsions can be considered good food emulsion delivery systems, but their applications are still limited under certain conditions due to their instability to creaming and aggregation. Therefore, the purpose of this review is to provide a complete overview of how different environmental stresses and processing conditions affect the stability of CAS-stabilized emulsions and how to improve their stability. Initially, the general properties of CAS as emulsifiers and the characterization of CAS-stabilized oil-in-water (O/W) emulsions were summarized. Second, the major instability mechanisms that operate in CAS-stabilized emulsions were presented. Furthermore, the general factors such as pH, emulsifier concentration, ionic strength, oxidation, and processing conditions, affecting the stability of CAS-stabilized O/W emulsion, were discussed. On this basis, the commonly used methods for evaluating emulsion stability are introduced. Finally, state-of-the-art strategies to improve CAS-based emulsion stability are also described and summarized. This review is expected to provide a theoretical basis for the future applications of CAS in food emulsions.

KEYWORDS

emulsion characterization, emulsion stability, instability mechanisms, sodium caseinate

1 | INTRODUCTION

Food emulsions, a dispersion system composed of two or more incompatible phases, play an essential role in food systems since they directly affect the color, the texture, and the mouthfeel of food products (McClements, 2015). Typically, emulsions can be prepared in the presence of emulsifiers, which are usually composed of hydrophilic and hydrophobic parts to reduce the interfacial tension at

the oil–water or water–oil interface. Until now, synthetic emulsifiers food additives, such as sorbitan esters, sugar esters, and polysorbates, are still intensively applied in the most frequently consumed foods, although some reports showed their possible harmful effects on intestinal barriers and microbiota (Csáki & Sebestyén, 2019). Currently, there is a growing worldwide trend in the food field to replace commercial synthetic emulsifiers with natural “label-friendly” ones. Consequently, food manufactures

have focused on identifying and characterizing natural emulsifiers, such as proteins, lipids, polysaccharides, saponins, and so forth (Dammak et al., 2020), that can be labeled as “clean” in emulsion-based food products. Some food proteins from different sources such as milk, whey, eggs, legume, oilseed, and so on (Kim et al., 2020) have been shown to act as natural emulsifiers by adsorbing at oil droplets because of their good solubility and amphiphilic ability.

At present, the most widely applied commercial protein-based emulsifiers are casein proteins (Wang et al., 2013), which are generally sold industrially in the form of sodium caseinate (CAS). CAS are composed of all casein fractions— α_{s1} - and α_{s2} -caseins, β -casein, and κ -casein—which have strong amphiphilic properties and have the ability to rapidly reduce the oil–water interfacial tension during emulsification process (Walstra & Jenness, 1984). Different emulsification techniques, such as high-pressure homogenization (Liao, Gharsallaoui, et al., 2021), ultrasonication (Wan et al., 2022), microfluidizer (Ebert et al., 2017), and so forth, have been employed to produce stable CAS-based oil-in-water (O/W) emulsion systems. Nevertheless, CAS-based emulsions are prone to instability at certain unfavorable compositional and environmental conditions, such as different solution conditions (pH, protein concentration, ionic strength, homogenization conditions) and different environmental stresses (thermal processing and oxidation). These specific conditions limit the application of CAS-based emulsions in certain high-value fields. In recent years, several reviews have summarized various formulations of nanoemulsions, preparation methods, food applications, and methods to improve stability through using mixed emulsifiers, protein–polysaccharide complexation, or conjugates (Dammak et al., 2020; Evans et al., 2013; Kim et al., 2020; McClements, 2007; Ribeiro et al., 2021). In this context, it is necessary to understand the factors that influence the stability of emulsions. Nonetheless, there are still few review papers that have systematically explored the factors affecting CAS-stabilized emulsions. In the present review, we will provide general factors affecting the stability of CAS-stabilized O/W emulsions, such as environmental stress and process conditions, and the relative importance of the various instability mechanisms of CAS-based emulsions as well as the relationships between them. In addition, the methodology for detecting emulsion stability and how to improve the stability of CAS-stabilized food emulsions will be discussed.

2 | CAS AND ITS EMULSIFYING ABILITY

CAS shares similar composition with casein micelles, which is a partially aggregated mixture of four individ-

ual caseins, α_{s1} - and α_{s2} -caseins, β -casein, and κ -casein. In industry, CAS is generally manufactured by acid precipitation of casein micelles and then neutralized with alkali for spray drying (Wusigale et al., 2020). By adding the cation of the alkalizing agent, various types of caseinate could be produced, such as sodium, calcium, potassium, and ammonium caseinate. Among those, CAS is more commercially available. The aqueous suspension of CAS has been reported to be a particle suspension with a weight-average molar mass of 1200–4700 kDa and a diameters range of 50–120 nm (Wusigale et al., 2020). As an important dairy ingredient, CAS can endow food with certain functionalities in terms of water solubility, viscosity, emulsification, foamability, and encapsulation ability. The application of CAS as an alternative source of food emulsifiers in the food industry has attracted considerable attention, such as coffee whiteners, cream liqueurs, and whipping ingredients (Euston & Goff, 2019).

Compared to the most other food proteins, CAS is more disordered and hydrophobic with an extremely open and flexible conformation (Dickinson, 1999). α_{s1} -Casein and β -casein are the two main individual caseins that account for approximately 75% of the total milk casein. Both casein proteins have been shown to be the main contributors to the emulsifying properties of CAS and they can rapidly adsorb at the O/W interface during emulsification to protect newly formed droplets against incipient flocculation and coalescence. This is the fact that the high proportion of proline residues disrupts α -helix and β -sheet secondary structures and there are almost no cysteine residues in α_{s1} - and β -casein (Dickinson, 1994). Even though both caseins proteins exhibited strong tendency to adsorb at hydrophobic surface, the mechanisms of α_{s1} - and β -casein acting on the O/W interface are significantly different. Dickinson (1988) compared the adsorption of α_{s1} - and β -casein in O/W emulsion and the data indicated that β -casein predominates at the interface since its equilibrium interfacial free energy is slightly lower than α_{s1} -casein. The train–loop–tail model has been used to explain the adsorbed layer structure by CAS (Dalgleish, 1996). As shown in Figure 1a, β -casein develops a highly charged tail dangling away from the droplet surface as the *N*-terminal of the chain is the hydrophilic charged residue, and the remaining parts adsorbed on the surface in the shape as “trains” and small “loops” are predominantly hydrophobic. The adsorbed layer thickness is mainly determined by the distribution of “loops” and the dangling “tails” that also provide steric repulsions in the emulsion systems. The “tails” parts are very sensitive to the solution environmental parameters such as pH and ionic strength, but the hydrophobic parts “loops” of the chain are relatively insensitive (Dickinson, 1999). α_{s1} -Casein-adsorbed layer also develops the “loops” (Figure 1a) on the O/W interfaces as it contains three

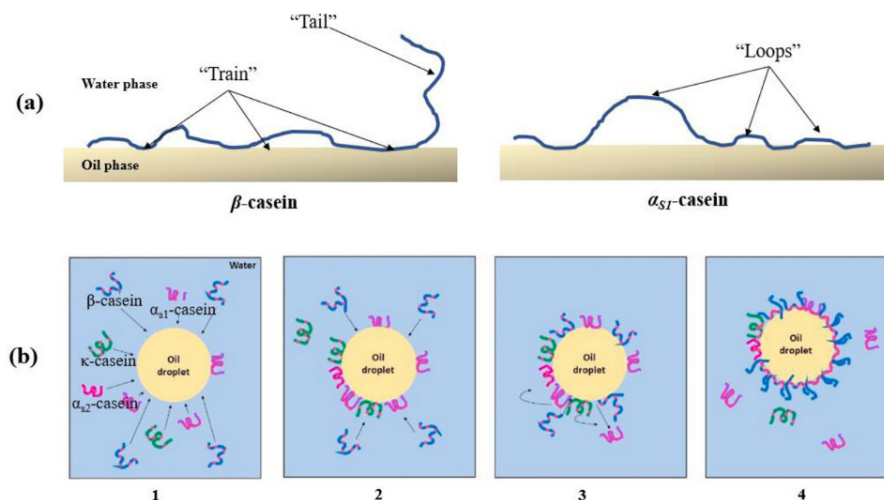


FIGURE 1 (a) Schematic diagram of typical adsorption configurations of α_{S1} -casein and β -casein at oil/water interface. (b) Mechanisms for adsorption of CAS at oil/water interface. Adapted from Kim et al. (2020)

discontinuous hydrophobic regions (Shimizu et al., 1986). It was reported that α_{S1} -casein provides less surface coverage and thinner layer during emulsification than β -casein (Dalglish, 1996), which inefficiently provides steric repulsions. However, α_{S1} -casein provides higher electrostatic repulsions than β -casein since the amino acid sequence is significantly different. On the other hand, the hydrophobic plots of amino acid residues in α_{S2} - and κ -casein indicated that they have surface-active properties (Su & Everett, 2003) and these caseins could also be adsorbed on the O/W interfaces and contribute to the surface stability. Kim et al. (2020) drew a schematic diagram (Figure 1b) of the adsorption of four casein proteins at the O/W interface based on the research of Dickinson (1989), which is mainly divided into three steps: (1) simultaneous adsorption of α_{S1} - and κ -casein in the initial diffusion stage; (2) subsequent displacement of α_{S1} - and κ -casein by β -casein from the interface; and (3) formation of a mixture with β -casein as the main component film. In fact, due to the interactions between casein molecules and other food ingredients, the characteristics of the CAS layer adsorbed in many food emulsions are much more complicated than just described.

3 | THE MAJOR INSTABILITY MECHANISMS IN CAS-STABILIZED O/W EMULSIONS

Generally, a food emulsion system is prepared using a high shear device (e.g., colloidal grinding, high-speed agitator, and high-pressure homogenizer) in which the emulsion mixes oil and water in the presence of emulsi-

fiers (McClements, 2015). For instance, the basic process of preparing a CAS-based emulsion by high-pressure homogenization is to force a coarse mixture of oil and CAS aqueous solution through narrow crevices, resulting in cavitation and intense laminar shear to disperse well. In this process, the casein molecules are adsorbed to the O/W interface through unfolding and rearrangement, forming a stable interface layer around the oil molecules. The degree of protein molecules unfolding relies on the flexibility of their molecular structure, which depends on the strength of the forces that maintain the secondary and tertiary structures. As CAS has a fairly flexible structure, it can expand rapidly at the interface and then form an extended layer of about 10 nm (Dalglish, 1990). The colloidal stability of the CAS-stabilized emulsion systems is eventually determined together by electrostatic repulsions and steric repulsions caused by all the interactions between adsorbed casein layers.

It is well established that emulsions are thermodynamically unstable, therefore various physical and chemical mechanisms (including creaming, flocculation, coalescence, Ostwald ripening, and phase separation, as shown in Figure 2) occur over time (Dickinson, 2019). Indeed, these instability mechanisms can occur simultaneously in CAS-stabilized emulsion systems, and the emergence of one instability mechanism encourages other mechanisms. When the free energy of surface interactions is repelling at all droplet surface-to-surface separation values, the emulsion will be stable. However, when the free energy of interactions has an attraction within a certain separation range, the droplets will tend to flocculate, which may adversely affect coalescence and creaming. These

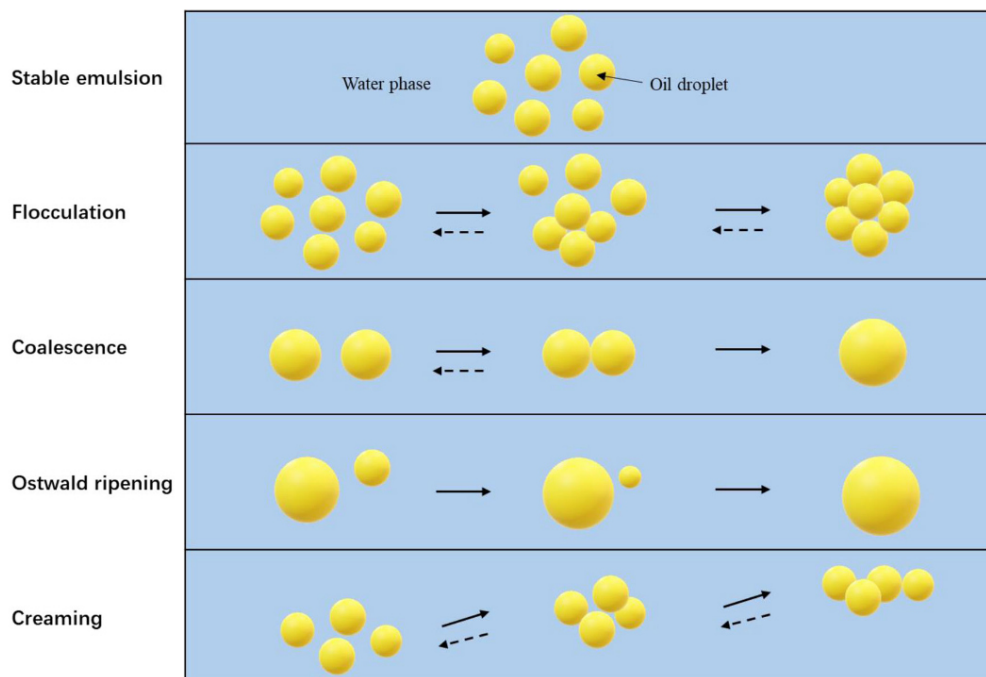


FIGURE 2 Schematic diagram of the major instability mechanisms undergone by oil-in-water emulsions

instability mechanisms occur in CAS-based emulsion depending on the overall balance among electrostatic forces, steric forces, and van der Waals forces. Generally, CAS-based emulsions are unstable under unfavorable compositional and environmental conditions, such as a pH value close to the isoelectric point (pI) of CAS (pH 4.6) (Bhat et al., 2016), high pressure processing (Mao et al., 2010), high temperatures (Mao et al., 2010), freeze-thaw cycles (Wang et al., 2020), and high ionic strength (Sharma et al., 2017). In the following part, we discuss several common instability mechanisms in CAS-based emulsion.

3.1 | Flocculation

Flocculation is a process in which two or more droplets combine with each other, but each remains intact. When attractive interactions between droplets outweigh repulsive interactions, droplets tend to flocculate (Dickinson, 2019). Due to the Brownian motion, droplets are usually close to each other. The occurrence of flocculation will depend on the forces acting on the droplets and the time whether they stay close together for long period time. Under certain situations, the presence of flocs is related to visible changes in the appearance of emulsion (Martinez-Padilla et al., 2021). The concentration of emulsifiers plays an essential role in the stability of CAS-based emulsions.

For example, to avoid flocculation, even in emulsions prepared at pH 7, the oil/protein ratio must be neither too low nor too high. At low caseinate content, casein molecules are generally shared by two or more oil droplets in emulsion systems that can lead to bridging flocculation, apparently accompanied by some coalescence. This type of flocculation is, at least partly, irreversible. In the presence of an excess of nonabsorbent caseins in the continuous phase, depletion flocculation will occur that is reversible with no measurable change in droplet size distribution after dilution (Dickinson et al., 1997). Typically, only strong shear forces such as high-speed homogenization could destroy the bridging flocculation, while depletion flocculation can be simply disrupted by gentle stirring or dilution. Our recent study (Liao et al., 2022) supported that depleted flocculation-induced droplet aggregation is reversible. The high content of pectin promoted extensive aggregation of CAS-based droplets (observed by microscopy), but the droplet size of the emulsion did not change significantly. In addition, caseinate molecules are sensitive to both pH and ionic strength. Different pH values and ionic forces in the continuous phase can affect the dissociation of ionized groups, thus determining the states of flocculation in emulsion systems. The macroscopic properties of CAS-based emulsions like appearance, rheology, and sensory property are strongly influenced by the degree and nature of emulsion flocculation. Generally, the occurrence of

flocculation is harmful, which leads to an increase in particle size to speed up gravity separation in some foods such as emulsion-based soft drinks. However, in some specific cases, flocculation can be used to control the creation of an ideal texture feature. On the other hand, the flocculation state has a significant influence on other instable phenomena, such as droplet coalescence, phase separation, and Ostwald ripening (Ma & Chatterton, 2021)

3.2 | Coalescence

Coalescence is defined as the process of two or more droplets coming into contact and merging, creating larger droplets. This can happen if two droplets are very close for a while. As described above, the occurrence of flocculation in the emulsion is usually accompanied by coalescence. Moreover, the mechanism and the intermolecular forces of flocculation and coalescence are similar. One is considered reversible (flocculation), in which a strong force can be used to separate the aggregates. The other is irreversible (coalescence). The occurrence of coalescence in emulsion systems significantly affects the processing or shelf life of O/W emulsions. It was reported that appropriate content of CAS-based emulsion systems was very stable toward creaming and coalescence due to the thicker interfacial film formed by casein proteins (Dickinson et al., 1997). The adsorbed film formed by the emulsifier may rupture spontaneously during storage. The formation of a thicker water phase film at the O/W interface helps prevent droplet coalescence (droplet melting) and achieve reasonable stability, thus providing the appropriate life for the final emulsified product (Costa et al., 2019). The larger the droplet diameter, the thinner the film thickness, and the lower the O/W interfacial tension, the easier the film ruptures to lead to irreversible coalescence (Fredrick et al., 2010). However, under certain circumstances, CAS-based emulsions have a tendency to coalesce. A recent study (Lamothe et al., 2019) reported that, under gastric conditions, CAS-stabilized emulsions showed extensive fat droplet coalescence, whereas coalescence was very limited in the whey protein-stabilized emulsions. They attributed this difference to the fact that CAS has highly flexible and disordered molecules that are more sensitive to the gastric environment. In an O/W emulsion, the coalescence eventually forms a layer of oil on top of the solution, called demulsification. In the manufacture of some products, partial coalescence is desired to obtain the specific properties in products like ice cream. It contributes to the structure and physical and sensory flavors like fattiness and creaminess of the final products (Chen et al., 2019).

3.3 | Gravitational separation

Emulsions tend to be divided into different layers of oil and water due to the different densities and the different polarities between oil and water molecules. Under the effect of gravitational separation, if the density of the droplets is lower than that of the surrounding liquid, they tend to move upward, which is termed creaming. Conversely, if they are denser than the surrounding liquid, they tend to move downward, which is termed sedimentation. This phenomenon is usually accompanied by emulsion separation, resulting in a droplet-rich cream layer and a droplet-depleted watery layer. Gravitational separation can be used to measure emulsion stability by visual or optical imaging, but it usually takes a long time. In addition, the correlation between creaming and bridging flocculation was observed in the CAS-stabilized O/W emulsion (Dickinson et al., 1997). In a dilute O/W emulsion, the occurrence of bridging flocculation can speed up the creaming of emulsion since the larger buoyance forces acting on flocs are stronger than those acting on individual droplets (Dickinson et al., 1997). On the contrary, in a higher concentrated O/W emulsion, bridging flocculation can retard creaming as a network structure is formed in emulsion system. Meanwhile, the creaming generally occurs before coalescence, followed by phase separation, and its degree in O/W emulsion can be described by creaming index (Onsaard et al., 2006). Therefore, the creaming index can predict the degree of droplet aggregation: the higher the index, the more the droplet aggregation.

3.4 | Ostwald ripening

Ostwald ripening is a time-lapse phenomenon, as the oil molecules diffuse through continuous phases and smaller droplets in the emulsion system increase the size of larger droplets at the expense of themselves (Jiao & Burgess, 2003). The driving force in this process is the curvature effect, in which oil molecules near smaller droplets are more soluble than larger droplets. Prof. Laplace pointed out that the concave pressure of the curved interface is higher than the convex pressure, which is proportional to the tension of the interface multiplied by the curvature. For a sphere, the curvature is given by the reciprocal of its radius. As a result, the dispersion of the smaller particles increases their solubility in the continuous phase, the smaller particles shrink (eventually disappear), and the larger particles become larger. Generally, Ostwald ripening is negligible in food emulsions containing low water-soluble long chain triglycerides. However, when more water-soluble oils (essential oils, flavor oils, short-chain triglycerides) are used in O/W emulsions, Ostwald

ripening is a major obstacle that should be carefully controlled during long-term storage (Park et al., 2020). Our previous study indicated that altering the oil composition by adding medium or long-chain carrier oil before homogenization can significantly inhibit Ostwald ripening of CAS-based emulsions containing essential oils (Liao et al., 2021). In addition, to prevent or delay Ostwald ripening in food emulsions, another effective method is to combine protein emulsifiers with some amphiphilic polysaccharides to form a thicker interfacial film around the oil droplets (Artiga-Artigas et al., 2020; Dickinson, 2019).

4 | MAIN FACTORS DETERMINING THE STABILITY OF CAS-STABILIZED EMULSIONS

Physical instability refers to changes in the spatial arrangement or size distribution of the emulsifier droplets over time, such as gravitational separation, flocculation, and aggregation, while chemical instability involves changes in the composition of the emulsion, such as oxidation and hydrolysis (McClements, 2015). To meet the requirements of industrial applications, researchers must understand the factors that determine emulsion stability. As reported by McClements (2007), effective methods to prevent adverse changes in food emulsions need to be determined based on the physical and chemical properties of the ingredients used to stabilize these emulsions. As we described above, fine O/W emulsions prepared by CAS as the only emulsifier are very sensitive to the influence of various factors such as temperature, pH, ionic strength, calcium ion content, protein/oil ratio, and so forth. These most important factors influencing the stability of CAS-stabilized O/W emulsions will be discussed in the following section.

4.1 | Effect of pH

One disadvantage of using CAS as an emulsifier is known to be its limited applicability in acidified foods (Perugini et al., 2018). It is well known that the environmental pH has a great influence on protein solubility, surface charge (zeta potential), and surface hydrophobicity. Casein proteins in milk are very stable systems that can withstand the stringent conditions imposed during commercial processing (Bhat et al., 2016). However, they are still destroyed under certain temperature and pH conditions, especially acidic pH (near their pI: ~4.6), resulting in reduced stability, which is reflected by visible flocculation or serum separation. Perrechil and Cunha (2010) studied the effect of pH on the stability of CAS-stabilized W/O emulsions and their

results showed that the creaming behavior of emulsions was largely influenced by the pH of the emulsions.

As expected, the weakest emulsifying property of CAS was observed around its pI (Wang et al., 2019). When the pH value is far from its pI, the absolute value of zeta potential of CAS-coated droplets increases and then it can provide enough electrostatic repulsions between droplets against flocculation. This is the fact that more negatively or positively charged proteins allow for more protein-solvent interactions and greater diffusion rates to the interface, which also contributes to increased interfacial tension of particles and the stability of emulsions. The interfacial tension can also be changed by pH. Amine e et al. (2014) reported that the interfacial tension of CAS particles is usually lower at alkaline pH than at pH 7, which contributes to a more expansive structure of the protein at the interface and then leads to a smaller emulsion size. Dickinson (1999) described that the “tail” extension around oil droplet formed by β -casein and the maximum extent of the loop-like region formed by α_{s1} -casein are diminished as pH is reduced from 7 to 5.5, resulting in lower steric repulsion. Nevertheless, by mixing other emulsifiers such as adsorbed polysaccharides (Shi et al., 2021; Surh et al., 2006) and non-ionic surfactants (Perugini et al., 2018), CAS can also be used in acidic environments to stabilize emulsions. Perugini et al. (2018) used a nonionic surfactant (Tween 20) in combination with CAS as blending emulsifiers of O/W nanoemulsions to prepare nanoemulsions and their results showed that the addition of Tween 20 effectively enhanced the stability of the emulsion under acidic conditions. As shown in Figure 3, the effects of pH and pectin type on the zeta potential and creaming stability of O/W emulsion stabilized by CAS were well investigated (Surh et al., 2006). The addition of pectin to CAS-based emulsions leads to an obvious change in the pH dependence of the surface droplet charge. At pH value around the pI of caseinate, the blending emulsifier is negatively charged. Optical microscope measurements from their results also showed that CAS-stabilized emulsion is dispersed well at a pH value higher than 5.0 and aggregates near the pI.

4.2 | Effect of ionic strength

As the ionic strength is able to screen the electrostatic repulsions between the droplets, the presence of certain ions, especially calcium, may affect the interactions between protein-stabilized droplets and induce flocculation (Dickinson, 2019). Targeted screening can promote aggregation and reduce adsorption at the emulsion interface, depending on the type and concentration of ions. Generally, protein-based food products usually need to be

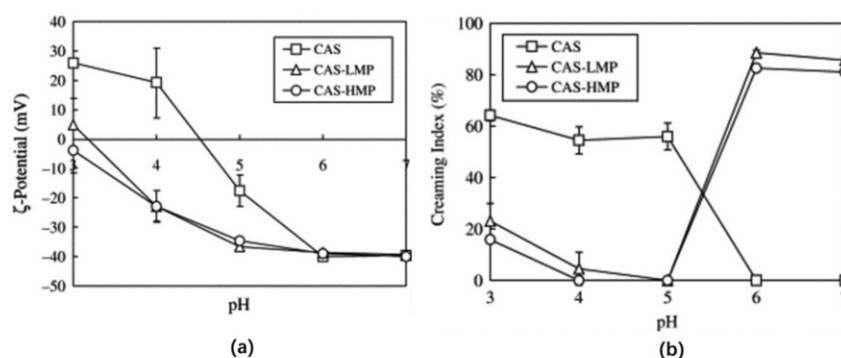


FIGURE 3 Dependence of (a) electrical charge of droplets (ζ -potential) and (b) creaming index on pH and pectin type for emulsion encapsulated by CAS (Surh et al., 2006)

TABLE 1 Influence of ionic strength on the mean particle diameter and ζ -potential of the sodium caseinate-stabilized emulsions (Qin et al., 2018)

Concentration (mg/ml)	Z-average diameter (nm)	ζ -potential (mV)	
NaCl	0	199.27 \pm 1.56 ^{bc}	-36.7 \pm 0.7 ^a
	0.1	197.76 \pm 1.59 ^c	-36.9 \pm 0.4 ^a
	0.35	202.25 \pm 2.51 ^{ab}	-36.8 \pm 1.1 ^a
	0.60	203.65 \pm 1.92 ^a	-36.9 \pm 0.7 ^a
	0.85	202.62 \pm 1.65 ^{ab}	-37.5 \pm 0.8 ^a
CaCl ₂	0	199.27 \pm 1.56 ^c	-36.7 \pm 0.7 ^d
	0.25	197.50 \pm 0.75 ^c	-32.6 \pm 1.6 ^c
	0.55	210.94 \pm 1.94 ^d	-31.7 \pm 0.9 ^c
	0.85	230.37 \pm 2.38 ^c	-29.3 \pm 0.6 ^b
	1.15	254.43 \pm 1.74 ^b	-26.6 \pm 0.5 ^a
1.45	265.18 \pm 4.39 ^a	-25.9 \pm 0.4 ^a	

Note: Mean values within the same column followed by the same lowercase letters are not significantly different ($p > .05$) between NaCl (or CaCl₂) levels.

used in combination with various minerals in practical applications to meet different needs. Thus, the effect of different minerals on emulsion stability should be better taken into account. It has been shown that the addition of 15 mM CaCl₂ to a CAS-stabilized emulsion caused destabilization (Dickinson, 2010). Qin et al. (2018) investigated the effect of ionic strength on the diameter and zeta potential of CAS-stabilized emulsion by sodium and calcium ions, respectively. As shown in Table 1, the addition of NaCl in different concentration (0.0–1.1 mg/ml) exhibited no obvious effect on the size and zeta potential of caseinate-stabilized emulsions, while the addition of CaCl₂ showed a higher influence. With the increase of CaCl₂ concentration, the zeta potential was significantly decreased, which may be caused by higher ionic strength shielding the surface charge of CAS-stabilized droplets.

The reduction of electrostatic repulsions between droplets promoted flocculation and then increased the size of droplets. A similar phenomenon was reported in the study of caseinate-stabilized clove oil nanoemulsion (Sharma et al., 2017). Multivalent counteracting ions such as Ca²⁺, Fe²⁺, or Fe³⁺ are more effective than monovalent ions in promoting emulsion instability because they are shielded; electrostatic interactions are more effective and they can be combined with the droplet surface, thus reducing the zeta potential (Liang, Matia-Merino, et al., 2017). Moreover, Dickinson and Davies (1999) found that the addition of calcium salts before or after homogenization had significantly different effects on the stability of CAS-stabilized emulsions under the same preparing process. These different behaviors of electrostatic force can be regarded as the changes of charge density and protein aggregation state, and these changes will further work on the adsorption layer structure and protein surface coverage.

It is worth noting that, in the presence of excessive unabsorbed CAS, the addition of appropriate amounts of CaCl₂ to emulsions can eliminate the effect of depletion flocculation (Ye & Singh, 2001). This is the fact that the addition of ionic molecules in the aqueous phase results in an increased size of casein aggregates due to the screen effect, thereby decreasing the amount of depleting unabsorbed proteins.

4.3 | Effect of emulsifier concentration

The protein concentration plays an important role in the stability, color, nutrition, and taste of the final emulsion. To improve stability against aggregation, it is significant to make sure that the protein/oil ratio is in the appropriate range even for an emulsion formed at neutral pH and low ionic strength. Otherwise, protein-stabilized emulsions are susceptible to different types of flocculation during

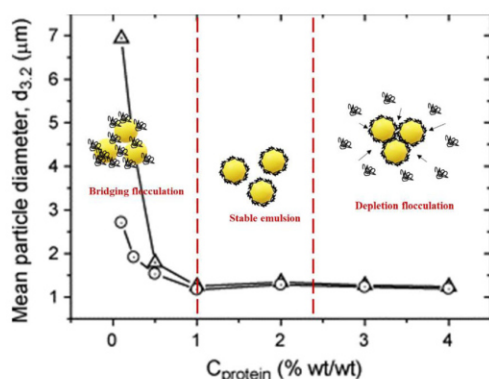


FIGURE 4 The effect of CAS concentration (% w/w) on mean particle diameter of O/W emulsions in the absence of SDS (Δ) or in the presence of SDS (O) with the schematic diagram of bridging flocculation and depletion flocculation in emulsion systems. Adapted from Sánchez and Patino (2005)

storage, leading to increased creams or serum separation. As reported by Singh (2011), with sufficient CAS molecules to cover the oil droplets during homogenization, emulsions are usually stable for long-term storage against coalescence. However, when the concentration is relatively low, casein proteins are insufficient to completely cover the O/W interfaces during the homogenization process. As a result, casein molecules are shared by two or more droplets, leading to bridging flocculation. The effect of CAS concentration on the stability of emulsion through high-pressure homogenization was studied by Sánchez and Patino (2005). As shown in Figure 4, their results indicated that there is a critical concentration of CAS in the aqueous phase: when CAS concentrations were above 1% (w/w), the emulsifying capacity was constant and the size distribution of droplets was monomodal; however, at CAS concentrations below 1% (w/w), the size distribution of droplets in the emulsion was bimodal and the emulsions exhibited some degree of flocculation, which was inhibited to some extent by the presence of sodium dodecyl sulfate (SDS). It is worth noting that excess of caseinate ($>2\%$ [w/w]) increased the rate of creaming that may be attributed to the presence of depletion flocculation. Dickinson (1997) similarly reported that attractive depletion interactions may exist between pairs of dispersed particles when a colloidal system contains a large amount (>3.0 wt.%) of smaller size of unabsorbed molecules. However, a recent rheological study of nanoemulsions prepared with CAS as the sole emulsifying agent found no evidence of depletion flocculation over a wide range of protein contents (Rouillet et al., 2019). This could be attributed to the relatively small droplet size ($d_{43} \sim 130$ nm). It has been reported that sufficiently high protein concen-

trations may lead to a stronger droplet network and this network can lead to partial restabilization of the emulsion against creaming and serum separation (Dickinson, 2019). Liang et al. (2014) investigated the relationship between creaming behavior and depleted flocculation of CAS-stabilized O/W emulsions with different contents of CAS (1%–10% [w/w]). At low CAS concentrations (less than 3% [w/w]), depletion-induced droplet networks formed and showed fast phase separation. At middle CAS concentrations (3%–5% [w/w]), the increase of nonadsorbed casein concentration increases the number of droplets involved in the network, thus stabilizing the emulsion structure dynamically to prevent creaming. Surprisingly, at higher caseinate concentrations ($\geq 6\%$ [w/w]), the formation of droplet network shows obvious delay that was probably caused by the higher continuous phase viscosity decreasing the formation of the droplet network. These results show that there is an optimal protein concentration for CAS that can produce good, saturated surface coverage and maximum emulsion stability against these instability mechanisms.

4.4 | Effect of homogenization process

The stability of an emulsion during storage is closely related to its homogeneity, especially its size distribution. Indeed, nanoemulsions (diameter <200 nm) generally have better physical and chemical stability than conventional emulsions ($>1 \mu\text{m}$) because they are kinetically stable which are more stable to gravitational separation, coalescence, and flocculation than conventional emulsions (Sneha & Kumar, 2021). There are two types of emulsification techniques used to produce emulsified systems: a top-down approach and a bottom-up approach (Liao, Badri, et al., 2021). The top-down methods generally need large energy input for breaking up the dispersed phase into small structures by reducing the size and shaping the structure. The bottom-up methods generally include self-assembly, phase inversion, and spontaneous emulsification, which require the use of organic solvents or the addition of industrial surfactants. For food emulsion-based products, a top-down approach was normally selected for security reasons. High-speed homogenization, high-pressure homogenization, ultrasonic emulsification, membrane emulsification, microfluidization, and so on have been widely used in different experimental laboratories for the preparation of nanoemulsions. The advantages and disadvantages of these techniques are summarized in previous reports (Saffarionpour, 2019; Sneha & Kumar, 2021). There are significant differences in droplet size and distribution available in different homogenization devices, and these differences will further affect the stability of

the emulsions (Jacobsen, 2016). For example, it has been reported that high-pressure homogenizers can be used to produce nanoemulsions, but excessive ultrasonic power or ultrasonic time course can lead to increased temperature, resulting in flocculation or coalescence (Mao et al., 2010). Hebshy et al. (2017) compared different methods to prepare CAS-stabilized emulsions. Their results showed that nanoemulsions produced by high-pressure homogenizers exhibited lower size and much higher stability than those produced by conventional homogenization. At the same time, different pressure settings in high-pressure homogenization also have a significant effect on the stability of the emulsion. When sufficient CAS concentrations are used, pressure higher than 200 MPa resulted in physically and oxidatively stable emulsions, while the use of lower homogenization pressure (100 MPa) resulted in significant creaming. A similar trend was observed in Carpenter and Saharan's (2017) study where mustard oil nanoemulsions were prepared by different ultrasound powers, and they found that time and power parameters of ultrasonic can lead to increases or reductions in mean particle size. Another study (Let et al., 2007) indicated that less lipid oxidation of milk-based emulsions was obtained at high pressure (22.5 MPa) than at lower pressure (5 MPa).

4.5 | Effect of heating process

Food products based on emulsions generally undergo heat treatment at higher temperatures such as cooking and sterilization. One of the reasons why CAS has been widely used in food emulsions is that it has a relatively higher heating resistance ability than other common protein emulsifiers such as whey proteins and pea proteins (Liang, Matia-Merino, et al., 2017). This is the fact that relatively flexible casein molecules do not undergo significant heat-induced conformational changes like globular proteins (Srinivasan et al., 2002). Nevertheless, dephosphorylation, proteolysis, and polymerization of CAS solutions can occur at higher temperatures and longer heating time (Liang, Gillies, et al., 2017). Therefore, it is still important to fully understand the physical and chemical changes in CAS-stabilized emulsions caused by heating and to develop strategies to control the destabilizing processes. Qin et al. (2018) studied the effect of different heating temperatures on CAS-stabilized emulsions, and their results indicated that CAS has an excellent heating tolerance. The average diameter of CAS-based emulsions did not show obvious change even when the emulsions were heated to 90°C. McSweeney (2004) reported that higher heating can affect the particle size of milk protein-stabilized emulsions. The particle size distribution (PSD) curve of the model emul-

sions (at pH 6.8) gradually increased from 1 μm before heating to $\sim 10 \mu\text{m}$ when heated at 140°C for 80 s. In this case, the unadsorbed caseinate protein fraction acts as "glue," causing the emulsion droplets to entangle into large aggregates. On the other hand, the disulfide bond between the milk proteins during the heating process can also grow the particle size due to the flocculation of the droplets. Liang, Gillies, et al. (2017) found that the phase separation of CAS-stabilized emulsions was markedly dependent on the duration of the heat treatment. The heat treatment at 120°C caused casein proteins degradation and changed the intact CAS concentration in the continuous phase, thereby resulting in a greater extent of flocculation. Srinivasan et al. (2002) found a very interesting phenomenon: after heating treatment (121°C for 15 min), the stability ratings of heated emulsions were higher than that of unheated systems. In fact, at high temperatures, the molecular structure of the protein will fully unfold, and all hydrophobic residues will enter the oil phase, making the droplets less likely to aggregate. However, it was reported that adsorbed CAS molecules are more susceptible to thermally induced degradation than unadsorbed ones in solution (Liang, Gillies, et al., 2017). This difference has been attributed to protein structure and conformational differences between adsorbed and unadsorbed caseinate. In some cases, especially when the final product is a gelatinous system (such as the formation of a gel matrix for casein emulsions), thermally induced emulsion destabilization is ideal (Silva et al., 2019).

4.6 | Effect of oxidation

Preventing oxidation is an important consideration when designing food emulsion systems since oxidation of an emulsion can greatly affect flavor, sense, and color of the food products during storage. The factors that cause lipid oxidation in an emulsion are very complex because they may include oxidation or electron transfer events in all the different phases of the system (Jacobsen, 2016). CAS has been reported to be very effective in protecting coated oils from oxidation, due to its unique iron-chelating properties and ability to generate thick interfacial layers around small oil droplets (McClements & Decker, 2018). For this reason, CAS has been used as an emulsifier to design delivery systems for omega-3 fatty acids, as well as for real food emulsified systems such as milk, yogurt, and cheese (Walker et al., 2015). Currently, a variety of methods and techniques can be used to detect the oxidation process of lipids in emulsions, such as peroxide value, *p*-Anisidine (*para*-anisidine) value, and thiobarbituric acid reactive substances (TBARS) assays (Jacobsen, 2016). O' Dwyer et al. (2013) measured the lipid hydroperoxide values and *p*-Anisidine values to

monitor the oxidative stability of CAS-stabilized emulsions containing various oils (sunflower, camelina, and fish). Their results showed that CAS, as emulsifier, was able to improve their oxidative stability compared to pure oils. Hebishy et al. (2017) reported that higher oxidative stable emulsions were prepared by ultrahigh-pressure homogenized emulsions with sufficient CAS concentration (5 g/100 g). The oxidative stability of O/W emulsions is also related to the size of the droplets, the interfacial properties of the droplets, and the type of emulsifier. Ries et al. (2010) found that CAS and whey protein-stabilized emulsions with small droplet size had greater oxidative stability than emulsions with large droplet size. Meanwhile, the antioxidant capacity of CAS-stabilized emulsion was proportional to the concentration of CAS in the preparation. Higher concentrations of protein molecules can even offset the effects of milk droplet size and protein type (Ries et al., 2010). This may be because higher concentrations of unabsorbed casein molecules in the continuous phase inhibit free radical invasion of the O/W emulsion. In general, oxidation occurs faster in O/W emulsions than in bulk oils (Jacobsen, 2016), which may be due to the relatively harsh processing conditions required to produce the emulsion, such as exposure to air (oxygen), higher heating temperatures, or direct production through ultrasonic cavitation. These processes will promote the oxidation of the emulsion. In addition, the higher the unsaturated lipid content in O/W emulsion, the more it is sensitive to lipid oxidation in general (Chen et al., 2022).

5 | GENERAL TECHNOLOGIES FOR DETECTING AND EVALUATING CAS EMULSION STABILITY

To meet specific applications needed in food industries, detailed information on the emulsion matrix and droplet properties should be obtained to understand and estimate the stability of O/W emulsions. Essential emulsion characteristics such as droplet size, droplet charge, morphology, and rheological behavior could be measured and monitored by analytical instruments and standardized methods. These characteristics could be used to represent the physicochemical, appearance, and sensory properties of emulsion systems. For this reason, researchers can achieve information about instability mechanisms by combining several techniques such as particle size and surface charge with microscopic observations. Table 2 summarizes the advantages and limitations of the various techniques most commonly used to test the stability of O/W emulsions. In the following section, these techniques for evaluating the stability of O/W emulsions stabilized by CAS will be discussed.

5.1 | Visual observation

The stability of an emulsion substantially affects the quality, appearance, color, and odor of food products. In turn, changes in appearance, color, and odor of emulsion-based products can also be used to determine whether the emulsion is still stable. In some cases, the instability of the emulsion, such as creaming or precipitation, can be directly observed by the naked eye. Visual observation is probably the simplest, cheapest, and fastest method of evaluating emulsion gravity separation without the need for expensive and complex analytical devices. From the viewpoint of gravity separation, the macroscopic changes of emulsions may have two mechanisms: creaming and sedimentation. As shown in Figure 5a, creaming can be observed clearly as the density of the dispersed phase is lower than that of the continuous phase. Conversely, sedimentation occurs when a dispersed phase with a higher density than the continuous phase moves upward and produces a thicker separation layer. In this regard, the degree of precipitation or creaming generally can be assessed by observing the thickness of the cream or precipitation layer with the naked eye, and then by instrumental measurement and recording. However, visual observation, though convenient, is not suitable for studying the mechanisms of instability phenomena such as flocculation, coalescence, and Ostwald maturation. In addition, the emulsion layer is usually visible only when the degree of instability is quite high. Therefore, the initial stage of emulsion stability usually needs to be observed accurately with the help of other analytical instruments.

5.2 | Microscopy observation

Visual observation is insufficient to study most instability mechanisms and smaller droplets, such as individual droplets, flocs, fat crystals, bubbles, and ice crystals. Several microscopy techniques have been established to observe these fine features of emulsions. Currently, the most widely used are optical, confocal fluorescent, scanning electron microscopy (SEM), transmitting electron microscopy (TEM), and atomic force microscopy (AFM). These techniques provide detailed information about complex systems in the form of “images” that are often relatively easy to understand. Meanwhile, each technique is based on a different physicochemical principle and can be used to further study the stability mechanism of emulsions with different particle sizes and types.

Among the developed techniques, the optical microscope is the most commonly used emulsion observation equipment, because it is very convenient in handling and sample preparation, especially suitable for the observation

TABLE 2 Advantages and limitations of various techniques for detecting the instability of emulsions

	Techniques	Advantages	Disadvantages
Visual observation	Appearance, color, and odor of emulsions	Simple and rapid. The extent of creaming or sedimentation can be observed with naked eyes.	Long measuring period; unable to study other instability phenomena, such as flocculation, coalescence, and Ostwald ripening
Microscopy observation	Optical microscopy	Easy sample preparation; easy to operate and available in most research facilities; quick view at the shape and integrity of emulsions	Unable to provide comprehensive information about the physical status of the dispersed phase. The contrast between the different components of an emulsion is usually poor.
	Confocal laser scanning microscopy (CLSM)	Three-dimensional images and surface profiles can be available. The ability to eliminate or reduce background information far from the focal plane results in better optical resolution and contrast.	The ingredients in the emulsion need to be stained prior to analysis; not suitable for light sensitive samples; depending on the target sample and its stain agent; the dyeing process is complex.
	Scanning electron microscopy (SEM)	In-depth study of the structure and morphology of the emulsion is possible; able to obtain detailed size, three-dimensional images, and surface structure as well as multifunctional information	The emulsion needs to be dried and gold/platinum coated before visualization; detailed information on the pellet layering and internal structure cannot be provided; hard to operate
	Transmitting electron microscopy (TEM)	Very high magnification and resolution of emulsion droplet are available; provides detailed information on morphology, size distribution, homogeneity, and surface structure	Staining and dehydration can result in structural artifacts; hard to construct three-dimensional image from two-dimensional slices; tedious operating procedure
	Atomic force microscope (AFM)	High resolution; easy sample preparation; accurate height information; works in vacuum, air, and liquids; three-dimensional images and surface roughness	Limited vertical range; small scan size and slow scan speed; data not independent of tip; tip or sample can be damaged
Particle size analysis	Laser diffraction measurement	The measuring range for static light and dynamic light scattering is 100 nm to 1000 μm and 3 nm to 5 μm , respectively; easy to operate; easy sample preparation; provides detailed information about droplet size and homogeneity in a short time	The sample needs to be diluted, which may damage the sample structure; the instrument should be flushed frequently to ensure the accuracy of the results
	Electrical pulse counting	The measuring range is 0.4 and 1200 μm ; easy to operate; rapid and accurate; volume distribution and particle count are available	The samples should be diluted before analyzing; pores are easily clogged
	Ultrasonic spectrometry	The measuring range is 10 nm to 1000 μm ; samples with high concentration (>50%) can be measured; suitable for measuring opaque emulsions; nondestructive	Not suitable for sample with concentration less than 1%; tedious operating procedure
Surface charge	Microelectrophoresis	Easy to operate; easy sample preparation; provides detailed information about the surface charge of particle	The sample needs to be diluted; the instrument should be flushed frequently to ensure the accuracy of the results.
	Electroacoustic spectroscopy	Samples with high concentration (>50%) can be measured; nondestructive	Not suitable for sample with concentration less than 1%

(Continues)

TABLE 2 (Continued)

	Techniques	Advantages	Disadvantages
Rheological properties	Rheometer	A wider dynamic range of control and measurement parameters are available; detailed information about flow, deformation, and the tackiness is available.	Tedious operating procedure; equipment cleaning is complicated; device is large and less portable.
	Viscometer	Simple and rapid; small and portable; accurate viscosity for a wide variety of fluids available	Speed and torque capabilities are limited; difficult to clean the capillary tube

of micron-scale emulsions. However, the main components of emulsion droplets captured by optical microscopy (the location of the O/W phase) are often difficult to detect when using bright light fields since they have similar refractive indices or colors (McClements, 2007). The good news is that various methods using chemical stains have been established to enhance the contrast between different components, resulting in improving the overall image quality and providing spatial information about component locations (Malvey et al., 2020). Emulsion components can be prestained using various types of chemical stains that bind to specific components of the emulsion (such as proteins, polysaccharides, or lipids). After homogenizing, different colors are distributed in the oil phase or water phase, which therefore can be observed by using a conventional optical or fluorescent microscope because some chemical dyes are fluorescent. As an example, the photographs of CAS-based emulsion obtained for optical microscopy (Xu et al., 2020) and fluorescent microscopy (Li & Xiang, 2019) are presented in Figure 5b,c. Very clear droplet distribution can be observed as the oil droplets were stained with Nile red fluorescent dye. Confocal laser scanning microscopy (CLSM) is another important innovation in microscopy for studying the interfacial structure of emulsions. The device focuses a very narrow laser beam on a specific point on the sample being analyzed, and the resulting laser signal is then sent through an adjustable pinhole before reaching the detector to prevent defocusing. This equipment allows to obtain cross-section images of emulsions with basic morphology, structure, and interface information (Kwok & Ngai, 2016). Álvarez Cerimedo et al. (2010) used CLSM to observe CAS-stabilized emulsions as shown Figure 5d. Their results showed that the droplet distribution profiles of confocal images obtained after 24 h were consistent with the emulsion stability data obtained from Turbiscan^{LAB} stability analyzer (a technique that is able to quickly and sensitively identify instability mechanisms of emulsions, such as creaming, sedimentation, flocculation, coalescence, etc. [Jiang & Charcosset, 2022]).

However, from the perspective of magnification factor (as low as about 1 μm), the image obtained from the opti-

cal microscope cannot provide clear information about the structural characteristics of the emulsion (such as particle aggregation, interfacial layer thickness, etc.) (Low et al., 2020). Electron microscopy is an alternative to optical one and uses electron beams with much smaller wavelengths than light to help visualize material structures that are much smaller than visible light. Two types of electron microscopes, SEM and TEM, are used to study the structure and physicochemical properties of nanoparticles, nanoemulsions, or Pickering emulsions. SEM allows observing the surface morphology of a sample by measuring the secondary electrons produced when the sample is bombarded with an electron beam (McClements, 2015). Typically, SEM sample preparation requires stringent conditions (fixation and dehydration) because electrons are easily scattered by atoms or molecules in the gas. Unfortunately, the sample preparation procedures are generally not applicable to emulsions, as dehydration of emulsions usually results in droplet rupture and oil leakage. The recent development of Cryo-SEM enables us to visualize the microstructure of an emulsion in a frozen state. High-pressure freezing could help inhibit ice crystal formation and preserve emulsion integrity. Xu et al. (2021) observed the complete structure of CAS-coated nanoemulsions by cryo-SEM (Figure 5e), through rapid emulsion freezing in a liquid nitrogen environment. The morphology, particle size, and thickness of solid particles on the surface of the emulsion can be clearly calculated by the corresponding software. TEM has also been widely used to characterize the structure and morphology of CAS emulsions. For TEM, the electron beam can pass directly through the sample to be analyzed, where the electron beam transmitted to the sample is amplified and captured as an image, as shown in Figure 5f (Zhang et al., 2020). It should be noted that the droplet distribution of emulsion samples can be visualized by TEM without additional sample preparation steps. However, in some cases, the difference between the dispersed and continuous phases of emulsion in the resulting image remains unclear. This problem can be solved by the staining of emulsion (Zhai et al., 2018).

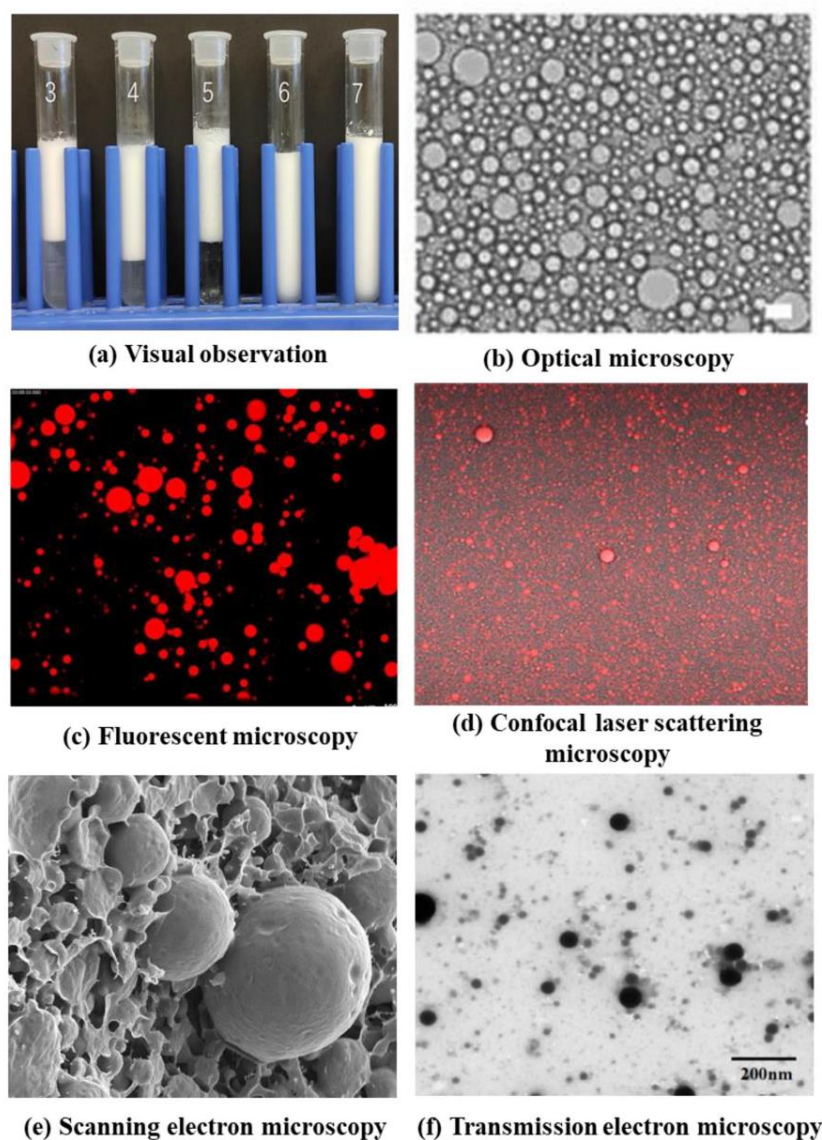


FIGURE 5 (a) Appearance of CAS-stabilized nanoemulsions at different pH (3–7). (b) Optical image of a tea seed oil emulsions stabilized by CAS (Xu et al., 2020). (c) Fluorescent microscopy of a coconut O/W emulsion stabilized by CAS (Li & Xiang, 2019). (d) Confocal laser scattering microscopy of a fish oil emulsion stabilized by 0.5 wt.% CAS (Álvarez Cerimedo et al., 2010). (e) Scanning electron microscopy of a soybean oil emulsion stabilized by CAS (Xu et al., 2021) and (f) transmission electron microscopy of a CAS-stabilized nanoparticles (Zhang et al., 2020)

5.3 | Particle size analysis

Under certain storage conditions, the stability of the original emulsion can be studied by measuring the droplet size of the sample. Meanwhile, by monitoring changes in PSD of the emulsion system, the incidence of flocculation between droplet interactions can be determined. As described by Stokes's Law, the stability of an emulsion

increases with the decrease of droplet size:

$$V_{\text{Stokes}} = -2gr^2(\rho_2 - \rho_1) / 9\eta,$$

where V_{Stokes} is separation rate, r is the radius of the particles, g is the action of gravity acceleration, ρ_1 and ρ_2 are the density of the two phases, and η is the shear viscosity of the target system. According to the droplet size,

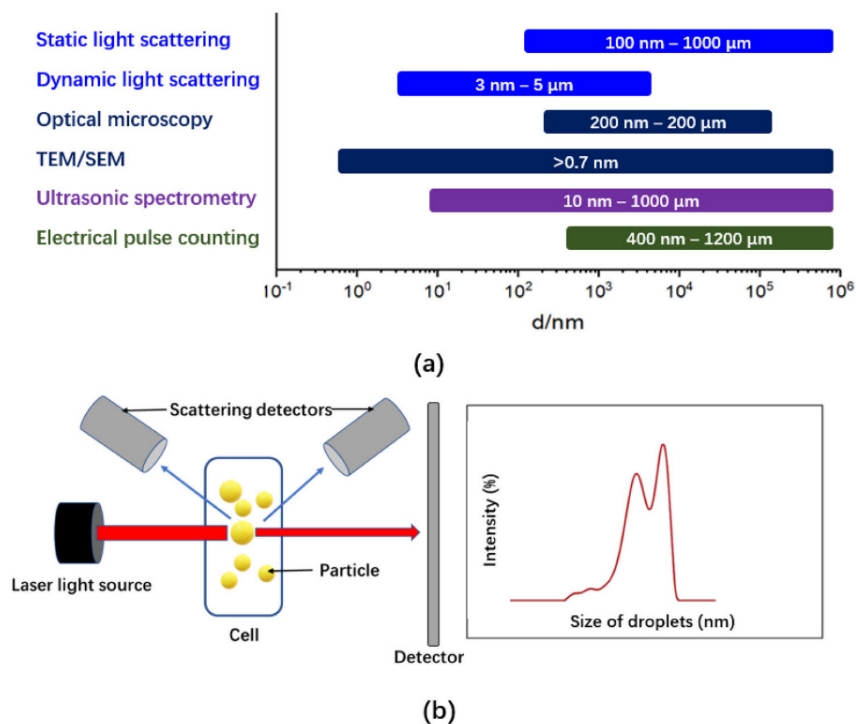


FIGURE 6 (a) The measuring range of common droplet size analysis techniques and (b) schematic diagram of particle size distribution detected by light scattering

the emulsion was further divided into three types, namely, conventional emulsion ($d > 200$ nm), nanoemulsion ($d < 200$ nm), and microemulsion ($d < 100$ nm). As stated by Piorkowski and McClements (2014), microemulsions are usually a combination of specific components (high levels of synthetic surfactants) through simple mixing and they are considered to be thermodynamically stable systems, therefore they usually have good long-term stability. Both conventional emulsions and nanometer emulsions are thermodynamically unstable systems and are consequently decomposed during storage by various instability mechanisms. In addition to microscopy techniques, a variety of commercially available analytical instruments have been developed to provide more information about the size and droplet distribution of emulsions, such as light scattering (static or dynamic light scattering), electrical pulse counting, and ultrasonic spectrometry, which are commonly used (McClements, 2015). Figure 6a summarizes the measurement ranges of several commonly used particle size analysis techniques (Zhang et al., 2021). These particle size analysis techniques are suitable for emulsion with different droplet sizes and concentrations and have the following advantages: easy to use, fully automatic, and large amount of information about droplet size provided in a short time. Even so, since different instruments oper-

ate on different physical principles, they must be chosen carefully.

Light scattering (also called laser diffraction) particle sizing instrument is a well-established technique to investigate properties of particles in solutions, as shown in Figure 6b. The basic principle is that the laser beam is irradiated on the sample, and the scattered intensity is detected by the detector at a certain angle θ (Blott et al., 2004). The evaluation of fluctuation is often referred to “dynamic light scattering (DLS),” and the analysis of absolute mean intensity is known as “static light scattering (SLS).” DLS-based devices usually operate with a specific scattering angle (fixed or variable), and then convert the flocculation strength math to PSD, which is used to detect smaller particles between 3 nm and 5 μ m (Zhang et al., 2021). SLS is assessed by measuring the angle change of scattering light intensity when laser passes through emulsion medium. The droplet size of emulsions directly affects the diffraction angle, and the emulsion with larger particle size will lead to a lower diffraction angle, and vice versa (Blott et al., 2004). Meanwhile, the laser diffraction systems generally use the precise input particle characteristics (such as refractive index, shape, and size) to determine the particle size between 100 nm to 1000 μ m (Zhang et al., 2021). Our previous studies have successfully used DSL and

laser diffraction to detect the average droplet size of CAS-based nanoemulsions and conventional emulsions (Liao et al., 2021). Multiple scattering is a common problem in light scattering measurements that leads to overestimation of particle size. This problem can generally be solved by diluting before the measurement process.

The electrical pulse counting (i.e., electro-zone sensing) technique is based on measurements of the change of electrical conductivity as the diluted emulsion passes through a small orifice (Church et al., 2019). Since oil has a lower conductivity than water, the current decreases with each drop of emulsion passing through the pores. The emulsion droplet size can be calculated since larger particles move more slowly and it will generate larger electrical pulses. The droplet concentration and PSD are determined by calculating the collected information from these electrical pulses. Commercial pulse counting techniques are currently available for measuring particles with diameters ranging from 0.4 to 1200 μm . However, this measurement is limited by the size of the holes in the glass tube and may require constant modification in the device to accommodate the measurement range. Brakstad et al. (2018) measured 2.0–60 and 5.6–100 μm oil droplets by 100 and 280 μm aperture, respectively. A recent study (Fang & Nakagawa, 2020) applied tunable resistive pulse sensing with micropores (2–10 μm) to analyze the particle size of CAS suspensions. Notably, electrical pulse counting instruments are usually only suitable for relatively low droplet concentrations (<0.1 wt.%) so that only one particle passes through the hole each time. Consequently, this method is particularly appropriate for particle size analysis, but is not fit for studying flocculation in the system, because dilution will destroy the aggregated particles and lead to misunderstanding of sample stability (Church et al., 2019).

Ultrasonic spectroscopy is another technique that relies on measuring ultrasonic attenuation and/or changes in ultrasonic velocity as a function of frequency. The attenuation level of ultrasonic velocity frequency is related to concentration and PSD in emulsion samples. Unlike other techniques, it is usually not necessary to dilute the emulsion before measurement as electroacoustic spectroscopy can be applied to high concentrated emulsions ($\leq 50\%$). Nevertheless, the strength of the received signal is related to the density ratio between the particle and the surrounding liquid; therefore, the application of electroacoustic measurements in some systems should be limited. The droplet size of CAS-based emulsions by DLS and ultrasonic attenuation has been compared (Gülseren & Corredig, 2011). The results indicated the mean diameter from DLS was larger than that measured by ultrasonics. This difference is attributed to the differences in the size dependence of the ultrasonic and light scattering signals.

5.4 | Charge analysis

The strength and sign of the surface charge on the dispersed droplets are derived from the ionization properties of the absorbing CAS; therefore, the surface charge is another important factor for detecting emulsion stability (McClements, 2015). The droplet charge of emulsion is subject to a variety of environmental factors including pH, ionic strength, and chemical reactions, which may ultimately lead to changes in surface charge and stability throughout the emulsion system. Electrostatic repulsions occur between droplets with the same surface charge symbol, which prevents particle flocculation and inhibits the propagation of most emulsion instable paths. On the contrary, electrostatic attractions occur when particles with opposite charges come into contact, depending on the degree of attraction, and may cause droplet instability (McClements, 2015). It should be noted that when the attraction is weak, the droplets tend to gather close to one another but do not physically coalesce into larger particles, while when the attraction is greater, the droplets coalesce, resulting in larger droplets at the expense of smaller ones. As we described above, the charge characteristic of CAS is really sensitive to the pH and the presence of ions as well as other charged species in the aqueous phase. Zeta potential (ζ) is the potential at the “shear plane” that is a good reflection of the electrical properties of emulsion droplets because it stems from the fact that ions tend to adsorb onto the droplets (McClements, 2007). In our previous study, measuring the ζ -potential of the CAS-coated droplets can reflect the stability of the emulsion to a certain extent (Liao et al., 2021).

A variety of analytical instruments have been used to measure the ζ -potential on emulsion droplets and the most widely used analytical systems include microelectrophoresis and electroacoustic spectroscopy. Microelectrophoresis measures the electrochemical properties of the surface of a charged drop based on the velocity and direction at which it moves in the emulsion when an electric field is applied. In the development of recent technologies, the combination of microelectrophoresis and DLS was used to measure electrophoretic mobility, from which zeta potential can then be calculated. The emulsion sample is placed in the measuring cell and an electric field is applied to it through a pair of electrodes. Any charged particles in the emulsion will then move toward the opposite charge at different speeds, depending on their charge. Thus, the symbol and magnitude of the charges on the particles can be collected and then converted into particle potentials by fitting software. Similarly, samples analyzed by light scattering techniques should be diluted to a lower concentration to avoid multiple scattering effects. Moreover,

special care should be taken when diluting samples, as the electrical properties are sensitive to changes in the surrounding water environment (Li et al., 2017).

Electroacoustic spectroscopy can also be used to determine the ζ -potential of the emulsion (Gülseren & Corredig, 2011). Unlike other techniques, it is usually not necessary to dilute the emulsion before measurement because electroacoustic spectroscopy can be applied to high concentrated emulsions ($\leq 50\%$). The measurements using electroacoustic spectroscopy can be designed in two operating modes: Electro-Sonic Amplitude (ESA) and Colloid Vibration Potential (CVP). For both modes, the measurements use an electrical or acoustic signal applied to the emulsion and record the acoustic or electrical signal produced by the oscillating particles, which are then converted to zeta potential by software fitting. Nevertheless, the strength of the received signal is related to the density ratio between the particle and the surrounding liquid; therefore, the application of electroacoustic measurements in some systems should be limited.

5.5 | Rheological properties

The rheological properties of emulsions strongly influence the processing behavior and shelf life stability of liquid foods, as well as their appearance, texture, taste, and flavor release. As reported by Tadros (1994), the rheological properties of emulsions are related to pH, electrolyte concentration in the continuous phase, shape, size distribution, internal viscosity and concentration of oil droplets, as well as their ability to participate in various interactions with other components. Therefore, studying the rheological properties of CAS emulsions can provide more information for studying their instability mechanisms.

Currently, the most commonly used instruments for characterizing the rheological properties of food emulsions are rheometer and viscometer. The viscometer is a very convenient system to obtain viscosity information by applying a fixed rate of shear force in a short period, but the information obtained is limited and cannot be used to deeply study the instability mechanism and rheological properties of emulsions. According to Stokes Law, as viscosity increases, O/W emulsions are generally more resistant to instability caused by particle flocculation. The rheometer is another device designed to apply shear deformation forces to study liquids, solids, or other viscoelastic samples that are the most widely used instruments for measuring the rheological properties of fluids (Tavares et al., 2022). It can provide detailed information on viscosity, yield stress, elastic modulus, and fracture behavior of emulsion systems by controlled-stress and controlled-strain modes. A typical method for measur-

ing rheological properties of emulsions is to measure the system's resistance to applied stresses, such as rotary or oscillating stresses, where stress can cause emulsion system deformation (Tavares et al., 2022). Briefly, the greater the deformation resistance, the higher the viscosity of the system, and the linearity of the deformation depends on the interactions between its components. Sosa-Herrera et al. (2008) studied the relationship between rheological properties of CAS-stabilized emulsions (30 wt.% sunflower oil) and the physicochemical characteristics of the water phase. They found that the addition of gellan gum into emulsion can help to prevent both flocculation and creaming, as the rheological behavior strongly increased. This is the fact that the polysaccharides act as filler particles between the oil droplets and the casein aggregates. A recent study also reported that the presence of polysaccharides (inulin and konjac glucomannan) has the potential to modulate the stability and rheological properties of CAS-based emulsions (Xu et al., 2020).

6 | STRATEGIES TO IMPROVE THE STABILITY OF CAS-STABILIZED EMULSIONS

CAS-stabilized emulsions are considered excellent systems for providing protection and transportation of nutrients in the food industry, but instability under certain conditions still limits their further applications. For example, at pH values close to their pI, the charge of casein proteins adsorbed at the O/W interface is gradually lost, and the thickness of the adsorbed layer becomes thinner as the "loops" and "tails" change, resulting in droplet instability. Based on the characteristics of CAS stable emulsions, this protein can be used in combination with other emulsifiers to deal with these unstable conditions, ensuring effective control of the emulsion, thereby reliably producing products with a consistent appearance, uniform consistency, and satisfactory shelf life. In this section, the main methods that can be used to improve CAS-stabilized emulsion properties will be discussed and some recent cases are summarized in Table 3.

6.1 | Optimizing emulsion formulation

First, optimizing the process of producing the emulsification is one of the most and safest ways to improve emulsion stability. During this process, several factors such as protein concentration, homogenization conditions, protein solubilization, ionic strength, and pH conditions can be optimized at the laboratory level to achieve better emulsion stability. At the same time, optimization of the formulation, selection of the right type of emulsifying equipment,

TABLE 3 Summary of recent progress in improving the stability of sodium caseinate-stabilized emulsions

Methods	Biopolymer addition	Core material	Results	References
Optimizing emulsion formulation	\	Sunflower and olive oils	Pressure (200–300 MPa) and 5 g/100 g CAS increased emulsion stability; the droplet size of CAS-based emulsions has an effect on the oxidation rate.	Hebshy et al., 2017
	\	Sunflower, camelina, and fish oil	Lipid hydroperoxide and p-Anisidine values of emulsions generally decreased as CAS concentration increased.	O' Dwyer et al., 2013
	\	Sunflower oil	When ethanol was added after processing emulsions, CAS-based emulsions suffered from a slower destabilization.	Erxleben et al., 2021
	\	Cinnamaldehyde, MCT oil, and sunflower oil	Mixing medium or long-chain carrier oil before homogenization can significantly inhibit Ostwald ripening of CAS-based emulsions containing essential oils.	Liao et al., 2021
	\	Soybean oil	Ultrasound treatment improved oxidative stability of CAS-based emulsions containing high level of soybean oil and enhanced the concentration of adsorbed CAS.	Li et al., 2020
	\	Canola oil	Depletion interaction energy calculation showed that droplet size reduction makes nanoemulsions more resistant to flocculation than conventional emulsions.	Yerramilli & Ghosh, 2017
Mixed emulsifiers	Soy protein isolate	MCT oil	Mixed proteins contributed to good stability of the encapsulated liposoluble nutrient.	Ji et al., 2015
	Pea protein	Canola oil	Mixed protein-based nanoemulsions were more stable than the individual ones and SDS-PAGE confirmed the presence of both proteins at the O/W interface.	Yerramilli et al., 2017
	Whey protein	Canola oil	Mixed protein-based emulsions had better oxidative stability to protect volatile compounds.	Loi et al., 2019
	Sucrose stearate	Thymol	Interactions between the emulsifiers enhanced the exposure of tryptophan and tyrosine residues, favoring binding to thymol during heating.	Su & Zhong, 2016
	Tween 20	Rice bran oil	Mixed emulsifier systems offered a suited solution to absorption because they allow the intake of a high amount of curcumin together with a low fat content.	Cuomo et al., 2019
	Tween 20	Rice bran oil	The presence of Tween 20 ensured the steric stabilization promoting the use of CAS as an emulsion stabilizer at acid pH.	Perugini et al., 2018
	Phosphatidylcholine (PC)	Fish oil	The partial substitution of CAS by PC increased the oxidative stability of the emulsions while maintaining their physical stability.	Yesiltas et al., 2019
	Soy lecithin	MCT	Blends of CAS and lecithin produced O/W emulsions with similar appearance, color, particle size, and electrical properties as those stabilizers used alone.	Chung et al., 2019
Soy lecithin	Coconut oil	The addition of amphiphilic lecithin could help decrease the droplet size of emulsion and increase the solubility of microcapsules.	Wu et al., 2022	

(Continues)

TABLE 3 (Continued)

Methods	Biopolymer addition	Core material	Results	References
Complexation	Konjac glucomannan	Canola oil	The increase in the concentration of konjac glucomannan is beneficial to strengthen the emulsion gel network and prevent creaming of the emulsion.	Martínez-Padilla et al., 2021
	Low methoxyl pectin (LMP)	Sunflower oil	At low LMP concentrations, CAS/LMP complexes-stabilized emulsions were more stable than layer-by-layer (LBL)-stabilized emulsions, while at high LMP concentrations, LBL-stabilized emulsions exhibited better stability.	Wang et al., 2018
	Lactoferrin	Sunflower oil	The formation of heteroaggregates by mixing two emulsions stabilized by proteins with opposite charges, varying the emulsion volume ratio and ionic strength, allowed producing systems with distinct properties.	de Figu et al., 2016
	Four different polysaccharides	Fish oil	Multilayer emulsion with targeted functions was formulated using polysaccharides; especially, κ -carrageenan could reach the demand of rapid digestion.	Shi et al., 2023
	Sulfated fucan	Fish oil	The sulfated fucans with higher molecular weights could significantly increase the initial digestibility rate of CAS-based emulsions.	Shi et al., 2021
	γ -Cyclodextrin and alginate	Corn oil	γ -CD/CAS/alginate-stabilized nanoemulsions exhibited nanoscale droplet diameter and high stability even under acid, alkali, and high-temperature conditions.	Wang et al., 2022
	Quillaja saponin	MCT oil	The emulsifying performance of the mixed binary emulsifier and the subsequent stability of the emulsion are highly dependent on the concentration ratio of the emulsifier.	Salminen et al., 2019
	Pectin and gum Arabic	α -Tocopherol and resveratrol	Both polysaccharides enhance the accumulation and stability of resveratrol at the oil-water interface.	Cheng et al., 2020
	Trehalose	Fish oil, sunflower oil, or olive oil	The addition of trehalose diminished the volume-weighted mean diameter and the protein-sugar interactions played a key role in creaming and flocculation processes.	Álvarez Cerimedo et al., 2010
	Carboxymethyl cellulose	Corn oil	The results indicated that the complex formed at O/W interfaces can protect the oil droplets against flocculation and coalescence upon acidification.	Liu et al., 2012
	Dextran sulfate (DS)	n-Tetradecane	CAS-based emulsions containing 1 wt.% DS exhibited good shelf life stability on quiescent storage for 3 weeks, especially when the emulsion was prepared at low pH.	Jourdain et al., 2008
	Inulin and konjac glucomannan	Tea seed oil	Above the critical inulin/KGM ratio of 2:0.1, the droplet size of CAS-based emulsions was significantly decreased, and the creaming stability was greatly enhanced.	Xu et al., 2020
	Gellan gum	Sunflower oil	CAS-based emulsions containing gellan gum were stable against both flocculation and creaming.	Sosa-Herrera et al., 2008

(Continues)

TABLE 3 (Continued)

Methods	Biopolymer addition	Core material	Results	References
	Succinylated alginate	Fish oil	The modified alginate increased the stability of the emulsion, and the emulsion had a lower creaming index.	Yesiltas et al., 2018
Conjugation	Propylene glycol alginate (PGA)	Soybean oil	PGA and CAS undergo transacylation during pH changes. This reaction imparts a gel-like structure to the emulsions and improves thermal stability of emulsions.	Sun & Zhong, 2022
	Maltodextrin	Palm-based triacylglycerol	Glycation has the ability to reduce moisture and surface oil content and produce larger particle size of spray-dried powders.	Lee et al., 2015
	Dextran	Fish oil	Glycoconjugates of CAS and dextrans were explored and glycoconjugates of CD70 displayed the best emulsifying antioxidant activity and emulsion stability with improved activity.	Liu et al., 2018
	Locust bean gum (LBG)	Soybean oil	Emulsions prepared by CAS-LBG biopolymers presented high stability and reduced particle size at pH 3.5 and 7, which could be regarded as promising alternative to emulsifying agents in neutral or acidified products.	Barbosa et al., 2019
	Sodium alginate	Corn oil	The conjugates produced stable emulsions with low surfactant to oil ratios, and the content of CAS played a major role in determining droplet size.	Li & Zhong, 2022
	Corn starch hydrolysates	Palm oil	Protein-polysaccharide conjugates have lower interfacial tension, and the conjugates formed by heating improve their ability to stabilize emulsions.	Consoli et al., 2018
	Pectin	Conjugated linoleic acid	The aggregation and creaming stability of the emulsions formulated by conjugates increased as the pectin-to-caseinate ratio increased.	Cheng & McClements, 2016
	Maltodextrin	MCT oil	CAS and maltodextrin conjugates-stabilized $W_1/O/W_2$ double emulsions had improved general stability when compared to CAS-stabilized $W_1/O/W_2$ double emulsions.	O'Regan & Mulvihill, 2010
	Bitter almond gum	Fish oils	The conjugate-based emulsions showed similar physical stability to CAS-stabilized emulsions, and lower antioxidant capacity.	Rahimi et al., 2021
	Lactose	Canola oil	Better CAS-lactose interactions were achieved at pH 11, with enhanced adsorption of the conjugates at the oil droplet particles and stability.	Li et al., 2017
	Soybean soluble polysaccharides	Sunflower oil	Conjugated-based emulsions exhibited a decreasing trend in droplet size and emulsification index and have better performance at low pH and higher heat conditions.	Tavasoli et al., 2022
	Maltodextrins and pectin	Eugenol-olive mixed oil	Higher stability of nanoemulsions was obtained by Maillard conjugate compared to protein or polysaccharides alone.	Nagaraju et al., 2021

addition of antioxidants, and optimization of packaging and storage conditions will also contribute to the stability of emulsions and prolong the shelf life of food products.

Hebisy et al. (2017) studied the effects of protein concentration and pressure on the stability of CAS stable emulsions and demonstrated that high-pressure treatment with sufficient CAS content can produce nanoscale emulsions with unimodal peaks and high physical properties. Compared with emulsions produced by conventional homogenization, oxidation stability of emulsion produced by high-pressure homogenization was improved. In another study by O' Dwyer et al. (2013), the effects of CAS concentration on the emulsion stability of O/W emulsions were examined. The authors reported that lipid hydroperoxide and p-Anisidine values of emulsions generally decreased as CAS concentration increased. Erxleben et al. (2021) investigated the effect of ethanol on the stability of CAS-stabilized emulsions and they observed a slower destabilization mechanism for these emulsions when ethanol was added after the processing step.

6.2 | Noncovalent bond

Compared to emulsions prepared with CAS as the sole emulsifying agent, emulsions prepared from mixed emulsifiers (Cuomo et al., 2019; McClements & Jafari, 2018) and protein-polysaccharide complexes (Cheng et al., 2020; Cheng & McClements, 2016) have been reported with increased resistance to environmental stresses such as pH, ionic strength, and temperature. This is because CAS can noncovalently bond with other biopolymers on the droplet surface, via electrostatic interactions, hydrophobic bonds, hydrogen bonds, and van der Waals interactions, among which electrostatic interactions are widely used.

A recent review (McClements & Jafari, 2018) detailed the many advantages of using mixed emulsifiers in improving emulsion formation, stability, and performance. Generally, proteins, small molecule surfactants, and phospholipids are the most used emulsifiers in food applications. Ji et al. (2015) used CAS and soy protein isolate (SPI) as natural emulsifiers to successfully develop an enteral nutrition system with enhanced stability. The results showed that the flexible protein CAS and the rigid globular protein SPI were adsorbed on the O/W interface. Another study (Yerramilli et al., 2017) also showed that by using CAS and pea protein, the mixed protein-based nanoemulsion was more stable than individual ones. They confirmed the presence of both pea protein and casein at the interface by SDS-PAGE. Perugini et al. (2018) used a nonionic surfactant (Tween 20) in combination with CAS as blending emulsifiers to prepare nanoemulsions and their results showed that the addition of Tween 20 effectively enhanced

the stability of the CAS-based emulsion under acidic conditions. Another study (Cuomo et al., 2019) also used a blend of CAS and Tween 20 to prepare O/W nanoemulsions. The results showed that, after an *in vitro* simulated digestion process, the mixed emulsifier system provided higher amounts of lipophilic compounds and lower fat intake compared to the CAS-stabilized nanoemulsion. In addition to proteins and small molecule surfactants, soy lecithin (Chung et al., 2019; Wu et al., 2022; Xue et al., 2015) is also used as a co-emulsifier with CAS in preparing food emulsions. Xue et al. (2015) reported that the combination of CAS and soy lecithin facilitates the formation of transparent and stable thyme oil nanoemulsions when compared with treatments applying the two emulsifiers individually. Nonetheless, there may be adsorption competition between the different emulsifier components, which may adversely affect emulsion formation and stability (McClements & Jafari, 2018).

Unlike other emulsifiers, polysaccharides are generally not used as the only emulsifiers in food emulsions because typical hydrophilic polysaccharide molecules are nearly surface inactive unless they contain protein moieties responsible for their emulsifying ability, such as gum Arabic (Ishii et al., 2018). However, polysaccharides are widely used as stabilizers in emulsion preparation, usually in combination with proteins, which can effectively improve the viscosity, texture, and appearance of food products as well as for introducing some nutritional components. As Ghosh and Bandyopadhyay (2012) described, the relative thickness of the liquid films between two approaching droplets lies in the order of hydrocolloids (5–10 nm) > proteins (1–5 nm) > surfactants (0.5–1 nm). Thus, the stability is expected to be higher when the emulsion is stabilized by protein-polysaccharide complexes or conjugates compared to the same systems stabilized by protein or surfactants alone. Effective binding of CAS and polysaccharides can be achieved by utilizing electrostatic attractions (noncovalent binding) through complexation at acidic pH (Artiga-Artigas et al., 2020; Xu et al., 2020) or by covalently binding polysaccharides (Consoli et al., 2018; Sato et al., 2015).

The prerequisite for the formation of electrostatic complexes is naturally the presence of opposite charges on the different polymers. Our previous study (Wang et al., 2019) has investigated the formation of CAS and low methoxyl pectin (LMP) complexes at different pH values (Figure 7). The charge density of CAS is strongly dependent on the suspension pH, which can induce the formation of complexes with LMP through strong electrical interactions at pH 3. The complexes formed by CAS and anionic polysaccharides could be used to prepare emulsions containing oil-soluble active molecules. The effect of complexation on CAS emulsion has been reported in many literatures by

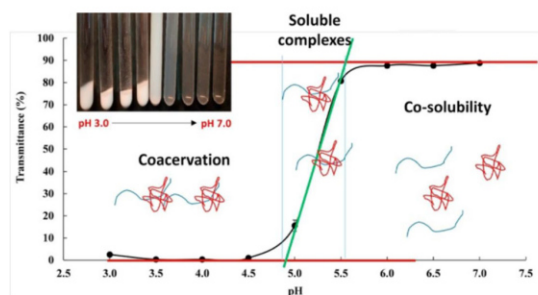


FIGURE 7 Transmittance (%) at 850 nm and photographs of CAS and pectin suspensions at different pHs (3.0–7.0) with ratio 2.5 (Wang et al., 2019)

either one- or two-step complex coacervation techniques. As shown in Figure 8a, the one-step method uses a mixture of two biopolymers to form a complex coacervate before preparing the emulsion, while the two-step method (Figure 8b) uses only CAS to form the emulsion and then adds the polysaccharide as a second layer. Yesiltas et al. (2018) used CAS and commercial sodium alginate as combined emulsifiers to prepare fish O/W emulsions. Their results indicated that mixed emulsifiers performed better in terms of physical stability compared to emulsions produced with only CAS. Cheng et al. (2020) also used the one-step method to prepare emulsions with CAS/pectin or gum Arabic. Both polysaccharides exhibited the ability to enhance the accumulation and stability of resveratrol at the O/W interface, while also increasing the absolute value of the droplet zeta potential. However, one-step methods tend to promote droplet flocculation or coalescence in the process, and aggregation is generally irreversible (Burgos-Díaz et al., 2016). Liu et al. (2012) prepared multilayer emulsions using carboxymethyl cellulose (CMC) and CAS by the two-step method that can result in more uniform droplets. First, CAS emulsion containing CMC in an aqueous phase was prepared under neutral pH, in which two biopolymers were negatively charged, and then the pH was adjusted to acidic values. A complex interface layer can be formed at a pH around the pI of proteins, consisting of a first layer generated by the direct adsorption of CAS molecules on the exposed interfaces, and a second layer composed of CMC molecules interacting with CAS molecules through attractive electrostatic interactions. Emulsions containing drops prepared by CAS/CMC exhibited fairly stability since polysaccharide outer layers increase the net surface charge and create steric hindrance (Liu et al., 2012). A recent study compared the effect of different anionic polysaccharides on the stability of CAS-based emulsion by the two-step method (Shi et al., 2023). All four polysaccharides tested in this study were able to adsorb to the surface of CAS-based lipids when the pH

of the mixture was reduced from neutral to 5, 4, and 3, and enhanced the performance of the multilayer emulsion. In particular, multilayer emulsions prepared from κ -carrageenan were shown to accelerate the digestion in the gastrointestinal tract.

Furthermore, it was also reported that the presence of free polysaccharides can improve the salt stability of protein-stabilized emulsion even without interactions with proteins (Qiu et al., 2015). This result was attributed to the fact that the unadsorbed xanthan gum increased the viscosity of the emulsion and formed a thickening network around the protein, which reduces the particle movement rate and thus improves the emulsion stability. However, improving the stability of CAS-stabilized emulsions by electrostatic complexing (sequential adsorption or mixed emulsification) still suffers from a major disadvantage: improvements may be limited to narrow pH or ionic strength ranges.

6.3 | Covalent bond (conjugation)

The chemical modification of proteins, such as acetylation, deamidation, succinylation, and glycation, is another considering modification method to improve physicochemical and functional properties of protein-stabilized emulsions. In food industries, the most common protein-polysaccharide conjugation method is the Maillard reaction, which is a series of nonenzymatic browning reactions that occur naturally between reducing sugars and amino acids (Evans et al., 2013). Unlike other protein modification methods, Maillard reaction is usually triggered by temperature elevation without other chemical reagents. In recent years, protein-polysaccharide conjugates as emulsifiers provided more diverse possibilities for the improvement of emulsifying, stabilizing, solubility, and thermal stability as well as better stability against pH variations. Casein and CAS have been reported to bound to a variety of galactose, lactose, and dextran under controlled conditions and these glycoconjugates showed improved emulsifying properties compared to natural CAS (Barbosa et al., 2019; Consoli et al., 2018; Liu et al., 2018). In fact, the open and hydrated random structure in caseins makes them more likely than globular proteins to benefit from glycosylation via the Maillard reaction (Consoli et al., 2018). Furthermore, as mentioned above, CAS has higher stability to temperature, which is required for glycosylation. A recent study formulated the Maillard conjugates biopolymers by CAS–locust bean gum (Barbosa et al., 2019). These conjugates appeared to be a promising alternative emulsifier to address the application deficiencies of CAS in acidic situations. Furthermore, the emulsions prepared from the conjugates showed a reduction in droplet

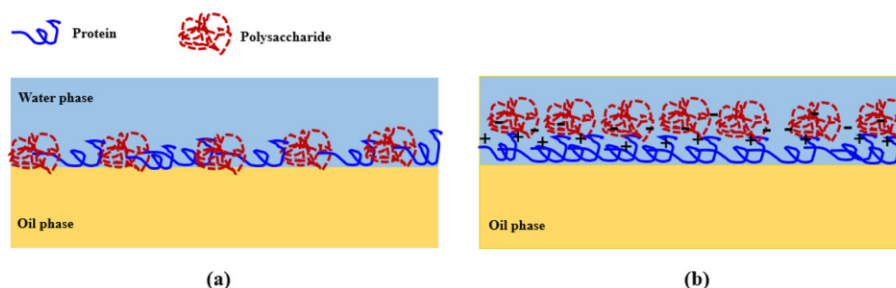


FIGURE 8 Schematic representation of two different methods for formulating oil–water emulsions with protein–polysaccharide complexes as emulsifiers. (a) Mixed protein and polysaccharide before emulsification. (b) Double layer emulsion, polysaccharide added to the emulsion, stabilized with protein first

size, which can be attributed to the formation of conjugates that promote steric repulsion between droplets and avoid attractive droplet interactions. Similar explanations were also reported by the study of CAS–sugar beet pectin conjugates (Juyang & Wolf, 2021). Improved antioxidant stability and creaming stability of emulsions have been also reported when CAS Maillard reaction products were applied as emulsifiers (Consoli et al., 2018; Lee et al., 2015). Li et al. (2017) investigated the effect of pH variation on the emulsion stability of CAS–lactose conjugates formed via the Maillard reaction for better oil encapsulation in spray-dried powder. They found that conjugates formulated at pH 11 exhibited better emulsifying properties and stability and enhanced conjugate adsorption on oil droplets. This improvement was due to the change of the hydrophilic/hydrophobic balance of emulsion systems and the resulting strong steric repulsions allowing slow droplet flocculation. Finally, although Maillard reaction products can demonstrate these improved physicochemical properties of emulsions, rigorous safety testing should be performed before using these products as ingredients, as Maillard reaction might produce advanced glycation end-products, causing side effects in healthy individuals (Wei et al., 2018).

In addition, modifying the protein by breaking down its structure has been investigated as an alternative strategy to improve the emulsification properties, which can be done enzymatically (Sato et al., 2015) or by heating treatments (Liang, Gillies, et al., 2017), where controlled hydrolysis can increase the solubility, emulsification, and foaming properties of protein emulsifiers.

7 | CONCLUSIONS

CAS provides interesting emulsifying properties that allow it to meet current consumer demands for the stabilization of food emulsions, but instability under some specific con-

ditions limits its applications. Therefore, there is an urgent need to better understand the effects of different environmental and processing conditions on emulsion stability, and how to improve the stability of CAS-formed food emulsions. This review presented the structural properties of CAS and its emulsifying ability and summarized the recent applications of CAS for stabilizing food emulsions. From our results and others discussed in the literature, it is clear that the stability of emulsions is strongly affected by pH, protein concentration, ionic strength, heating process, and oxidation. The instability mechanisms occurred in CAS-stabilized emulsions can be recorded and tracked by some instruments and methods, such as microscopy observation, droplet size distribution, droplet charge, and rheological measurements. Those technologies have advantages and disadvantages and provide different insights into the destabilization mechanisms. According to the general factors that control the stability of CAS-stabilized emulsions, some general strategies for preventing instability are pointed out: using enough protein emulsifier to fully saturate the interface during emulsification; avoiding any large excess of nonadsorbed protein; working away from pH values around the protein's pI; keeping the ionic strength as low as possible; and using high-energy methods in order to reduce particle size. In addition to the above proposals, a reliable strategy for preventing instability in CAS-stabilized emulsions can be improved by binding proteins to other biopolymers, especially polysaccharides by using complexation or conjugation. In summary, this review can serve as a template for researchers to understand the fundamental properties of CAS-stabilized emulsions and study their stabilization methods.

AUTHOR CONTRIBUTIONS

Wei Liao: Conceptualization; Formal analysis; Resources; Writing – original draft. **Adem Gharsallaoui:** Conceptualization; Supervision; Validation; Writing – review & editing. **Emilie Dumas:** Supervision; Validation; Writing

– review & editing. **Abdelhamid Elaissari**: Supervision; Validation; Writing – review & editing.

ACKNOWLEDGMENT

Wei Liao greatly thanks Chinese Scholarship Council for support (No. 201807565014).

CONFLICT OF INTEREST

The authors declare no conflict of interest.

ORCID

Adem Gharsallaoui  <https://orcid.org/0000-0001-6000-1994>

Abdelhamid Elaissari  <https://orcid.org/0000-0002-2151-9894>

REFERENCES

- Álvarez Cerimedo, M. S., Iriart, C. H., Candal, R. J., & Herrera, M. L. (2010). Stability of emulsions formulated with high concentrations of sodium caseinate and trehalose. *Food Research International*, 43(5), 1482–1493. <https://doi.org/10.1016/j.foodres.2010.04.008>
- Amine, C., Dreher, J., Helgason, T., & Tadros, T. (2014). Investigation of emulsifying properties and emulsion stability of plant and milk proteins using interfacial tension and interfacial elasticity. *Food Hydrocolloids*, 39, 180–186.
- Artiga-Artigas, M., Reichert, C., Salvia-Trujillo, L., Zeeb, B., Martín-Belloso, O., & Weiss, J. (2020). Protein/Polysaccharide complexes to stabilize decane-in-water nanoemulsions. *Food Biophysics*, 15(3), 335–345.
- Barbosa, J. M., Ushikubo, F. Y., de Figueiredo Furtado, G., & Cunha, R. L. (2019). Oil in water emulsions stabilized by Maillard conjugates of sodium caseinate-locust bean gum. *Journal of Dispersion Science and Technology*, 40(5), 634–645.
- Bhat, M. Y., Dar, T. A., & Singh, L. R. (2016). Casein proteins: Structural and functional aspects. In I. Ghigi (Ed.), *Milk proteins—From structure to biological properties and health aspects* (pp. 1–17). IntechOpen.
- Blott, S. J., Croft, D. J., Pye, K., Saye, S. E., & Wilson, H. E. (2004). Particle size analysis by laser diffraction. *Geological Society, London, Special Publications*, 232(1), 63–73.
- Brakstad, O. G., Farooq, U., Ribicic, D., & Netzer, R. (2018). Dispersibility and biotransformation of oils with different properties in seawater. *Chemosphere*, 191, 44–53.
- Burgos-Díaz, C., Wandersleben, T., Marqués, A. M., & Rubilar, M. (2016). Multilayer emulsions stabilized by vegetable proteins and polysaccharides. *Current Opinion in Colloid & Interface Science*, 25, 51–57. <https://doi.org/10.1016/j.cocis.2016.06.014>
- Carpenter, J., & Saharan, V. K. (2017). Ultrasonic assisted formation and stability of mustard oil in water nanoemulsion: Effect of process parameters and their optimization. *Ultrasonics Sonochemistry*, 35, 422–430.
- Cerimedo, M. S. Á., Iriart, C. H., Candal, R. J., & Herrera, M. L. (2010). Stability of emulsions formulated with high concentrations of sodium caseinate and trehalose. *Food Research International*, 43(5), 1482–1493.
- Chen, W., Liang, G., Li, X., He, Z., Zeng, M., Gao, D., Qin, F., Goff, H. D., & Chen, J. (2019). Effects of soy proteins and hydrolysates on fat globule coalescence and meltdown properties of ice cream. *Food Hydrocolloids*, 94, 279–286.
- Chen, X.-W., Hu, Q.-H., Li, X.-X., & Ma, C.-G. (2022). Systematic comparison of structural and lipid oxidation in oil-in-water and water-in-oil biphasic emulsions: Effect of emulsion type, oil-phase composition, and oil fraction. *Journal of the Science of Food and Agriculture*, 102(10), 4200–4209.
- Cheng, H., Fan, Q., Liu, T., & Liang, L. (2020). Co-encapsulation of α -tocopherol and resveratrol in oil-in-water emulsion stabilized by sodium caseinate: Impact of polysaccharide on the stability and bioaccessibility. *Journal of Food Engineering*, 264, 109685.
- Cheng, W., & McClements, D. J. (2016). Biopolymer-stabilized conjugated linoleic acid (CLA) oil-in-water emulsions: Impact of electrostatic interactions on formation and stability of pectin-caseinate-coated lipid droplets. *Colloids and Surfaces A: Physicochemical and Engineering Aspects*, 511, 172–179.
- Chung, C., Koo, C. K. W., Sher, A., Fu, J.-T. R., Rousset, P., & McClements, D. J. (2019). Modulation of caseinate-stabilized model oil-in-water emulsions with soy lecithin. *Food Research International*, 122, 361–370. <https://doi.org/10.1016/j.foodres.2019.04.032>
- Church, J., Lundin, J. G., Diaz, D., Mercado, D., Willner, M. R., Lee, W. H., & Paynter, D. M. (2019). Identification and characterization of bilgewater emulsions. *Science of The Total Environment*, 691, 981–995. <https://doi.org/10.1016/j.scitotenv.2019.06.510>
- Consoh, L., Dias, R. A., Rabelo, R. S., Furtado, G. F., Sussulini, A., Cunha, R. L., & Hubinger, M. D. (2018). Sodium caseinate-corn starch hydrolysates conjugates obtained through the Maillard reaction as stabilizing agents in resveratrol-loaded emulsions. *Food Hydrocolloids*, 84, 458–472.
- Costa, C., Medronho, B., Filipe, A., Mira, I., Lindman, B., Edlund, H., & Norgren, M. (2019). Emulsion formation and stabilization by biomolecules: The leading role of cellulose. *Polymers*, 11(10), 1570.
- Csáki, K. F., & Sebestyén, É. (2019). Who will carry out the tests that would be necessary for proper safety evaluation of food emulsifiers? *Food Science and Human Wellness*, 8(2), 126–135.
- Cuomo, F., Perugini, L., Marconi, E., Messia, M. C., & Lopez, F. (2019). Enhanced curcumin bioavailability through nonionic surfactant/caseinate mixed nanoemulsions. *Journal of Food Science*, 84(9), 2584–2591.
- Dalgleish, D. G. (1990). The conformations of proteins on solid/water interfaces—Caseins and phosphovitin on polystyrene latices. *Colloids and Surfaces*, 46(2), 141–155.
- Dalgleish, D. G. (1996). Conformations and structures of milk proteins adsorbed to oil-water interfaces. *Food Research International*, 29(5–6), 541–547.
- Dammak, I., Sobral, P. J. A., Aquino, A., Neves, M. A. d., & Conte-Junior, C. A. (2020). Nanoemulsions: Using emulsifiers from natural sources replacing synthetic ones—A review. *Comprehensive Reviews in Food Science and Food Safety*, 19(5), 2721–2746.
- de Figueiredo Furtado, G., Michelson, M., de Oliveira, D. R. B., & da Cunha, R. L. (2016). Heteroaggregation of lipid droplets coated with sodium caseinate and lactoferrin. *Food Research International*, 89, 309–319. <https://doi.org/10.1016/j.foodres.2016.08.024>
- Dickinson, E. (1989). Surface and emulsifying properties of caseins. *Journal of Dairy Research*, 56(3), 471–477.
- Dickinson, E. (1994). Protein-stabilized emulsions. In P. Fito, A. Mulet, & B. MacKenna (Eds.), *Water in foods* (pp. 59–74). Elsevier.

- Dickinson, E. (1997). Aggregation processes, particle interactions, and colloidal structure. *Special Publication-Royal Society of Chemistry*, 192, 107–126.
- Dickinson, E. (1999). Caseins in emulsions: Interfacial properties and interactions. *International Dairy Journal*, 9(3–6), 305–312.
- Dickinson, E. (2010). Food emulsions and foams: Stabilization by particles. *Current Opinion in Colloid & Interface Science*, 15(1–2), 40–49.
- Dickinson, E. (2019). Strategies to control and inhibit the flocculation of protein-stabilized oil-in-water emulsions. *Food Hydrocolloids*, 96, 209–223.
- Dickinson, E., & Davies, E. (1999). Influence of ionic calcium on stability of sodium caseinate emulsions. *Colloids and Surfaces B: Biointerfaces*, 12(3), 203–212. [https://doi.org/10.1016/S0927-7765\(98\)00075-7](https://doi.org/10.1016/S0927-7765(98)00075-7)
- Dickinson, E., Golding, M., & Povey, M. J. (1997). Creaming and flocculation of oil-in-water emulsions containing sodium caseinate. *Journal of Colloid and Interface Science*, 185(2), 515–529.
- Dickinson, E., Rolfe, S. E., & Dalgleish, D. G. (1988). Competitive adsorption of α 1-casein and β -casein in oil-in-water emulsions. *Food Hydrocolloids*, 2(5), 397–405. [https://doi.org/10.1016/S0268-005X\(88\)80004-3](https://doi.org/10.1016/S0268-005X(88)80004-3)
- Ebert, S., Koo, C. K., Weiss, J., & McClements, D. J. (2017). Continuous production of core-shell protein nanoparticles by antisolvent precipitation using dual-channel microfluidization: Caseinate-coated zein nanoparticles. *Food Research International*, 92, 48–55.
- Erxleben, S. W. J., Pelan, E., & Wolf, B. (2021). Effect of ethanol on the stability of sodium caseinate stabilised emulsions. *Food Hydrocolloids*, 121, 107058. <https://doi.org/10.1016/j.foodhyd.2021.107058>
- Euston, S. R., & Goff, H. D. (2019). Emulsifiers in dairy products and dairy substitutes. In G.L. Hasenhuettl & R.W. Hartel (Eds.), *Food emulsifiers and their applications* (pp. 217–254). Springer.
- Evans, M., Ratcliffe, L., & Williams, P. A. (2013). Emulsion stabilisation using polysaccharide-protein complexes. *Current Opinion in Colloid & Interface Science*, 18(4), 272–282.
- Fang, B., & Nakagawa, K. (2020). Modification of casein aggregate microstructures under frozen conditions: A study using tunable resistive pulse sensing. *Food Hydrocolloids*, 98, 105259. <https://doi.org/10.1016/j.foodhyd.2019.105259>
- Fredrick, E., Walstra, P., & Dewettinck, K. (2010). Factors governing partial coalescence in oil-in-water emulsions. *Advances in Colloid and Interface Science*, 153(1), 30–42. <https://doi.org/10.1016/j.cis.2009.10.003>
- Ghosh, A. K., & Bandyopadhyay, P. (2012). Polysaccharide-protein interactions and their relevance in food colloids. *The Complex World of Polysaccharides*, 14, 395–406.
- Gülseren, İ., & Corredig, M. (2011). Changes in colloidal properties of oil in water emulsions stabilized with sodium caseinate observed by acoustic and electroacoustic spectroscopy. *Food Biophysics*, 6(4), 534. <https://doi.org/10.1007/s11483-011-9236-x>
- Hebishi, E., Buffa, M., Juan, B., Blasco-Moreno, A., & Trujillo, A.-J. (2017). Ultra high-pressure homogenized emulsions stabilized by sodium caseinate: Effects of protein concentration and pressure on emulsions structure and stability. *LWT - Food Science and Technology*, 76, 57–66. <https://doi.org/10.1016/j.lwt.2016.10.045>
- Ishii, T., Matsumiya, K., Aoshima, M., & Matsumura, Y. (2018). Microgelation imparts emulsifying ability to surface-inactive polysaccharides—Bottom-up vs top-down approaches. *npj Science of Food*, 2(1), 1–12.
- Jacobsen, C. (2016). Oxidative Stability and shelf life of food emulsions. In M. Hu & C. Jacobsen (Eds.), *Oxidative stability and shelf life of foods containing oils and fats* (pp. 287–312). AOCS Press. <https://doi.org/10.1016/B978-1-63067-056-6.00008-2>
- Ji, J., Zhang, J., Chen, J., Wang, Y., Dong, N., Hu, C., Chen, H., Li, G., Pan, X., & Wu, C. (2015). Preparation and stabilization of emulsions stabilized by mixed sodium caseinate and soy protein isolate. *Food Hydrocolloids*, 51, 156–165. <https://doi.org/10.1016/j.foodhyd.2015.05.013>
- Jiang, T., & Charcosset, C. (2022). Encapsulation of curcumin within oil-in-water emulsions prepared by premix membrane emulsification: Impact of droplet size and carrier oil on the chemical stability of curcumin. *Food Research International*, 157, 111475. <https://doi.org/10.1016/j.foodres.2022.111475>
- Jiao, J., & Burgess, D. J. (2003). Ostwald ripening of water-in-hydrocarbon emulsions. *Journal of Colloid and Interface Science*, 264(2), 509–516.
- Jourdain, L., Leser, M. E., Schmitt, C., Michel, M., & Dickinson, E. (2008). Stability of emulsions containing sodium caseinate and dextran sulfate: Relationship to complexation in solution. *Food Hydrocolloids*, 22(4), 647–659. <https://doi.org/10.1016/j.foodhyd.2007.01.007>
- Juyang, Z., & Wolf, B. (2021). Impact of type of sugar beet pectin-sodium caseinate interaction on emulsion properties at pH 4.5 and pH 7. *Foods*, 10(3), 631.
- Kim, W., Wang, Y., & Selomulya, C. (2020). Dairy and plant proteins as natural food emulsifiers. *Trends in Food Science & Technology*, 105, 261–272. <https://doi.org/10.1016/j.tifs.2020.09.012>
- Kwok, M., & Ngai, T. (2016). A confocal microscopy study of micron-sized poly (N-isopropylacrylamide) microgel particles at the oil-water interface and anisotropic flattening of highly swollen microgel. *Journal of Colloid and Interface Science*, 461, 409–418.
- Lamothe, S., Desroches, V., & Britten, M. (2019). Effect of milk proteins and food-grade surfactants on oxidation of linseed oil-in-water emulsions during in vitro digestion. *Food Chemistry*, 294, 130–137. <https://doi.org/10.1016/j.foodchem.2019.04.107>
- Lee, Y.-Y., Tang, T.-K., Tan, C.-P., Alitheen, N. B. M., Phuah, E.-T., Karim, N. A. A., & Lai, O.-M. (2015). Entrapment of palm-based medium-and long-chain triacylglycerol via Maillard reaction products. *Food and Bioprocess Technology*, 8(7), 1571–1582.
- Let, M. B., Jacobsen, C., Sørensen, A.-D. M., & Meyer, A. S. (2007). Homogenization conditions affect the oxidative stability of fish oil enriched milk emulsions: Lipid oxidation. *Journal of Agricultural and Food Chemistry*, 55(5), 1773–1780.
- Li, K., Woo, M. W., Patel, H., & Selomulya, C. (2017). Enhancing the stability of protein-polysaccharides emulsions via Maillard reaction for better oil encapsulation in spray-dried powders by pH adjustment. *Food Hydrocolloids*, 69, 121–131.
- Li, K., Li, Y., Liu, C.-L., Fu, L., Zhao, Y.-Y., Zhang, Y.-Y., Wang, Y.-T., & Bai, Y.-H. (2020). Improving interfacial properties, structure and oxidative stability by ultrasound application to sodium caseinate prepared pre-emulsified soybean oil. *LWT - Food Science and Technology*, 131, 109755. <https://doi.org/10.1016/j.lwt.2020.109755>
- Li, N., & Zhong, Q. (2022). Impacts of preparation conditions on the structure and emulsifying properties of casein-alginate conjugates produced by transacylation reaction. *International Journal of*

- Biological Macromolecules*, 201, 242–253. <https://doi.org/10.1016/j.ijbiomac.2021.12.169>
- Li, Y., & Xiang, D. (2019). Stability of oil-in-water emulsions performed by ultrasound power or high-pressure homogenization. *PLoS ONE*, 14(3), e0213189.
- Liang, Y., Gillies, G., Matia-Merino, L., Ye, A., Patel, H., & Golding, M. (2017). Structure and stability of sodium-caseinate-stabilized oil-in-water emulsions as influenced by heat treatment. *Food Hydrocolloids*, 66, 307–317. <https://doi.org/10.1016/j.foodhyd.2016.11.041>
- Liang, Y., Gillies, G., Patel, H., Matia-Merino, L., Ye, A., & Golding, M. (2014). Physical stability, microstructure and rheology of sodium-caseinate-stabilized emulsions as influenced by protein concentration and non-adsorbing polysaccharides. *Food Hydrocolloids*, 36, 245–255. <https://doi.org/10.1016/j.foodhyd.2013.10.006>
- Liang, Y., Matia-Merino, L., Gillies, G., Patel, H., Ye, A., & Golding, M. (2017). The heat stability of milk protein-stabilized oil-in-water emulsions: A review. *Current Opinion in Colloid & Interface Science*, 28, 63–73.
- Liao, W., Badri, W., Dumas, E., Ghnimi, S., Elaissari, A., Saurel, R., & Gharsallaoui, A. (2021). Nanoencapsulation of essential oils as natural food antimicrobial agents: An overview. *Applied Sciences*, 11(13), 5778.
- Liao, W., Dumas, E., Ghnimi, S., Elaissari, A., & Gharsallaoui, A. (2021). Effect of emulsifier and droplet size on the antibacterial properties of emulsions and emulsion-based films containing essential oil compounds. *Journal of Food Processing and Preservation*, 45(12), e16072.
- Liao, W., Elaissari, A., Ghnimi, S., Dumas, E., & Gharsallaoui, A. (2022). Effect of pectin on the properties of nanoemulsions stabilized by sodium caseinate at neutral pH. *International Journal of Biological Macromolecules*, 209, 1858–1866.
- Liao, W., Gharsallaoui, A., Dumas, E., Ghnimi, S., & Elaissari, A. (2021). Effect of carrier oil on the properties of sodium caseinate stabilized O/W nanoemulsions containing Trans-cinnamaldehyde. *LWT - Food Science and Technology*, 146, 111655.
- Liu, J., Liu, W., Salt, L. J., Ridout, M. J., Ding, Y., & Wilde, P. J. (2018). Fish oil emulsions stabilized with caseinate glycosylated by dextran: Physicochemical stability and gastrointestinal fate. *Journal of Agricultural and Food Chemistry*, 67(1), 452–462.
- Liu, L., Zhao, Q., Liu, T., Kong, J., Long, Z., & Zhao, M. (2012). Sodium caseinate/carboxymethylcellulose interactions at oil–water interface: Relationship to emulsion stability. *Food Chemistry*, 132(4), 1822–1829.
- Loi, C. C., Eyres, G. T., & Birch, E. J. (2019). Effect of milk protein composition on physicochemical properties, creaming stability and volatile profile of a protein-stabilised oil-in-water emulsion. *Food Research International*, 120, 83–91. <https://doi.org/10.1016/j.foodres.2019.02.026>
- Low, L. E., Siva, S. P., Ho, Y. K., Chan, E. S., & Tey, B. T. (2020). Recent advances of characterization techniques for the formation, physical properties and stability of Pickering emulsion. *Advances in Colloid and Interface Science*, 277, 102117.
- Ma, X., & Chatterton, D. E. W. (2021). Strategies to improve the physical stability of sodium caseinate stabilized emulsions: A literature review. *Food Hydrocolloids*, 119, 106853. <https://doi.org/10.1016/j.foodhyd.2021.106853>
- Malvey, J., Pérez-Anker, J., Toll, A., Pigem, R., Garcia, A., Alos, L. L., & Puig, S. (2020). Ex vivo confocal microscopy: Revolution in fast pathology in dermatology. *British Journal of Dermatology*, 183(6), 1011–1025.
- Mao, L., Yang, J., Xu, D., Yuan, F., & Gao, Y. (2010). Effects of homogenization models and emulsifiers on the physicochemical properties of β -carotene nanoemulsions. *Journal of Dispersion Science and Technology*, 31(7), 986–993.
- Martínez-Padilla, L. P., Sosa-Herrera, M. G., & Osnaya-Becerril, M. (2021). Effect of the konjac glucomannan concentration on the rheological behaviour and stability of sodium caseinate oil-in-water emulsions. *International Dairy Journal*, 117, 104993. <https://doi.org/10.1016/j.idairyj.2021.104993>
- McClements, D. J. (2007). Critical review of techniques and methodologies for characterization of emulsion stability. *Critical Reviews in Food Science and Nutrition*, 47(7), 611–649.
- McClements, D. J. (2015). *Food emulsions: Principles, practices, and techniques*. CRC Press.
- McClements, D. J., & Decker, E. (2018). Interfacial antioxidants: A review of natural and synthetic emulsifiers and coemulsifiers that can inhibit lipid oxidation. *Journal of Agricultural and Food Chemistry*, 66(1), 20–35.
- McClements, D. J., & Jafari, S. M. (2018). Improving emulsion formation, stability and performance using mixed emulsifiers: A review. *Advances in Colloid and Interface Science*, 251, 55–79.
- McSweeney, S. L., Mulvihill, D. M., & O'Callaghan, D. M. (2004). The influence of pH on the heat-induced aggregation of model milk protein ingredient systems and model infant formula emulsions stabilized by milk protein ingredients. *Food Hydrocolloids*, 18(1), 109–125.
- Nagaraju, P. G., Sindhu, P., Dubey, T., Chinnathambi, S., Poornima Priyadarshini, C. G., & Rao, P. J. (2021). Influence of sodium caseinate, maltodextrin, pectin and their Maillard conjugate on the stability, in vitro release, anti-oxidant property and cell viability of eugenol-olive oil nanoemulsions. *International Journal of Biological Macromolecules*, 183, 158–170. <https://doi.org/10.1016/j.ijbiomac.2021.04.122>
- O' Dwyer, S. P., O' Beirne, D., Eidhin, D. N., & O' Kennedy, B. T. (2013). Effects of sodium caseinate concentration and storage conditions on the oxidative stability of oil-in-water emulsions. *Food Chemistry*, 138(2), 1145–1152. <https://doi.org/10.1016/j.foodchem.2012.09.138>
- Onsaard, E., Vittayanont, M., Srigan, S., & McClements, D. J. (2006). Comparison of properties of oil-in-water emulsions stabilized by coconut cream proteins with those stabilized by whey protein isolate. *Food Research International*, 39(1), 78–86.
- O'Regan, J., & Mulvihill, D. M. (2010). Sodium caseinate–maltodextrin conjugate stabilized double emulsions: Encapsulation and stability. *Food Research International*, 43(1), 224–231. <https://doi.org/10.1016/j.foodres.2009.09.031>
- Park, S. H., Hong, C. R., & Choi, S. J. (2020). Prevention of Ostwald ripening in orange oil emulsions: Impact of surfactant type and Ostwald ripening inhibitor type. *LWT - Food Science and Technology*, 134, 110180. <https://doi.org/10.1016/j.lwt.2020.110180>
- Perrechil, F. A., & Cunha, R. L. (2010). Oil-in-water emulsions stabilized by sodium caseinate: Influence of pH, high-pressure homogenization and locust bean gum addition. *Journal of Food Engineering*, 97(4), 441–448.

- Perugini, L., Cinelli, G., Cofelice, M., Ceglie, A., Lopez, F., & Cuomo, F. (2018). Effect of the coexistence of sodium caseinate and Tween 20 as stabilizers of food emulsions at acidic pH. *Honoring Piero Baglioni*, 168, 163–168. <https://doi.org/10.1016/j.colsurfb.2018.02.003>
- Piorkowski, D. T., & McClements, D. J. (2014). Beverage emulsions: Recent developments in formulation, production, and applications. *Special Issue: A Festschrift in Honour of Professor Eric Dickinson*, 42, 5–41. <https://doi.org/10.1016/j.foodhyd.2013.07.009>
- Qin, X., Yang, R., Zhong, J., Shabani, K. I., & Liu, X. (2018). Ultrasound-assisted preparation of a human milk fat analog emulsion: Understanding factors affecting formation and stability. *Journal of Food Engineering*, 238, 103–111.
- Qiu, C., Zhao, M., & McClements, D. J. (2015). Improving the stability of wheat protein-stabilized emulsions: Effect of pectin and xanthan gum addition. *Food Hydrocolloids*, 43, 377–387. <https://doi.org/10.1016/j.foodhyd.2014.06.013>
- Rahimi, P., Hosseini, E., Rousta, E., & Bostar, H. (2021). Digestibility and stability of ultrasound-treated fish oil emulsions prepared by water-soluble bitter almond gum glycosylated with caseinate. *LWT - Food Science and Technology*, 148, 111697. <https://doi.org/10.1016/j.lwt.2021.111697>
- Ribeiro, E. F., Morell, P., Nicoletti, V. R., Quiles, A., & Hernando, I. (2021). Protein- and polysaccharide-based particles used for Pickering emulsion stabilisation. *Food Hydrocolloids*, 119, 106839. <https://doi.org/10.1016/j.foodhyd.2021.106839>
- Ries, D., Ye, A., Haisman, D., & Singh, H. (2010). Antioxidant properties of caseins and whey proteins in model oil-in-water emulsions. *International Dairy Journal*, 20(2), 72–78.
- Roulet, M., Clegg, P. S., & Frith, W. J. (2019). Viscosity of protein-stabilized emulsions: Contributions of components and development of a semipredictive model. *Journal of Rheology*, 63(1), 179–190.
- Saffarionpour, S. (2019). Preparation of food flavor nanoemulsions by high-and-low-energy emulsification approaches. *Food Engineering Reviews*, 11(4), 259–289.
- Salminen, H., Bischoff, S., & Weiss, J. (2019). Impact of concentration ratio on the formation and stability of emulsions stabilized by Quillaja saponin–sodium caseinate mixtures. *Food Biophysics*, 14(2), 109–119.
- Sánchez, C. C., & Patino, J. M. R. (2005). Interfacial, foaming and emulsifying characteristics of sodium caseinate as influenced by protein concentration in solution. *Food Hydrocolloids*, 19(3), 407–416. <https://doi.org/10.1016/j.foodhyd.2004.10.007>
- Sato, A. C. K., Perrechil, F. A., Costa, A. A. S., Santana, R. C., & Cunha, R. L. (2015). Cross-linking proteins by laccase: Effects on the droplet size and rheology of emulsions stabilized by sodium caseinate. *Food Research International*, 75, 244–251.
- Sharma, M., Mann, B., Sharma, R., Bajaj, R., Athira, S., Sarkar, P., & Pothuraju, R. (2017). Sodium caseinate stabilized clove oil nanoemulsion: Physicochemical properties. *Journal of Food Engineering*, 212, 38–46. <https://doi.org/10.1016/j.jfoodeng.2017.05.006>
- Shi, F., Chang, Y., Shen, J., Chen, G., & Xue, C. (2023). A comparative investigation of anionic polysaccharides (sulfated fucan, *ι*-carrageenan, *κ*-carrageenan, and alginate) on the fabrication, stability, rheology, and digestion of multilayer emulsion. *Food Hydrocolloids*, 134, 108081. <https://doi.org/10.1016/j.foodhyd.2022.108081>
- Shi, F., Tian, X., McClements, D. J., Chang, Y., Shen, J., & Xue, C. (2021). Influence of molecular weight of an anionic marine polysaccharide (sulfated fucan) on the stability and digestibility of multilayer emulsions: Establishment of structure-function relationships. *Food Hydrocolloids*, 113, 106418. <https://doi.org/10.1016/j.foodhyd.2020.106418>
- Shimizu, M., Ametani, A., Kaminogawa, S., & Yamauchi, K. (1986). The topography of α 1-casein adsorbed to an oil/water interface: An analytical approach using proteolysis. *Biochimica et Biophysica Acta (BBA)-Protein Structure and Molecular Enzymology*, 869(3), 259–264.
- Silva, J. V. C., Jacquette, B., Amagliani, L., Schmitt, C., Nicolai, T., & Chassenieux, C. (2019). Heat-induced gelation of micellar casein/plant protein oil-in-water emulsions. *Colloids and Surfaces A: Physicochemical and Engineering Aspects*, 569, 85–92. <https://doi.org/10.1016/j.colsurfa.2019.01.065>
- Singh, H. (2011). Aspects of milk-protein-stabilised emulsions. *Food Hydrocolloids*, 25(8), 1938–1944.
- Sneha, K., & Kumar, A. (2021). Nanoemulsions: Techniques for the preparation and the recent advances in their food applications. *Innovative Food Science & Emerging Technologies*, 76, 102914.
- Sosa-Herrera, M. G., Berli, C. L. A., & Martinez-Padilla, L. P. (2008). Physicochemical and rheological properties of oil-in-water emulsions prepared with sodium caseinate/gellan gum mixtures. *Food Hydrocolloids*, 22(5), 934–942.
- Srinivasan, M., Singh, H., & Munro, P. A. (2002). Formation and stability of sodium caseinate emulsions: Influence of retorting (121°C for 15 min) before or after emulsification. *Food Hydrocolloids*, 16(2), 153–160.
- Su, D., & Zhong, Q. (2016). Formation of thymol nanoemulsions with combinations of casein hydrolysates and sucrose stearate. *Journal of Food Engineering*, 179, 1–10. <https://doi.org/10.1016/j.jfoodeng.2016.01.030>
- Su, J., & Everett, D. W. (2003). Adsorption of κ -casein onto native milk fat globule, latex particle, and emulsion surfaces. *Food Hydrocolloids*, 17(4), 529–537. [https://doi.org/10.1016/S0268-005X\(03\)00015-8](https://doi.org/10.1016/S0268-005X(03)00015-8)
- Sun, C., & Zhong, Q. (2022). Alkaline conjugation of caseinate and propylene glycol alginate to prepare biopolymer complexes stabilizing oil-in-water emulsion gels. *Food Hydrocolloids*, 123, 107192. <https://doi.org/10.1016/j.foodhyd.2021.107192>
- Surh, J., Decker, E. A., & McClements, D. J. (2006). Influence of pH and pectin type on properties and stability of sodium-caseinate stabilized oil-in-water emulsions. *Food Hydrocolloids*, 20(5), 607–618. <https://doi.org/10.1016/j.foodhyd.2005.07.004>
- Tadros, T. F. (1994). Fundamental principles of emulsion rheology and their applications. *Colloids and Surfaces A: Physicochemical and Engineering Aspects*, 91, 39–55.
- Tavares, L., Zapata Noreña, C. P., Barros, H. L., Smaoui, S., Lima, P. S., & Marques de Oliveira, M. (2022). Rheological and structural trends on encapsulation of bioactive compounds of essential oils: A global systematic review of recent research. *Food Hydrocolloids*, 129, 107628. <https://doi.org/10.1016/j.foodhyd.2022.107628>
- Tavasoli, S., Maghsoudlou, Y., Jafari, S. M., & Tabarestani, H. S. (2022). Improving the emulsifying properties of sodium caseinate through conjugation with soybean soluble polysaccharides. *Food*

- Chemistry*, 377, 131987. <https://doi.org/10.1016/j.foodchem.2021.131987>
- Walker, R., Decker, E. A., & McClements, D. J. (2015). Development of food-grade nanoemulsions and emulsions for delivery of omega-3 fatty acids: Opportunities and obstacles in the food industry. *Food & Function*, 6(1), 41–54.
- Walstra, P., & Jenness, R. (1984). *Dairy chemistry & physics*. John Wiley & Sons.
- Wan, L., Li, L., Xiao, J., He, N., Zhang, R., Li, B., & Zhang, X. (2022). The interfacial digestion behavior of crystalline oil-in-water emulsions stabilized by sodium caseinate during in vitro gastrointestinal digestion. *Food Hydrocolloids*, 130, 107734. <https://doi.org/10.1016/j.foodhyd.2022.107734>
- Wang, C., Li, X., Sang, S., Julian McClements, D., Chen, L., Long, J., Jiao, A., Wang, J., Jin, Z., & Qiu, C. (2022). Preparation, characterization and in vitro digestive behaviors of emulsions synergistically stabilized by γ -cyclodextrin/sodium caseinate/alginate. *Food Research International*, 160, 111634. <https://doi.org/10.1016/j.foodres.2022.111634>
- Wang, J., Maoulida, F., Ben Amara, C., Ghnimi, S., Chihib, N.-E., Dumas, E., & Gharsallaoui, A. (2019). Spray-drying of protein/polysaccharide complexes: Dissociation of the effects of shearing and heating. *Food Chemistry*, 297(1), 124943.1–124943.6.
- Wang, J., Souihi, S., Amara, C. B., Dumas, E., & Gharsallaoui, A. (2018). Influence of low methoxyl pectin on the physicochemical properties of sodium caseinate-stabilized emulsions. *Journal of Food Process Engineering*, 41(8), e12906.
- Wang, J., Su, Y., Jia, F., & Jin, H. (2013). Characterization of casein hydrolysates derived from enzymatic hydrolysis. *Chemistry Central Journal*, 7(1), 1–8.
- Wang, L., Zhang, S., Jiang, W., Zhao, H., & Fu, J. (2020). Ability of casein hydrolysate-carboxymethyl chitosan conjugates to stabilize a nanoemulsion: Improved freeze-thaw and pH stability. *Food Hydrocolloids*, 101, 105452.
- Wei, Q., Liu, T., & Sun, D.-W. (2018). Advanced glycation end-products (AGEs) in foods and their detecting techniques and methods: A review. *Trends in Food Science & Technology*, 82, 32–45.
- Wu, F., Chen, F., Pu, Y., Qian, F., Leng, Y., Mu, G., & Zhu, X. (2022). Effects of soy lecithin concentration on the physicochemical properties of whey protein isolate, casein-stabilised simulated infant formula emulsion and their corresponding microcapsules. *International Journal of Dairy Technology*, 75(3), 513–526.
- Wusigale, L. L., & Luo, Y. (2020). Casein and pectin: Structures, interactions, and applications. *Trends in Food Science & Technology*, 97, 391–403. <https://doi.org/10.1016/j.tifs.2020.01.027>
- Xu, N., Wu, X., Zhu, Y., Miao, J., Gao, Y., Cheng, C., Peng, S., Zou, L., Julian McClements, D., & Liu, W. (2021). Enhancing the oxidative stability of algal oil emulsions by adding sweet orange oil: Effect of essential oil concentration. *Food Chemistry*, 355, 129508. <https://doi.org/10.1016/j.foodchem.2021.129508>
- Xu, W., Xiong, Y., Li, Z., Luo, D., Wang, Z., Sun, Y., & Shah, B. R. (2020). Stability, microstructural and rheological properties of complex prebiotic emulsion stabilized by sodium caseinate with inulin and konjac glucomannan. *Food Hydrocolloids*, 105, 105772.
- Xue, J., Michael Davidson, P., & Zhong, Q. (2015). Antimicrobial activity of thyme oil co-nanoemulsified with sodium caseinate and lecithin. *International Journal of Food Microbiology*, 210, 1–8. <https://doi.org/10.1016/j.ijfoodmicro.2015.06.003>
- Ye, A., & Singh, H. (2001). Interfacial composition and stability of sodium caseinate emulsions as influenced by calcium ions. *Food Hydrocolloids*, 15(2), 195–207.
- Yerramilli, M., & Ghosh, S. (2017). Long-term stability of sodium caseinate-stabilized nanoemulsions. *Journal of Food Science and Technology*, 54(1), 82–92.
- Yerramilli, M., Longmore, N., & Ghosh, S. (2017). Improved stabilization of nanoemulsions by partial replacement of sodium caseinate with pea protein isolate. *Food Hydrocolloids*, 64, 99–111. <https://doi.org/10.1016/j.foodhyd.2016.10.027>
- Yesiltas, B., Garcia-Moreno, P. J., Sørensen, A.-D. M., Akoh, C. C., & Jacobsen, C. (2019). Physical and oxidative stability of high fat fish oil-in-water emulsions stabilized with sodium caseinate and phosphatidylcholine as emulsifiers. *Food Chemistry*, 276, 110–118. <https://doi.org/10.1016/j.foodchem.2018.09.172>
- Yesiltas, B., Sørensen, A.-D. M., Garcia-Moreno, P. J., Anankanbil, S., Guo, Z., & Jacobsen, C. (2018). Combination of sodium caseinate and succinylated alginate improved stability of high fat fish oil-in-water emulsions. *Food Chemistry*, 255, 290–299.
- Zhai, X., Lin, D., Liu, D., & Yang, X. (2018). Emulsions stabilized by nanofibers from bacterial cellulose: New potential food-grade Pickering emulsions. *Food Research International*, 103, 12–20.
- Zhang, S., Jiang, W., Zhang, Z., Zhu, Y., Wang, L., & Fu, J. (2020). A nanoparticle/oil double epigallocatechin gallate-loaded Pickering emulsion: Stable and delivery characteristics. *LWT - Food Science and Technology*, 130, 109369. <https://doi.org/10.1016/j.lwt.2020.109369>
- Zhang, S., Zhang, Q., Shang, J., Mao, Z.-S., & Yang, C. (2021). Measurement methods of particle size distribution in emulsion polymerization. *Chinese Journal of Chemical Engineering*, 39, 1–15.

How to cite this article: Liao, W., Gharsallaoui, A., Dumas, E., & Elaissari, A. (2022). Understanding of the key factors influencing the properties of emulsions stabilized by sodium caseinate. *Comprehensive Reviews in Food Science and Food Safety*, 1–27. <https://doi.org/10.1111/1541-4337.13062>

Literature review II

Nanoencapsulation of Essential Oils as Natural Food Antimicrobial
Agents: An Overview

Published in: Applied Sciences

Summary of literature review II

As consumer awareness increases, there is a growing concern of the potential carcinogenic and mutagenic risks associated with chemical preservatives. “Fresher,” “more natural,” and “minimally processed” food is being demanded. Essential oils (EOs) possess strong antimicrobial activity that could play a remarkable role as a novel source of food preservative. Despite the excellent efficacy of EOs as antimicrobials, their use is limited due to some major inherent barriers, such as low water solubility, bioavailability, volatility, and stability in food systems. Nanoencapsulation has been shown to be an effective mean of addressing these issues. In addition, nanoemulsions have been reported to have better bioavailability than conventional emulsions to encapsulate bioactive ingredients due to their nano-size (20-500 nm) and high specific surface area. In this review, we explore recent advances concerning the natural active molecules as antibacterial agents and the different strategies for the nanoencapsulation of these natural antibacterial agents, especially EOs. On this basis, the advantages and limitations of nano-encapsulation technology and “traditional” packaging technology are compared and discussed. The state-of-the-art antibacterial properties of EOs were summarized. Finally, the latest applications of nano-encapsulated antibacterial agents in food systems were introduced in detail.

Review

Nanoencapsulation of Essential Oils as Natural Food Antimicrobial Agents: An Overview

Wei Liao ¹, Waisudin Badri ¹, Emilie Dumas ¹, Sami Ghnimi ^{1,2} , Abdelhamid Elaissari ³ , Rémi Saurel ⁴ 
and Adem Gharsallaoui ^{1,*} 

¹ Laboratoire d'Automatique, de Génie des Procédés et de Génie Pharmaceutique, CNRS, University Claude Bernard Lyon 1, 43 Bd 11 Novembre 1918, 69622 Villeurbanne, France; wei.liao@etu.univ-lyon1.fr (W.L.); waisudin.badri@univ-lyon1.fr (W.B.); emilie.dumas@univ-lyon1.fr (E.D.); sghnimi@isara.fr (S.G.)

² ISARA, 23 Rue Jean Baldassini, 69007 Lyon, France

³ Institute of Analytical Sciences, CNRS, University Claude Bernard Lyon 1, 69622 Villeurbanne, France; abdelhamid.elaissari@univ-lyon1.fr

⁴ Procédés Alimentaires Et Microbiologiques, L'Unité Mixte de Recherche, University Bourgogne Franche-Comté, AgroSup Dijon, F-21000 Dijon, France; remi.saurel@agrosupdijon.fr

* Correspondence: adem.gharsallaoui@univ-lyon1.fr; Tel.: +33-4-74-45-52-52

Abstract: The global demand for safe and healthy food with minimal synthetic preservatives is continuously increasing. Natural food antimicrobials and especially essential oils (EOs) possess strong antimicrobial activities that could play a remarkable role as a novel source of food preservatives. Despite the excellent efficacy of EOs, they have not been widely used in the food industry due to some major intrinsic barriers, such as low water solubility, bioavailability, volatility, and stability in food systems. Recent advances in nanotechnology have the potential to address these existing barriers in order to use EOs as preservatives in food systems at low doses. Thus, in this review, we explored the latest advances of using natural actives as antimicrobial agents and the different strategies for nanoencapsulation used for this purpose. The state of the art concerning the antibacterial properties of EOs will be summarized, and the main latest applications of nanoencapsulated antimicrobial agents in food systems will be presented. This review should help researchers to better choose the most suitable encapsulation techniques and materials.

Keywords: essential oils; antimicrobial activity; nanoencapsulation; food preservation



Citation: Liao, W.; Badri, W.; Dumas, E.; Ghnimi, S.; Elaissari, A.; Saurel, R.; Gharsallaoui, A. Nanoencapsulation of Essential Oils as Natural Food Antimicrobial Agents: An Overview. *Appl. Sci.* **2021**, *11*, 5778. <https://doi.org/10.3390/app11135778>

Academic Editors: Giorgia Spigno and Raed Abu-Reziq

Received: 23 April 2021

Accepted: 17 June 2021

Published: 22 June 2021

Publisher's Note: MDPI stays neutral with regard to jurisdictional claims in published maps and institutional affiliations.



Copyright: © 2021 by the authors. Licensee MDPI, Basel, Switzerland. This article is an open access article distributed under the terms and conditions of the Creative Commons Attribution (CC BY) license (<https://creativecommons.org/licenses/by/4.0/>).

1. Introduction

In recent decades, the global food loss caused by microbial spoilage has increased year by year [1]. Moreover, the recent outbreaks of foodborne diseases associated with *Escherichia coli* O157:H7, *Salmonella Saintpaul*, *Listeria monocytogenes*, and so on, have made microbiological safety a priority, especially during food processing and storage [2].

Food antimicrobial agents are chemicals which can prevent and inhibit the growth of microorganisms, and they are usually used in conjunction with other preservation procedures to extend the shelf life of foods. Currently, the main preservatives used in the food industry are chemically synthesized ones [3]. As consumer awareness increases, there is a growing concern of the potential carcinogenic and mutagenic risks associated with chemical preservatives like nitrites and parabens. “Fresher”, “more natural”, and “minimally processed” food is being demanded. In this sense, the development of alternative natural and low-toxic antimicrobial agents to replace traditional synthetic antimicrobial substances has received a lot of attention.

Essential oils (EOs) are volatile and aromatic secondary metabolites of plants, which are mainly developed for their flavor, fragrances, and biological properties. In recent years, EOs and their biologically active compounds have been widely explored for their antibacterial and antifungal efficacy against foodborne pathogens (bacteria, molds, and related toxins) [4]. However, the use of EOs in food preservation is often limited because of

their processing costs and other disadvantages, such as their low efficacy as compared to synthetic antimicrobial agents, their intense aroma, and their instability or insolubility in water. Therefore, an effective intervention system is necessary to preserve the activity of natural food antimicrobials when using them in the food industry. Nanotechnology has proven to be a useful tool for this purpose, which could provide the protection of natural antimicrobial agents against degradation, and improve the bioavailability and the target delivery of antimicrobial agents, thereby decreasing the amount of antimicrobials required for effective food preservation [3]. Hence, the application of nanotechnology in the food industry has been one of the fastest growing fields in the past few years.

Based on what has been learned so far, the aim of this review is to summarize the up-to-date account and advances concerning the potential of EOs as food antimicrobial agents. Meanwhile, the strategy for nanoencapsulation of EOs and its application in food are also discussed.

2. Synthetic and Natural Food Antimicrobial Agents

Food antimicrobial agents can destroy and inhibit the growth of microorganisms and consequently improve food safety for the consumers, as well as extend the shelf life of food products. According to their sources, they can be classified in two groups: synthetic antimicrobial agents and natural antimicrobial agents.

2.1. Synthetic Antimicrobial Agents

Although consumers have begun to worry about the safety of synthetic antimicrobials used in food products, they are still widely used in the food industry to date. The main synthetic antimicrobials used are sorbic acid and its salts, benzoic acid and its salts, parabens, propionic acid and its salts, and sodium diacetate (Table 1). They have the advantages of having strong antimicrobial activity at low concentrations, high industrial availability, and low cost, but most of the end products of their metabolism can lead to food color change and flavor and nutrient deterioration, and even endanger human health [5].

Table 1. Commonly used synthetic antimicrobial agents for Food.

Chemical Compound	Application Range	Mechanism of Action or Application Effect
Benzoic acid and benzoates	Particularly used in acidic foods	Destruction of bacterial cell membrane, inhibition of cell membrane absorption of amino acid and respiratory enzymes, blocking condensation of acetyl-CoA, etc.
Sorbic acid and sorbates	Dried meats and acidic foods	Binding to biological enzymes and inhibiting enzyme activity.
Paraben (Hydroxybenzoates)	Bakery products, soft drinks, cosmetic	Destruction of cell membranes, denaturation of intracellular proteins, inhibition of the activity of respiratory enzymes and electron transport enzymes.
Propionic acid and propionates	Baked products such as pastries, bread, etc.	Binding to biological enzymes and inhibiting their biological activity. They have a good inhibitory effect on molds and Gram-negative bacteria under acidic pH, especially to prevent the production of aflatoxins.
Dimethyl dicarbonate	Beverages	Passing through the cell membrane and interacting with enzymes in the microbial cells to block intracellular metabolism.
Sulfur dioxide and sulfites	Dried fruits, wine making	Hydrogen ions generated by the decomposition of sulfite can cause damage of bacterial surface proteins and nucleic acids to kill microorganisms.

2.2. Natural Antimicrobial Agents

“Natural antimicrobial agent” refers to natural active substances extracted from plants, animals, or microorganisms, such as polyphenols, flavonoids, tannins, alkaloids, terpenoids, isothiocyanates, polypeptides, and oxidized derivatives thereof. Based on the safety issues and the exploration of healthier and natural products, natural antimicrobial agents are more acceptable to consumers than synthetic antimicrobials [6]. The activities of some common natural antimicrobials against bacteria and fungi are summarized in Table 2. In the past few years, many researchers have conducted a large number of experiments about active substances to study their antibacterial effects. The main antibacterial mechanisms are: (i) destruction of cell membranes; (ii) complexation of metal ions; (iii) damage of the genetic material of microorganisms; (iv) leakage of cell contents; (v) inhibition of metabolic enzymes; and (vi) consumption of cellular energy in the form of ATP [7,8]. The bacteriostatic effects of these natural active substances are influenced by many factors, such as their own chemical properties (acid dissociation constant, hydrophobic/hydrophilic ratio, solubility, and volatility), target microorganisms (species, strains, and genes), environmental factors (pH, ionic strength, water activity, temperature, and atmospheric composition) and food properties (ingredients and initial bacterial amount) [8].

Table 2. Commonly used natural antimicrobial agents for food preservation.

Antimicrobial Compound	Main Source	Target Microorganism			Reference
		Gram-Positive Bacteria	Gram-Negative Bacteria	Fungi	
Plant Origin					
	Thyme	<i>Staphylococcus aureus</i> <i>Listeria monocytogenes</i>	<i>Shigella sonnei</i> <i>Shigella flexneri</i> <i>Escherichia coli</i> O157:H7 <i>E. coli</i> <i>Salmonella enteritidis</i> <i>Salmonella typhimurium</i>	<i>Botrytis cinerea</i> <i>Candida albicans</i> <i>Penicillium digitatum</i>	[9,10]
Essential oils	Clove	<i>S. aureus</i> <i>Bacillus cereus</i> <i>L. monocytogenes</i>	<i>E. coli</i> <i>S. enteritidis</i>	<i>C. albicans</i> <i>Trichophyton mentagrophytes</i>	[10,11]
	Cinnamon	<i>Lactobacillus delbrueckii</i> <i>L. monocytogenes</i> <i>S. aureus</i>	<i>E. coli</i>	<i>Saccharomyces cerevisiae</i>	[12]
	Oregano	<i>L. monocytogenes</i> <i>Bacillus subtilis</i> <i>S. aureus</i>	<i>E. coli</i> <i>Pseudomonas aeruginosa</i> <i>Salmonella enterica</i> <i>S. typhimurium</i>	<i>C. albicans</i> <i>P. digitatum</i> <i>S. cerevisiae</i>	[10,13]
Plant Extracts	Grape seed	<i>L. monocytogenes</i>	<i>S. typhimurium</i> <i>E. coli</i> O157:H7	<i>Candida maltosa</i>	[14,15]
	Olive leaves extracts	<i>B. cereus</i> <i>L. monocytogenes</i>	<i>E. coli</i> <i>E. coli</i> O157:H7	<i>Candida oleophila</i>	[16]
	Rosemary	<i>B. cereus</i> <i>L. monocytogenes</i> <i>S. aureus</i>	<i>E. coli</i> <i>S. enteritidis</i> <i>S. typhimurium</i>	<i>Aspergillus</i> <i>S. cerevisiae</i> <i>C. albicans</i>	[17]
Animal origin					
Lysozyme	Chicken eggs Vegetables Insects	<i>Bacillus</i> <i>Clostridium</i> <i>L. monocytogenes</i> <i>L. spp.</i>	Weak inhibitory effects	<i>Aspergillus</i> , <i>Candida</i> , <i>Fusarium</i> , <i>Sporothrix</i> , <i>Paecilomyces</i> , <i>Penicillium</i> , <i>Saccharomyces</i> .	[18]
Lactoferrin	Milk	<i>B. cereus</i> <i>Bacillus stearothermophilus</i> <i>L. monocytogenes</i>	<i>E. coli</i> <i>S. enteritidis</i> . <i>Klebsiella</i> spp. <i>S. enteritidis</i>	No effect	[18]
Chitosan	Shellfish	<i>S. aureus</i> <i>L. monocytogenes</i> <i>B. cereus</i>	<i>S. typhimurium</i> <i>Yersinia enterocolitica</i>	<i>Aspergillus flavus</i> <i>S. cerevisiae</i> <i>Zygosaccharomyces bailii</i>	[19]

Table 2. Cont.

Antimicrobial Compound	Main Source	Target Microorganism			Reference
		Gram-Positive Bacteria	Gram-Negative Bacteria	Fungi	
					Microbial origin
Natamycin	<i>Streptomyces natalensis</i>	No effect	No effect	<i>Penicillium candidum</i> <i>Aspergillus flavus</i> <i>S. cerevisiae</i> <i>Byssoschlamys nitvea</i> <i>Hemerocallis fulva</i> <i>Zygosaccharomyces bailii</i>	[20]
Nisin	<i>Lactococcus lactis</i>	<i>C. botulinum</i> (spores) <i>L. monocytogenes</i> <i>S. aureus</i> <i>Lactobacillus plantarum</i>	No effect	No effect	[21]
Polylysine	<i>Streptomyces</i>	<i>S. aureus</i> <i>Lactococcus lactis</i> <i>B. subtilis</i>	<i>E. coli</i> <i>S. typhimurium</i>	<i>Aspergillus niger</i> <i>T. mentagrophytes</i>	[22]

3. Essential Oils as Food Preservatives: Current Status and Challenges

Essential oils (EOs) are synthesized as secondary metabolites in different plant organs to provide protection against external factors [23]. They have strong antibacterial activity and are often used as sanitary products and cosmetics, and so on [6]. EOs are naturally derived substances that can be distilled by water vapor from different tissues of plants, such as flowers, leaves, stems, roots, and fruits. EOs are volatile, usually lipophilic, with a low molecular weight and a strong odor [23]. In addition, most of the EOs have low mammalian toxicity and are ephemeral in nature, which makes them relatively safe for the health and environment [24].

3.1. Advances in Research on EOs as Antimicrobial Agent

A large body of literature has shown that EOs are proven to have antimicrobial properties, allowing them to be used for the preservation of several food products [6]. Many EOs have been tested in vitro against different microorganisms, such as bacterial cells to fungi as summarized in Table 3. The chemical constituents of plant EOs are mainly divided into four types: terpenoids, aromatic compounds, aliphatic compounds, and sulfur-containing nitrogen compounds [23]. The bacteriostatic mechanism of different components is usually not a single mode of action, but a multi-point mechanism of action [25,26]. There are two main ways in which plant EOs and their main components affect microorganisms: one is to change the morphological structure and composition of microbial cells and mycelia, such as cell membrane, cell wall, and organelles [27]; the second is to reduce or inhibit the production and germination of spores, reducing or blocking the pathogens from continuing to harm the offspring [28].

Table 3. Summary of the main recent studies concerning the antibacterial mechanisms and effects of essential oils (MIC: Minimum Inhibitory Concentration).

Essential Oils	Bacteriostatic Mechanism	Antimicrobial Activity
Cumin	Cuminaldehyde and cuminalcohol can destroy cell membrane	Antimicrobial activity against <i>Aspergillus flavus</i> (MIC: 650 µg/mL) [29]; cumin EOs (≥30 µL/100 mL) combined with nisin (≥0.5 µg/mL) can inhibit <i>S. typhimurium</i> ; cumin EOs (≥15 µL/100 mL) in combination with nisin (≥0.5 µg/mL) inhibited <i>S. aureus</i> [30]; inhibition of <i>S. typhimurium</i> and <i>E. coli</i> (MIC: 0.125% and 0.250%, v/v) [31].
Oregano	Caused by carvacrol and thymol	2% (w/v) oregano EOs inhibited <i>S. aureus</i> , <i>E. coli</i> , and <i>Pseudomonas aeruginosa</i> (inhibition zone diameters: 342.36, 21.53, and 9.70 mm, respectively) [32]; antimicrobial activity against <i>L. monocytogenes</i> , <i>S. typhimurium</i> , <i>E. coli</i> , etc. [33].
Lemon	Limonene inhibits cellular respiration	Antimicrobial activity against <i>C. jejuni</i> C338, <i>C. coli</i> , and <i>B. cereus</i> (inhibition zone diameter: 28.3, 35.3, and 23.7 mm, respectively) [34]; inhibition of <i>S. cerevisiae</i> MB-21, fission yeast MB-89, <i>Geotrichum candidum</i> MB-102, and <i>Pichia pastoris</i> MB-196 (MIC: 0.245–0.51, 0.06–0.25, 0.5–1.0, and 0.5–0.73 µL/mL, respectively) [35].

Table 3. Cont.

Essential Oils	Bacteriostatic Mechanism	Antimicrobial Activity
Cinnamon	Cinnamaldehyde can act on enzymes and cell wall. It can alter cell membrane permeability, inhibit ATPase activity and amino acid synthesis, and deplete proton potential energy	0.1–0.3% (w/v) cinnamon EO inhibited <i>L. monocytogenes</i> (6.0 log CFU/mL) [36]; 2.0% (w/v) cinnamon EO inhibited <i>E. coli O157:H7</i> (2.0 log CFU/mL) [37].
Marjoram	Ethanol steroids (protein denaturation and dehydration), terpin-4-opening (destruction of cell membrane results, leakage of intracellular substances) [38]	Antimicrobial activity against <i>S. cerevisiae</i> , <i>Fission yeast</i> , <i>Geotrichum candidum</i> , and <i>Pichia pastoris</i> (MIC: 0.5–1.0, 0.0625, 0.5 and 0.5 µL/mL, respectively) [35].
Peppermint	Caused by menthone, menthol, menthyl acetate, limonene and β-pinene	Gaseous peppermint EOs inhibits <i>E. coli O157:H7</i> (MIC: 0.625 µL/mL); inhibition of <i>S. aureus</i> , <i>Bacillus cereu</i> , <i>E. coli MTCC108</i> , and <i>Yersinia colitis</i> (0.10%: 1.3–4.8 log CFU/ mL, 0.20%: 1.8–5.7 log CFU/mL, 0.25%: 0.4–2.6 log CFU/mL and 0.15%: 1.1–5.2 log CFU/mL, respectively) [39].
Clove	Eugenol can destroy the structure of cells	Antimicrobial activity against <i>S. mutans</i> (MIC: 1000 µg/mL) [40], <i>L. monocytogenes</i> (1.6–4.3 log CFU/mL), <i>L. sinensis</i> (0.2–0.8 log CFU/mL) [37].
Garlic	Organic sulfur compounds destroy cell membrane and intracellular macromolecular structure	Inhibition of <i>E. coli O157:H7</i> , <i>S. aureus</i> , <i>S. enteritidis</i> , <i>L. monocytogenes</i> , and <i>L. plantarum</i> (inhibition zone diameter: 9.3–11.36, 11.36–13.45, 8.43–10.48, 9.89–11.96, and 6.13–9.21 mm, respectively) [41].
Clary sage	Ethanol steroids (protein denaturation and dehydration), linalool (destroying cell membrane structure, inhibiting Gram-negative bacteria), caryophyllene (inhibiting Gram-positive bacteria) [35]	Antimicrobial activity against <i>S. cerevisiae</i> , <i>Fission yeast</i> , <i>Geotrichum candidum</i> , and <i>Pichia pastoris</i> (MIC: 0.5–1.0, 0.375–0.875, 1.0, and 0.5–1.0 µL/mL, respectively) [35]; 20,000 µg/mL EOs prolonged the lag phase of <i>E. coli</i> (3.20–6.40 h) and inhibited <i>L. monocytogenes</i> [42].
Rosemary	Camphor and eucalyptus oil have an oxidizing effect and enhance the antibacterial activity of terpenoids	Antimicrobial activity against <i>S. aureus</i> , <i>L. monocytogenes</i> , <i>E. coli</i> , and <i>Vibrio cholerae</i> [42].

3.2. Challenges in the Use of EOs as Food Antimicrobials

Due to their “green” nature, essential oils have received consumer attention for their use as a substitute for traditional food preservatives, which is a considerable market. However, EOs have a variety of internal and external critical challenges hindering their process as food preservatives: (i) EOs normally have low solubility in aqueous mediums and the reached concentrations are not able to exert significant biological activities; (ii) the scarcity of raw materials means that the quantity of EO obtained after extraction is generally insufficient for commercial applications; (iii) the high processing cost are also some of the major challenges; (iv) EOs are unstable due to their volatilization and oxidation, and thus are difficult to store, which may change the functional composition of active compounds (in actual production, it is necessary to rely on suitable carriers or adopt appropriate methods to achieve good antibacterial and fresh-keeping effects); (v) some EOs have a strong aroma even at low doses (in food systems, EOs can bind to lipids, proteins, and carbohydrates, so for a certain dose to achieve antibacterial effects, it may have a negative impact on food sensory qualities) [29]; and (vi) the collection and identification of plants, as well as the quality of raw materials, require a more systematic evaluation, especially safety assessment.

There is still a lack of systematic research on the effects of plant EOs and their main components on the quality of food, fruit, and vegetable flavor [43]. Until now, most of the current studies are studying EOs as a whole or selecting single components in EOs. However, there are few studies about the interactions between various components and different EOs. Most of the research is carried out in the presence of a single microorganism and constant environmental conditions [26]. There are few studies on the coexistence of various microorganisms and the mode of action in food systems, because temperature, moisture, pH, and other factors in food products have a certain influence on the bacteriostatic effect and can be a barrier factor. Therefore, it is necessary to conduct an in-depth study on the synergistic antimicrobial effect of the barrier factors [25].

The main challenges of using EOs as food-preserving agents can be overcome to some extent by using nanoencapsulation, rather than applying the EOs directly to food products as free antimicrobials. The incorporation of EOs into nanosized encapsulation systems can significantly improve their physical properties, such as dispersibility, dispersion stability, turbidity, and viscosity, and thus promote their functional activities, in comparison to free EOs [44]. Moreover, nanoencapsulation can also be used to protect EOs against oxygen, light, pH, moisture, and degradation during processing and storage; to improve the solubility of lipophilic compounds in aqueous media; to mask unpleasant taste and aroma; and to release them in the desired location at an appropriate rate through efficient design of the capsules and proper selection of wall materials [45].

4. Nanoencapsulation versus Microencapsulation

In order to enhance the applicability of active compounds for food products, or to protect them against deteriorating environmental conditions, encapsulation is considered a viable alternative [46]. In general, encapsulation is defined as a carrier matrix in which a bioactive substance is entrapped, which allows one to control the rate of bioactive release [47]. A comparison of the functionality of micro- and nanoencapsulation has been reported by [48], as shown in Figure 1.

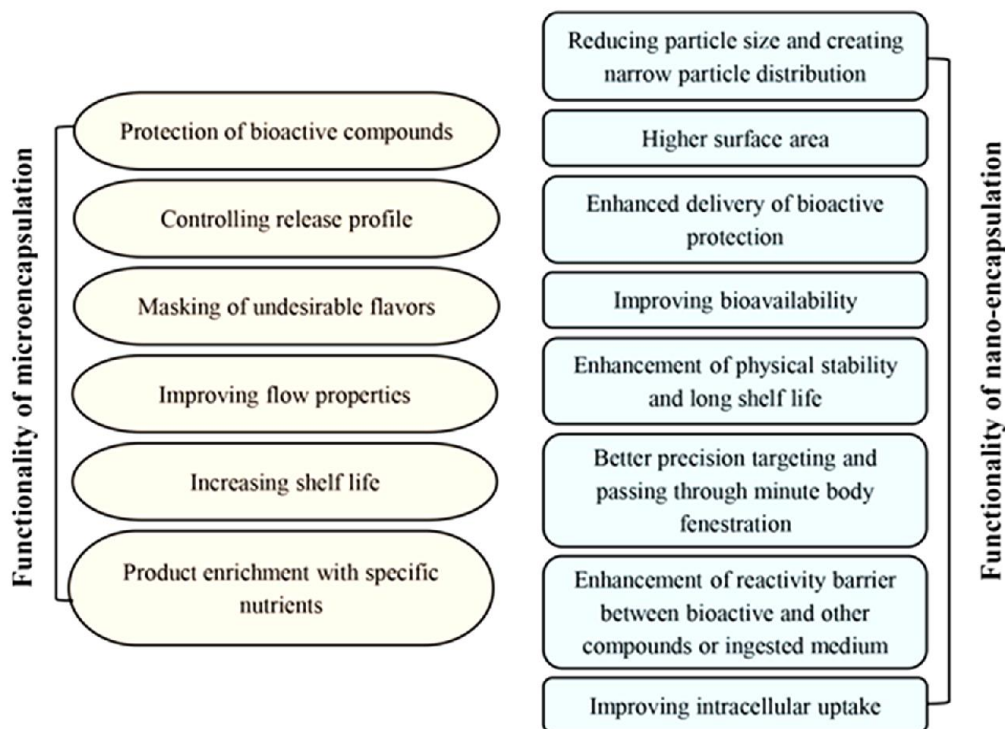


Figure 1. Advantages of nano- and microencapsulation [48]. Reprinted with permission from Ref. [48]. Copyright 2018 Elsevier.

Particle size has been shown to be an important factor affecting the functional characteristics of capsules [49]. Nanoencapsulation is considered to be the use of a carrier with a size of less than 1 micron (1000 nm), possessing different properties than ordinary encapsulation. According to some specific regulations, however, particularly in the pharmaceutical field, the size of carriers should be less than 100 nm for them to be considered

as nanocapsules [50]. The nanometric size of delivery systems can increase the surface area and consequently the dispersion in the food matrices. They are easier to disperse and to suspend in water to form uniform and stable colloidal suspensions and may have good sustained-release effects in comparison to microsized delivery systems. Based on their smaller size, nanocapsules have the potential to increase the passive cellular absorption mechanisms, promoting the effective release of active substances inside the target cells, and consequently increasing the efficiency of active substances and their bioavailability. Meanwhile, nanoparticles may penetrate into the tissues (such as the liver) through the capillaries, and are absorbed by the cells in the tissues; thus, the active substance can be efficiently delivered to the target cells in the body [51]. In the case of emulsions-based delivery systems, there are some interesting physical properties that can be used to distinguish nano- and microemulsions. Microemulsions generally exhibit multiple scattering of visible light, which means they have an opaque white appearance. Conversely, nanoemulsions are much smaller than visible wavelengths, and therefore, appear almost optically transparent [52]. This character can be considered as a very advantageous feature for nanoemulsions in the beverage industry.

Despite the numerous technologies for the encapsulating of biologically active compounds which have been studied, only a few techniques, namely spray-drying and freeze-drying, are widely applied in the food industry [53]. Typically, emulsification technology is the first step of encapsulation. There are two types of emulsification techniques used to produce encapsulation systems: a top-down approach and a bottom-up approach. The top-down methods involve changing large structural materials into small structures by reducing the size, and shaping the structure through external mechanical destructive forces. Top-down methods generally include high-pressure homogenization, microfluidization, and microchannel homogenizers [48]. They are commonly used for the encapsulation of hydrophilic and hydrophobic compounds, but have less control over the particle size and structure of the produced emulsion, and are only suitable for a limited type of matrix [54]. The bottom-up approach generally includes self-assembly, phase inversion, and spontaneous emulsification, which are affected by factors such as pH, temperature, concentration, and ionic strength. Meanwhile, low-energy methods are also used as preparatory steps for other nanoencapsulation methods (e.g., spray-drying, complex coacervation, extrusion, electro-spinning, and electro-spraying [55]). They allow better control of the properties of the capsules and consume less energy. However, low-energy methods require large amounts of stabilizers and are used with limited types of oils and surfactants. [56]. Various techniques for encapsulating have been proposed in the literature, but none of them can be considered as standard and suitable for the encapsulation of all biologically active compounds [55]. However, the best strategy could be selected according to the properties of the core compound and the encapsulated material, including their molecular weight, polarity, solubility, particle size distribution, and food matrix composition.

To date, for microencapsulation, a number of methods have been developed. However, for nanoencapsulation, the method is more complex than those used for microencapsulation [48]. Table 4 summarizes the commonly used encapsulation techniques to encapsulate active substances and lists some recent research reports about nano- and microencapsulation.

Table 4. Summary of recent studies on micro- and nanoencapsulation of food bioactive compounds.

Encapsulation Method	Description	Nanoencapsulation	Microencapsulation
Emulsification	Emulsification is a process of mixing two immiscible solvents, and the resulting product is referred to as an emulsion. It can be divided into top-down approaches (high-shear stirring, high pressure homogenization, microfluidization, and ultrasonication) and bottom-up (phase inversion temperature, emulsion phase inversion, and spontaneous nanoemulsification) approaches.	Vitamin E encapsulated by Tween-80 [57]; vanillin encapsulated in poly (lactic-acid) nanoparticles [58]	Curcumin encapsulated by Tween 80 and polyglycerol polyricinoleate [59]; lycopene encapsulated in plant (soy and pea) or dairy (whey and sodium caseinate) proteins [60]
Spray drying	The basic theory of spray-drying is to feed the liquid into a drying chamber in the form of tiny droplets containing biologically active compounds, supplying hot air to the drying chamber, forming microcapsules in the drying chamber, and recovering them through a cyclone.	Folic acid encapsulated by whey proteins and resistant starch [61]; curcumin encapsulated by chitosan/Tween 20 [62]	Propolis extracts bioactive compounds encapsulated by maltodextrin matrices with or without nature gums [63]; cocoa volatile compounds encapsulated by maltodextrins and modified starch [64]
Freeze drying	The basic principle of freeze-drying is to freeze water contained in a solution or suspension and then evaporate the water molecules from the solution or suspension.	Fish oil encapsulated by poly-ε-caprolactone and Pluronic F68 [65]	Blackberry by-product extract encapsulated by maltodextrins [66]; flaxseed oil encapsulated by sodium alginate, whey protein, and maltodextrin [67]
Extrusion	Extrusion technique involves the injection of a bio-based solution into another solution to promote gelation and produce a hard and dense encapsulation system.	Seed oils encapsulated by sodium alginate and high methoxyl pectin [68]	Canola oil encapsulated by alginate and high methoxyl pectin [69]; quercetin encapsulated by carnauba wax, shellac, or zein [70]
Complex coacervation	Coacervation is a well-known implemented technique to produce micro- and nanosystems. The basic mechanism is the formation of an emulsion by electrostatic attraction between oppositely charged molecules to produce the encapsulating structure.	Folic acid encapsulated by casein nanoparticles [71]; anthocyanins encapsulated by whey protein isolate and beet pectin [72]	Algal oil encapsulated by soy protein isolate and chitosan [73]; β-carotene encapsulated by casein and gum tragacanth [74]
Electro-spinning and electro-spraying	They are two modes of electrohydrodynamic processes that use a charged jet to rotate or spray a polymer solution to produce fibers or particles.	Rose hip seed oil encapsulated by zein prolamine fiber [75]; β-carotene encapsulated by zein prolamine fiber [76]	D-limonene encapsulated by seed gum and tween 20 [77]; fish oil encapsulated by a composite zein fiber [78]

5. Main Strategies for Nanoencapsulation of Essential Oils

Nanoencapsulation has promising applications to solve the existing problems of essential oils (EOs), since it has been shown to be an effective means to enhance the stability of EOs against degradation during storage, mask unpleasant taste, and release the antimicrobial at a controlled rate [44,79]. In this review, data surveys in the literature have found the most applied methods for essential oils and various types of nanocarriers, which are summarized in Figure 2. According to the different encapsulating materials, they are mainly divided into two categories: lipid-based nanoencapsulation systems and polymer-based nanoencapsulation systems. In addition, some nanoencapsulation of antimicrobial agents can be implemented with specially developed equipment, such as electro-spinning, electro-spraying, and nanospraying dryer.

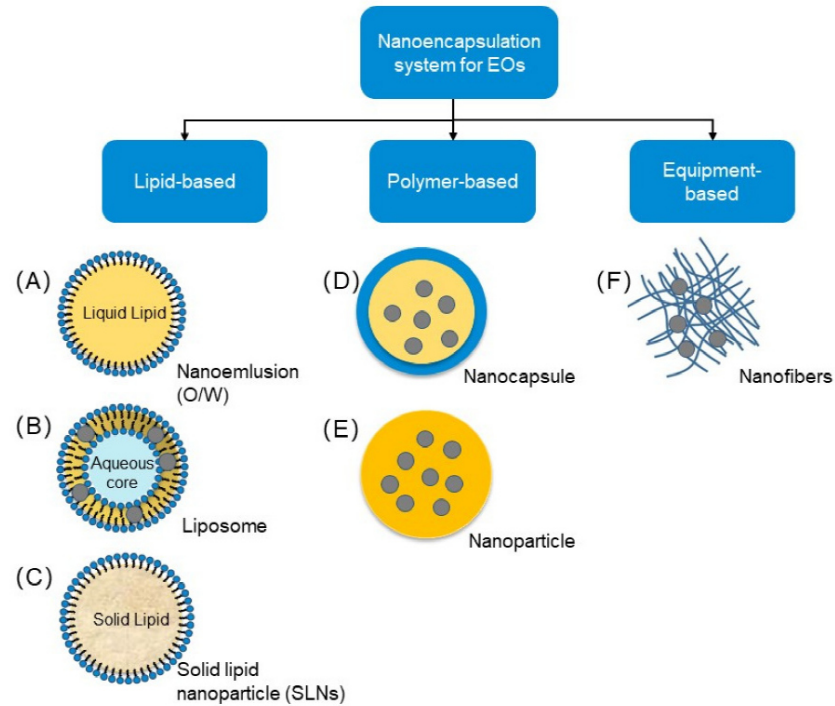


Figure 2. Schematic representation of the different nanoencapsulation systems for EOs.

5.1. Biopolymer-Based Nanoencapsulation

Biopolymers are widely used as a wall material for the encapsulation of antimicrobial agents. Various sources serve as the origin of the biopolymer, which can be used in its native form or modified to acquire certain required properties. In general, EOs can be encapsulated in food-grade biopolymers such as proteins (whey proteins, caseins, zein, gelatin, etc.) and polysaccharides (starch, chitosan, cyclodextrin, pectin, alginate, etc.), as well as derived composite materials [2]. Biopolymer-based nanoencapsulation can produce nanocapsules (Figure 2D) or nanospheres (Figure 2E). In nanocapsules, the oily core is surrounded by polymer walls, while nanospheres are matrix systems in which the core is dispersed in the polymer matrix [80]. Several different technologies are normally used for the production of nanocapsules or nanospheres, such as complex coacervation [71], freeze-drying [81], spray-drying [61], and ionic gelation [82].

5.1.1. Polysaccharide-Based Biopolymers

Polysaccharide-based biopolymers can be classified as homopolysaccharides or heteropolysaccharides depending on the number and types of monosaccharide units constituting the chain. Because of the different chemical properties of the monosaccharide units, the polysaccharides also have different degrees of polymerization (unit monosaccharide number), molecular weight, hydrophobicity/hydrophilicity, electrostatic charge, gelation properties, and viscosity, which are different from each other. Polysaccharides used for encapsulation usually have the following advantages: low toxicity and low cost, high stability in a wide pH range, and good biodegradability [81].

Cyclodextrins (CDs) are cyclic oligosaccharides with a truncated cone shape and are derived from starch, which is a traditional wall material used to prepare nanocapsules [83]. In this process, the inner side of β -cyclodextrin is an inner wall of a cavity formed by a combination of a hydrophobic epoxy group and a C-H bond, and the outer side of the

ring is a primary alcoholic hydroxyl group on C₆, which exhibits a hydrophobic inner side and a special structure of the outer hydrophilic structure. The molecular structure can form an inclusion complex with many guest molecules, and the core material is coated in the cavity, which can slow down the reaction with the control of light and oxygen. Meanwhile, β-cyclodextrin can mask the pungent odor of some oils, compared with other wall materials. Lee et al. [84] used β-cyclodextrin as a cryoprotectant to prepare eugenol nanocapsules by the emulsion diffusion method. The morphology and structure of the nanocapsules were analyzed by scanning electron microscopy. The results showed that β-cyclodextrin can be used as a cryoprotectant to maintain the physical stability of eugenol and protect eugenol from freezing damage [85].

Chitosan (CS) is a cationic polysaccharide found in nature, which is obtained by deacetylation of chitin. CS is suitable for the preparation of nanocarrier systems because of its biodegradability, pH sensitivity, and easy chemical modification [86]. Although chitosan nanoparticles can be prepared by different methods, ionic gelation is the most widely used method. The method is simple and mild, and the activity of the encapsulated substances can be maximized. Mohammadi, Hashemi et al. [87] prepared chitosan nanoparticles (125–175 nm) by this method, and their results showed that encapsulated EOs improved stability and enhanced antifungal activity against *Botrytis cinerea*. In another study, ionic gelation, applied to prepare O/W emulsion, was carried out to obtain chitosan nanoparticles enclosing thyme essential oil [88].

Starch is an interesting renewable polysaccharide and one of the main sources of glucose in the human body. Moreover, the modifications of its physical, chemical, or biochemical characteristics can impart a variety of unique properties to this biopolymer. Therefore, starch and/or its derivatives are often used for the encapsulation of active substances such as carotenoids and essential oils [89]. Chin et al. [90] obtained starch nanoparticles (300–400 nm) by dissolving sago starch in NaOH/urea, adding the obtained starch solution dropwise to absolute ethanol under magnetic stirring, and centrifuging the obtained suspension.

5.1.2. Protein-Based Biopolymers

Proteins are promising nanocarriers for delivery purposes due to their interesting functional properties: their molecular structures are dependent on their amino acid sequence and environmental factors such as pH, ionic strength, temperature, good emulsifying capacity, solubility, stability, and so on, as well as their ability to modify the texture, the flavor, and the color of the food matrices into which they will be incorporated [2].

Casein is an amphiphilic protein that has a strong tendency to spontaneously self-assemble into micelles in aqueous solution, and it can also interact with other proteins or organic compounds to form micellar complexes. Casein or caseinate have been found to be of valuable use as nanoencapsulating natural biopolymers due to their balanced hydrophobic and hydrophilic amino acid moieties. Zimet et al. [91] self-assembled omega-3 polyunsaturated fatty acids and casein to prepare nanomicelles with a particle size of 50–60 nm. Narayanan et al. [92] used a polylactic acid-glycolic acid copolymer to assemble with casein to prepare nanoparticles with a distinct core-shell structure. In another study, the authors used casein micelles and nano-gold particles to obtain casein-nano-gold-conjugated nanoparticles with a particle size of about 200 nm [93]. The interactions between iron oxide nanoparticles and casein micelles were also studied to prepare iron oxide/casein composite nanoparticles with an average particle diameter of 38 nm [94].

Zein is a group of prolamins that are insoluble in water. It has both hydrophilic and lipophilic properties and good biocompatibility. Its hydrophobic region can be polymerized into colloidal particles with a diameter of 50–550 nm. Using the phase separation technique, [95] encapsulated three essential oils—oregano, red thyme and cassia seed essential oils—into zein nanospheres. Whey proteins have been reported as an effective encapsulation system for different hydrophobic antimicrobial agents, and they were widely used in the design of protein-polysaccharide complex systems [96]. Polysaccharides-protein

encapsulation systems are more valuable than pure single biopolymer systems because of their higher chemical and colloidal protection. Ghasemi et al. [97] embedded orange peel oil into whey protein and pectin matrices by complex coacervation. Their results showed that the obtained nanocomposites had particle sizes of 360, 182, and 185 nm at pH 3, 6, and 9, respectively. Encapsulating materials based on complexed biopolymers are discussed in the next section.

5.1.3. Complexation of Biopolymers

The combined use of various biopolymers provides different functions and promising properties compared to a single biopolymer [98]. Biopolymer nanoparticles can be synthesized from food-grade biopolymers by self-association of individual biopolymers or by phase separation in biopolymer mixtures [99]. The ability to control and modify the interactions involved can help food technicians in designing new molecular structures to develop foods with more desirable structural properties.

Among the cited techniques, the most widely used to prepare nanocapsule systems is the complex coacervation method, as shown in Figure 3. Two kinds of polyelectrolytes with opposite charges are used as the wall material, and the core material is dispersed in the wall material solution. By changing the pH value, temperature, and concentration of the solution, or by adding an inorganic salt electrolyte to modify the electrostatic interactions in the system, the solubility of the wall material can be reduced to form nano/microcapsules. The commonly used polyelectrolytes are oppositely charged proteins and polysaccharides, such as gelatin, gum Arabic, carboxymethyl cellulose, alginate, chitosan, and polylysine. To obtain stable complexes, it is important to control the environmental conditions to form oppositely charged polymers with sufficient intensity of ionic interactions. The process of the complex coacervation method is relatively mild. Esfahani et al. [100] successfully prepared nano-sized fish oil capsules (26–114 nm) with high encapsulation efficiency using gum Arabic and gelatin.

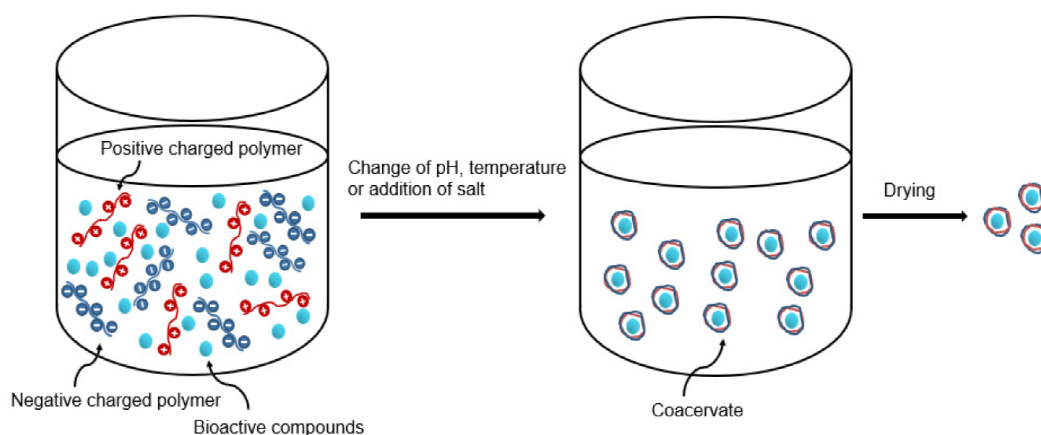


Figure 3. General process scheme for capsule preparation by complex coacervation.

5.2. Lipid-Based Nanoencapsulation

Although biopolymer-based nanoencapsulation methods have different advantages, they do not have the potential for mass production due to the need to apply different complicated chemical or thermal processes for monitoring. Lipid-based nanocarriers have the potential for industrial production with the advantages of high encapsulation efficiency and low toxicity [101]. Lipid-based nanoencapsulation, such as nanoemulsions, liposomes, and solid lipid nanoparticles, are formed from lipid components, which are

generally biodegradable and are believed to be available in the pharmaceutical and food industries [101].

5.2.1. Nanoemulsions

Nanoemulsions (Figure 2A) are nanoscale droplets of a multiphase colloidal dispersion formed by dispersing one liquid in another immiscible liquid by mechanical agitation [102]. Depending on the hydrophobic or hydrophilic nature of the antimicrobial agent, an O/W or W/O emulsion system can be used to stabilize the oil-soluble or water-soluble agent, respectively. Emulsions containing nanodroplets with a size range less than 100 nm have properties different from those of conventional emulsions, especially the viscosity, color, and dispersion [52]. The emulsion stability is also different. In fact, while microemulsions are thermodynamically stable and form spontaneously, nanoemulsions are kinetically stable [103]. On the other hand, nanoemulsions are generally prepared by both top-down (high-energy) and bottom-up (low-energy) approaches, while microemulsions are produced by low-energy approaches only [104]. Top-down approaches use mechanical energy to form nanodroplets; however, low-energy methods are based on changes in process parameters, such as temperature and phase composition, to achieve nanoemulsions with less energy input [105].

For high-energy methods, the most generally used methods are high-shear mixing, high-pressure homogenization, microfluidization, and microchannel homogenization [2]. The emulsification process is divided into two stages: (i) breaking down the coarse droplets into smaller droplets, and (ii) absorbing the emulsifier onto the newly formed interface to prevent re-coalescing [106]. Nanoemulsions obtained by high-energy methods are thermodynamically unstable colloidal systems dispersed in the second phase in the form of 50–1000 nm droplets. Since the droplets of the nanoemulsions are small, they have kinetic stability under certain conditions, and phase separation, flocculation, coalescence, or precipitation in the system will not occur for a long time. Hashtjin and Abbasi [107] used ultrasonic as the external energy source, and used the response surface method to optimize the nano-emulsification of orange peel EOs. The results showed that when the ultrasonic power was 94%, the ultrasonic time was 138 s, and when the ultrasonic treatment temperature was 37 °C, the prepared orange peel EOs nanoemulsion can reach a particle size of 12.68 nm. Nirmal, Mereddy et al. [108] successfully incorporated lemon myrtle EOs (LMEO) into a water system by using ultrasonication to form a nanoemulsion. The minimum average droplet size achieved for LMEO was 16.07 ± 0.13 nm, and LMEO nanoemulsions showed higher antibacterial activity than LMEO alone. For low-energy methods, the most commonly used techniques are phase inversion temperature, emulsion phase inversion, and spontaneous nanoemulsification. Nanoemulsions obtained by low energy are thermodynamically stable systems formed by the action of oil phase, water phase, and a large amount of emulsifier or surfactant. Meanwhile, the compatibility is better, and the droplets are uniform and small in size [109]. A limitation of this approach is that a large amount of organic solvent surfactant is required to prepare the emulsion, so the application of the low energy method is limited in the food field. Jun et al. [110] used Span-80 and Tween-80 as surfactants and glycerin as a co-surfactant to prepare grapefruit EOs oil-in-water type nanoemulsions. The particle size was about 21 nm, and the stability was good. Xue et al. [111] used casein and soy lecithin to finely emulsify thyme oil by nanoemulsification and obtained a thyme oil nanoemulsion with better antibacterial activity than free oil. In another study, the authors successfully prepared a thyme EOs nanoemulsion with a particle size of 150–250 nm using triglyceride as an additive [112].

5.2.2. Nanoliposomes

Nanoliposomes (Figure 2B) (also known as lipid vesicles) are lipid-based encapsulation carriers commonly used in foods and drugs [113]. Their structure is a phospholipid bilayer. Liposomes have many excellent properties, such as the ability to bring drugs into cells (cell targeting), biological affinity, and low drug toxicity, as well as increasing drug stability

and tolerance [114]. Compared to common liposomes, nanoliposomes can simultaneously embed two active substances with different solubilities [115]. Another important advantage of nanoliposomes is targeting, delivering and releasing their load at target sites in vivo and in vitro [116]. In order to encapsulate lipophilic antimicrobials and essential oils into liposomes, these compounds should be pre-dissolved together with the phospholipids. This procedure needs to input energy, allowing the phospholipids to aggregate to form a double-layered capsule and to obtain a thermodynamic equilibrium in the aqueous phase to attain the nanoscale size [117]. Various nanoliposome preparation techniques have been employed, including lyophilization, freezing, spray-drying, and supercritical fluid (SCF) technology [101]. Nieto et al. [118] used a membrane dispersion ultrasonic method to prepare liposome-embedded EOs, and found that the liposomes played a better role in the protection of foods, especially meat. Bai et al. [119] used ethanol injection combined with spray-drying technology to prepare liposome-encapsulated coix seed oil, thus overcoming the shortcomings of coix seed oil instability and its poor water solubility, and enhancing its absorption in the intestine. Detoni et al. [120] developed a liposome-based carrier agent for the *Zanthoxylum tinguassuiba* EO in multi- and unilamellar vesicle, and they observed that the carrier system successfully enhanced the thermal stability and bioactivity of EO. The liposome-encapsulated nisin fully inhibited the growth of *E.coli* O157:H7 at concentrations lower than that reportedly required for unencapsulated nisin.

5.2.3. Solid Lipid Nanoparticles

Solid lipid nanoparticles (SLNs), also known as nanostructured lipid carriers, are suspensions of nano-sized solid lipid particles dispersed in an aqueous medium. SLNs (Figure 2C) are mainly prepared from solid lipids, such as fatty acids (e.g., palmitic acid), triglycerides (e.g., trilaurin), steroids (e.g., cholesterol), and partial glycerides (e.g., glyceryl monostearate) [114]. From a formulation point of view, SLNs are very similar to emulsions, but they are obtained using a lipid that is solid at room temperature to form a lipid phase, which results in solid dispersed particles rather than oil droplets. Due to the solid nature of SLNs, they have higher stability and longer storage time than aqueous liposomes [121]. The volatility and instability of EOs could be significantly reduced by SLNs systems [122,123]. Nevertheless, there are only two basic production techniques for large-scale production of SLNs in food processing: thermal homogenization and cold homogenization [124]. Nasser et al. [123] prepared *Z. multiflora* essential oil-loaded SLNs as delivery agents of eugenol using glyceryl monostearate (lipid phase), Tween 80, and Poloxamer (surfactant). Their results showed that solid lipid nanoparticles exhibited stronger antifungal activity at low doses than free oil. Prisa et al. [125] prepared cholesterol-loaded curcumin SLNs using the high-pressure homogenization method. The prepared SLNs showed a particle size range of 112–163 nm, and the drug embedding rate was up to 71%. The results have shown that cholesterol lipid structure leads to enhanced permeability of bacteria, and this can improve the antibacterial ability of curcumin.

5.3. Equipment-Based Nanoencapsulation

In order to encapsulate bioactive compounds, it is usually necessary to use some general equipment, including homogenizers, grinders, mixing equipment, and so on. However, certain specific requirements, such as nanofibers and nanofibrous scaffolds, can be implemented only by specialized developed equipment such as electrospinning and electrospray (Figure 4) [126]. Electrospinning and electrospray are two types of electrohydrodynamic procedures that use charged jets to rotate or spray a polymer solution to produce fibers or particles. The prospect of using both technologies in food preservation is promising due to the following advantages: amendable size with large surface area, ability to carry heat-sensitive compounds, and possibility of mass production. Electrospinning technology has been used to prepare antimicrobial nanofibers (Figure 2F) to encapsulate bacteriocin in probiotics for sustained release during food processing and storage [127]. Ghayem-pour and Mortazavi [128] successfully encapsulated peppermint essential oil into alginate

biopolymer using the electro-spraying method. Their results showed that the peppermint EOs did not degrade during the encapsulation process and showed a high encapsulation efficiency (96.4%).

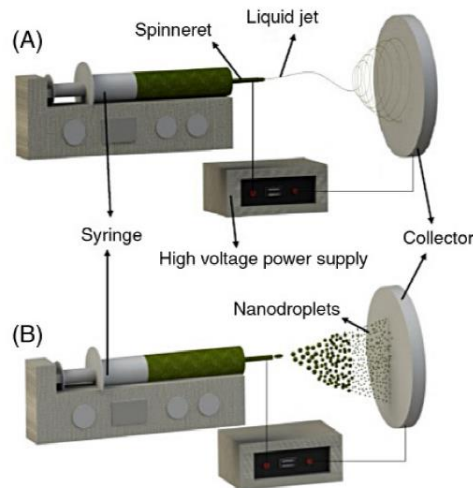
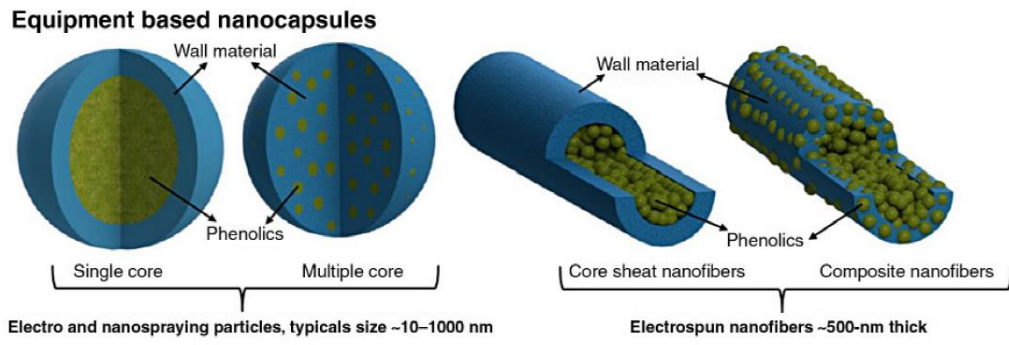


Figure 4. Examples of equipment-based nanoencapsulation: (A) electrospinning and (B) electrospraying [129]. Reprinted with permission from Ref. [129]. Copyright 2017 Elsevier.

6. Effect of Nanoencapsulation on the Antimicrobial Activity of Essential Oils

As mentioned above, the direct application of essential oils as food antibacterial agents in the food industry faces challenges such as water insolubility, physical and chemical degradation, and effects on the sensory properties of foods. In the past few decades, nanotechnology has gradually become one of the most important technologies in the food industry, especially to improve the anti-corrosion potential of EOs, which may solve these shortcomings in their application [79]. Table 5 reports the latest studies on the efficacy of encapsulated EOs and their bioactive compounds against foodborne pathogens.

Aguitar et al. [130] and Pesavento et al. [131] reported studies about the antibacterial effects of clove basil, left-handed aroma, oregano, rosemary, and thyme EOs against *Staphylococcus aureus*, *Escherichia coli*, *Pseudomonas aeruginosa*, and *Listeria*. They found the low water solubility and oxidizability of EOs reduce the antibacterial activity of EOs. It has been reported that the EOs are encapsulated by a suitable wall material to prepare nano-

sized particles, which can improve the low water solubility of the EOs and improve the stability of its biological activity, thereby improving the antibacterial properties of EOs [132]. Salvia et al. [133] found that emulsified citronella oil and clove EOs with nanoemulsification had a stronger antibacterial effect on *Escherichia coli*. Li et al. [134] studied the effect of surfactant and oil phase composition on the antibacterial activity of eugenol cyanophenol nanoemulsion. It was found that the antibacterial activity could be strengthened after nanoemulsification. In the process of nanoemulsification of eugenol, when adding the ionic surfactant (Tween-80), the antibacterial activity of the nanoemulsion is higher than that of the added non-ionic surfactant (dodecyl sulfate) during the ripening process. Moreover, the lower the amount of soybean oil added to the clove oil, the stronger the bacteriostatic action against *Escherichia coli*. Esmaeili et al. [135] used chitosan to encapsulate sesame oil into nano-sized granules to explore its sustained-release effect and biological activity. As a result, the antioxidant activity of unencapsulated celery oil was stronger than that of chitosan-embedded EOs nanoparticles, but the encapsulated EOs showed stronger antibacterial ability against *Staphylococcus aureus*, *Staphylococcus epidermidis*, *Cactus rod*, *Escherichia coli*, *Salmonella typhimurium*, and *Bacillus subtilis* than unencapsulated EOs. The same situation was observed when studying the antibacterial activity of D-limonene and oregano EOs after emulsification [136].

Compared with the free EOs, encapsulation can improve the water solubility of EOs, and when the size of EO droplets reaches the nanometer level, this helps to reduce the mass transfer resistance of the nano-scale transport system and enhances the ability of somatic cells to passively adsorb droplets of EOs, thereby reinforcing the antibacterial activity of EOs [137]. Acevedo et al. [138] found that the emulsified thyme EOs after nano-emulsification had a significant enhancement effect on the bacteriostasis of *E. coli*. Moghimi et al. [139] prepared EO nanocapsules from *thymus daenensis* by sonication. They then compared the antibacterial effect of nanocapsules on food spoilage bacteria with that of unencapsulated EO. The results showed that the minimum inhibitory concentration of EOs nanoemulsions was 0.4 mg/mL, and its antibacterial activity was 10 times that of unencapsulated EOs. Studies have found that different sizes of limonene and cinnamic acid nanoemulsions have no significant difference in the inhibitory effect on spoilage yeast or *Escherichia coli*, which was closely related to the composition of the emulsion system [12].

In addition, compared to a conventional emulsion, nanoencapsulated lipophilic antimicrobial agents are generally believed to penetrate more easily through the microbial membrane, resulting in an improved bactericidal activity. This is because the dispersion of the lipophilic antimicrobial agent in the nanoemulsion will result in an increase of the interactions with the binding sites on the targeting bacteria. It can be assumed that antimicrobial agents may more fully contact the cells and promote efficient release of the active substance in the cell, thereby providing an opportunity to increase its bioavailability and consequently enhancing the bacteriostatic effect. However, there have been results reported by Salvia-Trujillo [133] and Buranasuksombat et al. [140] which showed that the antibacterial activity of encapsulated EOs was not affected by the droplet size. These clearly controversial results suggest that a decrease in droplet size does not necessarily mean the enhancement of the function of the essential oil nanoemulsions.

Table 5. Efficacy of nanoencapsulated essential oils and other bioactive compounds as food preservatives.

Delivery System	Bioactive Compounds	Encapsulating Material	Techniques	Size	Major Findings	References
Nanoemulsion (prepared by low-energy methods)	Thymol	Zein-Sodium caseinate	Emulsion polymerization	65.8–87.6 nm	Compared with the control, the encapsulated thymol was more effective in lowering <i>S. aureus</i> counts during a period of 13 days	[141]
	Vitamin E	Edible mustard oil with Tween-80	Emulsion diffusion	~86 nm	High encapsulation efficiency close to 100%; the antioxidant and antimicrobial activity of nanoemulsions was improved	[57]
	Cuminum cyminum oil	Chitosan-caffeic acid	Ionic gelation	<100 nm	When tested under unsealed condition, nanogel-containing oils showed better antimicrobial activity than the free oils against <i>Aspergillus flavus</i>	[29]

Table 5. Cont.

Delivery System	Bioactive Compounds	Encapsulating Material	Techniques	Size	Major Findings	References
Nanoemulsion (prepared by high-energy methods)	Peppermint oil	Medium-chain triacylglycerol	High pressure homogenization	<200 nm	Nanoemulsions containing EO showed improved antimicrobial activity against <i>Listeria monocytogenes</i> and <i>Staphylococcus aureus</i>	[112]
	Eucalyptus oil	Tween 80	Ultrasonication	17.1 nm	Nanoemulsions containing eucalyptus showed to inactivate <i>B. cereus</i> at 0 min, <i>S. aureus</i> at 15 min, and <i>E. coli</i> at 1 h	[142]
	Essential oils (Lemongrass, clove, tea tree, thyme, geranium, marjoram, palmarosa, rosewood, sage or mint)	Sodium alginate and tween 80	Microfluidization	<20 nm	The antibacterial activity depends on the type of essential oil used in the formulation, not their droplet size	[133]
	<i>Thymus capitatus</i> oil	Soybean oil and SDS (sodium dodecylsulfate)	High pressure micro-fluidizer	~110 nm	Nanoencapsulated EO exhibited higher antibacterial inhibition diameters against <i>Staphylococcus aureus</i> compared to those formed by free EO	[143]
SLNs	Nisin	Cetyl palmitate, Softisan 378, Softisan 154, Imwitor 900 and Witapol E85	High pressure homogenization	119 nm	The antibacterial activity of nisin-loaded SLNs against <i>L. monocytogenes</i> and <i>L. plantarum</i> was up to 20 and 15 days, respectively, while the free nisin was only 1 day and 3 days, respectively.	[144]
	<i>Zataria multiflora</i> oil	Glyceryl monostearat and Precirol®	High-shear homogenization and ultrasound	255.5 nm	<i>Z. multiflora</i> essential-oil-loaded SLNs exhibited strong antifungal activity compared to free oil against <i>Aspergillus ochraceus</i> , <i>Aspergillus niger</i>	[123]
Nanoliposome	Nisin	Soy and marine lecithin	Microfluidization	151–181 nm	Lecithin-encapsulated nisin exhibited higher stability for 6 weeks and showed better antibacterial activity compared to free nisin	[145]
	Rose essential oil	Phosphatidylcholine and cholesterol	Supercritical fluid technology	<100 nm	The liposomes formed by the supercritical process have high encapsulation efficiency and small particle size with a unimodal distribution	[146]
Polysaccharide-based	Cardamom oil	Chitosan nano-particles	Ionic gelation	50–100 nm	The encapsulation efficiency of chitosan nano-composites was more than 90%; it exhibited excellent anti-microbial potential against <i>Escherichia coli</i> and <i>Staphylococcus aureus</i> .	[147]
	Lemon ironbark oil	Cashew gum	Spray dryer	27.7–432.6 nm	Nanoencapsulated oil showed improved activity against Salmonella Enteritidis.	[148]
	Lime oil	Chitosan	Phase inversion emulsification	100–300 nm	Nanoencapsulated lime EO exhibited enhanced antibacterial activity against <i>Staphylococcus aureus</i> , <i>Listeria monocytogenes</i> , <i>Shigella dysenteriae</i> , and <i>Escherichia coli</i>	[149]
Protein-based	Thymol/carvacrol	Zein	Emulsion diffusion	263 nm / 275 nm	The encapsulated EOs in zein nanoparticles can increase their solubility by up to 14 times without affecting their ability to scavenge free radicals or to control <i>E. coli</i> growth	[150]
	Thymol	Sodium Caseinate	High shear homogenization	~130 nm	Compared with thymol crystals, the encapsulated thymol exhibited significantly improved anti- <i>Listeria</i> activity in milk with different fat levels	[82]
Biopolymer-based	Eugenol oil	Whey protein and maltodextrin	High-speed homogenizer	100–300 nm	The nanoencapsulated eugenol showed improved antimicrobial activity against <i>E. coli</i> and <i>L. monocytogenes</i> than the free oil	[151]
	Terpenes mixture and D-limonene	Starch and soy lecithin	High Pressure Homogenization	100–400 nm	The addition of low dose of the nanoencapsulated terpenes can delay the microbial growth (1.0 g/L terpenes) or completely inactivate microorganisms such as <i>Lactobacillus delbrueckii</i> , <i>Saccharomyces</i>	[117]
Equipment-based	Peppermint oil	Alginate biopolymer	Electrospinning and electrospaying	~80 nm	The nanoencapsulated peppermint oil exhibited a high antimicrobial activity against <i>E. coli</i> and <i>S. aureus</i> bacteria	[128]

7. Applications of Nanoencapsulated Natural Antimicrobial Agents

The use of nanoencapsulated natural antimicrobial agents in food is a crucial challenge. A large number of spoilage and pathogenic microorganisms that contaminate food systems require extensive activity of the antibacterial systems [152]. The purposes of using the nanoencapsulation system in food industries include the following four: (1) stabilizing the volatile antimicrobial agents, such as essential oils, to prevent evaporation during processing; (2) reducing the interaction of antimicrobials with food substrates; (3) controlling the release rate of antimicrobial agents in food matrices to extend the exposure of microorganisms to antimicrobial agents; (4) improving the solubility of antibiotics in unhealthy foods to expand the range of applications of antibacterial drugs. It is reported that more than 400 companies have used nanoscience to manufacture food and packaging materials [153].

7.1. Aqueous Food Systems

The two most common beverage systems are divided into carbohydrate-based products and dairy-based products. Carbohydrate-based products, such as juices and soft drinks, normally contain a certain amount of carbohydrates, but no or only a small amount of protein and lipids. A problem with the application of antimicrobial agents to carbohydrate-based products is the incorporation of hydrophobic compounds into the food system. Dairy-based products such as milk generally contain large amounts of proteins and fats, so the interactions between antimicrobial agents and these complex food compounds and their stability during pasteurization can be a serious challenge for the food industry. Nanoencapsulation technology can be used to solve these problems. In this context, zein-encapsulated nisin and thymol oil showed better bacteriostatic effects than free antimicrobial agents after 4 h [154]. The use of nanoencapsulated thymol essential oil resulted in a prolonged effect on *Listeria monocytogenes* within seven days of shelf life at 32 °C, making the number of bacteria lower than the detectable limit in skim milk [82]. In juices, both tea tree oil and cinnamaldehyde nanoemulsions showed concentration-dependent inhibition of microbial load on inoculation [117]. Juices containing minimal concentration of nanoencapsulated terpene showed retarding microbial growth (1.0 g/L of terpene) or complete inactivation of microbes (5.0 g/L of terpene), while minimizing sensory properties [117].

7.2. Solid Food Systems

Nanoencapsulation technologies are also used in solid food matrices to improve uniform mixing and extend shelf life. Gökmen et al. [155] used spray-drying method to encapsulate omega-3 unsaturated fatty acid with high-linear corn starch, and added it to dough in different amounts to study its effect on bread quality. The results show that nanocapsules can effectively reduce the oxidation of unsaturated fatty acids during the bread baking process, thereby greatly improving the quality of bread products, and reducing the oxidation of harmful fatty acids and the production of harmful substances during the baking process [155]. Degnan and Luchansky [156] investigated the activity of liposome-encapsulated pediocin AcH in beef slurries. Their results showed that encapsulating pediocin AcH in liposomes can increase the recovery of pediocin activity in heated beef muscle and beef tallow pulp by an average of 27.5% and 28.9%, respectively, compared with similar beef pulp with free pediocin.

7.3. Active Food Packaging

In order to improve food packaging and extend the quality and freshness of perishable products, the food industry has established a new packaging system named “active packaging”. It is intended to deliberately incorporate functional ingredients that release or absorb substances from the food or food matrices [157]. In this regard, the usage of essential oils in active packaging has become a good alternative to improve the shelf life of food products [158]. Chitosan in the form of films and nanoparticles has been reported

to be used in food packaging to prevent microbial infections [159]. Chitosan nanoparticles (110 nm) have been developed and can be used as a coating by spraying directly onto the surface of apple slices to produce a discontinuous coating [160]. Compared to uncoated samples, the chitosan nanoparticle coating showed more effective antimicrobial activity against yeast and mold, as well as thermophilic and mesophilic bacteria [160]. Chitosan/pentasodium tripolyphosphate nanoparticles containing carvacrol have been shown to have antibacterial activity, with the minimum inhibitory concentration being determined to be 0.257 mg/mL [161]. This suggests that the encapsulated carvacrol in chitosan nanoparticles improved its antibacterial activity. Edible coatings based on chitosan-containing lemon oil have been successfully used to inhibit the endogenous flora present on sesame leaves, and their shelf life was extended by seven days compared to untreated samples [162].

8. Legislative Aspects Concerning the Use of Nanoparticles in Food Products

As shown in the previous section, food nanotechnology is applied into many aspects of the food field, such as food packaging, additives, and food preservation. Many conventional molecules used as food additives or in packaging materials can be found at nanometer scale in food products. For example, food-grade TiO₂ nanoparticles have been found up to approximately 40% in the nanometer range [163,164]. Although nanomaterials like TiO₂ nanoparticles are generally recognized as low in toxicity at conventional conditions, long-term exposure to such nanomaterials may cause adverse damages. The United States Food and Drug Administration (FDA or USFDA) and the European Commission (EC) are the main sources for legislation and regulation on food nanotechnology. A recent literature review summarized the risk assessment of the conventional particle size of substances in food products [165]. However, the development of nanotechnology in the food industry should not be blamed. Before applying nanomaterials to the food field, appropriate risk assessments can be made on the physical and chemical properties of nanomaterials and their absorption, biodistribution, metabolism, and body excretion, to alleviate the effects of nanotoxicity.

9. Conclusions

Consumer demand for safe natural products has driven the search for mild food preservatives in recent years. In this case, natural antibacterial agents, such as essential oils, have the potential to provide quality and safety benefits and have a reduced impact on human health, but they still have some drawbacks. The advancements in nanotechnology can protect active compounds from degradation, improve their solubility, and control their release compared to adding the antimicrobial compound directly to the food products. However, most of them are only produced on a laboratory scale because there is still a lack of systematic research. Before these natural bacteriostatic agents are widely used in the research and development of food, the following challenges need to be properly addressed: (i) a better understanding of the mechanisms of encapsulated natural bacteriostats is necessary to provide a solid foundation for engineering new antimicrobial systems and strategies; (ii) costs should be carefully evaluated, because the use of some natural antimicrobial agents is still expensive, as well as the production of nanocapsules; and (iii) future research must address the synthesis of new synergistic formulations based on EOs and their nanoencapsulation, to reduce their adverse effects on sensory properties and improve their antimicrobial efficacy in food matrices.

Author Contributions: Conceptualization, W.L. and A.G.; methodology, W.L.; validation, A.G., S.G. and E.D.; formal analysis, A.E.; investigation, W.L.; data curation, W.L.; writing—original draft preparation, W.L.; writing—review and editing, W.B., A.E., A.G., S.G., and E.D.; supervision, A.G., S.G., A.E., R.S. and E.D.; project administration, A.G. All authors have read and agreed to the published version of the manuscript.

Funding: This research received no external funding.

Informed Consent Statement: Not applicable.

Conflicts of Interest: The authors declare no conflict of interest.

References

- Gustafsson, J.; Cederberg, C.; Sonesson, U.; Emanuelsson, A. *The Methodology of the FAO Study: Global Food Losses and Food Waste—Extent, Causes and Prevention—FAO, 2011*; SIK Institutet för Livsmedel och Bioteknik: Gothenburg, Sweden, 2013.
- Zhang, Y.; Chen, H.; Pan, K. Chapter 5—Nanoencapsulation of Food Antimicrobial Agents and Essential Oils. In *Nanoencapsulation of Food Bioactive Ingredients*; Jafari, S.M., Ed.; Academic Press: Cambridge, MA, USA, 2017; pp. 183–221.
- Prakash, B.; Kujur, A.; Yadav, A.; Kumar, A.; Singh, P.P.; Dubey, N. Nanoencapsulation: An efficient technology to boost the antimicrobial potential of plant essential oils in food system. *Food Control* **2018**, *89*, 1–11. [[CrossRef](#)]
- Zhu, Y.; Li, C.; Cui, H.; Lin, L. Encapsulation strategies to enhance the antibacterial properties of essential oils in food system. *Food Control* **2021**, *123*, 107856. [[CrossRef](#)]
- Shatalov, D.; Kedik, S.; Zhavoronok, E.; Aydakova, A.; Ivanov, I.; Evseeva, A.; Beliakov, S.; Biryulin, S.; Kovalenko, A.; Mikhailenko, E. The current state and development of perspectives of application of synthetic antimicrobial agents. *Polym. Sci. Ser. D* **2017**, *10*, 293–299. [[CrossRef](#)]
- Falleh, H.; Ben Jemaa, M.; Saada, M.; Ksouri, R. Essential oils: A promising eco-friendly food preservative. *Food Chem.* **2020**, *330*, 127268. [[CrossRef](#)]
- Zeng, W.C.; He, Q.; Sun, Q.; Zhong, K.; Gao, H. Antibacterial activity of water-soluble extract from pine needles of *Cedrus deodara*. *Int. J. Food Microbiol.* **2012**, *153*, 78–84. [[CrossRef](#)]
- Gould, G.W. *Mechanisms of Action of Food Preservation Procedures*; Elsevier Applied Science: London, UK, 1989.
- Bagamboula, C.; Uyttendaele, M.; Debevere, J. Inhibitory effect of thyme and basil essential oils, carvacrol, thymol, estragol, linalool and p-cymene towards *Shigella sonnei* and *S. flexneri*. *Food Microbiol.* **2004**, *21*, 33–42. [[CrossRef](#)]
- Cortés-Rojas, D.F.; de Souza, C.R.F.; Oliveira, W.P. Clove (*Syzygium aromaticum*): A precious spice. *Asian Pac. J. Trop. Biomed.* **2014**, *4*, 90–96. [[CrossRef](#)]
- Chaieb, K.; Hajlaoui, H.; Zmantar, T.; Kahla-Nakbi, A.B.; Rouabhia, M.; Mahdouani, K.; Bakhrouf, A. The chemical composition and biological activity of clove essential oil, *Eugenia caryophyllata* (*Syzygium aromaticum* L. Myrtaceae): A short review. *Phytother. Res.* **2007**, *21*, 501–506. [[CrossRef](#)] [[PubMed](#)]
- Donsi, F.; Annunziata, M.; Vincenzi, M.; Ferrari, G. Design of nanoemulsion-based delivery systems of natural antimicrobials: Effect of the emulsifier. *J. Biotechnol.* **2012**, *159*, 342–350. [[CrossRef](#)] [[PubMed](#)]
- Bozin, B.; Mimica-Dukic, N.; Simin, N.; Anackov, G. Characterization of the volatile composition of essential oils of some Lamiaceae spices and the antimicrobial and antioxidant activities of the entire oils. *J. Agric. Food Chem.* **2006**, *54*, 1822–1828. [[CrossRef](#)]
- Schlüter, B.; Pflügel, P.; Lindequist, U.; Jülich, W. Aspects of the antimicrobial efficacy of grapefruit seed extract and its relation to preservative substances contained. *Die Pharm.* **1999**, *54*, 452–456.
- Levy, J.; Boyer, R.R.; Neilson, A.P.; O’Keefe, S.F.; Chu, H.S.S.; Williams, R.C.; Dorenkott, M.R.; Goodrich, K.M. Evaluation of peanut skin and grape seed extracts to inhibit growth of foodborne pathogens. *Food Sci. Nutr.* **2017**, *5*, 1130–1138. [[CrossRef](#)]
- Rahmanian, N.; Jafari, S.M.; Wani, T.A. Bioactive profile, dehydration, extraction and application of the bioactive components of olive leaves. *Trends Food Sci. Technol.* **2015**, *42*, 150–172. [[CrossRef](#)]
- Moreno, S.; Scheyer, T.; Romano, C.S.; Vojnov, A.A. Antioxidant and antimicrobial activities of rosemary extracts linked to their polyphenol composition. *Free Radic. Res.* **2006**, *40*, 223–231. [[CrossRef](#)] [[PubMed](#)]
- Davidson, P.M.; Critzer, F.J.; Taylor, T.M. Naturally occurring antimicrobials for minimally processed foods. *Annu. Rev. Food Sci. Technol.* **2013**, *4*, 163–190. [[CrossRef](#)] [[PubMed](#)]
- Davidson, P.; Zivanovic, S. The use of natural antimicrobials. In *Food Preservation Techniques*; Elsevier: Amsterdam, The Netherlands, 2003; pp. 5–30.
- Elsser-Gravesen, D.; Elsser-Gravesen, A. Biopreservatives. In *Biotechnology of Food and Feed Additives*; Springer: Berlin, Germany, 2013; pp. 29–49.
- Bergholz, T.M.; Tang, S.; Wiedmann, M.; Boor, K.J. Nisin resistance of *Listeria monocytogenes* is increased by exposure to salt stress and is mediated via LiaR. *Appl. Environ. Microbiol.* **2013**, *79*, 5682–5688. [[CrossRef](#)] [[PubMed](#)]
- Yoshida, T.; Nagasawa, T. *ε*-Poly-L-lysine: Microbial production, biodegradation and application potential. *Appl. Microbiol. Biotechnol.* **2003**, *62*, 21–26. [[CrossRef](#)] [[PubMed](#)]
- Bakkali, F.; Averbeck, S.; Averbeck, D.; Idaomar, M. Biological effects of essential oils—A review. *Food Chem. Toxicol.* **2008**, *46*, 446–475. [[CrossRef](#)] [[PubMed](#)]
- Calo, J.R.; Crandall, P.G.; O’Bryan, C.A.; Ricke, S.C. Essential oils as antimicrobials in food systems—A review. *Food Control* **2015**, *54*, 111–119. [[CrossRef](#)]
- Sperotto, A.R.; Moura, D.J.; Péres, V.F.; Damasceno, F.C.; Caramão, E.B.; Henriques, J.A.; Saffi, J. Cytotoxic mechanism of *Piper gaudichaudianum* Kunth essential oil and its major compound nerolidol. *Food Chem. Toxicol.* **2013**, *57*, 57–68. [[CrossRef](#)]
- Burt, S. Essential oils: Their antibacterial properties and potential applications in foods—A review. *Int. J. Food Microbiol.* **2004**, *94*, 223–253. [[CrossRef](#)] [[PubMed](#)]

27. Hammer, K.A.; Carson, C.F.; Riley, T.V. Melaleuca alternifolia (tea tree) oil inhibits germ tube formation by *Candida albicans*. *Med. Mycol.* **2000**, *38*, 355–362. [[CrossRef](#)] [[PubMed](#)]
28. Shao, X.; Cheng, S.; Wang, H.; Yu, D.; Mungai, C. The possible mechanism of antifungal action of tea tree oil on *Botrytis cinerea*. *J. Appl. Microbiol.* **2013**, *114*, 1642–1649. [[CrossRef](#)]
29. Zhavah, S.; Mohsenifar, A.; Beiki, M.; Khalili, S.T.; Abdollahi, A.; Rahmani-Cherati, T.; Tabatabaei, M. Encapsulation of *Cuminum cyminum* essential oils in chitosan-caffeic acid nanogel with enhanced antimicrobial activity against *Aspergillus flavus*. *Ind. Crop Prod.* **2015**, *69*, 251–256. [[CrossRef](#)]
30. Tavakoli, H.R.; Mashak, Z.; Moradi, B.; Sodagari, H.R. Antimicrobial activities of the combined use of *Cuminum cyminum* L. essential oil, nisin and storage temperature against *Salmonella Typhimurium* and *Staphylococcus aureus* in vitro. *Jundishapur J. Microbiol.* **2015**, *8*, e24838. [[CrossRef](#)]
31. Bisht, D.S.; Menon, K.; Singhal, M.K. Comparative Antimicrobial Activity of Essential oils of *Cuminum cyminum* L. and *Foeniculum vulgare* Mill. seeds against *Salmonella typhimurium* and *Escherichia coli*. *J. Essent. Oil Bear. Plants* **2014**, *17*, 617–622. [[CrossRef](#)]
32. Aguirre, A.; Borneo, R.; León, A. Antimicrobial, mechanical and barrier properties of triticale protein films incorporated with oregano essential oil. *Food Biosci.* **2013**, *1*, 2–9. [[CrossRef](#)]
33. Bhargava, K.; Conti, D.S.; da Rocha, S.R.; Zhang, Y. Application of an oregano oil nanoemulsion to the control of foodborne bacteria in fresh lettuce. *Food Microbiol.* **2015**, *47*, 69–73. [[CrossRef](#)]
34. Kurekci, C.; Padmanabha, J.; Bishop-Hurley, S.L.; Hassan, E.; Al Jassim, R.A.; McSweeney, C.S. Antimicrobial activity of essential oils and five terpenoid compounds against *Campylobacter jejuni* in pure and mixed culture experiments. *Int. J. Food Microbiol.* **2013**, *166*, 450–457. [[CrossRef](#)]
35. Tserennadmid, R.; Takó, M.; Galgóczy, L.; Papp, T.; Pesti, M.; Vágvölgyi, C.; Almássy, K.; Krisch, J. Anti yeast activities of some essential oils in growth medium, fruit juices and milk. *Int. J. Food Microbiol.* **2011**, *144*, 480–486. [[CrossRef](#)] [[PubMed](#)]
36. Yuste, J.; Fung, D. Inactivation of *Listeria monocytogenes* Scott A 49594 in apple juice supplemented with cinnamon. *J. Food Prot.* **2002**, *65*, 1663–1666. [[CrossRef](#)]
37. Gill, A.O.; Holley, R.A. Mechanisms of bactericidal action of cinnamaldehyde against *Listeria monocytogenes* and of eugenol against *L. monocytogenes* and *Lactobacillus sakei*. *Appl. Environ. Microbiol.* **2004**, *70*, 5750–5755. [[CrossRef](#)]
38. Kim, J.; Marshall, M.R.; Wei, C.-I. Antibacterial activity of some essential oil components against five foodborne pathogens. *J. Agric. Food Chem.* **1995**, *43*, 2839–2845. [[CrossRef](#)]
39. Catherine, A.A.; Deepika, H.; Negi, P.S. Antibacterial activity of eugenol and peppermint oil in model food systems. *J. Essent. Oil Res.* **2012**, *24*, 481–486. [[CrossRef](#)]
40. Du, E.; Gan, L.; Li, Z.; Wang, W.; Liu, D.; Guo, Y. In vitro antibacterial activity of thymol and carvacrol and their effects on broiler chickens challenged with *Clostridium perfringens*. *J. Anim. Sci. Biotechnol.* **2015**, *6*, 58. [[CrossRef](#)]
41. Seydim, A.; Sarikus, G. Antimicrobial activity of whey protein based edible films incorporated with oregano, rosemary and garlic essential oils. *Food Res. Int.* **2006**, *39*, 639–644. [[CrossRef](#)]
42. Gutierrez, J.; Barry-Ryan, C.; Bourke, P. The antimicrobial efficacy of plant essential oil combinations and interactions with food ingredients. *Int. J. Food Microbiol.* **2008**, *124*, 91–97. [[CrossRef](#)]
43. Bucar, F.; Wube, A.; Schmid, M. Natural product isolation—How to get from biological material to pure compounds. *Nat. Prod. Rep.* **2013**, *30*, 525–545. [[CrossRef](#)] [[PubMed](#)]
44. Blanco-Padilla, A.; Soto, K.M.; Hernández Iturriaga, M.; Mendoza, S. Food antimicrobials nanocarriers. *Sci. World J.* **2014**, *2014*, 837215. [[CrossRef](#)] [[PubMed](#)]
45. Bazana, M.T.; Codevilla, C.F.; de Menezes, C.R. Nanoencapsulation of Bioactive Compounds: Challenges and Perspectives. *Curr. Opin. Food Sci.* **2019**, *26*, 47–56. [[CrossRef](#)]
46. Yada, R.Y.; Buck, N.; Canady, R.; DeMerlis, C.; Duncan, T.; Janer, G.; Juneja, L.; Lin, M.; McClements, D.J.; Noonan, G. Engineered nanoscale food ingredients: Evaluation of current knowledge on material characteristics relevant to uptake from the gastrointestinal tract. *Compr. Rev. Food Sci. Food Saf.* **2014**, *13*, 730–744. [[CrossRef](#)]
47. Zhang, Y.; Hsu, B.Y.; Ren, C.; Li, X.; Wang, J. Silica-based nanocapsules: Synthesis, structure control and biomedical applications. *Chem. Soc. Rev.* **2014**, *44*, 315–335. [[CrossRef](#)]
48. Shishir, M.R.I.; Xie, L.; Sun, C.; Zheng, X.; Chen, W. Advances in micro and nano-encapsulation of bioactive compounds using biopolymer and lipid-based transporters. *Trends Food Sci. Technol.* **2018**, *78*, 34–60. [[CrossRef](#)]
49. Fery, A.; Weinkamer, R. Mechanical properties of micro-and nanocapsules: Single-capsule measurements. *Polymer* **2007**, *48*, 7221–7235. [[CrossRef](#)]
50. Shin, G.H.; Kim, J.T.; Park, H.J. Recent developments in nanoformulations of lipophilic functional foods. *Trends Food Sci. Technol.* **2015**, *46*, 144–157. [[CrossRef](#)]
51. Prakash, A.; Baskaran, R.; Paramasivam, N.; Vadivel, V. Essential oil based nanoemulsions to improve the microbial quality of minimally processed fruits and vegetables: A review. *Food Res. Int.* **2018**, *111*, 509–523. [[CrossRef](#)] [[PubMed](#)]
52. McClements, D.J.; Li, Y. Structured emulsion-based delivery systems: Controlling the digestion and release of lipophilic food components. *Adv. Colloid Interface Sci.* **2010**, *159*, 213–228. [[CrossRef](#)]
53. de Souza Simões, L.; Madalena, D.A.; Pinheiro, A.C.; Teixeira, J.A.; Vicente, A.A.; Ramos, O.L. Micro-and nano bio-based delivery systems for food applications: In vitro behavior. *Adv. Colloid Interface Sci.* **2017**, *243*, 23–45. [[CrossRef](#)]

54. Joye, I.J.; McClements, D.J. Biopolymer-based nanoparticles and microparticles: Fabrication, characterization, and application. *Curr. Opin. Colloid Interface Sci.* **2014**, *19*, 417–427. [[CrossRef](#)]
55. Jia, Z.; Dumont, M.-J.; Orsat, V. Encapsulation of phenolic compounds present in plants using protein matrices. *Food Biosci.* **2016**, *15*, 87–104. [[CrossRef](#)]
56. Saberi, A.H.; Fang, Y.; McClements, D.J. Influence of surfactant type and thermal cycling on formation and stability of flavor oil emulsions fabricated by spontaneous emulsification. *Food Res. Int.* **2016**, *89*, 296–301. [[CrossRef](#)]
57. Dasgupta, N.; Ranjan, S.; Mundra, S.; Ramalingam, C.; Kumar, A. Fabrication of food grade vitamin E nanoemulsion by low energy approach, characterization and its application. *Int. J. Food Prop.* **2016**, *19*, 700–708. [[CrossRef](#)]
58. Dalmolin, L.F.; Khalil, N.M.; Mainardes, R.M. Delivery of vanillin by poly (lactic-acid) nanoparticles: Development, characterization and in vitro evaluation of antioxidant activity. *Mater. Sci. Eng. C* **2016**, *62*, 1–8. [[CrossRef](#)]
59. Aditya, N.; Aditya, S.; Yang, H.; Kim, H.W.; Park, S.O.; Ko, S. Co-delivery of hydrophobic curcumin and hydrophilic catechin by a water-in-oil-in-water double emulsion. *Food Chem.* **2015**, *173*, 7–13. [[CrossRef](#)]
60. Ho, K.K.; Schröen, K.; San Martín-González, M.F.; Berton-Carabin, C.C. Physicochemical stability of lycopene-loaded emulsions stabilized by plant or dairy proteins. *Food Struct.* **2017**, *12*, 34–42. [[CrossRef](#)]
61. Pérez-Masiá, R.; López-Nicolás, R.; Periago, M.J.; Ros, G.; Lagaron, J.M.; López-Rubio, A. Encapsulation of folic acid in food hydrocolloids through nanospray drying and electrospraying for nutraceutical applications. *Food Chem.* **2015**, *168*, 124–133. [[CrossRef](#)] [[PubMed](#)]
62. O'Toole, M.G.; Henderson, R.M.; Soucy, P.A.; Fasciotto, B.H.; Hoblitzell, P.J.; Keynton, R.S.; Ehringer, W.D.; Gobin, A.S. Curcumin encapsulation in submicrometer spray-dried chitosan/Tween 20 particles. *Biomacromolecules* **2012**, *13*, 2309–2314. [[CrossRef](#)] [[PubMed](#)]
63. Busch, V.; Pereyra-Gonzalez, A.; Šegatin, N.; Santagapita, P.; Ulrih, N.P.; Buera, M. Propolis encapsulation by spray drying: Characterization and stability. *LWT* **2017**, *75*, 227–235. [[CrossRef](#)]
64. Sanchez-Reinoso, Z.; Osorio, C.; Herrera, A. Effect of microencapsulation by spray drying on cocoa aroma compounds and physicochemical characterisation of microencapsulates. *Powder Technol.* **2017**, *318*, 110–119. [[CrossRef](#)]
65. Bejrappa, P.; Min, S.-G.; Surassmo, S.; Choi, M.-J. Physicochemical properties of freeze-dried fish oil nanocapsules frozen under different conditions. *Dry. Technol.* **2010**, *28*, 481–489. [[CrossRef](#)]
66. Yamashita, C.; Chung, M.M.S.; dos Santos, C.; Mayer, C.R.M.; Moraes, I.C.F.; Branco, I.G. Microencapsulation of an anthocyanin-rich blackberry (*Rubus* spp.) by-product extract by freeze-drying. *LWT* **2017**, *84*, 256–262. [[CrossRef](#)]
67. Fioramonti, S.A.; Rubiolo, A.C.; Santiago, L.G. Characterisation of freeze-dried flaxseed oil microcapsules obtained by multilayer emulsions. *Powder Technol.* **2017**, *319*, 238–244. [[CrossRef](#)]
68. Chew, S.-C.; Nyam, K.-L. Microencapsulation of kenaf seed oil by co-extrusion technology. *J. Food Eng.* **2016**, *175*, 43–50. [[CrossRef](#)]
69. Wang, W.; Waterhouse, G.I.; Sun-Waterhouse, D. Co-extrusion encapsulation of canola oil with alginate: Effect of quercetin addition to oil core and pectin addition to alginate shell on oil stability. *Food Res. Int.* **2013**, *54*, 837–851. [[CrossRef](#)]
70. Khor, C.M.; Ng, W.K.; Kanaujia, P.; Chan, K.P.; Dong, Y. Hot-melt extrusion microencapsulation of quercetin for taste-masking. *J. Microencapsul.* **2017**, *34*, 29–37. [[CrossRef](#)]
71. Penalva, R.; Esparza, I.; Agüeros, M.; Gonzalez-Navarro, C.J.; Gonzalez-Ferrero, C.; Irache, J.M. Casein nanoparticles as carriers for the oral delivery of folic acid. *Food Hydrocoll.* **2015**, *44*, 399–406. [[CrossRef](#)]
72. Arroyo-Maya, I.J.; McClements, D.J. Biopolymer nanoparticles as potential delivery systems for anthocyanins: Fabrication and properties. *Food Res. Int.* **2015**, *69*, 1–8. [[CrossRef](#)]
73. Yuan, Y.; Kong, Z.-Y.; Sun, Y.-E.; Zeng, Q.-Z.; Yang, X.-Q. Complex coacervation of soy protein with chitosan: Constructing antioxidant microcapsule for algal oil delivery. *LWT* **2017**, *75*, 171–179. [[CrossRef](#)]
74. Jain, A.; Thakur, D.; Ghoshal, G.; Katore, O.; Shivhare, U. Characterization of microcapsulated β -carotene formed by complex coacervation using casein and gum tragacanth. *Int. J. Biol. Macromol.* **2016**, *87*, 101–113. [[CrossRef](#)]
75. Yao, Z.-C.; Chang, M.-W.; Ahmad, Z.; Li, J.-S. Encapsulation of rose hip seed oil into fibrous zein films for ambient and on demand food preservation via coaxial electrospinning. *J. Food Eng.* **2016**, *191*, 115–123. [[CrossRef](#)]
76. Fernandez, A.; Torres-Giner, S.; Lagaron, J.M. Novel route to stabilization of bioactive antioxidants by encapsulation in electrospun fibers of zein prolamine. *Food Hydrocoll.* **2009**, *23*, 1427–1432. [[CrossRef](#)]
77. Khoshakhlagh, K.; Koocheki, A.; Mohebbi, M.; Allafchian, A. Development and characterization of electrosprayed *Alyssum homolocarpum* seed gum nanoparticles for encapsulation of D-limonene. *J. Colloid Interface Sci.* **2017**, *490*, 562–575. [[CrossRef](#)] [[PubMed](#)]
78. Yang, H.; Feng, K.; Wen, P.; Zong, M.-H.; Lou, W.-Y.; Wu, H. Enhancing oxidative stability of encapsulated fish oil by incorporation of ferulic acid into electrospun zein mat. *LWT* **2017**, *84*, 82–90. [[CrossRef](#)]
79. El Asbahani, A.; Miladi, K.; Badri, W.; Sala, M.; Addi, E.A.; Casabianca, H.; El Mousadik, A.; Hartmann, D.; Jilale, A.; Renaud, F. Essential oils: From extraction to encapsulation. *Int. J. Pharm.* **2015**, *483*, 220–243. [[CrossRef](#)] [[PubMed](#)]
80. Bilia, A.R.; Guccione, C.; Isacchi, B.; Righeschi, C.; Firenzuoli, F.; Bergonzi, M.C. Essential oils loaded in nanosystems: A developing strategy for a successful therapeutic approach. *Evid. Based Complementary Altern. Med.* **2014**, *2014*, 651593. [[CrossRef](#)]
81. Hill, L.E.; Gomes, C.; Taylor, T.M. Characterization of beta-cyclodextrin inclusion complexes containing essential oils (trans-cinnamaldehyde, eugenol, cinnamon bark, and clove bud extracts) for antimicrobial delivery applications. *LWT Food Sci. Technol.* **2013**, *51*, 86–93. [[CrossRef](#)]

82. Pan, K.; Chen, H.; Davidson, P.M.; Zhong, Q.J. Thymol nanoencapsulated by sodium caseinate: Physical and antilisterial properties. *J. Agric. Food Chem.* **2014**, *62*, 1649–1657. [[CrossRef](#)]
83. Karathanos, V.T.; Mourtzinos, I.; Yannakopoulou, K.; Andrikopoulos, N.K. Study of the solubility, antioxidant activity and structure of inclusion complex of vanillin with β -cyclodextrin. *Food Chem.* **2007**, *101*, 652–658. [[CrossRef](#)]
84. Lee, M.-Y.; Min, S.-G.; You, S.-K.; Choi, M.-J.; Hong, G.-P.; Chun, J.-Y. Effect of β -cyclodextrin on physical properties of nanocapsules manufactured by emulsion–diffusion method. *J. Food Eng.* **2013**, *119*, 588–594. [[CrossRef](#)]
85. Lee, M.-Y.; Min, S.-G.; Bourgeois, S.; Choi, M.-J. Development of a novel nanocapsule formulation by emulsion-diffusion combined with high hydrostatic pressure. *J. Microencapsul.* **2009**, *26*, 122–129. [[CrossRef](#)]
86. Wang, X.; Chen, Y.; Dahmani, F.Z.; Yin, L.; Zhou, J.; Yao, J. Amphiphilic carboxymethyl chitosan-quercetin conjugate with P-gp inhibitory properties for oral delivery of paclitaxel. *Biomaterials* **2014**, *35*, 7654–7665. [[CrossRef](#)]
87. Mohammedi, A.; Hashemi, M.; Hosseini, S.M. Nanoencapsulation of Zataria multiflora essential oil preparation and characterization with enhanced antifungal activity for controlling Botrytis cinerea, the causal agent of gray mould disease. *Innov. Food Sci. Emerg. Technol.* **2015**, *28*, 73–80. [[CrossRef](#)]
88. Ghaderi-Ghahfarokhi, M.; Barzegar, M.; Sahari, M.A.; Azizi, M.H. Nanoencapsulation approach to improve antimicrobial and antioxidant activity of thyme essential oil in beef burgers during refrigerated storage. *Food Bioprocess Technol.* **2016**, *9*, 1187–1201. [[CrossRef](#)]
89. Fathi, M.; Martin, A.; McClements, D.J. Nanoencapsulation of food ingredients using carbohydrate based delivery systems. *Trends Food Sci. Technol.* **2014**, *39*, 18–39. [[CrossRef](#)]
90. Chin, S.F.; Pang, S.C.; Tay, S.H. Size controlled synthesis of starch nanoparticles by a simple nanoprecipitation method. *Carbohydr. Polym.* **2011**, *86*, 1817–1819. [[CrossRef](#)]
91. Zimet, P.; Rosenberg, D.; Livney, Y.D. Re-assembled casein micelles and casein nanoparticles as nano-vehicles for ω -3 polyunsaturated fatty acids. *Food Hydrocoll.* **2011**, *25*, 1270–1276. [[CrossRef](#)]
92. Narayanan, S.; Pavithran, M.; Viswanath, A.; Narayanan, D.; Mohan, C.C.; Manzoor, K.; Menon, D. Sequentially releasing dual-drug-loaded PLGA–casein core/shell nanomedicine: Design, synthesis, biocompatibility and pharmacokinetics. *Acta Biomater.* **2014**, *10*, 2112–2124. [[CrossRef](#)] [[PubMed](#)]
93. Liu, Y.; Guo, R. The interaction between casein micelles and gold nanoparticles. *J. Colloid Interface Sci.* **2009**, *332*, 265–269. [[CrossRef](#)]
94. Sangeetha, J.; Philip, J. The interaction, stability and response to an external stimulus of iron oxide nanoparticle–casein nanocomplexes. *Colloids Surf. A Physicochem. Eng. Asp.* **2012**, *406*, 52–60. [[CrossRef](#)]
95. Parris, N.; Cooke, P.H.; Hicks, K.B. Encapsulation of essential oils in zein nanospherical particles. *J. Agric. Food Chem.* **2005**, *53*, 4788–4792. [[CrossRef](#)]
96. Livney, Y.D. Milk proteins as vehicles for bioactives. *Curr. Opin. Colloid Interface Sci.* **2010**, *15*, 73–83. [[CrossRef](#)]
97. Ghasemi, S.; Jafari, S.M.; Assadpour, E.; Khomeiri, M. Production of pectin–whey protein nano-complexes as carriers of orange peel oil. *Carbohydr. Polym.* **2017**, *177*, 369–377. [[CrossRef](#)] [[PubMed](#)]
98. Hosseini, S.M.H.; Emam-Djomeh, Z.; Sabatino, P.; Van der Meer, P. Nanocomplexes arising from protein–polysaccharide electrostatic interaction as a promising carrier for nutraceutical compounds. *Food Hydrocoll.* **2015**, *50*, 16–26. [[CrossRef](#)]
99. Gupta, A.K.; Gupta, M. Synthesis and surface engineering of iron oxide nanoparticles for biomedical applications. *Biomaterials* **2005**, *26*, 3995–4021. [[CrossRef](#)] [[PubMed](#)]
100. Esfahani, R.; Jafari, S.M.; Jafarpour, A.; Dehnad, D. Loading of fish oil into nanocarriers prepared through gelatin–gum Arabic complexation. *Food Hydrocoll.* **2019**, *90*, 291–298. [[CrossRef](#)]
101. Fathi, M.; Mozafari, M.-R.; Mohebbi, M. Nanoencapsulation of food ingredients using lipid based delivery systems. *Trends Food Sci. Technol.* **2012**, *23*, 13–27. [[CrossRef](#)]
102. Solans, C.; Esquena, J.; Forgiarini, A.M.; Uson, N.; Morales, D.; Izquierdo, P.; Azemar, N.; Garcia-Celma, M.J. Nano-emulsions: Formation, properties, and applications. *Surfactant Sci. Ser.* **2003**, *109*, 525–554.
103. Henry, J.V.; Fryer, P.J.; Frith, W.J.; Norton, I.T. The influence of phospholipids and food proteins on the size and stability of model sub-micron emulsions. *Food Hydrocoll.* **2010**, *24*, 66–71. [[CrossRef](#)]
104. Galanakis, C.M. *Food Waste Recovery: Processing Technologies and Industrial Techniques*; Academic Press: Cambridge, MA, USA, 2015.
105. Koroleva, M.Y.; Yurtov, E.V. Nanoemulsions: The properties, methods of preparation and promising applications. *Russ. Chem. Rev.* **2012**, *81*, 21. [[CrossRef](#)]
106. Donsi, F.; Sessa, M.; Ferrari, G. Effect of emulsifier type and disruption chamber geometry on the fabrication of food nanoemulsions by high pressure homogenization. *Ind. Eng. Chem. Res.* **2011**, *51*, 7606–7618. [[CrossRef](#)]
107. Hashitjin, A.M.; Abbasi, S. Nano-emulsification of orange peel essential oil using sonication and native gums. *Food Hydrocoll.* **2015**, *44*, 40–48. [[CrossRef](#)]
108. Nirmal, N.P.; Mereddy, R.; Li, L.; Sultanbawa, Y. Formulation, characterisation and antibacterial activity of lemon myrtle and anise myrtle essential oil in water nanoemulsion. *Food Chem.* **2018**, *254*, 1–7. [[CrossRef](#)] [[PubMed](#)]
109. Silva, H.D.; Cerqueira, M.Á.; Vicente, A.A. Nanoemulsions for food applications: Development and characterization. *Food Bioprocess Technol.* **2012**, *5*, 854–867. [[CrossRef](#)]
110. Jun, H.E.; Yao, X.L.; Feng, G.R.; Wang, R.; Yang, B.L. Preparations of the Nano-emulsion Grapefruit Essential Oil and Its Quality Evaluation. *Food Res. Dev.* **2015**, *36*, 3–6.

111. Xue, J.; Davidson, P.M.; Zhong, Q. Antimicrobial activity of thyme oil co-nanoemulsified with sodium caseinate and lecithin. *Int. J. Food Microbiol.* **2015**, *210*, 1–8. [[CrossRef](#)] [[PubMed](#)]
112. Chang, Y.; McLandsborough, L.; McClements, D.J. Physical properties and antimicrobial efficacy of thyme oil nanoemulsions: Influence of ripening inhibitors. *J. Agric. Food Chem.* **2012**, *60*, 12056–12063. [[CrossRef](#)] [[PubMed](#)]
113. da Silva Malheiros, P.; Daroit, D.J.; Brandelli, A. Food applications of liposome-encapsulated antimicrobial peptides. *Trends Food Sci. Technol.* **2010**, *21*, 284–292. [[CrossRef](#)]
114. Zhang, L.; Pornpattananangkul, D.; Hu, C.-M.; Huang, C.-M. Development of nanoparticles for antimicrobial drug delivery. *Curr. Med. Chem.* **2010**, *17*, 585–594. [[CrossRef](#)]
115. Mozafari, M.R.; Flanagan, J.; Matia-Merino, L.; Awati, A.; Omri, A.; Suntres, Z.E.; Singh, H. Recent trends in the lipid-based nanoencapsulation of antioxidants and their role in foods. *J. Sci. Food Agric.* **2006**, *86*, 2038–2045. [[CrossRef](#)]
116. Mozafari, M.R. *Nanocarrier Technologies: Frontiers of Nanotherapy*; Springer: Berlin, Germany, 2006.
117. Donsì, F.; Annunziata, M.; Sessa, M.; Ferrari, G. Nanoencapsulation of essential oils to enhance their antimicrobial activity in foods. *LWT Food Sci. Technol.* **2011**, *44*, 1908–1914. [[CrossRef](#)]
118. Nieto, G.; Huvaere, K.; Skibsted, L.H. Antioxidant activity of rosemary and thyme by-products and synergism with added antioxidant in a liposome system. *Eur. Food Res. Technol.* **2011**, *233*, 11–18. [[CrossRef](#)]
119. Bai, C.; Peng, H.; Xiong, H.; Liu, Y.; Zhao, L.; Xiao, X. Carboxymethylchitosan-coated proliposomes containing coix seed oil: Characterisation, stability and in vitro release evaluation. *Food Chem.* **2011**, *129*, 1695–1702. [[CrossRef](#)]
120. Detoni, C.B.; de Oliveira, D.M.; Santo, I.E.; Pedro, A.S.; El-Bacha, R.; da Silva Velozo, E.; Ferreira, D.; Sarmento, B.; de Magalhães Cabral-Albuquerque, E.C. Evaluation of thermal-oxidative stability and antiglioma activity of Zanthoxylum tingoassuiba essential oil entrapped into multi- and unilamellar liposomes. *J. Liposome Res.* **2012**, *22*, 1–7. [[CrossRef](#)]
121. Guan, P.; Lu, Y.; Qi, J.; Niu, M.; Lian, R.; Wu, W. Solidification of liposomes by freeze-drying: The importance of incorporating gelatin as interior support on enhanced physical stability. *Int. J. Pharm.* **2015**, *478*, 655–664. [[CrossRef](#)] [[PubMed](#)]
122. Cortés-Rojas, D.F.; Souza, C.R.; Oliveira, W.P. Encapsulation of eugenol rich clove extract in solid lipid carriers. *J. Food Eng.* **2014**, *127*, 34–42. [[CrossRef](#)]
123. Nasser, M.; Golmohammadzadeh, S.; Arouiee, H.; Jaafari, M.R.; Neamati, H. Antifungal activity of Zataria multiflora essential oil-loaded solid lipid nanoparticles in-vitro condition. *Iran. J. Basic Med. Sci.* **2016**, *19*, 1231.
124. Schwarz, C.; Mehnert, W.; Lucks, J.; Müller, R. Solid lipid nanoparticles (SLN) for controlled drug delivery. I. Production, characterization and sterilization. *J. Control. Release* **1994**, *30*, 83–96. [[CrossRef](#)]
125. Joughanian, P.; Ghaffari, S.; Ardjmand, M.; Haghghat, S.; Mohammadnejad, M. Sustained release curcumin loaded solid lipid nanoparticles. *Adv. Pharm. Bull.* **2016**, *6*, 17. [[CrossRef](#)]
126. Bhushani, J.A.; Anandharamkrishnan, C. Electrospinning and electrospaying techniques: Potential food based applications. *Trends Food Sci. Technol.* **2014**, *38*, 21–33. [[CrossRef](#)]
127. Heunis, T.D.J.; Botes, M.; Dicks, L.M.T. Encapsulation of Lactobacillus plantarum 423 and its Bacteriocin in Nanofibers. *Probiotics Antimicrob. Proteins* **2010**, *2*, 46–51. [[CrossRef](#)]
128. Ghayempour, S.; Mortazavi, S. Antibacterial activity of peppermint fragrance micro-nanocapsules prepared with a new electro-spraying method. *J. Essent. Oil Res.* **2014**, *26*, 492–498. [[CrossRef](#)]
129. Jafari, S.M. *Nanoencapsulation Technologies for the Food and Nutraceutical Industries*; Academic Press: Cambridge, MA, USA, 2017.
130. Aguiar, J.J.; Sousa, C.P.; Araruna, M.K.; Silva, M.K.; Portelo, A.C.; Lopes, J.C.; Carvalho, V.R.; Figueredo, F.G.; Bitu, V.C.; Coutinho, H.D. Antibacterial and modifying-antibiotic activities of the essential oils of *Ocimum gratissimum* L. and *Plectranthus amboinicus* L. *Eur. J. Integr. Med.* **2015**, *7*, 151–156. [[CrossRef](#)]
131. Pesavento, G.; Calónico, C.; Bilia, A.; Barnabei, M.; Calesini, F.; Addona, R.; Mencarelli, L.; Carmagnini, L.; Di Martino, M.; Nostro, A.L. Antibacterial activity of Oregano, Rosmarinus and Thymus essential oils against Staphylococcus aureus and Listeria monocytogenes in beef meatballs. *Food Control* **2015**, *54*, 188–199. [[CrossRef](#)]
132. Hamed, S.F.; Sadek, Z.; Edris, A. Antioxidant and antimicrobial activities of clove bud essential oil and eugenol nanoparticles in alcohol-free microemulsion. *J. Oleo Sci.* **2012**, *61*, 641–648. [[CrossRef](#)]
133. Salvia-Trujillo, L.; Rojas-Graü, A.; Soliva-Fortuny, R.; Martín-Belloso, O. Physicochemical characterization and antimicrobial activity of food-grade emulsions and nanoemulsions incorporating essential oils. *Food Hydrocoll.* **2015**, *43*, 547–556. [[CrossRef](#)]
134. Li, W.; Chen, H.; He, Z.; Han, C.; Liu, S.; Li, Y. Influence of surfactant and oil composition on the stability and antibacterial activity of eugenol nanoemulsions. *LWT Food Sci. Technol.* **2015**, *62*, 39–47. [[CrossRef](#)]
135. Esmaeili, A.; Asgari, A. In vitro release and biological activities of Carum copticum essential oil (CEO) loaded chitosan nanoparticles. *Int. J. Biol. Macromol.* **2015**, *81*, 283–290. [[CrossRef](#)] [[PubMed](#)]
136. Zhang, Z.; Vriesekoop, F.; Yuan, Q.; Liang, H. Effects of nisin on the antimicrobial activity of D-limonene and its nanoemulsion. *Food Chem.* **2014**, *150*, 307–312. [[CrossRef](#)] [[PubMed](#)]
137. Donsì, F.; Sessa, M.; Ferrari, G. Nanoencapsulation of essential oils to enhance their antimicrobial activity in foods. *J. Biotechnol.* **2010**, *67*, 1908–1914. [[CrossRef](#)]
138. Acevedo-Fani, A.; Salvia-Trujillo, L.; Rojas-Graü, M.A.; Martín-Belloso, O. Edible films from essential-oil-loaded nanoemulsions: Physicochemical characterization and antimicrobial properties. *Food Hydrocoll.* **2015**, *47*, 168–177. [[CrossRef](#)]
139. Moghimi, R.; Ghaderi, L.; Rafati, H.; Aliahmadi, A.; McClements, D.J. Superior antibacterial activity of nanoemulsion of Thymus daenensis essential oil against E. coli. *Food Chem.* **2016**, *194*, 410–415. [[CrossRef](#)] [[PubMed](#)]

140. Buranasuksombat, U.; Kwon, Y.J.; Turner, M.; Bhandari, B. Influence of emulsion droplet size on antimicrobial properties. *Food Sci. Biotechnol.* **2011**, *20*, 793–800. [[CrossRef](#)]
141. Li, K.-K.; Yin, S.-W.; Yin, Y.-C.; Tang, C.-H.; Yang, X.-Q.; Wen, S.-H. Preparation of water-soluble antimicrobial zein nanoparticles by a modified antisolvent approach and their characterization. *J. Food Eng.* **2013**, *119*, 343–352. [[CrossRef](#)]
142. Sugumar, S.; Nirmala, J.; Ghosh, V.; Anjali, H.; Mukherjee, A.; Chandrasekaran, N. Bio-based nanoemulsion formulation, characterization and antibacterial activity against food-borne pathogens. *J. Basic Microbiol.* **2013**, *53*, 677–685. [[CrossRef](#)]
143. Jemaa, M.B.; Falleh, H.; Serairi, R.; Neves, M.A.; Snoussi, M.; Isoda, H.; Nakajima, M.; Ksouri, R. Nanoencapsulated Thymus capitatus essential oil as natural preservative. *Innov. Food Sci. Emerg. Technol.* **2018**, *45*, 92–97. [[CrossRef](#)]
144. Prombutara, P.; Kulwathanasal, Y.; Supaka, N.; Sramala, I.; Chareonpornwattana, S. Production of nisin-loaded solid lipid nanoparticles for sustained antimicrobial activity. *Food Control* **2012**, *24*, 184–190. [[CrossRef](#)]
145. Imran, M.; Revol-Junelles, A.-M.; Paris, C.; Guedon, E.; Linder, M.; Desobry, S. Liposomal nanodelivery systems using soy and marine lecithin to encapsulate food biopreservative nisin. *LWT Food Sci. Technol.* **2015**, *62*, 341–349. [[CrossRef](#)]
146. Wen, Z.; You, X.; Jiang, L.; Liu, B.; Zheng, Z.; Pu, Y.; Cheng, B. Liposomal incorporation of rose essential oil by a supercritical process. *Flavour Fragr. J.* **2011**, *26*, 27–33. [[CrossRef](#)]
147. Jamil, B.; Abbasi, R.; Abbasi, S.; Imran, M.; Khan, S.U.; Ihsan, A.; Javed, S.; Bokhari, H. Encapsulation of cardamom essential oil in chitosan nano-composites: In-vitro efficacy on antibiotic-resistant bacterial pathogens and cytotoxicity studies. *Front. Microbiol.* **2016**, *7*, 1580. [[CrossRef](#)] [[PubMed](#)]
148. Herculano, E.D.; de Paula, H.C.; de Figueiredo, E.A.; Dias, F.G.; Pereira, V.D.A. Technology. Physicochemical and antimicrobial properties of nanoencapsulated Eucalyptus staigeriana essential oil. *LWT Food Sci. Technol.* **2015**, *61*, 484–491. [[CrossRef](#)]
149. Sotelo-Boyas, M.E.; Correa-Pacheco, Z.N.; Bautista-Baños, S.; Corona-Rangel, M.L. Physicochemical characterization of chitosan nanoparticles and nanocapsules incorporated with lime essential oil and their antibacterial activity against food-borne pathogens. *LWT* **2017**, *77*, 15–20. [[CrossRef](#)]
150. Wu, Y.; Luo, Y.; Wang, Q. Antioxidant and antimicrobial properties of essential oils encapsulated in zein nanoparticles prepared by liquid–liquid dispersion method. *LWT Food Sci. Technol.* **2012**, *48*, 283–290. [[CrossRef](#)]
151. Shah, B.; Davidson, P.M.; Zhong, Q. Nanodispersed eugenol has improved antimicrobial activity against Escherichia coli O157:H7 and Listeria monocytogenes in bovine milk. *Int. J. Food Microbiol.* **2013**, *161*, 53–59. [[CrossRef](#)]
152. Donsi, F.; Ferrari, G. Essential oil nanoemulsions as antimicrobial agents in food. *J. Biotechnol.* **2016**, *233*, 106–120. [[CrossRef](#)]
153. Neethirajan, S.; Jayas, D.S. Nanotechnology for the food and bioprocessing industries. *Food Bioprocess Technol.* **2011**, *4*, 39–47. [[CrossRef](#)]
154. Xiao, D.; Davidson, P.M.; Zhong, Q. Spray-dried zein capsules with coencapsulated nisin and thymol as antimicrobial delivery system for enhanced antilisterial properties. *J. Agric. Food Chem.* **2011**, *59*, 7393–7404. [[CrossRef](#)]
155. Gökmen, V.; Mogol, B.A.; Lumaga, R.B.; Fogliano, V.; Kaplun, Z.; Shimoni, E. Development of functional bread containing nanoencapsulated omega-3 fatty acids. *J. Food Eng.* **2011**, *105*, 585–591. [[CrossRef](#)]
156. Degan, A.J.; Luchansky, J.B. Influence of beef tallow and muscle on the antilisterial activity of pediocin AcH and liposome-encapsulated pediocin AcH. *J. Food Prot.* **1992**, *55*, 552–554. [[CrossRef](#)]
157. Commission, E.; Regulation, E.C. No 1935/2004 of the European Parliament and of the Council of 27 October 2004 on materials and articles intended to come into contact with food and repealing Directives 80/590/EEC and 89/109/EEC. *Off. J. Eur. Union L.* **2004**, *338*, 4–16.
158. Sacchetti, G.; Maietti, S.; Muzzoli, M.; Scaglianti, M.; Manfredini, S.; Radice, M.; Bruni, R. Comparative evaluation of 11 essential oils of different origin as functional antioxidants, antiradicals and antimicrobials in foods. *Food Chem.* **2005**, *91*, 621–632. [[CrossRef](#)]
159. Kenawy, E.-R.; Worley, S.; Broughton, R. The chemistry and applications of antimicrobial polymers: A state-of-the-art review. *Biomacromolecules* **2007**, *8*, 1359–1384. [[CrossRef](#)]
160. Pilon, L.; Spricigo, P.C.; Miranda, M.; de Moura, M.R.; Assis, O.B.G.; Mattoso, L.H.C.; Ferreira, M.D. Chitosan nanoparticle coatings reduce microbial growth on fresh-cut apples while not affecting quality attributes. *Int. J. Food Sci. Technol.* **2015**, *50*, 440–448. [[CrossRef](#)]
161. Keawchaon, L.; Yoksan, R. Preparation, characterization and in vitro release study of carvacrol-loaded chitosan nanoparticles. *Colloids Surf. B Biointerfaces* **2011**, *84*, 163–171. [[CrossRef](#)]
162. Sessa, M.; Ferrari, G.; Donsi, F. Novel edible coating containing essential oil nanoemulsions to prolong the shelf life of vegetable products. *Chem. Eng. Trans.* **2015**, *43*, 55–60.
163. Duféoi, W.; Terrisse, H.; Richard-Plouet, M.; Gautron, E.; Popa, F.; Humbert, B.; Ropers, M.H. Criteria to define a more relevant reference sample of titanium dioxide in the context of food: A multiscale approach. *Food Addit. Contam. Part A* **2017**, *34*, 653–665. [[CrossRef](#)] [[PubMed](#)]
164. Dorier, M.; Béal, D.; Marie-Desvergne, C.; Dubosson, M.; Barreau, F.; Houdeau, E.; Herlin-Boime, N.; Carriere, M. Continuous in vitro exposure of intestinal epithelial cells to E171 food additive causes oxidative stress, inducing oxidation of DNA bases but no endoplasmic reticulum stress. *Nanotoxicology* **2017**, *11*, 751–761. [[CrossRef](#)]
165. He, X.; Deng, H.; Hwang, H. The current application of nanotechnology in food and agriculture. *J. Food Drug Anal.* **2019**, *27*, 1–21. [[CrossRef](#)]

Chapter II

Effect of emulsifier and droplet size on the antibacterial properties of emulsions and emulsion-based films containing essential oil compounds

Published in: Journal of Food Processing and Preservation

Summary of Chapter II

In this study, sodium caseinate (CAS) and lecithin were selected as emulsifiers, and TC and citral were selected as core materials to form different O/W emulsion systems. The physical properties and antibacterial effects against Escherichia coli and Listeria innocua of these nanoemulsions were investigated. In addition, the effect of droplet size on the stability and antibacterial activity of nano-size and micro-size emulsions based on CAS and TC was studied. The results showed that the four different nanoemulsions had nanometric sizes with relatively high negative zeta potential. Nanoemulsions containing TC exhibited higher antimicrobial activities against the two bacteria than nanoemulsions containing citral whatever the emulsifier used. These nanoemulsions were then incorporated into low methoxyl pectin (LMP) films and the obtained results showed that films containing TC droplets stabilized by CAS had a larger inhibition zone than that stabilized by lecithin whatever the EO used. Finally, the obtained results showed that nanosized emulsions were more stable than microsized ones, but no significant differences were observed concerning their antibacterial activity. These results could provide new ways for the use of natural active biomolecules for manufacturing food emulsions or food packaging with functional abilities.

Effect of emulsifier and droplet size on the antibacterial properties of emulsions and emulsion-based films containing essential oil compounds

Wei Liao¹ | Emilie Dumas¹ | Sami Ghnimi¹ | Abdelhamid Elaissari² |
Adem Gharsallaoui¹ 

¹Univ. Lyon, University Claude Bernard
Lyon 1, CNRS, LAGEPP UMR 5007,
Villeurbanne, France

²Univ. Lyon, University Claude Bernard
Lyon 1, CNRS, ISA-UMR 5280, Villeurbanne,
France

Correspondence

Adem Gharsallaoui, Univ. Lyon, University
Claude Bernard Lyon 1, CNRS, LAGEPP
UMR 5007, 43 Bd 11 Novembre 1918,
69622 Villeurbanne, France.
Email: adem.gharsallaoui@univ-lyon1.fr

Funding Information

The authors are indebted to Conseil
Départementale de l'Ain for their financial
support

Abstract

In this study, the physical properties and antibacterial activity of emulsions prepared through four different combinations of essential oils (EOs) (trans-cinnamaldehyde [TC] and citral) and emulsifiers (sodium caseinate and lecithin) were investigated. The results showed that the four different nanoemulsions had nanometric sizes ranging from 142.3 to 273.1 nm, exhibiting high negative zeta potential (−25.3 to −42.7 mV) at pH 7. Nanoemulsions containing TC exhibited higher antimicrobial activities against *Escherichia coli* and *Listeria innocua* than nanoemulsions containing citral irrespective of the emulsifier used. These nanoemulsions were then incorporated into low methoxyl pectin films and the obtained results showed that films containing TC stabilized by sodium caseinate had a larger inhibition zone than the one stabilized by lecithin irrespective of the EO used. Finally, the obtained results showed that nanosized emulsions were more stable than microsized ones, but no significant differences were observed concerning their antibacterial activity.

Practical applications

This work should be an interesting basis for developing innovative antimicrobial packaging containing nanoemulsions. The interfacial membrane that surrounds the droplets of the emulsified antimicrobial provides an additional barrier that the active agent should cross before leaving the polymer matrix of the packaging film. Thus, the release kinetics will be modified and the efficiency could be improved.

1 | INTRODUCTION

Due to the increasing consumer demand for natural plant-based foods with improved microbial safety, interest in using nontoxic bioactive compounds, such as natural antibacterial agents and preservatives, in the food industry has attracted much attention in recent years (Cliceri et al., 2018). Certain essential oils (EOs) extracted from plants have a wide range antibacterial activity against common foodborne pathogens, and have attracted widespread attention as a potential resource to replace synthetic preservatives in the food industry. Especially, it is reported that some EOs are nontoxic and

classified as generally recognized as safe (GRAS) (Burt, 2004) by the U.S. Food and Drug Administration (FDA). The rational use of these biologically active compounds is currently a problem worthy of research. In this context, many natural antibacterial EO compounds have been studied, such as cinnamon oil (Wang et al., 2018), geraniol, and carvacrol (Syed et al., 2020) as food preservatives. These bioactive agents can be used directly, emulsified, or incorporated in polymer films. In fact, edible films, prepared with biodegradable and ecofriendly materials, can be used as a carrier for natural biologically active substances, such as EOs. Such active and edible films have great potential to reduce food waste and extend the shelf life

of different types of foods compared to petroleum-based food packaging films (Dutta et al., 2009).

Trans-cinnamaldehyde (3-phenyl-2-propenal, TC, FEMA 2286) is a major constituent of volatile *Cinnamon* EO (Adams et al., 2004). TC has been reported as a flavoring agent in chewing gums, ice creams, candies, and beverages. In addition, it has been used to provide a cinnamon flavor to medical products, cosmetics, and perfumes (Ribeiro-Santos et al., 2017; Shreaz et al., 2016; Yang et al., 2022). Citral (3,7-dimethyl-2, 6-octadienal, FEMA 2303), a natural flavoring molecule used for its strong lemon odor, is widely applied as an additive in foods and beverages (Zhang et al., 2020). These two molecules have been reported to have relatively strong antibacterial activities against a variety of foodborne pathogens (Lu et al., 2018; Sedaghat Doost et al., 2018; Wang et al., 2018; Zhang et al., 2020).

Nevertheless, EOs in their free forms shows low water solubility and it is complicated to introduce them into aqueous-based foods. In addition, they are volatile compounds at room temperature, which limits their processing in industries (Jo et al., 2015). To overcome these problems, oil-in-water (O/W) emulsions are promising encapsulation systems for incorporating these hydrophobic bioactive ingredients into food aqueous matrices. These encapsulation systems not only minimize the direct impact of bioactive compounds on sensory attributes but also protect them in different media during food processing and transportation (Bergensstahl, 2008). Meanwhile, emulsions are also able to improve the chemical stability of these active compounds by protecting them from environmental factors (such as oxygen, light, moisture, and pH) as well as from interactions with other food ingredients, which could decrease their activity. To allow the complete dispersion of EO into oil-in-water emulsions, synthetic surfactants such as Tween® have been commonly used. However, most synthetic surfactants still have potential safety hazards in food applications (Nerin et al., 2018). Thus, some more reassuring molecules (e.g., proteins, polysaccharides, and phospholipids) have been increasingly developed in recent years as delivery systems to encapsulate hydrophobic bioactive compounds for enhancing their stability and effectiveness (Liu et al., 2019). Among food emulsifiers, sodium caseinate, can be used as an encapsulating material because of its considerable emulsification, gelling, and stabilizing activity (Choi et al., 2009). Phospholipids are a group of polar lipids that contain both nonpolar fatty acyl groups and polar head groups, making them amphiphilic and useful as natural emulsifiers (Li et al., 2017). Among them, lecithin has been widely used as a natural emulsifier to stabilize O/W emulsions in the food industry (Belayneh et al., 2018), which was mainly attributed to the presence of various phospholipids. Concerning emulsions containing EOs, it can be assumed that different emulsifiers may produce emulsions with different physical stabilities, as well as antibacterial activities.

Thus, in this study, sodium caseinate and lecithin were selected as emulsifiers, TC and citral were selected as core materials to form different O/W emulsion systems as well as emulsion-based pectin films, and the physical properties and antibacterial activity against *Escherichia coli* and *Listeria innocua* of these emulsions were compared. Another purpose of this article was to study the

effect of diameter size on the antimicrobial activity of emulsions and emulsion-based films. In fact, the size of an emulsion-based delivery system could be a key factor that determines the properties of emulsions such as stability, solubility, and release of the emulsified bioactive molecules. Indeed, nanoemulsions may have better physical and chemical stability over traditional micrometric emulsions (>1 µm) for encapsulating bioactive components due to their nanometric size (20–500 nm) and high surface area (Polychniatou & Tzia, 2018). Thus, nanoemulsion-based systems can provide many advantages because they are more thermodynamically stable than micrometric emulsions (McClements & Rao, 2011), limiting the volatility of emulsified EOs, increasing their biological activity, and minimizing the impact on the organoleptic characteristics of food products (Donsi et al., 2011). In order to deeply investigate the size effect, we selected sodium caseinate as the emulsifier and TC as the core material to prepare nanosized and microsized emulsions and then examined the impact of the droplets' size on the antibacterial activity of emulsions and emulsion-based films.

2 | MATERIALS AND METHODS

2.1 | Materials

Trans-cinnamaldehyde (TC, 99%) and citral (99%) were purchased from Sigma-Aldrich (St Quentin Fallavier, France). Low methoxyl pectin (LMP) (Unipectine™ OF 305 C SB, degree of esterification from 22% to 28% and degree of acetylation from 20% to 23%) was purchased from Cargill (Baupte, France) and used for the preparation of films containing emulsions. Sodium caseinate powder (protein content = 93.20%) and soy lecithin powder (40% phosphatidylcholine) were purchased from Fisher Scientific (United Kingdom). Analytical grade imidazole (C₃H₄N₂), acetic acid, sodium hydroxide (NaOH), hydrochloric acid (HCl), and glycerol were purchased from Sigma-Aldrich Chimie (St Quentin Fallavier, France). Tryptone Salt broth (TS), Tryptone Soy broth (TSB), and Tryptone Soy Agar (TSA) were purchased from (Biokar Diagnostics, Beauvais, France) and used for the determination of the antibacterial activity of emulsions and films. Deionized water was used for the preparation of all solutions. The target strains used in this study were *L. innocua* (ATCC 33090) and *E. coli* (ATCC10536). All stains were maintained at -80°C in TSB supplemented with 20% (vol/vol) glycerol.

2.2 | Preparation of nanoemulsions containing essential oils (EOs)

As shown in the preparation flow chart (Figure 1), the oil phase (TC or citral) (10 wt%), the aqueous phase (90 wt%) (imidazole-acetate buffer, 5 mmol/L, pH 7), and the emulsifier (caseinate or lecithin at 1 g/L) were combined and mixed under high-shear homogenization (HSH) for 5 min under 13 500 rpm to form a coarse emulsion. Nanoemulsions were obtained by passing coarse emulsions



FIGURE 1 The flow chart of the preparation of nanoemulsions

TABLE 1 Abbreviations of the nanoemulsions according to their composition

Abbreviation	Oily phase	Emulsifier
TCC	Trans-cinnamaldehyde	Caseinate
TCL	Trans-cinnamaldehyde	Lecithin
CC	Citral	Caseinate
CL	Citral	Lecithin

through a high-pressure homogenizer (HPH) (Microfluidics LM20, Microfluidics Corp., Newton, MA, USA) five times at 300 bar. The pH was then adjusted to 7 by adding HCl (0.1 mol/L) or NaOH (0.1 mol/L). All samples were stored in sealed glass bottles (volume: 100 ml) at room temperature in the dark for physical stability evaluation. The abbreviations and formulations of the four different emulsions obtained by the different combinations of EO/emulsifier are shown in Table 1.

2.3 | Preparation of films containing EOs

Low methoxyl pectin was separately dissolved (1 wt%) in imidazole-acetate buffer (5 mM, pH 7.0) at 25°C for 3 hr under magnetic stirring. After complete dissolution, LMP solution was gradually added to the prepared nanoemulsions at a ratio of 1:1, and glycerol (1.5 g/L) was used as plasticizer. The pH of the mixture was adjusted to 7 and the film forming mixture was stirred with a magnetic stirrer at 800 rpm for 1 hr until complete homogenization. Each film was then prepared by weighing 40 g of film-forming suspensions that was spread evenly over a plastic Petri dish (90 mm). Films were formed by drying during 48 hr at 25°C under a constant airflow in an extractor hood. To ensure that the surface of the prepared films is smooth enough, the thickness of dry films was measured at five random positions with a Käfer micrometer (Erichsen, Rueil-Malmaison, France). The thickness of films with different combinations of TCC, TCL, CC, and CL varied between 96 and 231 nm.

2.4 | Hydrodynamic particle size and size distribution

Average droplet size and size distribution were determined by dynamic light scattering using a Zetasizer Nano-ZS90 (Malvern Instruments, Worcestershire, UK) at a fixed angle of 90°. To perform the measurement, nanoemulsions were diluted to an oil droplet concentration around 0.1 wt.% using imidazole-acetate buffer (5 mM, pH 7.0) prior to analysis to eliminate multiple scattering effects. After 90 s of equilibrium, each sample was scanned three times. Then, the average droplet size and polydispersity index (Pdl) were reported to represent, respectively, the mean droplet size and size distribution for each sample.

2.5 | Zeta potential measurement

Initially, nanoemulsions were diluted to a concentration of around 0.05wt% with imidazole-acetate buffer (5 mM, pH 7.0). Diluted samples were poured into cells of disposable cuvettes for electrophoretic mobility measurement (Malvern Instruments, Worcestershire, UK). All measurements were performed three times and the zeta-potential values were reported as the average of three individual measurements ($\pm SD$ [standard deviation]).

2.6 | Antibacterial activity of emulsions

The agar well diffusion method was used for the determination of the antimicrobial activity of nanoemulsions containing EOs against *L. innocua* ATCC 33090 (as a surrogate of the foodborne pathogen *Listeria monocytogenes*) and *E. coli* ATCC10536. Firstly, both bacteria were precultured in TSB at 10% (vol/vol) for 8 hr at 37°C and then precultured in TSB at 10% (vol/vol) for 16 hr at 37°C. Bacterial cultures were diluted in TSB to final concentrations of 1×10^6 CFU/ml and 1 ml was incorporated in melted TSA at 5% (vol/vol) and cooled in Petri dishes at room temperature. A sterilized glass pipette (6 mm in diameter, Fisher Scientific) was used to make a hole in the inoculated

TSA Petri plates. Fifty microliters of each nanoemulsion (TCC, TCL, CC, and CL) was placed in different wells. Nanoemulsions stabilized by caseinate and lecithin containing sunflower oil were used as negative controls of inhibition. The Petri dishes were incubated for 2 hr at 4°C to allow nanoemulsion diffusion and then incubated at 37°C. Bacterial growth inhibition zones were measured after 24 hr and each experiment was repeated three times.

2.7 | Antibacterial activity of films

The antimicrobial activity of nanoemulsion-based LMP films against *L. innocua* ATCC33090 and *E. coli* ATCC10536 were determined by using the “zone of inhibition” assay. Each film sample (TCC, TCL, CC, and CL) was aseptically cut into 15-mm-diameter discs and sterilized by ultraviolet irradiation. Thereafter, samples were transferred to TSA Petri plates inoculated as explained in Section 2.6 with bacteria at a final concentration of 1×10^7 CFU/ml. After incubating the plates at 37°C for 24 hr, the size of the zone of bacterial growth inhibition was visually observed and measured. Each experiment was repeated three times.

2.8 | Effect of emulsion size

In order to further study the effect of emulsion size on the physical properties and antibacterial activity of emulsified EOs, we selected sodium caseinate as emulsifier and TC as core material to prepare nanosized and microsized emulsions. As detailed in Section 2.3, coarse emulsions were obtained after the process of HSH and nanoemulsions were obtained after a HSH step followed by a HPH step. The particle size distributions of nanoemulsions and coarse emulsions were measured by a Zetasizer NanoZS90 and a Mastersizer 3000 equipment (Malvern Instruments, Worcestershire, UK), respectively. Antimicrobial activities against *L. innocua* ATCC33090 and *E. coli* ATCC10536 of nanoemulsions and coarse emulsions were measured before and after their incorporation in LMP films.

2.9 | Statistics

All the experiments were performed in triplicate, and at least three replicate analyses of each sample were carried out. Data were expressed as arithmetic mean \pm standard deviation (SD). SPSS 19.0 package (IBM, New York) was used to perform the analysis of variance. Values were considered significantly different at $p \leq .05$.

3 | RESULTS AND DISCUSSION

3.1 | Particle size distribution and zeta-potential of nanoemulsions

In this study, the combined effects of emulsifiers and EOs on the physical properties of nanoemulsions were evaluated. Consequently,

four different nanoemulsions were prepared by 10 wt% EO as the oily phase and 1 wt% sodium caseinate or lecithin as the emulsifier through high-pressure homogenization. The mean droplet size, Pdl, and zeta potential of these nanoemulsions were measured and reported in Table 2. The different emulsions showed significantly different average droplet sizes and size distributions (Pdl values ranged between 0.3 and 0.5). However, all nanoemulsions had relatively small average particle diameters (from 142 to 273 nm) due to the used homogenization process (high-pressure valve rigged up to 300 MPa), and the lowest droplet size was obtained for the TCL nanoemulsions (142 nm). The higher Pdl value means that the particle size distribution of these nanoemulsions was significantly wide. This phenomenon may be due to the fact that high pressure generates small droplets that can rapidly grow during storage due to Ostwald ripening mechanism (McClements, 2018).

For zeta-potential, the droplets of all nanoemulsions were negatively charged (-25 to -42 mV) at pH 7 and lecithin-based nanoemulsions showed significant higher ($p < .05$) absolute values of zeta-potential than caseinate-based ones. As described by Lieberman and Rieger (2008), an absolute value of zeta-potential around 25 mV is enough to consider that the electrostatic repulsions are able to ensure good stability of an emulsion (in salt-free medium or in moderate salt conditions). Thus, it could be deduced that the use of sodium caseinate or lecithin as emulsifier could provide sufficient repulsive forces between the droplets to obtain good physical stability of these two types of nanoemulsions containing EOs. According to Table 2, we can also notice that, irrespective of the emulsifier used, the type of EO affected the particle size and the zeta potential of the formed nanoemulsions. In fact, the nature of the oily phase (e.g., surface properties) could affect the interfacial membrane composition, structure, and rheological properties, and modify consequently the properties of the droplets. Moreover, according to the water solubility of EO, part of the oily phase could come out of the droplets and end up in the continuous phase, which can modify the interactions between the nanoscale droplets. Similar results were reported by Walker et al. (2017). In their study, the authors compared the physical properties of nanoemulsions containing a medium chain triglyceride, thyme oil, and lemon oil stabilized by Tween 80, and results showed that these three nanoemulsions have different mean particle diameters and zeta-potential values. From the viewpoint of Bonilla et al. (2012), the difference in the zeta potential of emulsions and nanoemulsions formulated with different EOs may be due to the differences in the number of ionizable compounds in the oil that can interact differently with the emulsifier molecules.

3.2 | Antibacterial activity on nanoemulsions and films

The agar diffusion method was applied to evaluate the antimicrobial activity of nanoemulsions and films against a gram-positive and a gram-negative bacteria, *L. innocua* ATCC33090 and *E. coli* ATCC10536, respectively. By maintaining the same amount of EO

(50 μ l) regardless of the sample tested, the different nanoemulsions (TCC, TCL, CC, and CL) were added in each well of the bacteria-containing medium, and the same formulation containing sunflower oil (instead of EO) was used as control. An example of the inhibition zones obtained after 24 hr at 37°C is shown in Figure 2(a).

The size of the inhibition zone is usually related to the level of the antibacterial activity of the examined sample. The larger the inhibition zone, the stronger the antibacterial effect (Lu et al., 2018). From Figure 2(a), except for the control, all the nanoemulsions showed clearly inhibition zones against both bacterial strains. In fact, as stated by Weiss et al. (2009), encapsulation of EOs at the nanoscale could increase the physical stability of the bioactive compounds contained in these EOs and increases their bioactivity through modification of their interactions with cell membranes (adsorption). Inhibition zones with different sizes were measured by the software Image J (National Institutes of Health, USA) and results are shown in the form of a bar chart Figure 2(b). According to these results, nanoemulsions containing TC showed significantly higher antibacterial activities against both bacterial strains than nanoemulsions containing citral. The relatively strong antibacterial activity of TC

is generally attributed to its aldehyde functional group, which can effectively increase the permeability of bacterial cell walls (Doyle & Stephens, 2019). Moreover, a comparison of the antimicrobial activity of nanoemulsions against a gram-positive and a gram-negative bacteria did not show significant differences regardless of the emulsifier used and EO. Generally, gram-negative bacteria are more resistant to antimicrobial molecules than gram-positive bacteria. As it is not the case for these nanoemulsions, these results are quite encouraging to hope to combat a broad spectrum of foodborne pathogens and food spoilage microorganisms.

Nanoemulsions were incorporated in LMP films and their antibacterial activity was evaluated against the same two bacterial strains. As shown in Figure 3, there were no inhibition zones around the films prepared by CC and CL. Thus, irrespective of the emulsifier used, LMP films containing nanoemulsified citral were not active against the two bacterial strains. On the other hand, films prepared by TCC showed obvious inhibition of both strains after 24 hr at 37°C. Moreover, the films containing emulsified TC stabilized by caseinate (TCC) were more active against the two tested bacteria than the films containing emulsified TC but stabilized by lecithin (TCL). Indeed, the inhibition zone was smaller for *E. coli* ATCC10536 and absent for *L. innocua* ATCC33090. These results could be attributed to the combination of several phenomena such as (i) evaporation of free EOs during the formation of biopolymer films, (ii) diffusion of EOs through the interfacial membrane containing the emulsifier, (iii) diffusion of EOs through the pectin matrix, (iv) film structure, and (v) interactions between pectin, emulsifier, EO molecules, and the bacterial membranes. An in-depth analysis is then necessary to dissociate the effect of each of these parameters on the antimicrobial

TABLE 2 Properties of nanoemulsions produced by high-pressure homogenization

Sample name	Size (nm)	Polydispersity index	Zeta potential (mV)
TCC	273.10	0.313	-25.30 \pm 3.85
TCL	142.30	0.416	-33.30 \pm 7.29
CC	269.40	0.451	-28.90 \pm 4.60
CL	189.20	0.362	-42.70 \pm 6.13

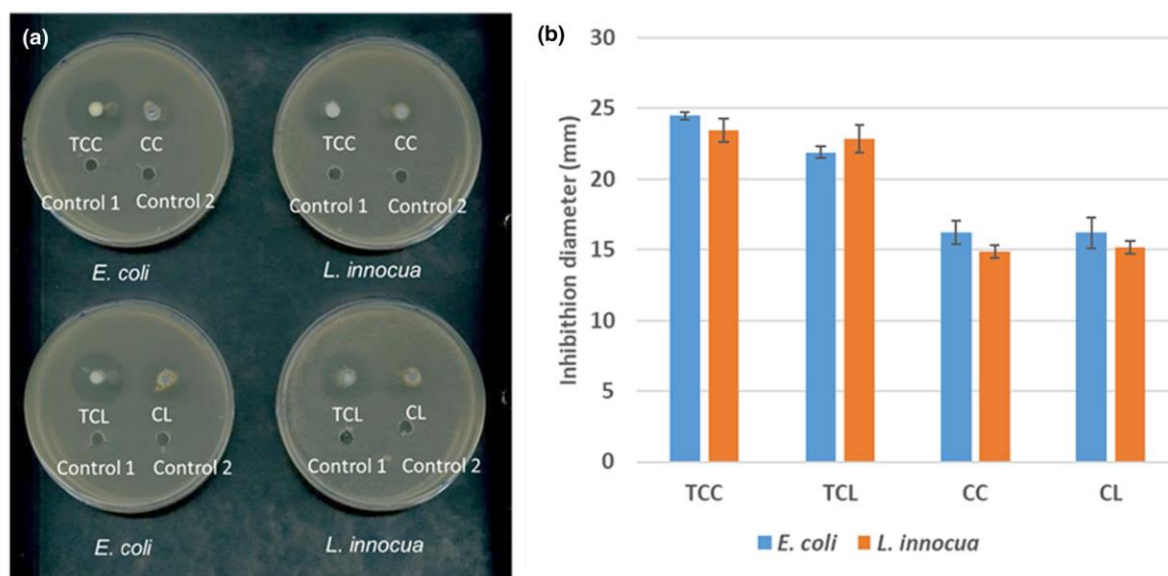


FIGURE 2 (a) Inhibition zones on culture medium containing *Escherichia coli* and *Listeria innocua* caused by four nanoemulsion samples: TCC, TCL, CC, and CL. Control 1 and Control 2 represent nanoemulsions stabilized by caseinate and lecithin containing sunflower oil. (b) The measured diameter of inhibition zone of nanoemulsions against *E. coli* and *L. innocua*

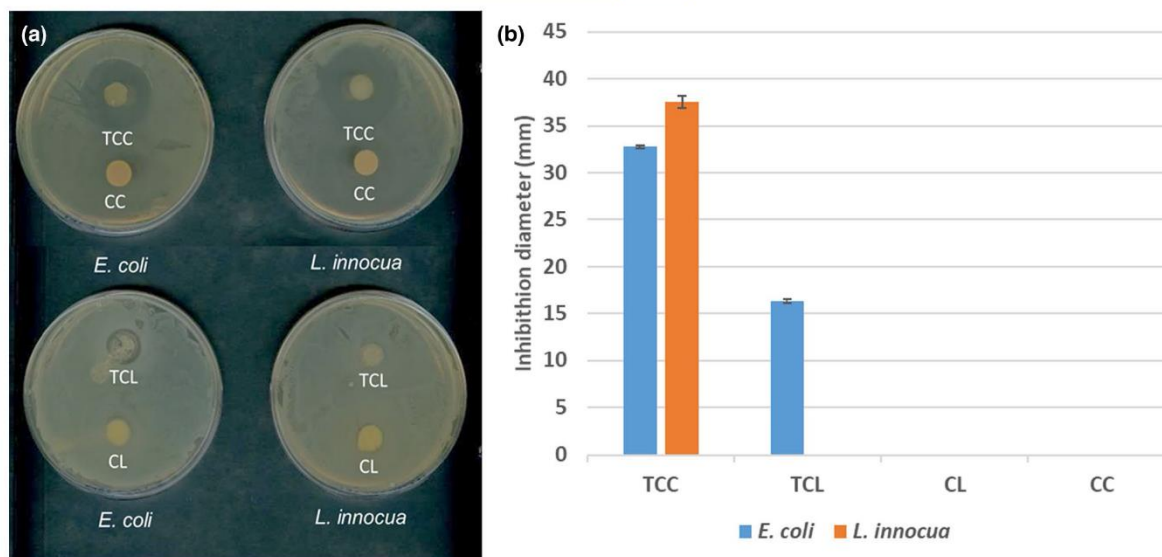


FIGURE 3 (a) Inhibition zones on culture medium containing *Escherichia coli* and *Listeria innocua* caused by four film samples containing TCC, TCL, CC, and CL. (b) The measured diameter of inhibition zone of films against *E. coli* and *L. innocua*

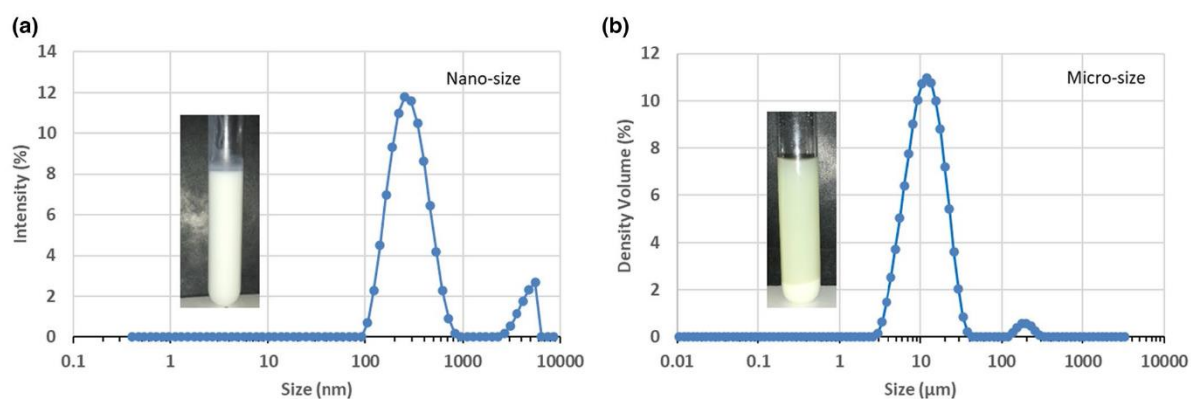


FIGURE 4 Droplet size distribution of nanoemulsions and coarse emulsions

activity of LMP films containing nanoemulsified EOs (Acevedo-Fani et al., 2015). In the present study, we will limit our interpretations to the formulation that has shown the greatest effectiveness, that is, TCC formulation. Thus, for practical applications, and based on these results, it can be assumed that the TC-containing nanoemulsions and stabilized by caseinate can be effectively incorporated into low-methylation pectin films for increasing the shelf life of foodstuffs.

3.3 | Effect of emulsion size

As indicated above, the TC/caseinate pair made it possible to obtain nanoemulsions and films having good antimicrobial activities. Thus, it is interesting to know whether the nanometric size of the

emulsions is necessary to achieve these objectives. Indeed, on an industrial scale, it is obvious that microemulsification is more economically advantageous than nanoemulsification. For this reason, the aim of the last part of the present study was to study if droplet size plays a role in the antimicrobial effectiveness of films. For this purpose, nanoemulsions containing TC and stabilized by caseinate were prepared with the same components and the preparation process was adapted to obtain nanoscale emulsions (nanoemulsions) and micro-scale emulsions (coarse emulsions).

The size distribution profiles of the two types of emulsions are shown in Figure 4 and the average diameter was 274 nm for nanoemulsions and 5.7 μm for coarse emulsions. In addition, nanoemulsions were relatively stable, while a precipitate appeared at the bottom of the coarse emulsion after 1 hr (Figure 4). The droplet

size distribution of coarse emulsions prepared using only HSH was found to range between 3 and 40 μm (Figure 4(b)). A small peak appeared and centered around 100 μm , which could be likely caused by gravitational separation, creaming, and/or coalescence of particles. For nanoemulsions (Figure 4(a)), a peak size between 100 and 1000 nm was found, which reflects a nanoscale droplet size distribution caused by the high-pressure homogenization process. In addition, a small peak was observed between 7 and 10 μm , which was likely caused by Ostwald ripening mechanism (McClements, 2018). It is interesting to notice that the prepared emulsions have been analyzed as such and without any filtration. The zeta-potential of the two emulsions was measured and the obtained values are reported in Table 3. The zeta potential was found to be negative (-25.3 ± 3.85 mV for nanoemulsion and -25.3 ± 4.67 for coarse emulsion) reflecting that the negative surface charge of the prepared emulsions was not significantly affected by the droplet size.

3.4 | Antibacterial activity of nanoemulsions, coarse emulsions, and their films

Samples of TCC nanoemulsions and coarse emulsions containing the same amount of TC were added in different wells of the agar media containing bacteria. The same formulation containing sunflower oil was used as a control. The inhibition zones obtained after 24 hr are shown in Figure 5a,b.

Except for the control, the different samples showed clearly inhibition zones against the two bacterial strains and the diameters of the inhibition zones had no significant disparity. Similar results were reported by Buranasuksombat et al. (2011). In this study, it was found that the droplet size of emulsions had no effect on the antibacterial properties of Lemon Myrtle oil. In contrast, other researchers found an effect of the droplet size on the antimicrobial properties: a decrease in droplet size resulted in an increase of the

TABLE 3 Properties of nanoemulsions and coarse emulsions

Sample name	Size	Polydispersity index	Span	Zeta potential (mV)
Nanoemulsions	274.20 nm	0.31	-	-25.30 ± 3.85
Coarse emulsions	5.70 μm	-	1.79	-25.30 ± 4.67

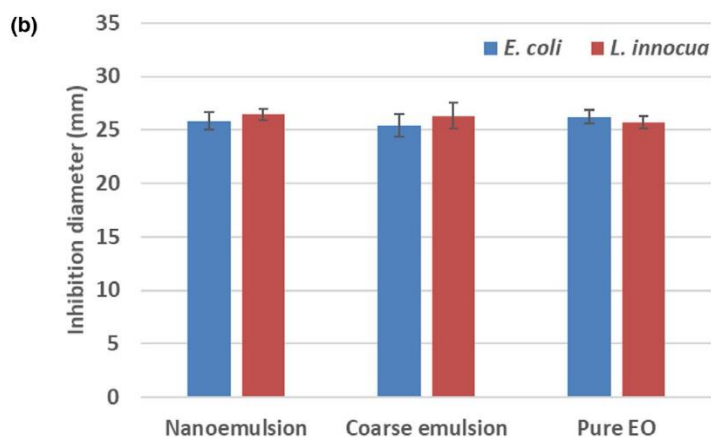
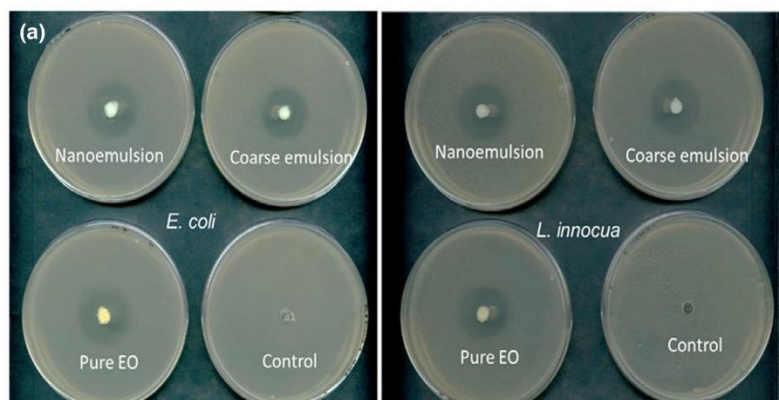


FIGURE 5 (a) Inhibition zones on culture medium containing *Escherichia coli* and *Listeria innocua* caused by nanoemulsion, coarse emulsion, and pure TC. Control represents nanoemulsions containing sunflower oil. (b) The measured diameter of inhibition of nanoemulsions against *E. coli* and *L. innocua*

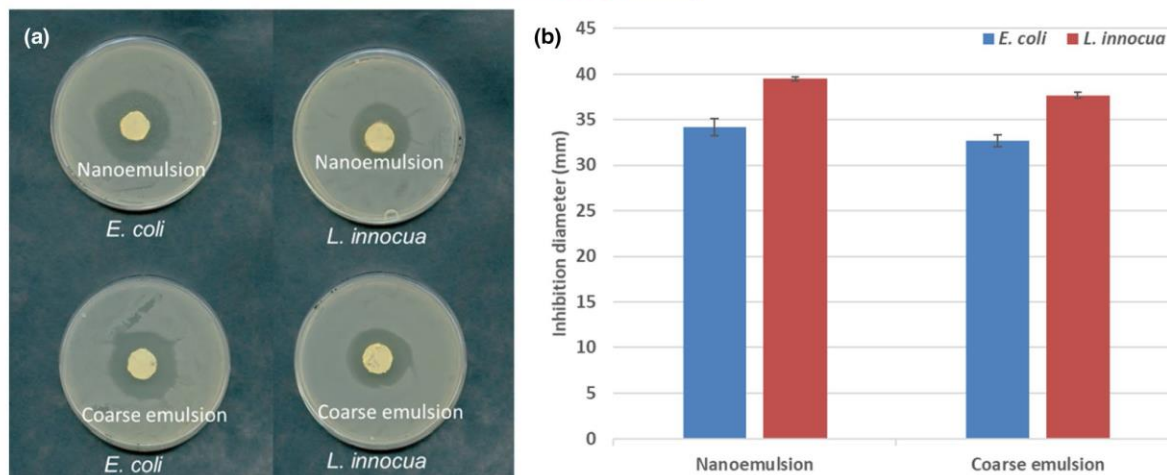


FIGURE 6 (a) Inhibition zones on culture medium containing *Escherichia coli* and *Listeria innocua* caused by films containing nanoemulsions and coarse emulsions. (b) The measured diameter of inhibition zone of two films against *E. coli* and *L. innocua*

antimicrobial properties (Chang et al., 2012). The authors explained their findings by the following hypothesis: nanoencapsulated lipophilic antimicrobials would be able to penetrate more easily through microbial membranes thus leading to an improved bactericidal activity (Chang et al., 2012). However, there is still insufficient evidence to explain this interpretation. These apparently contradictory facts indicate that a significant reduction in droplet size does not necessarily mean an increase in the functionality of EO emulsions because their antibacterial activity may be determined by the entire delivery system and its special ability to react with microbial membranes (Salvia-Trujillo et al., 2015).

As shown in Figure 6a,b, both films (containing nanoemulsions or coarse emulsions) showed obvious inhibition zones against the two bacterial strains after 24 hr of incubation. It is worthy to note that films containing nanoemulsions showed larger inhibition zone diameters than films containing coarse emulsions. This phenomenon may be explained by the fact that emulsions have more EO losses during the process of film formation than nanoemulsions because a part of TC could not yet be well encapsulated by only HSH used. However, from an application point of view, the preparation of films containing microsized emulsions should be sufficient to achieve the desired antimicrobial activity.

4 | CONCLUSION

Nanosized emulsions were obtained by different combinations of emulsifiers (sodium caseinate or lecithin) and EOs (TC and citral). Nanoemulsions containing TC exhibited higher antimicrobial activities against *E. coli* and *L. innocua* than that containing citral irrespective of the emulsifier used. Moreover, films containing TC emulsified by caseinate showed interesting antibacterial activity for both nanosized and microsized droplets. Thus, the antimicrobial activity of

nanoemulsions and nanoemulsion-based films was the highest if the combination TC and caseinate was used. These results are evidence of the potential advantages of emulsions as delivery systems of EOs as preservatives, but more factors should be considered in our future studies to evaluate the effect of the type, chemical structure, and physical properties of EOs on their antibacterial activities. Particularly, it would be interesting to verify certain hypotheses made in the present study such as the loss of EOs during the preparation of the films. This could be done by quantitating EO amounts in the films as well as evaluating their oxidation. It would also be important to measure the release kinetics of EOs from emulsions and films and to follow their diffusion in the pectin film matrices. This should explain in depth some of the results presented in this article. These results open up new ways for the use of natural active biomolecules for the manufacture of food packaging with stable biological activities.

ACKNOWLEDGEMENTS

Wei Liao greatly thanks Chinese Scholarship Council for support.

CONFLICTS OF INTEREST

The author declares that there is no conflict of interest that could be perceived as prejudicing the impartiality of the research reported.

AUTHOR CONTRIBUTIONS

Liao Wei: Data curation; Investigation; Writing-original draft. **Emilie Dumas:** Conceptualization; Formal analysis; Supervision. **Ghniemi Sami:** Resources; Supervision. **Elaissari Abdelhamid:** Conceptualization; Funding acquisition; Investigation. **Adem Gharsallaoui:** Conceptualization; Supervision; Validation.

DATA AVAILABILITY STATEMENT

The data that support the findings of this study are available from the corresponding author upon reasonable request.

ORCID

Adem Gharsallaoui  <https://orcid.org/0000-0001-6000-1994>

REFERENCES

- Acevedo-Fani, A., Salvia-Trujillo, L., Rojas-Graü, M. A., & Martín-Belloso, O. (2015). Edible films from essential-oil-loaded nanoemulsions: Physicochemical characterization and antimicrobial properties. *Food Hydrocolloids*, 47, 168–177. <https://doi.org/10.1016/j.foodhyd.2015.01.032>
- Adams, T. B., Cohen, S. M., Doull, J., Feron, V. J., Goodman, J. I., Marnett, L. J., Munro, I. C., Portoghese, P. S., Smith, R. L., Waddell, W. J., & Wagner, B. M. (2004). The FEMA GRAS assessment of cinnamyl derivatives used as flavor ingredients. *Food and Chemical Toxicology*, 42(2), 157–185. <https://doi.org/10.1016/j.fct.2003.08.021>
- Belayneh, H. D., Wehling, R. L., Cahoon, E., & Ciftci, O. N. (2018). Lipid composition and emulsifying properties of *Camelina sativa* seed lecithin. *Food Chemistry*, 242, 139–146. <https://doi.org/10.1016/j.foodchem.2017.08.082>
- Bergenstahl, B. (2008). Physicochemical aspects of an emulsifier functionality. In G. L. Hasenhuettl & R. W. Hartel (Eds.), *Food emulsifiers and their applications* (pp. 173–194). Springer.
- Bonilla, J., Atarés, L., Vargas, M., & Chiralt, A. (2012). Effect of essential oils and homogenization conditions on properties of chitosan-based films. *Food Hydrocolloids*, 26(1), 9–16. <https://doi.org/10.1016/j.foodhyd.2011.03.015>
- Buranasuksombat, U., Kwon, Y. J., Turner, M., & Bhandari, B. (2011). Influence of emulsion droplet size on antimicrobial properties. *Food Science and Biotechnology*, 20(3), 793–800. <https://doi.org/10.1007/s10068-011-0110-x>
- Burt, S. (2004). Essential oils: Their antibacterial properties and potential applications in foods—A review. *International Journal of Food Microbiology*, 94(3), 223–253. <https://doi.org/10.1016/j.ijfoodmicro.2004.03.022>
- Chang, Y., McLandsborough, L., & McClements, D. J. (2012). Physical properties and antimicrobial efficacy of thyme oil nanoemulsions: Influence of ripening inhibitors. *Journal of Agricultural and Food Chemistry*, 60(48), 12056–12063. <https://doi.org/10.1021/jf304045a>
- Choi, S. J., Decker, E. A., Henson, L., Popplewell, L. M., & McClements, D. J. (2009). Stability of citral in oil-in-water emulsions prepared with medium-chain triacylglycerols and triacetin. *Journal of Agricultural and Food Chemistry*, 57(23), 11349–11353. <https://doi.org/10.1021/jf902761h>
- Cliceri, D., Spinelli, S., Dinnella, C., Prescott, J., & Monteleone, E. (2018). The influence of psychological traits, beliefs and taste responsiveness on implicit attitudes toward plant- and animal-based dishes among vegetarians, flexitarians and omnivores. *Food Quality and Preference*, 68, 276–291. <https://doi.org/10.1016/j.foodqual.2018.03.020>
- Donsi, F., Annunziata, M., Sessa, M., & Ferrari, G. (2011). Nanoencapsulation of essential oils to enhance their antimicrobial activity in foods. *LWT-Food Science and Technology*, 44(9), 1908–1914. <https://doi.org/10.1016/j.lwt.2011.03.003>
- Doyle, A. A., & Stephens, J. C. (2019). A review of cinnamaldehyde and its derivatives as antibacterial agents. *Fitoterapia*, 139, 104405. <https://doi.org/10.1016/j.fitote.2019.104405>
- Dutta, P. K., Tripathi, S., Mehrotra, G. K., & Dutta, J. (2009). Perspectives for chitosan based antimicrobial films in food applications. *Food Chemistry*, 114(4), 1173–1182. <https://doi.org/10.1016/j.foodchem.2008.11.047>
- Jo, Y.-J., Chun, J.-Y., Kwon, Y.-J., Min, S.-G., Hong, G.-P., & Choi, M.-J. (2015). Physical and antimicrobial properties of trans-cinnamaldehyde nanoemulsions in water melon juice. *LWT-Food Science and Technology*, 60(1), 444–451. <https://doi.org/10.1016/j.lwt.2014.09.041>
- Li, J., Vosegaard, T., & Guo, Z. (2017). Applications of nuclear magnetic resonance in lipid analyses: An emerging powerful tool for lipidomics studies. *Progress in Lipid Research*, 68, 37–56. <https://doi.org/10.1016/j.plipres.2017.09.003>
- Lieberman, H. A., & Rieger, M. M. (2008). *Pharmaceutical dosage forms. Disperse systems*. Informa.
- Liu, G., Wang, Q., Hu, Z., Cai, J., & Qin, X. (2019). Maillard-reacted whey protein isolates and epigallocatechin gallate complex enhance the thermal stability of the pickering emulsion delivery of curcumin. *Journal of Agricultural and Food Chemistry*, 67(18), 5212–5220. <https://doi.org/10.1021/acs.jafc.9b00950>
- Lu, W.-C., Huang, D.-W., Wang, C.-C.-R., Yeh, C.-H., Tsai, J.-C., Huang, Y.-T., & Li, P.-H. (2018). Preparation, characterization, and antimicrobial activity of nanoemulsions incorporating citral essential oil. *Journal of Food and Drug Analysis*, 26(1), 82–89. <https://doi.org/10.1016/j.jfda.2016.12.018>
- McClements, D. J. (2018). Enhanced delivery of lipophilic bioactives using emulsions: A review of major factors affecting vitamin, nutraceutical, and lipid bioaccessibility. *Food & Function*, 9(1), 22–41. <https://doi.org/10.1039/C7FO01515A>
- McClements, D. J., & Rao, J. (2011). Food-grade nanoemulsions: Formulation, fabrication, properties, performance, biological fate, and potential toxicity. *Critical Reviews in Food Science and Nutrition*, 51(4), 285–330. <https://doi.org/10.1080/10408398.2011.559558>
- Nerin, C., Canellas, E., Vera, P., Garcia-Calvo, E., Luque-Garcia, J. L., Cámara, C., Ausejo, R., Miguel, J., & Mendoza, N. (2018). A common surfactant used in food packaging found to be toxic for reproduction in mammals. *Food and Chemical Toxicology*, 113, 115–124. <https://doi.org/10.1016/j.fct.2018.01.044>
- Polychniatou, V., & Tzia, C. (2018). Evaluation of surface-active and antioxidant effect of olive oil endogenous compounds on the stabilization of water-in-olive-oil nanoemulsions. *Food Chemistry*, 240, 1146–1153. <https://doi.org/10.1016/j.foodchem.2017.08.044>
- Ribeiro-Santos, R., Andrade, M., Madella, D., Martinazzo, A. P., de Aquino Garcia Moura, L., de Melo, N. R., & Sanches-Silva, A. (2017). Revisiting an ancient spice with medicinal purposes: Cinnamon. *Trends in Food Science & Technology*, 62, 154–169. <https://doi.org/10.1016/j.tifs.2017.02.011>
- Salvia-Trujillo, L., Rojas-Graü, A., Soliva-Fortuny, R., & Martín-Belloso, O. (2015). Physicochemical characterization and antimicrobial activity of food-grade emulsions and nanoemulsions incorporating essential oils. *Food Hydrocolloids*, 43, 547–556. <https://doi.org/10.1016/j.foodhyd.2014.07.012>
- Sedaghat Doost, A., Dewettink, K., Devlieghere, F., & Van der Meeren, P. (2018). Influence of non-ionic emulsifier type on the stability of cinnamaldehyde nanoemulsions: A comparison of polysorbate 80 and hydrophobically modified inulin. *Food Chemistry*, 258, 237–244. <https://doi.org/10.1016/j.foodchem.2018.03.078>
- Shreaz, S., Wani, W. A., Behbehani, J. M., Raja, V., Irshad, M., Karched, M., Ali, I., Siddiqi, W. A., & Hun, L. T. (2016). Cinnamaldehyde and its derivatives, a novel class of antifungal agents. *Fitoterapia*, 112, 116–131. <https://doi.org/10.1016/j.fitote.2016.05.016>
- Syed, I., Banerjee, P., & Sarkar, P. (2020). Oil-in-water emulsions of geraniol and carvacrol improve the antibacterial activity of these compounds on raw goat meat surface during extended storage at 4°C. *Food Control*, 107, 106757. <https://doi.org/10.1016/j.foodcont.2019.106757>
- Walker, R. M., Gumus, C. E., Decker, E. A., & McClements, D. J. (2017). Improvements in the formation and stability of fish oil-in-water nanoemulsions using carrier oils: MCT, thyme oil, & lemon oil. *Journal of Food Engineering*, 211, 60–68. <https://doi.org/10.1016/j.jfoodeng.2017.05.004>
- Wang, J., Li, Y., Gao, Y., Xie, Z., Zhou, M., He, Y., Wu, H., Zhou, W., Dong, X., Yang, Z., & Hu, Y. (2018). Cinnamon oil-loaded composite emulsion hydrogels with antibacterial activity prepared using concentrated emulsion templates. *Industrial Crops and Products*, 112, 281–289. <https://doi.org/10.1016/j.indcrop.2017.12.022>

- Weiss, J., Gaysinsky, S., Davidson, M., & McClements, J. (2009). Nanostructured encapsulation systems: Food antimicrobials. In G. Barbosa-Cánovas, A. Mortimer, D. Lineback, W. Spiess, K. Buckle & P. Colonna (Eds.), *Global issues in food science and technology* (pp. 425–479). Elsevier.
- Yang, Y.-L., Adel Al-Mahdy, D., Wu, M.-L., Zheng, X.-T., Piao, X.-H., Chen, A.-L., Wang, S.-M., Yang, Q., & Ge, Y.-W. (2022). LC-MS-based identification and antioxidant evaluation of small molecules from the cinnamon oil extraction waste. *Food Chemistry*, 366, 130576. <https://doi.org/10.1016/j.foodchem.2021.130576>
- Zhang, Y., Wei, J., Chen, H., Song, Z., Guo, H., Yuan, Y., & Yue, T. (2020). Antibacterial activity of essential oils against *Stenotrophomonas*

maltophilia and the effect of citral on cell membrane. *LWT*, 117, 108667. <https://doi.org/10.1016/j.lwt.2019.108667>

How to cite this article: Liao, W., Dumas, E., Ghnimi, S., Elaissari, A., & Gharsallaoui, A. (2021). Effect of emulsifier and droplet size on the antibacterial properties of emulsions and emulsion-based films containing essential oil compounds. *Journal of Food Processing and Preservation*, 00, e16072. <https://doi.org/10.1111/jfpp.16072>

Chapter III

Effect of carrier oil on the properties of sodium caseinate stabilized O/W
nanoemulsions containing Trans-cinnamaldehyde

Published in: LWT-Food Science and Technology

Summary of Chapter III

It is known that combining poor water-solubility carrier oils with hydrophobic bioactive phases could be able to enhance the physical stability of nanoemulsions by inhibiting Ostwald ripening. In this study, the impact of different contents of medium-chain triglycerides (MCT) and long-chain triglycerides (LCT) mixed with trans-cinnamaldehyde (TCA), as the active oily phase, on the sodium caseinate (CAS)-stabilized nanoemulsion was investigated. The physical properties of these nanoemulsions under different pHs, salt concentrations, and temperatures as well as their antibacterial activity were determined. Results showed that long-term stable CAS-based nanoemulsions cannot be developed by pure TCA, but they can be obtained by mixing TCA with MCT or LCT. The improved stability of these nanoemulsions can be attributed to a reduction of TCA solubility due to the addition of carrier oil, thereby inhibiting Ostwald ripening. In addition, carrier oils were shown to enhance the physical stability under common pH values, salt concentrations, and thermal processing. On the other hand, there was no obvious differences between the effects of the two carrier oils used in this study on the physical stability of nanoemulsions. Antibacterial testing revealed that nanoemulsions containing carrier oils exhibited better antibacterial activity than pure TCA. These results are useful for expanding the application of TCA as food preservative in the food industry.



Contents lists available at ScienceDirect

LWT

journal homepage: www.elsevier.com/locate/lwt

Effect of carrier oil on the properties of sodium caseinate stabilized O/W nanoemulsions containing *Trans*-cinnamaldehyde

Wei Liao^a, Adem Gharsallaoui^{a,*}, Emilie Dumas^a, Sami Ghnimi^a, Abdelhamid Elaissari^b

^a Univ. Lyon, University Claude Bernard Lyon 1, CNRS, LAGEPP UMR 5007, 43 Bd 11 Novembre 1918, 69622 Villeurbanne, France

^b Univ Lyon, University Claude Bernard Lyon 1, CNRS, ISA-UMR 5280, 69622 Villeurbanne, France

ARTICLE INFO

Keywords:

Nanoemulsion
Sodium caseinate
trans-Cinnamaldehyde
Carrier oil
Antibacterial activity

ABSTRACT

In this study, the impact of different contents of medium-chain triacylglycerols (MCT) and long-chain triacylglycerols (LCT) as carrier oils mixed with *trans*-cinnamaldehyde (TCA) on the properties of sodium caseinate-stabilized nanoemulsions was investigated. The obtained results showed that the use of a carrier oil improves significantly the TCA emulsion stability, which can be attributed to a reduction of TCA solubility in the aqueous phase followed by a decrease of Ostwald ripening. This stability improvement was observed at different pHs (3, 7 and 11), salt concentrations (0–300 mmol/L), and temperature (4, 25, 60, and 80 °C). However, the carrier oil type (MCT or LCT) did not show any significant effect on the nanoemulsions properties whatever the environmental conditions. Antibacterial testing revealed that the addition of carrier oil increased the antibacterial activity of TCA against *Escherichia coli* and *Listeria innocua*. These results are useful for expanding the application of TCA as food preservative in food industry.

1. Introduction

It is well established that food preservation is a great challenge and a significant concern in the food industries and the most serious concern of food spoilage remains that of foodborne pathogens. To solve these problems, synthetic preservatives and chemical antimicrobial agents are extensively applied in preventing microbial deterioration of food products and increasing their shelf lives. However, given the growing public concern associated with the use of chemical preservatives, there is an urgent need to be substituted by natural antimicrobial agents. Several natural antimicrobial agents, such as essential oils (EOs), lysozyme, bacteriocins, chitosan and phenolic compounds were applied for food preservation in different ways (Saeed et al., 2019).

Trans-Cinnamaldehyde (3-phenyl-2-propenal, TCA) is the major constituent of the essential volatile oil extracted from cinnamon, a traditional flavoring agent. TCA is an aromatic aldehyde regarded as a “Generally Regarded As Safe” (GRAS) molecule (Adams et al., 2004). In addition to food applications as a flavoring agent in chewing gums, ice creams, candies, and beverages, it has been used to provide a cinnamon flavor to medical products, cosmetics, and perfumes (Shreaz et al., 2016). Over the years, numerous studies have indicated that TCA possessed brilliant antibacterial activity with broad-spectrum against

bacteria, yeasts, and molds, such as *Salmonella* spp., *Campylobacter jejuni*, *Cronobacter sakazakii*, *Listeria innocua* (Doyle & Stephens, 2019a), *Laetiporus sulphureus*, *Clostridium difficile* (Mooyottu et al., 2014) and *Saccharomyces cerevisiae* (Mochida et al., 1988). Thus, TCA may act as a good alternative to synthetic chemical preservatives due to its potential antibacterial activity and safety. Nonetheless, TCA, in its free form, has a low water-solubility and it is difficult to introduce this EO into aqueous-based foods. Moreover, TCA is a volatile compound easily denatured at room temperature, which limits its use in food processing (Jo et al., 2015).

Recently, encapsulation techniques, such as emulsion-based encapsulation process, are generally used as delivery systems for EOs. Particularly, oil-in-water emulsion systems are particularly suitable for encapsulating these lipophilic bioactive components and the average size can play an important role in the efficiency of these systems. Indeed, nanoemulsions may have better physical and chemical stability compared to conventional emulsions for encapsulating bioactive components because of their nanometric size (20–500 nm) and high surface area (Polychniatou & Tzia, 2018). Thus, nanoemulsion-based systems can provide many advantages, such as protecting hydrophobic bioactive agents from chemical degradation, limiting their volatility, increasing their biological activity, and minimizing the impact on the organoleptic

* Corresponding author.

E-mail address: adem.gharsallaoui@univ-lyon1.fr (A. Gharsallaoui).

<https://doi.org/10.1016/j.lwt.2021.111655>

Received 17 September 2020; Received in revised form 19 April 2021; Accepted 4 May 2021

Available online 7 May 2021

0023-6438/© 2021 Elsevier Ltd. This is an open access article under the CC BY-NC-ND license (<http://creativecommons.org/licenses/by-nc-nd/4.0/>).

characteristics of food products (Donsi et al., 2011). In addition, nanoemulsions are more kinetically stable than conventional emulsions but they are more susceptible to Ostwald ripening due to their small droplet size (McClements & Rao, 2011). As a result, they tend to undergo physical changes during storage, which may lead to undesirable alterations in appearance, texture, and shelf life of food products. Chen et al. (2018) showed that nanoemulsions containing pure cinnamaldehyde encapsulated by whey proteins is not physically stable due to a significant change in their size. This phenomenon might be attributed to the high water solubility of cinnamaldehyde, which causes droplet growth through Ostwald ripening (Riquelme et al., 2019). Accordingly, it is necessary to properly design nanoemulsion-based delivery systems to ensure that they have good physical stability in different conditions. Walker et al. (2017) indicated that carrier oil can be incorporated into the oily phase of nanoemulsions to improve its physical and oxidative stability. In another study reported by Donsi et al. (2012), the authors added sunflower oil to the lipid phase to overcome Ostwald ripening of carvacrol, α -limonene and *trans*-cinnamaldehyde nanoemulsions prepared by high pressure homogenization. In the same context, McClements (2012) developed beverage emulsions by addition of poorly water soluble oils to inhibit Ostwald Ripening. Walker et al. confirmed (2017) that the key to enhance the stability of nanoemulsions depends on the physical properties of the carrier oil, such as viscosity, density, and water-solubility. For instance, it has been shown that: (i) combining poor water-solubility carrier oils with hydrophobic bioactive phase, has been shown to enhance physical stability of nanoemulsions by inhibiting Ostwald ripening (Julian McClements et al., 2012); (ii) combining low-viscosity carrier oils with hydrophobic bioactive phase can be used to reduce the size of nanoemulsion droplets during high-pressure homogenization (Qian & McClements, 2011); and (iii) combining carrier oils containing natural antioxidant or antibacterial agents with hydrophobic bioactive phase may endow different bioactive properties (Meroni & Raikos, 2018).

In order to study, the effect of the chain length of oil carrier, two different triacylglycerols were used in this work to improve the properties of TCA oil-in-water nanoemulsions: a medium chain triacylglycerol (MCT) and a long chain triacylglycerol (LCT). The used MCT is typically rich in saturated medium chain fatty acids ($C_{8:0}$ and $C_{10:0}$) and the LCT is derived from the linoleic acid and oleic acid ($C_{18:0}$). Both carrier oils show low water solubility compared with TCA, and they can be used to prepare nanoemulsions to inhibit Ostwald ripening. In addition, the consequences of these structural differences on the stability of emulsions, and consequently on their functional properties, deserve to be evaluated. Sodium caseinate was selected as emulsifier in this study because it is one of the most widely used proteins and has considerable emulsification, gelling and nutritional properties (Choi et al., 2009). The effects of parameters such as pH, ionic strength, and temperature on the stability as well as on the antibacterial activity of the nanoemulsions were also compared. The information generated by this study could be valuable for improving the functional performance and physical stability of food emulsion systems containing essential oil.

2. Materials and methods

2.1. Materials

Sodium caseinate powder was purchased from Fisher Scientific (United Kingdom). Protein content in sodium caseinate determined by the Kjeldahl method was 93.20% (nitrogen conversion factor $N = 6.38$). A medium chain triacylglycerol oil (MCT) was purchased from Gattefossé (Saint-Priest, France). A long chain triacylglycerol oil (sunflower oil, LCT) was purchased from a local Market. *Trans*-cinnamaldehyde (CA, 99%) was purchased from Sigma-Aldrich (St Quentin Fallavier, France). The summary of some physicochemical properties of three different oils are shown in Table 1. Analytical grade sodium chloride, imidazole, acetic acid, sodium hydroxide, and hydrochloric

Table 1

General physical properties of TCA, MCT and LCT.

Properties	(TCA) <i>trans</i> -Cinnamaldehyde	MCT	LCT (Sunflower oil)
Density (g/cm ³)	1.05	0.945	0.920
Viscosity (mPa.s)	5.08	22.88	30.68
Interfacial tension (mN/m)	2.70	7.30	10.90
Solubility in water (mg/100 mL)	1.42	Insoluble	Insoluble

acid, were purchased from Sigma-Aldrich Chimie (St Quentin Fallavier, France). All the solutions were prepared in deionized water.

2.2. Preparation of nanoemulsions

A pre-emulsion was formulated by dispersing the lipid phase (10 g/100 g) in the continuous phase, which consisted of (1 g/100 g) sodium caseinate and (89 g/100 g) buffer solution (5 mmol/L acetic acid-imidazole, 50 mg/100 g sodium benzoate, pH 7). Firstly, the resulting suspensions were stirred at room temperature until the protein was completely dissolved. The oily phase (10 g/100 g) and the aqueous phase (90 g/100 g) were mixed using high-speed homogenization for 5 min under 13 500 rpm to form coarse emulsions. Finally, nanoemulsions were obtained by passing coarse emulsions through a microfluidizer (Microfluidics LM20, Microfluidics Corp., Newton, MA, USA) 5 times at 5×10^7 Pa. The pH of the nanoemulsion was then immediately adjusted to 7.0. Each emulsion was produced in duplicate. All samples were stored in 100 mL sealed glass bottles at room temperature in the dark for physical stability evaluation.

2.3. Effect of carrier oil concentration

The overall oil content of the nanoemulsions (TCA and carrier oil) was kept constant at 10 g/100 g. TCA was mixed with MCT or LCT in different ratios (100/0, 90/10, 70/30, 50/50, 30/70 and 0/100, m/m) under stirring (15 min, 750 rpm). In order to study colloidal stability under storage, the prepared nanoemulsions were stored for 28 days and characterized in terms of hydrodynamic size and zeta potential as a function of time ranging from 1 day to one month.

2.4. Droplet hydrodynamic size and size distribution

Droplet size and size distribution were determined by dynamic light scattering using a Zetasizer Nano-ZS90 (Malvern Instruments, Worcestershire, UK) at fixed angle of 90°. To perform measurement, nanoemulsions were diluted to an oil droplet concentration around 0.1 wt% using imidazole acetate buffer to eliminate multiple scattering effects. After 90 s of equilibrium, each sample was analyzed three times. Then the average droplet size and polydispersity index (PDI) were obtained.

2.5. Zeta potential (ζ)

Nanoemulsions were diluted to a concentration around 0.05 wt% with imidazole acetate buffer to avoid multiple scattering effects. Diluted samples were transferred to the cell of disposable cuvettes for electrophoretic mobility measurement (Malvern Instruments, Worcestershire, UK). All measurements were performed three times and the ζ -potential values were reported as the average of three individual injections (\pm SD (standard deviation)).

2.6. Nanoemulsion stability to environmental stress

According to preliminary results, nanoemulsions containing mixed oily phase in the ratio TCA/MCT or LCT of 100/0 and 70/30 were investigated in the remainder of the study. The resultant nanoemulsions

were referred to as T100, T70M30 and T70L30 according to their oil compositions. To evaluate the effect of environmental stress on the properties of nanoemulsions, different pHs, salt concentrations, and temperatures were used to mimic scene which might be experienced during manufacture, cooking or utilization. For each dispersion, droplet size distribution and ζ -potential of samples were measured.

pH stability: Nanoemulsion samples were adjusted to pH values from 9.0 to 3.0 by adding 1.0 mol/L HCl or 1.0 mol/L NaOH and then stirred for 20 min to make sure the value of pH stable.

Salt stability: Nanoemulsion samples (pH 7.0) were mixed with different ratios of NaCl solution and distilled water while continuously stirring. The final NaCl concentration in the studied nanoemulsions were 0, 50, 100, and 300 mmol/L. Oil content and emulsifier contents after dilution were 5 g/100 g and 0.5 g/100 g, respectively.

Temperature stability: Selected nanoemulsion samples (pH 7.0) were heated in a water bath at different temperatures 60 °C and 80 °C for 1 h, and then cooled down to room temperature prior to analysis. Nanoemulsions stored in refrigerator (4 °C) and at room temperature (25 °C) were used as controls.

2.7. Viscosity

Viscosity of nanoemulsions was measured by Viscometers (LP-22, Brookfield, Canada) at 150 s⁻¹ at ambient temperature. Sample volume (0.5 mL) was kept constant and each measurement was repeated three times.

2.8. Interfacial tension

The oil-water interfacial tension was measured using an optical tensiometer equipped with an oscillating drop accessory (Tracker Teclis/TT Concept, France) at room temperature. In brief, the aqueous phase was placed in a glass cuvette, and the oil phase was injected into the aqueous phase using a syringe. The shape of the oil drop formed was recorded using a high-speed digital camera and the interfacial tension (mN/m) was calculated using the Tracker Software (Tracker Teclis/TT Concept, France). According to the density of the oil phase, the rising drop method or pendant drop method were used. Five different oil compositions (T100, T70M30, T70L30, M100 and L100) were studied and the initial volume of the oil drop was ~15 μ L. The aqueous phase contained 0.005 wt% caseinate in imidazole-acetate buffer (pH 7.0). The test was carried out at room temperature for 7200 s and each experiment was run in triplicate.

2.9. Antibacterial activity of nanoemulsions

The "zone of inhibition" assay on solid media was used for the determination of the antimicrobial effects of nanoemulsions against *Listeria innocua* (ATCC 33090) and *Escherichia coli* (ATCC 10536). Strains were stored at -20 °C in Tryptone Soy Broth (TSB) (Biokar diagnostics, Beauvais, France) with glycerol (15 mL/100 mL). One milliliter of the stock culture was transferred to 9 mL of TSB and incubated for 8 h at 37 °C. Then one milliliter of this pre-culture was transferred in 9 mL of TSB and incubated for 16 h at 37 °C. After that, pre-cultured bacteria were diluted in TSB to a final concentration of 10⁶ CFU/mL. One mL of bacterial suspension was incorporated at 5 mL/100 mL in melted Tryptone Soy Agar (TSA) and cooled in Petri dishes. A sterilized glass pipette (6 mm in diameter, Fisher Scientific) was used to make a well in the TSA Petri dishes inoculated. To maintain the same TCA concentration, 50 μ L of T70M30 and T70L30 and 35 μ L of T100 were placed in different wells. M100, L100, pure MCT and pure LCT were used as controls. The Petri dishes were then incubated for 2 h at 4 °C for making nanoemulsion diffusion and then incubated at 37 °C. Inhibition zone diameter was measured after 24 h and each experiment was repeated three times.

2.10. Statistical analysis

All assays were performed at least in triplicate. The data were presented as means \pm standard deviation of different samples. Statistical analyses were performed using one-way analysis of variance and multiple comparisons of means were done by Fishers Least Significant Difference (LSD) test. Statistical significance was defined as $p < 0.05$.

3. Results and discussion

3.1. Effect of carrier oil content on the properties of TCA nanoemulsions

The mean droplet size and polydispersity index of nanoemulsions containing different ratios of TCA/carrier oil (100/0, 90/10, 70/30, 50/50, 30/70 and 0/100) stored during 4 weeks were measured and the obtained results are reported in Fig. 1. Initially, all nanoemulsions had relatively small average hydrodynamic particle diameters ranging between 105.7–211.3 nm, and the lowest droplet size was obtained at the ratio TCA/LCT of 90/10. Except for nanoemulsions containing pure TCA (100/0), the other nanoemulsions have lower PDI value (<0.15) after one day storage. Low PDI value indicated that the droplet are narrowly size distributed. According to Stokes law, the smaller the droplet size was, the lower the sedimentation or creaming rate was (Paraskevopoulou et al., 2005). For nanoemulsions containing pure TCA, a transparent layer was detected in the top of the sample indicating the movement of the oil droplets to the bottom of the test tube during storage (data not shown). Results showed that, when the content of carrier oil was above 30% in the oil phase, caseinate-coated nanoemulsions containing the mixed oil phase can remain stable for a long time (>28 days), which suggests that they were stable to Ostwald ripening, coalescence, and flocculation. In fact, it is known that low size of droplets is more prone to Ostwald ripening during storage, *i.e.*, diffusion of oil molecules from the smaller to the larger droplets (McClements et al., 2012, p.; Wooster et al., 2008). For this reason, it is possible for small droplets to be produced during homogenization process and then grow rapidly during storage. In our case, increased droplet size and relatively higher PDI value were present in the nanoemulsions containing oil phases with 100% and 90% TCA after two weeks. This is in agreement with results obtained for nanoemulsions containing pure thyme oil which was attributed to Ostwald ripening (Chang et al., 2012). In addition, it is worth noting that, by comparing the PDI values of nanoemulsions containing mixed oil phase of the 70/30, LCT as a carrier oil showed lower value of PDI than that of MCT, which may be attribute to the difference in properties between the two carriers. Similar results were reported by McClements (2012) who concluded that the properties of the droplets produced during homogenization depends on the viscosity and interfacial tension of the lipid phase.

Compared to nanoemulsions containing TCA, the improved stability observed after addition of a carrier oil could be attributed to a decrease in the solubility of the oily phase causing a drop in Ostwald ripening. In fact, TCA is slightly soluble in water (Seraj & Seyedarabi, 2019), while MCT and LCT have a relatively low water-solubility. Thus, the carrier oil can act as a ripening inhibitor through an entropy of mixing effect during homogenization (McClements et al., 2012). Density of oil is another factor that may affect the formation and stability of nanoemulsions. In fact, TCA has a higher density (1050 kg m⁻³) than water (997 kg m⁻³) at 25 °C, while MCT (945 kg m⁻³) and LCT (920 kg m⁻³) have a relatively lower density than water. The density of the mixed oil phase could be consequently close to that of the water phase which can reduce droplet creaming and sedimentation during long time storage. In addition, strong electrostatic repulsions between caseinate coated oil droplets is another important factor of nanoemulsion stability. On the other hand, the mean particle diameter of nanoemulsion increased with increasing carrier oil content in the organic phase, which could be probably attributed to the decreased diffusion of TCA from the oil droplets, resulting in an increase of particle diameter after

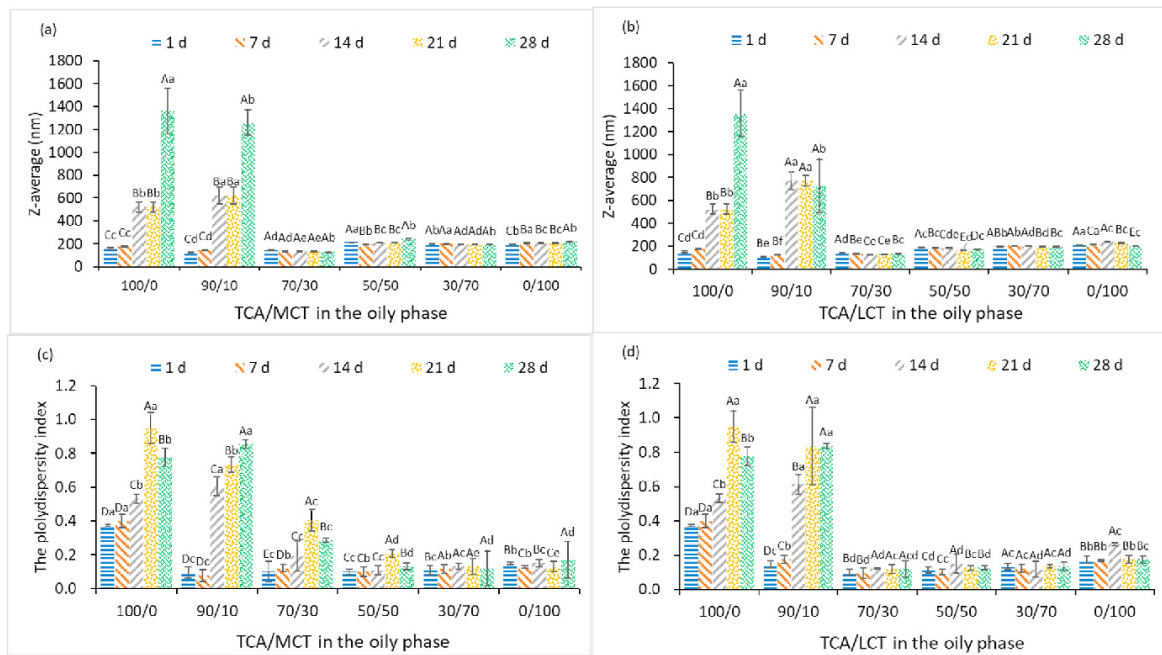


Fig. 1. Effect of MCT or LCT content on particle size (a and b) and polydispersity index (c and d) of sodium caseinate stabilized TGA nanoemulsions as a function of storage time. Samples with different uppercase superscripts (A–E) differ significantly ($p < 0.05$) when different nanoemulsions are compared at the same storage time; Samples with different lowercase superscripts (a–f) differ significantly ($p < 0.05$) when the same nanoemulsions are compared at different storage times.

homogenization.

To further explore the effect of the properties of carrier oil on the stability of nanoemulsions, the viscosity of nanoemulsions containing mixed oil phases in the ratio 100/0 and 70/30 were investigated (Fig. 2a). According to the results reported in this figure and measured at 22 °C, pure LCT showed highest viscosity (30.68 mPa s), while pure TCA showed the lowest one (5.08 mPa s) and the mixtures TCA/MCT and TCA/LCT showed intermediate viscosity values (7.56 mPa s and 9.87 mPa s, respectively). Therefore, the addition of carrier oil significantly increased the viscosity of the oily phase. As stated by Qian et al. (2011), the increased viscosity could improve stability of nanoemulsions, but their droplet size will be slight increased, which was consistent with our previous results (Fig. 1). Fig. 2b showed the interfacial tension reduction kinetics between different oily phases and sodium caseinate aqueous solution. Whatever the oily phase composition, the interfacial tension decreased over time, which can be attributed to the adsorption of caseinate molecules to the oil-water interface. Pure LCT and pure MCT showed that the equilibrium interfacial tensions were relatively high (around 10.9 mN/m and 7.3 mN/m, respectively), while pure TCA showed an equilibrium interfacial tension around 2.7 mN/m. This result can be attributed to the difference in polarity between TCA, LCT and MCT. Interestingly, the equilibrium interfacial tensions of the two mixed oil systems showed almost the same equilibrium interfacial tensions than that of pure TCA, suggesting that the interfacial tension between oil and water was mainly dependent on the presence of TCA. Similar results were found by Chen et al. (2018) as well as Felix et al. (2019). Indeed, Chen et al. (2018) found that, in the presence of TCA, the surface of the oil droplets stabilized by whey protein became crinkly, while the shape of the oil droplets without TCA did not change. This result indicates that TCA has the ability to improve the adsorption of caseinate to the oil/water interface, resulting in smaller size oil droplets after homogenization (Fig. 1).

As shown in Fig. 3, the ζ -potential of the nanoemulsions containing the two different carrier oils were measured within 4 weeks. At the first

day, all nanoemulsions had a relatively high negative surface potential (–50 to –30 mV), which can be attributed to the fact that the aqueous phase pH (7.0) during the preparing process was above the isoelectric point of the caseinate molecules (Wang et al., 2019). As described by Lieberman and Rieger (2008), when the absolute value of ζ -potential is greater than 25 mV, the electrostatic repulsions are high enough to maintain good colloidal stability of the prepared emulsion. Thus, it could be deduced that the presence of caseinate could provide high repulsive forces between the droplets to have good physical stability whatever the oil composition. However, the surface potential of oil droplets changed significantly after one week, especially for nanoemulsions containing pure TCA or a low amount of carrier oil (T90M10 and T90L10), which could indicate a change in the interface composition and/or structure.

Except for the system containing pure TCA (TCA100), the ζ -potential of the nanoemulsions became more negative with increasing carrier oil content, which means that the electrostatic repulsions between oil droplets are more intense when the carrier oil content was increased. Several different physicochemical mechanisms might account for the observed changes in surface charge of nanoemulsions. Firstly, the composition and structure of the adsorbed caseinate layer may depend on the properties of the oil phase (such as size, polarity and viscosity), which could indirectly change their surface potential (li Zhai et al., 2013). Secondly, there is a hypothesis that TCA may have chemically reacted with the adsorbed caseinate due to the presence of an aldehyde group in TCA molecules generally used as a cross-linking agent (Marin et al., 2014), and then changed their structure and electrical characteristics. Thirdly, there may be charged surface-active impurities in TCA, MCT and LCT that may affect the electrical properties of the droplets. Finally, as stated by Zhu (2017), cinnamaldehyde can rapidly be oxidized to cinnamic acid (Fig. 1. Supplementary data) during storage. Thus, the presence of cinnamic acid can affect the environmental properties, like pH, and then affect the ζ -potential of caseinate coated droplets.

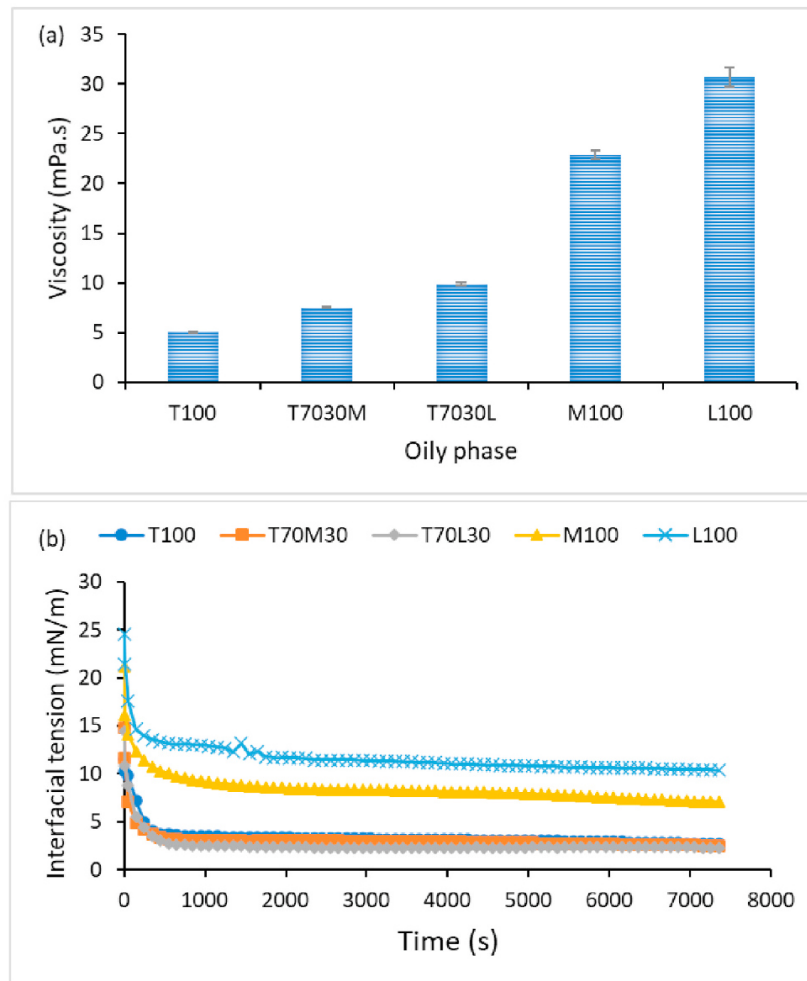


Fig. 2. Viscosity of five different oil compositions (a) and interfacial tension over time of five different oil compositions in the presence of 0.005 wt% sodium caseinate in the aqueous phase (b).

To explore this perspective, five nanoemulsions containing different oil mixtures (T100, T70M30, T70L30, T0M100 and T0L100) were selected and the pH of each sample was measured within 4 weeks (Fig. 4). The pH of nanoemulsions containing pure TCA or mixtures of TCA and carrier oils decreased with storage time, while the pH of nanoemulsions containing pure carrier oils (MCT and LCT) remained unchanged. This result can also explain the fact that the zeta potential of nanoemulsions containing high contents of carrier oil was relatively stable (Fig. 3). Interestingly, compared to pure TCA nanoemulsions, the nanoemulsions containing mixed oil phase (T70M30 and T70L30) appeared to be able to slow down the pH to the same extent after three weeks. In addition, LCT as carrier oil in nanoemulsions exhibited more ability ($p < 0.05$) to change the pH than MCT as carrier oil. This result can be explained by comparing the changes in PDI values of T70M30 and T70L30 as a function of time (Fig. 1c and d). In fact, a significant increase of PDI value was found when MCT was used as carrier oil after one week, while the PDI of T70L30 nanoemulsions remained stable. These effects may therefore depend on the physical properties of carrier oils. Similar tendency was also reported by Walker (2017) who found that the oxidation rate of fish oil was dependent on the carrier oil type.

3.2. Physical stability of nanoemulsions against environmental stress

Caseinate stabilized nanoemulsions are especially sensitive to environmental conditions which could affect their physical stability. The main three influencing parameters are pH, ionic strength, and temperature whose effects have been studied in the following sections.

pH stability: Three different pHs (3.0, 7.0 and 11.0) were used to study the effect of pH on the stability of nanoemulsions (Fig. 5). As shown in Fig. 5a, no significant difference was found in particle size of the three samples prepared at different pH values. For droplet size distribution, nanoemulsions containing mixed oil phases showed very low PDI values indicating that they were highly concentrated, while nanoemulsions containing pure TCA showed very high PDI values in each pH condition. In fact, as the pH increased from 3.0 to 11.0, the particle size of the three nanoemulsions slightly increased. This may be attributed to the electrostatic repulsion forces among amino and carboxyl groups of caseinate (Lovett et al., 2015). On the other hand, aqueous pH is related to the solubility of caseinate which will affect the particle size distribution of nanoemulsions after homogenization. As stated by Mezdour et al. (2008), the increase of the caseinate solubility allows to form thicker adsorption oil-in-water layer. The ζ -potential of the droplets in

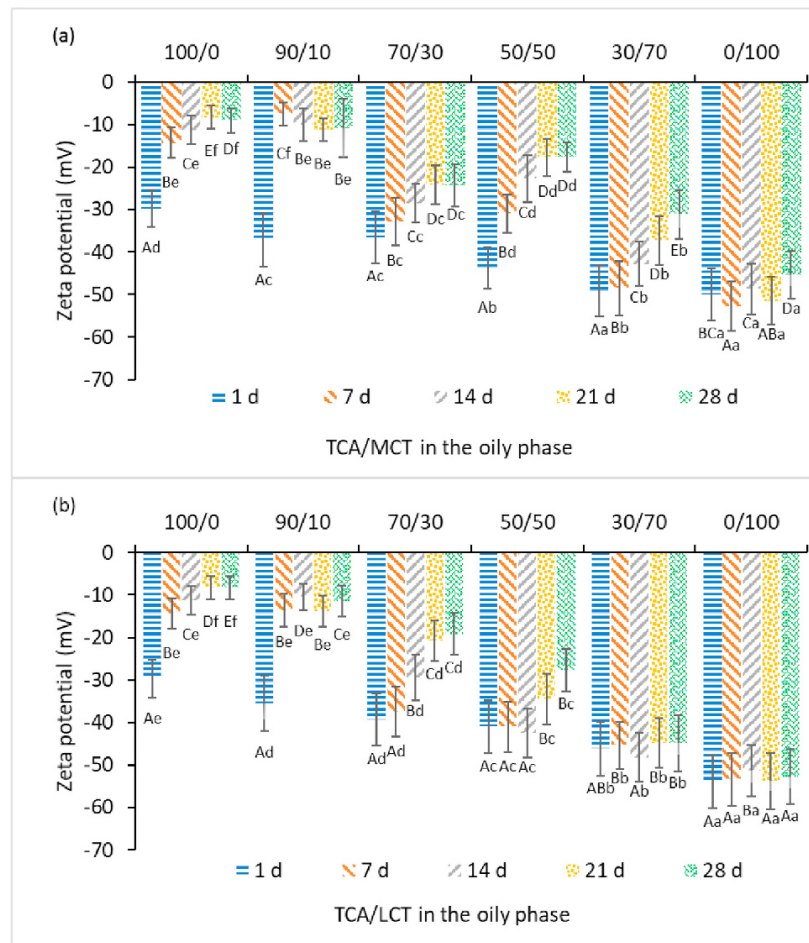


Fig. 3. Effect of MCT(a) or LCT (b) content on the ζ -potential of caseinate stabilized TCA nanoemulsions as a function of storage time. Samples with different uppercase superscripts (A–E) differ significantly ($p < 0.05$) when different nanoemulsions are compared at the same storage time; Samples with different lowercase superscripts (a–f) differ significantly ($p < 0.05$) when the same nanoemulsions are compared at different storage times.

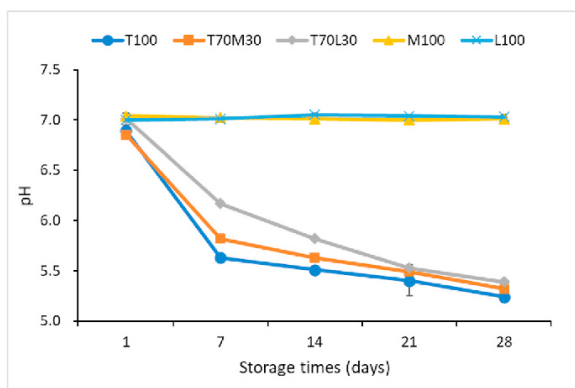


Fig. 4. pH values of caseinate stabilized nanoemulsions containing different oily phases during storage.

these emulsions was also evaluated (Fig. 5b). For all samples, the ζ -potential showed the similar trend and changed from positive to negative as the pH changed from 3 to 9, which can be attributed to the fact that the isoelectric point (I_p) of caseinate is around 4.5. The results are consistent with our previous studies that have shown that caseinate-coated oil droplets are highly unstable and aggregate in the vicinity of this pH (Wang et al., 2019). This result also showed that ζ -potential of emulsions mainly depends on the caseinate whatever the composition of the oily phase.

Ionic force: Nanoemulsions can be used as delivery systems in some food matrices containing different salt concentrations, and therefore it is important to verify the effect of ionic strength on droplet stability. Thus, the effect of different NaCl concentrations on the mean particle diameter and ζ -potential of nanoemulsions was examined (Fig. 6). All nanoemulsions showed an increase of the droplet size and PdI when NaCl concentration was increased for 0–300 mmol/L, especially for nanoemulsions containing pure TCA ($p < 0.05$, significantly). For nanoemulsions containing mixed oily phases, addition of low content of salt (<200 mmol/L) to the nanoemulsions caused little changes in the mean particle diameter after homogenization, but addition of higher salt content promoted a certain degree of droplet aggregation ($p < 0.05$). This droplet aggregation observed at higher salt concentrations is due to

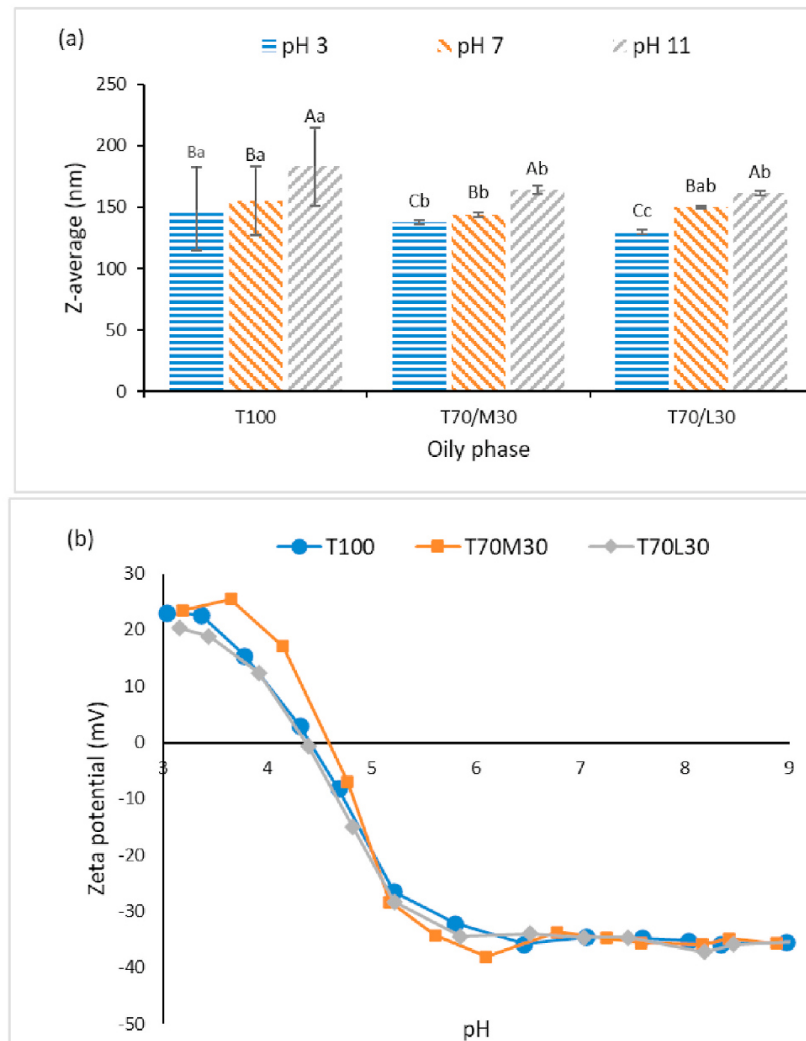


Fig. 5. Effect of pH on particle size (a) and ζ -potential (b) of caseinate-stabilized nanoemulsions containing different oily phases. The italic number above each bar refers to the PDI value. Samples with different uppercase superscripts (A–C) differ significantly ($p < 0.05$) when the same nanoemulsions are compared at different pHs; Samples with different lowercase superscripts (a–c) differ significantly ($p < 0.05$) when the different nanoemulsions are compared at the same pH.

a reduction in the electrostatic repulsion between the protein-coated droplets caused by electrostatic screening and ion binding effects.

Similar phenomenon was found upon addition of NaCl to β -lactoglobulin-stabilized emulsions (Qian et al., 2011). Moreover, our results showed that, in the presence of NaCl, the droplet size of nanoemulsions containing pure TCA turned to bimodal distribution (two peaks in one curve, data not shown), while the particle size distributions of nanoemulsions containing mixtures of TCA and carrier oil remained monomodal, though their peak shapes and locations were changed slightly. Thus, addition of carrier oil can prevent the emulsions to form bimodal distributions, which was consistent with the results obtained by Zhao et al. (2015). This phenomenon can be attributed to the fact that an increase in particle size leads to an increase in the rate of creaming of droplets in nanoemulsions (Paraskevopoulou et al., 2005). Fig. 6b showed that the ζ -potential of nanoemulsions was significantly affected by ionic strength. All samples showed a decrease trend when the NaCl concentration was increased suggesting an accumulation of counter-ions around oil droplets surfaces screening caseinate charged groups

preventing repulsions between oil droplets (Öztürk, 2017).

Temperature stability: In many commercial applications, it seems important that emulsions can withstand high temperatures during their production, storage or use. For this reason, the effect of heating treatments (60 °C and 80 °C) on the stability of nanoemulsions was examined, and 4 °C as well as 25 °C were used as control (Fig. 7). With the exception of pure TCA-containing nanoemulsions treated at 80 °C, all other nanoemulsions appeared to be relatively stable to heat treatment and showed a unimodal particle size distribution (Fig. 7a). This could be attributed to the good thermal stability of caseinate-coated droplets owing to their relatively high negative charge at pH 7, which led to stronger electrostatic repulsions between them. Meanwhile, caseinate stabilized emulsions generally have better stability during heating, because of the protein structure which does not affected by the heat-induced conformation changes as for globular proteins (Srinivasan et al., 2002). For nanoemulsions containing pure TCA, a slight increase in size was observed at 60 °C, but when the heating temperature was increased to 80 °C, the size increased significantly ($p < 0.05$). After

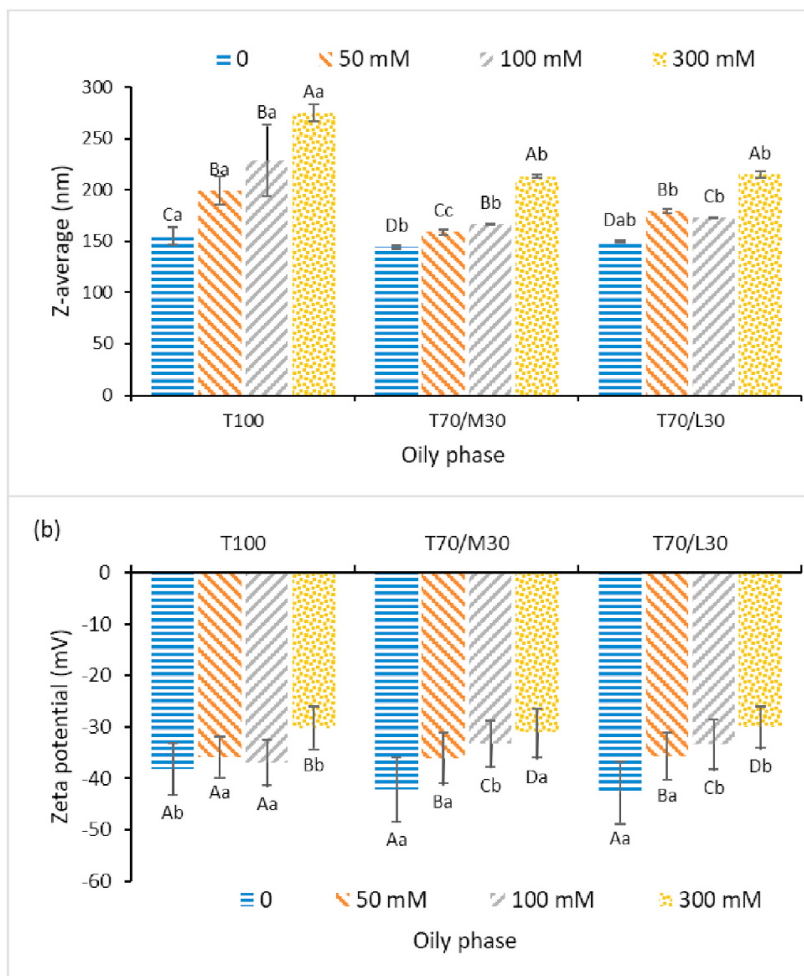


Fig. 6. The effect of salt concentration on particle size (a) and ζ -potential (b) of caseinate-stabilized nanoemulsions containing different oily phases. The italic number above each bar refers to the PDI value. Samples with different uppercase superscripts (A–D) differ significantly ($p < 0.05$) when the same nanoemulsions are compared at different salt concentrations; Samples with different lowercase superscripts (a–c) differ significantly ($p < 0.05$) when the different nanoemulsions are compared at the same salt concentration.

heating, the ζ -potential of nanoemulsions were also measured. According to Fig. 7b, there was no significant change in the ζ -potential for all nanoemulsions upon thermal treatments, suggesting that heating did not strongly influence the overall composition or structure of the caseinate coatings. The extreme condition may affect the physical stability of the nanoemulsion, however, MCT oil and LCT oil as carrier oils into the oily phase showed better tolerance than pure TCA.

3.3. Antibacterial activity of nanoemulsions

Nanoemulsions were studied for their antibacterial activity against a Gram-positive (*Listeria innocua*) and a Gram-negative (*Escherichia coli*) bacteria. Based on the same TCA content, three nanoemulsions (T100, T70M30 and T70L30) were added to each well of the bacterial-containing medium, and the same formulation without TCA as a control. Inhibition zones of nanoemulsions on medium containing bacteria after 24 h is shown in Fig. 8a. The three nanoemulsions showed clear inhibition zones against the two bacteria, whereas the control without TCA showed no inhibition zones. The size of the inhibition zones was measured by the software Image J (National Institutes of Health, USA) and the obtained values are shown in Fig. 8b. The antimicrobial activity of TCA is attributed to its aldehyde functional group and the antibacterial mechanism of TCA is probably due to the increase in permeability

of bacteria cell wall (Doyle & Stephens, 2019b). As stated by Weiss et al. (2009, pp. 425–479), encapsulation of TCA at the nanoscale could increase the physical stability of bioactive compounds and increases their bioactivity through activation of cell absorption mechanism. In addition, there was no significant disparity between antimicrobial activity of nanoemulsions containing MCT and LCT as carrier oils, but these two nanoemulsions exhibited larger inhibition zones than nanoemulsions containing pure TCA ($p < 0.05$). This phenomenon can be attributed to the fact that the addition of a carrier oil increases emulsion stability during storage, which can further increase its biological activity. Another reason may be considered to explain this result, is that nanoemulsions containing pure TCA may lose a small amount of TCA, because TCA is volatile and subject to oxidation. Meanwhile, the size of inhibition zones can be affected by several parameters, such as the amount of nanoemulsion, the spread area of nanoemulsions, the mechanism of TCA release, the number of bacteria in the medium, and the time of measuring inhibition zone. As far as possible, we have tried in this work to keep all these parameters constant and to vary only the composition of the emulsion in order to detect the effect of the carrier oil.

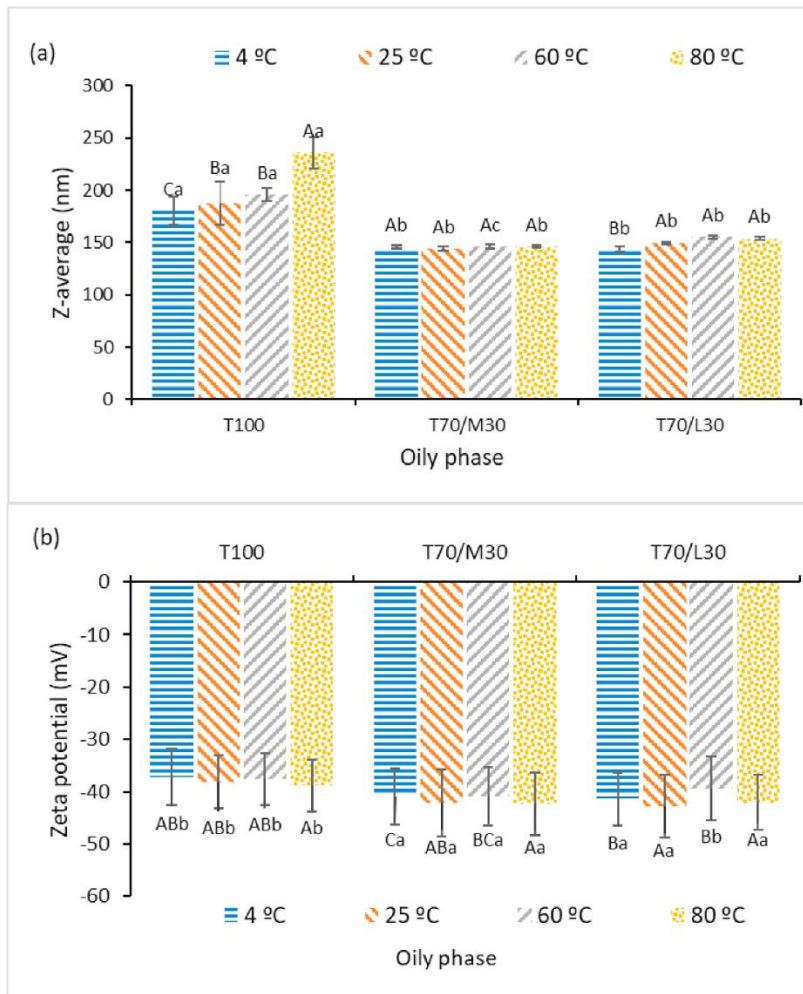


Fig. 7. The effect of temperature on particle size (a) and ζ -potential (b) of caseinate-stabilized nanoemulsions containing different oily phases. The italic number above each bar refers to the PDI value. Samples with different uppercase superscripts (A–D) differ significantly ($p < 0.05$) when the same nanoemulsions are compared at different temperatures; Samples with different lowercase superscripts (a–c) differ significantly ($p < 0.05$) when the different nanoemulsions are compared at the same temperature.

4. Conclusions

This study compared the ability of two different carrier oils to improve the properties of emulsions containing *trans*-cinnamaldehyde and stabilized by sodium caseinate. The influence of the oil type and content on the physical stability of nanoemulsions was investigated under different pHs, salt concentrations and temperature as well as their antibacterial activity against two common gram-positive and gram-negative bacteria. The analyses revealed that stable caseinate-coated nanoemulsions are difficult to formulate using pure TCA. However, nanoemulsions containing TCA mixed with carrier oil could keep stable for a relatively long period, especially when LCT is used as carrier oil. This stability improvement can be attributed to a reduction of TCA diffusion in the aqueous phase and an inhibition of Ostwald ripening. Antibacterial effect revealed that, compared to nanoemulsions containing pure TCA, the activity of nanoemulsions containing mixtures of TCA and carrier oils exhibited better antibacterial activity against *Escherichia coli* and *Listeria innocua*. The development of these nanoemulsions is in line with the growing interest of the food industry and consumers in using products based on natural substances and the incorporation of carrier oils into nanoemulsion-based systems containing TCA is a promising technique that can extend the shelf life of

perishable foods.

CRediT authorship contribution statement

Wei Liao: Conceptualization, Formal analysis, Writing – original draft, conception and design, or analysis and interpretation of the data; (b) drafting the article or revising it critically for important intellectual content; and (c) approval of the final version. **Adem Gharsallaoui:** Conceptualization, Formal analysis, Writing – original draft, conception and design, or analysis and interpretation of the data; (b) drafting the article or revising it critically for important intellectual content; and (c) approval of the final version. **Emilie Dumas:** Conceptualization, Formal analysis, Writing – original draft, conception and design, or analysis and interpretation of the data; (b) drafting the article or revising it critically for important intellectual content; and (c) approval of the final version. **Sami Ghnimi:** Conceptualization, Formal analysis, Writing – original draft, and conception and design, or analysis and interpretation of the data; (b) drafting the article or revising it critically for important intellectual content; and (c) approval of the final version. **Abdelhamid Elaissari:** Conceptualization, Formal analysis, Writing – original draft, conception and design, or analysis and interpretation of the data; (b) drafting the article or revising it critically for important intellectual

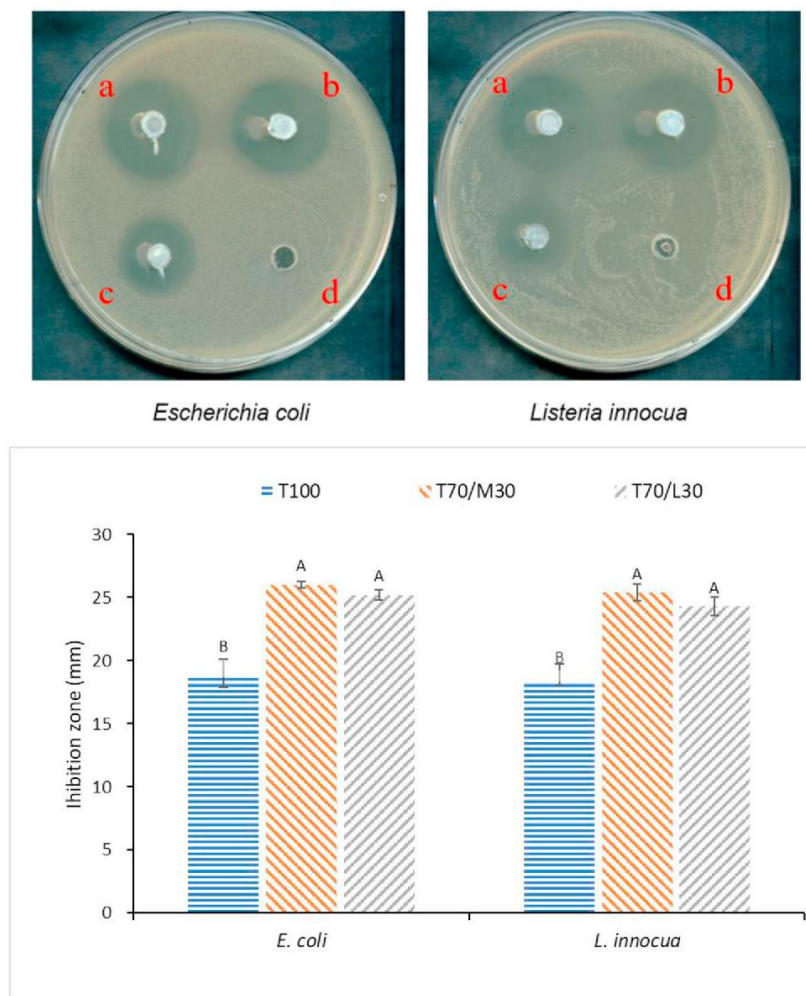


Fig. 8. Top: Example of inhibition zones on TSA containing *Escherichia coli* and *Listeria innocua* with four nanoemulsions: T100 (a), T70M30 (b), T70L30 (c) and M100 (d). Bottom: Measured diameter of inhibition zone of three nanoemulsions against *Escherichia coli* and *Listeria innocua*: T100, T70M30 and T70L30. Samples with different uppercase superscripts (A–B) differ significantly ($p < 0.05$).

content; and (c) approval of the final version.

Declaration of competing interest

The authors declare no conflicts of interest that pertain to this manuscript.

Appendix A. Supplementary data

Supplementary data to this article can be found online at <https://doi.org/10.1016/j.lwt.2021.111655>.

References

- Adams, T. B., Cohen, S. M., Doull, J., Feron, V. J., Goodman, J. I., Marnett, L. J., Munro, I. C., Portoghese, P. S., Smith, R. L., & Waddell, W. J. (2004). The FEMA GRAS assessment of cinnamyl derivatives used as flavor ingredients. *Food and Chemical Toxicology*, 42(2), 157–185.
- Chang, Y., McLandsborough, L., & McClements, D. J. (2012). Physical properties and antimicrobial efficacy of thyme oil nanoemulsions: Influence of ripening inhibitors. *Journal of Agricultural and Food Chemistry*, 60(48), 12056–12063.
- Chen, E., Cao, L., McClements, D. J., Liu, S., Li, B., & Li, Y. (2018). Enhancement of physicochemical properties of whey protein-stabilized nanoemulsions by interfacial cross-linking using cinnamaldehyde. *Food Hydrocolloids*, 77, 976–985. <https://doi.org/10.1016/j.foodhyd.2017.11.047>
- Choi, S. J., Decker, E. A., Henson, L., Popplewell, L. M., & McClements, D. J. (2009). Stability of citral in oil-in-water emulsions prepared with medium-chain triacylglycerols and triacetin. *Journal of Agricultural and Food Chemistry*, 57(23), 11349–11353.
- Donsi, F., Annunziata, M., Sessa, M., & Ferrari, G. (2011). Nanoencapsulation of essential oils to enhance their antimicrobial activity in foods. *LWT-Food Science and Technology*, 44(9), 1908–1914.
- Donsi, F., Annunziata, M., Vincenzi, M., & Ferrari, G. (2012). Design of nanoemulsion-based delivery systems of natural antimicrobials: Effect of the emulsifier. *Biotechnology for Enhancing Plant Production and Food Quality - IBS 2010 Part III*, 159(4), 342–350.
- Doyle, A. A., & Stephens, J. C. (2019a). A review of cinnamaldehyde and its derivatives as antibacterial agents. *Fitoterapia*, 139, 104405.
- Doyle, A. A., & Stephens, J. C. (2019b). A review of cinnamaldehyde and its derivatives as antibacterial agents. *Fitoterapia*, 139, 104405.
- Felix, M., Yang, J., Guerrero, A., & Sagis, L. M. C. (2019). Effect of cinnamaldehyde on interfacial rheological properties of proteins adsorbed at O/W interfaces. *Food Hydrocolloids*, 97.
- Jo, Y.-J., Chun, J.-Y., Kwon, Y.-J., Min, S.-G., Hong, G.-P., & Choi, M.-J. (2015). Physical and antimicrobial properties of trans-cinnamaldehyde nanoemulsions in water melon juice. *LWT-Food Science and Technology*, 60(1), 444–451.

- Julian McClements, D., Henson, L., Popplewell, L. M., Decker, E. A., & Jun Choi, S. (2012). Inhibition of Ostwald ripening in model beverage emulsions by addition of poorly water soluble triglyceride oils. *Journal of Food Science*, 77(1), C33–C38.
- Lieberman, H. A., & Rieger, M. M. (2008). *Pharmaceutical dosage forms: Disperse systems*. Informa.
- Lovett, J. R., Warren, M. J., Ratcliffe, L. P., Kocik, M. K., & Armes, S. P. (2015). pH-responsive non-ionic diblock copolymers: Ionization of carboxylic acid end-groups induces an order–order morphological transition. *Angewandte Chemie International Edition*, 54(4), 1279–1283.
- Marin, L., Moraru, S., Popescu, M.-C., Nicolăescu, A., Zgărdan, C., Simionescu, B. C., & Barboiu, M. (2014). Out-of-Water constitutional self-organization of chitosan–cinnamaldehyde dyads. *Chemistry—A European Journal*, 20(16), 4814–4821.
- McClements, D. J., Henson, L., Popplewell, L. M., Decker, E. A., & Choi, S. J. (2012). Inhibition of Ostwald ripening in model beverage emulsions by addition of poorly water soluble triglyceride oils. *Journal of Food Science*, 77(1), C33–C38.
- McClements, D. J., & Rao, J. (2011). Food-grade nanoemulsions: Formulation, fabrication, properties, performance, biological fate, and potential toxicity. *Critical Reviews in Food Science and Nutrition*, 51(4), 285–330.
- Meroni, E., & Raikos, V. (2018). Physicochemical stability, antioxidant properties and bioaccessibility of β -carotene in orange oil-in-water beverage emulsions: Influence of carrier oil types. *Food and Function*, 9(1), 320–330. <https://doi.org/10.1039/c7fo01170a>
- Mezdout, S., Boyaval, P., & Korolczuk, J. (2008). Solubility of α S1-, β - and κ -casein in water-ethanol solutions. *Dairy Science & Technology*, 88(3), 313–325.
- Mochida, K., Gomyoda, M., Fujita, T., & Yamagata, K. (1988). Toxicity of allyl isothiocyanate and cinnamic aldehyde assessed using cultured human KB cells and yeast, *Saccharomyces cerevisiae*. *Bulletin of Environmental Contamination and Toxicology*, 40(3).
- Mooyottu, S., Kollanoor-Johny, A., Flock, G., Bouillaut, L., Upadhyay, A., Sonenshein, A., & Venkitanarayanan, K. (2014). Carvacrol and trans-cinnamaldehyde reduce *Clostridium difficile* toxin production and cytotoxicity in vitro. *International Journal of Molecular Sciences*, 15(3), 4415–4430.
- Öztürk, B. (2017). Nanoemulsions for food fortification with lipophilic vitamins: Production challenges, stability, and bioavailability. *European Journal of Lipid Science and Technology*, 119(7), 1500539.
- Paraskevopoulou, A., Boskou, D., & Kiosseoglou, V. (2005). Stabilization of olive oil–lemon juice emulsion with polysaccharides. *Food Chemistry*, 90(4), 627–634.
- Polychniatou, V., & Tzia, C. (2018). Evaluation of surface-active and antioxidant effect of olive oil endogenous compounds on the stabilization of water-in-olive-oil nanoemulsions. *Food Chemistry*, 240, 1146–1153.
- Qian, C., Decker, E. A., Xiao, H., & McClements, D. J. (2011). Comparison of biopolymer emulsifier performance in formation and stabilization of orange oil-in-water emulsions. *Journal of the American Oil Chemists' Society*, 88(1), 47–55.
- Qian, C., & McClements, D. J. (2011). Formation of nanoemulsions stabilized by model food-grade emulsifiers using high-pressure homogenization: Factors affecting particle size. *Food Hydrocolloids*, 25(5), 1000–1008.
- Riquelme, N., Zúñiga, R. N., & Arancibia, C. (2019). Physical stability of nanoemulsions with emulsifier mixtures: Replacement of tween 80 with quillaja saponin. *LWT – Food Science and Technology*, 111, 760–766.
- Saeed, F., Afzaal, M., Tufail, T., & Ahmad, A. (2019). Use of natural antimicrobial agents: A safe preservation approach. In I. Var, & S. Uzurlu (Eds.), *Active antimicrobial food packaging*. IntechOpen (2019), pp. 0-18.
- Seraj, Z., & Seyedarabi, A. (2019). The role of cinnamaldehyde and phenyl ethyl alcohol as two types of precipitants affecting protein hydration levels. *International Journal of Biological Macromolecules*.
- Shreaz, S., Wani, W. A., Behbehani, J. M., Raja, V., Irshad, M., Karched, M., Ali, I., Siddiqi, W. A., & Hun, L. T. (2016). Cinnamaldehyde and its derivatives, a novel class of antifungal agents. *Fitoterapia*, 112, 116–131.
- Srinivasan, M., Singh, H., & Munro, P. A. (2002). Formation and stability of sodium caseinate emulsions: Influence of retorting (121 C for 15 min) before or after emulsification. *Food Hydrocolloids*, 16(2), 153–160.
- Walker, R. M., Gumus, C. E., Decker, E. A., & McClements, D. J. (2017). Improvements in the formation and stability of fish oil-in-water nanoemulsions using carrier oils: MCT, thyme oil, & lemon oil. *Journal of Food Engineering*, 211, 60–68.
- Wang, J., Dumas, E., & Gharsallaoui, A. (2019). Low Methoxyl pectin/sodium caseinate complexing behavior studied by isothermal titration calorimetry. *Food Hydrocolloids*, 88, 163–169.
- Weiss, J., Gaysinsky, S., Davidson, M., & McClements, J. (2009). Nanostructured encapsulation systems: Food antimicrobials. *Global issues in food science and technology*. Elsevier.
- Wooster, T. J., Golding, M., & Sanguansri, P. (2008). Impact of oil type on nanoemulsion formation and Ostwald ripening stability. *Langmuir*, 24(22), 12758–12765.
- Li Zhai, J., Day, L., Aguil ar, M.-I., & Wooster, T. J. (2013). Protein folding at emulsion oil/water interfaces. *Current Opinion in Colloid & Interface Science*, 18(4), 257–271.
- Zhao, X., Liu, F., Ma, C., Yuan, F., & Gao, Y. (2015). Effect of carrier oils on the physicochemical properties of orange oil beverage emulsions. *Food Research International*, 74, 260–268.
- Zhu, R., Liu, H., Liu, C., Wang, L., Ma, R., Chen, B., Li, L., Niu, J., Fu, M., & Zhang, D. (2017). Cinnamaldehyde in diabetes: A review of pharmacology, pharmacokinetics and safety. *Pharmacological Research*, 122, 78–89.

Chapter IV

Effect of pectin on the properties of nanoemulsions stabilized by sodium
caseinate at neutral pH

Published in: International Journal of Biological Macromolecules

Summary of Chapter IV

Unlike proteins can be adsorbed at the oil-water interfaces, most polysaccharides such as pectin, xanthan gum, alginate, Arabic gum, etc. have little inherent surface activity because of their relatively high hydrophilicity. The purpose of the present article was to study if anionic polysaccharides (LMP) could be used to improve physical and chemical stability of protein-based nanoemulsions at neutral pH. Our previous studies conducted by using isothermal titration calorimetry have indicated that no significant interactions were found at pH 7.0 between CAS and LMP. The effect of different concentrations of LMP on lipid oxidation and physical stability of CAS stabilized nanoemulsions under neutral pH was investigated. Results indicated that the addition of LMP at low concentration had no effect on the average size of nanoemulsions, but a slight size increase and phase separation were observed at higher concentrations of pectin. In addition, the presence of pectin could improve the physical (especially against high salt concentrations and freeze-thaw cycles) and chemical stability (inhibition of lipid and protein oxidation) of caseinate-stabilized nanoemulsions, depending on its concentration. This research could be interesting for the formulation of beverage emulsions with improved physical and chemical properties at neutral pH.



Effect of pectin on the properties of nanoemulsions stabilized by sodium caseinate at neutral pH

Wei Liao^a, Abdelhamid Elaissari^b, Sami Ghnimi^{a,b,c}, Emilie Dumas^a, Adem Gharsallaoui^{a,*}

^a Univ. Lyon, University Claude Bernard Lyon 1, CNRS, LAGEPP UMR 5007, 43 Bd 11 Novembre 1918, 69622 Villeurbanne, France

^b Univ Lyon, University Claude Bernard Lyon 1, CNRS, ISA UMR 5280, 69622 Villeurbanne, France

^c ISARA, 23 Rue Jean Baldissini, 69007 Lyon, France

ARTICLE INFO

Keywords:

Nanoemulsion
Physical stability
Lipid oxidation
Sodium caseinate
Pectin

ABSTRACT

The effect of different concentrations of low methoxyl pectin (LMP) on lipid oxidation and physical stability of sodium caseinate (CAS) stabilized nanoemulsions under neutral pH was investigated. The addition of pectin at low concentration (≤ 0.10 wt%) had no significant effect on the average size of nanoemulsions, but a slight size increase and phase separation were observed at higher concentrations of pectin (≥ 0.25 wt%). This result suggests that LMP can not adsorb at the oil/water interfacial CAS membrane at neutral pH. However, in the presence of LMP, the physical stability of nanoemulsions against high salt concentrations and freeze-thaw cycles was significantly enhanced. Moreover, nanoemulsions containing pectin have a better ability to inhibit lipid and protein oxidation than nanoemulsions without pectin after 3 weeks, and the lowest lipid hydroperoxide content was observed for nanoemulsions containing 0.25 wt% pectin.

1. Introduction

Over the last few years, substantial efforts have been concentrated on incorporating biologically active compounds into food formulations to endow food products with more functional properties. In addition, there is a great interest to produce delivery systems containing different types of natural lipophilic bioactive ingredients, such as carotenoids, phytosterols, vitamins, and essential oils [1]. Nevertheless, there are many technical challenges to overcome such as low water solubility, chemical instability, and sensitivity to oxidative degradation of lipophilic compounds during production and storage. Fortunately, most of these problems can be successfully solved by encapsulation technologies. Among these technologies, nanoemulsion-based encapsulation systems have been widely used to achieve these goals, such as protecting bioactive compounds, delivering active molecules to target sites, increasing bioavailability, and extending their shelf life...[2]. Indeed, compared with the conventional emulsions, nanoemulsion-based systems exhibited better functionality, such as enhanced protection, increased stability and improved bioavailability of bioactive compounds, due to their nanometric size (20–500 nm) and high surface area [3]. Moreover, nanoemulsions are kinetically stable systems which are more stable to gravitational separation, coalescence, and flocculation

than conventional emulsions, but they are more prone to Ostwald ripening due to their small droplet size [4] and generally narrowly size distributed.

The encapsulating wall material needs to be carefully selected, usually edible and inexpensive, especially in the food industry [1]. At present, many encapsulation systems based on synthetic polymers have been established and explored. However, some food safety issues may arise because the preparation of these polymer-based synthetic microcapsules may involve the use of toxic organic solvents [5]. Thus, it is increasingly necessary in the food industry to replace synthetic emulsifiers with natural ones. Proteins and polysaccharides as natural biopolymers have been applied in food industries. Particularly, many types of food proteins, such as walnut protein [6], legume protein [7], whey protein [8,9], soy protein [10,11], casein proteins [10,12], etc., have been well studied as wall materials for encapsulation systems due to their commercial availability, film-forming, and excellent amphiphilic properties. Among them, casein proteins, which are generally sold industrially in the form of sodium caseinate (CAS), have been widely used as commercial emulsifiers in the food industry [13]. CAS has rather flexible structure and composed of a soluble mixture of four different proteins, $\alpha(s1)$ - and $\alpha(s2)$ -caseins, β -casein, and κ -casein. As a result, they can be rapidly adsorbed by reducing the surface tension at the

* Corresponding author.

E-mail address: adem.gharsallaoui@univ-lyon1.fr (A. Gharsallaoui).

<https://doi.org/10.1016/j.ijbiomac.2022.04.160>

Received 9 March 2022; Received in revised form 16 April 2022; Accepted 21 April 2022

Available online 27 April 2022

0141-8130/© 2022 Elsevier B.V. All rights reserved.

oil–water interface and form thick interfacial films during the emulsification process [14,15]. CAS was also reported to be effective in protecting emulsified oils from oxidation due to its unique iron chelating properties [10]. Antioxidant proteins could slow down the oxidation of lipids in food, but during this process they are usually self-oxidized [16]. Meanwhile, the products of lipid oxidation generally could in turn promote the oxidation of proteins [17]. These changes typically result in modifications of the functional properties of proteins like their emulsifying ability [8] and produce toxic reaction products [18]. Therefore, it is necessary to simultaneously inhibit the oxidation of lipids and that of proteins in food emulsions.

Unlike proteins can be adsorbed at the oil-water interface, most polysaccharides such as pectin, xanthan gum, alginate, Arabic gum, etc. have little inherent surface activity because of their strong hydrophilicity [19,20]. Nevertheless, under the conditions that proteins and polysaccharides have opposite charges, they can be adsorbed on the surface of protein-encapsulated oil droplets through electrostatic interactions. Zhang et al. [12] investigated the effect of pH on emulsions stabilized by chitosan and casein and their results indicated that emulsification pH range of casein could be effectively expanded as the non-covalent protein-polysaccharide complexes formed by electrostatic attractions between casein and chitosan. Zang et al. [20] investigated the effect of different anionic polysaccharides on the properties of rice bran protein-stabilized emulsions and they found that the resistance of emulsions to environmental stresses (salt, pH) was significantly improved. On the other hand, even if the polysaccharide has the same charge as the protein, the polysaccharide can act as an emulsion stabilizer by forming an extended network, thereby affecting the viscosity of the continuous phase [6]. Khaloufi et al. [9] demonstrated that flaxseed gum is a non-interacting polysaccharide at neutral pH when mixed with whey protein isolate stabilized emulsions and there was no visible phase separation at low addition levels. Zhang et al. [21] developed almond proteins and *camellia* saponin based emulsions at pH 7. They found that the formation of lipid oxidation products was significantly lower in the almond protein stabilized emulsions containing *camellia* saponin, even though both the protein and the surfactant were negatively charged [21]. In this regard, many studies have begun to focus on the use of emulsifier blends to improve the emulsification effect and functional properties by combining the properties of many functional molecules. Particularly, based on electrostatic interactions between anionic polysaccharides and positively charged proteins below their isoelectric point (pI), the benefits of polysaccharides as an adsorbable layer in protein-stabilized emulsions have been widely reported [6,22]. On the other hand, when the pH of the emulsions is higher than the pI of protein emulsifiers, anionic polysaccharides cannot be adsorbed on the emulsion as a protective layer due to the electrostatic repulsions. Several studies have suggested that unadsorbed polysaccharides can also improve the stability of protein-stabilized emulsion and enhance its nutritional value [9,21]. Nevertheless, there are still few reports on the influence of unadsorbed polysaccharides on the physicochemical properties of protein-stabilized emulsions.

The purpose of the present article was to study if anionic polysaccharides could be used to improve physical and chemical stability of proteins nanoemulsions at neutral pH. Our previous study has indicated that no significant interactions were found at pH 7.0 between sodium caseinate and pectin by isothermal titration calorimetry [23]. Thus, sodium caseinate (CAS) and low methoxyl pectin (LMP) were selected as emulsifiers and stabilizers in this study to prepare nanoemulsions at pH 7.0. To achieve this goal, the effects of LMP concentration on particle size distribution, zeta potential (ζ -potential), creaming behavior, microstructure, and environmental stresses (salt addition, heating, freeze-thaw) of CAS stabilized nanoemulsions were measured. Moreover, the encapsulated lipid and protein oxidation was also evaluated.

2. Materials and methods

2.1. Materials

Sodium caseinate (CAS) powder with 93.20% protein content (determined by the Kjeldahl method, $N = 6.38$) was purchased from Fisher Scientific (United Kingdom). Low methoxyl pectin (LMP, esterification degree from 22% to 28% and acetylation degree from 20% to 23%) with 81.21% carbohydrate content was bought from Cargill (Baupre, France). Corn oil, trichloroacetic acid (TCA), thiobarbituric acid (TBA), 1,1,3,3-tetraethoxypropane, cumene hydroperoxide, ammonium thiocyanate, ferrous chloride, imidazole, acetic acid, sodium azide, sodium hydroxide, and hydrochloric acid were purchased from Sigma-Aldrich Chimie (St Quentin Fallavier, France). All the solutions were prepared in deionized water.

2.2. Preparation of oil-in-water (O/W) nanoemulsions

Imidazole-acetate buffer solution was prepared by dispersing 5 mM imidazole and 5 mM acetic acid in deionized water, and then adjusting the pH to 7.0 with 1 M NaOH. Stock solutions were prepared by dispersing separately 2.0 wt% CAS and different amounts of LMP into 5 mM imidazole-acetate buffer (pH 7.0) and stirring overnight at 4 °C to ensure complete hydration. The pH of the two stock solutions was adjusted to 7.0 before use.

Firstly, continuous phases were prepared by mixing 2.0 wt% CAS and 0.0, 0.1, 0.2, 0.5, or 1.0 wt% LMP stock solutions in a ratio of 1:1 at pH 7. Then, oil-in-water coarse emulsions were formulated by mixing 10 wt% corn oil and 90 wt% emulsifier aqueous solution by high-speed homogenization (IKA, Staufen, Germany) under 13,500 rpm for 5 min. Finally, nanoemulsions were obtained by passing coarse emulsions through a microfluidizer (Microfluidics LM20, Microfluidics Corp., Newton, MA, USA) 5 times at 5×10^7 Pa. The pH of the nanoemulsions was then immediately adjusted to 7.0. Sodium azide (0.02% final concentration) was added into emulsions to prevent microbial growth [24]. All nanoemulsions were stored in 100 mL sealed glass bottles at room temperature in the dark for three weeks. The hydrodynamic particle size of nanoemulsions as a function of time was recorded.

2.3. Droplet hydrodynamic size and size distribution

The hydrodynamic particle size (nm) and size distribution were determined by dynamic light scattering using a Zetasizer Nano-ZS90 (Malvern Instruments, Worcestershire, UK) at a fixed angle of 90°. To eliminate multiple scattering effects, nanoemulsions were diluted to a droplet concentration around 0.1 wt% by 5 mM imidazole acetate buffer (pH 7.0). After 90 s of equilibrium, each sample was analyzed at least three times. Then the average droplet size and polydispersity index (PdI) were obtained.

2.4. Zeta potential (ζ)

To avoid multiple scattering effects, the nanoemulsions were diluted to a concentration of around 0.05 wt% in imidazole acetate buffer. Diluted samples were transferred to the zeta potential cell for electrophoretic mobility measurement using a Zetasizer Nano-ZS90 (Malvern Instruments, Worcestershire, UK). All measurements were performed at least three times and the measured electrophoretic mobilities were converted to Smoluchowski's ζ -potential values via integrated software as the average of three individual measurements.

2.5. Creaming stability measurement

The creaming index can provide indirect information about the extent of droplet flocculation and aggregation in emulsion systems. Firstly, 10 mL of each nanoemulsion were transferred into a cylindrical

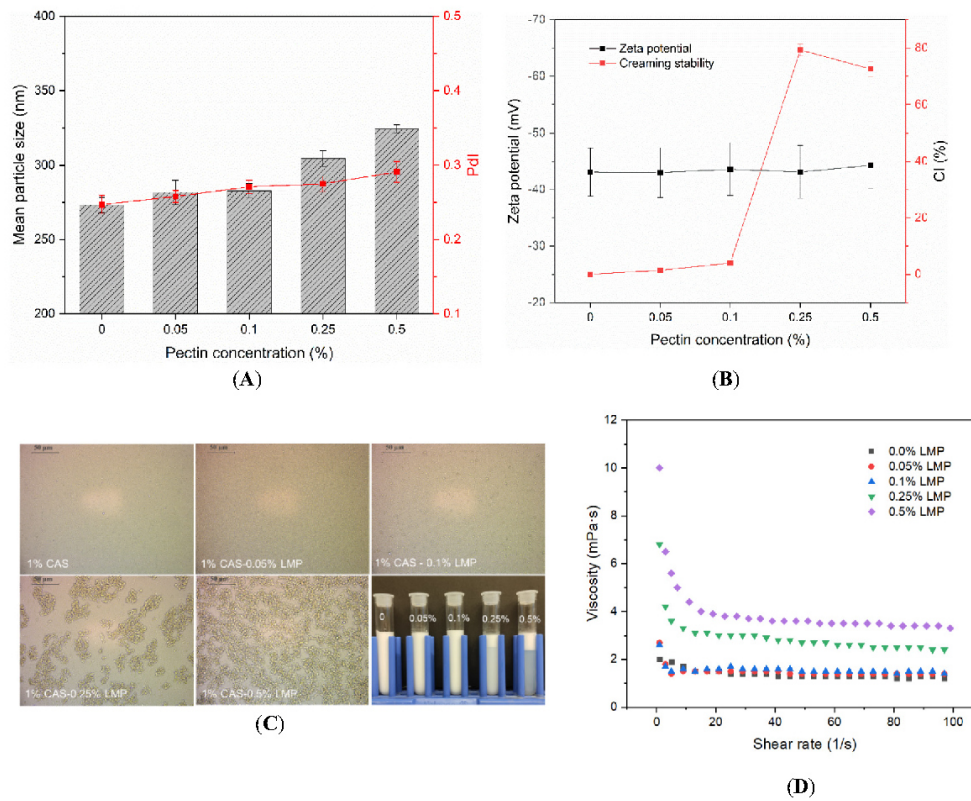


Fig. 1. Effect of pectin concentration on the mean particle size (A), zeta potential, creaming stability (B), visual appearance and microscopic structure (C) and viscosity (D) of caseinate stabilized nanoemulsions at pH 7.

test tube (inner diameter 1 cm, height 10 cm), tightly sealed with a rubber cap, and then stored at room temperature. If phase separation occurred, emulsions will be separated into an optically thin “creamed” layer at the top and a transparent (or turbid) ‘serum’ layer on the bottom during storage. The total height of the emulsions (HE) and the height of the serum layer (HS) were measured [25]. The creaming index (CI) was calculated as follows (Eq. (1)):

$$CI(\%) = \frac{HS}{HE} \times 100 \quad (1)$$

2.6. Viscosity measurements

The apparent viscosity of nanoemulsions was measured by a dynamic shear rheometer (Anton-Paar MCR 302, Graz, Austria) with a 40 mm parallel stainless-steel plate. The nanoemulsions were transferred to the platform, and the gap between the plate and the platform was adjusted to 1 mm. After equilibrating for 5 min at 25 °C, the interfacial viscosity measurement was carried out for a shear rate ranging from 0.01 to 100 s⁻¹. The flow data obtained was fitted with the Herschel-Bulkley model by Origin 8.0 software (Originlab, MicroCal, USA).

2.7. Nanoemulsion stability to environmental stress

2.7.1. Heating stability

10 mL of each nanoemulsion were transferred into a cylindrical test tube and then placed into water bath under 100 °C. After heating for 15 min, 30 min and 60 min, they were taken out and then cooled down to room temperature before measuring droplet size distribution.

2.7.2. Freeze-thaw stability

Nanoemulsion samples were transferred into 15 mL centrifuge tubes and incubated in a -20 °C freezer for 24 h. After incubation, the samples were thawed by incubating them in a water bath at 40 °C for 2 h. This freeze-thaw cycle was repeated from 0 to 3 times and the droplet size distribution of each nanoemulsion was recorded.

2.7.3. Salt stability

Nanoemulsions containing 0.1 wt% LMP was mixed with different ratios of NaCl solution under continuous stirring. The final NaCl concentrations of the studied nanoemulsions were 0, 50, 100, 200 and 300 mM. Lipid, CAS and LMP content after dilution were 5.00 g/100 g, 0.50 g/100 g and 0.05 g/100 g, respectively. The droplet size and zeta potential of these samples were measured. Meanwhile, the microstructure of the nanoemulsions was observed using conventional optical microscopy (DM2000, Wetzlar, Germany). Magnetic stirring is required before analysis to ensure that the nanoemulsions were homogeneous.

2.8. Lipid and protein oxidation measurements

According to the method of Zhu et al. [26], the nanoemulsions were incubated at 45 °C in the dark for 21 days to accelerate the oxidation. The degree of the lipid oxidation in these nanoemulsions was taken out periodically to evaluate the formation of primary (lipid hydroperoxides) and secondary (2-thiobarbituric acid reactive substances, TBARS) oxidation products. In addition, fluorescence spectroscopy was used to evaluate the impact of oxidation on the tertiary structure of CAS by means of tryptophan loss [27].

2.8.1. Primary reaction products (lipid hydroperoxides)

For the lipid hydroperoxide analysis, 0.3 mL of each nanoemulsion sample was mixed with 1.5 mL of an isooctane:2-propanol mixture (2:1, v/v) to extract the oil phase and then, vortexed for 1 min. Thereafter, the mixed solution was centrifuged at 2000 g for 5 min and the organic solvent phase was collected. Two hundreds μL of the organic phase were subsequently mixed with 2.8 mL of a methanol:1-butanol mixture (2:1, v/v), followed by the addition of 50 μL of 3.94 M ammonium thiocyanate and 50 μL of 0.132 M ferrous iron solution. After 20 min, the absorbance of the mixtures was measured at 510 nm using a UV-visible spectrophotometer (Mettler Toledo, Columbus Ohio, USA). The concentration of lipid hydroperoxides was calculated based on a standard curve prepared with cumene hydroperoxide.

2.8.2. Secondary oxidation products (TBARS)

For the TBARS analysis, 1.0 mL of each nanoemulsion was mixed with 2.0 mL of TBA reagent (formulated by mixing 15 g of trichloroacetic acid, 0.375 g of thiobarbituric acid (TBA), 1.76 mL of 12 M hydrochloric acid, and 82.9 mL of distilled water) in glass test tubes with screw caps and then vortexed for 1 min. These mixtures were then transferred in a boiling water bath for 15 min, cooled to room temperature for 10 min, and then mixed with 3 mL chloroform under stirring for 1 min. After centrifugation at 3000 rpm for 15 min, the supernatant was collected. The absorbance of the samples was measured at 532 nm using a UV-visible spectrophotometer. The concentration of TBARS formed during storage was calculated based on a standard curve prepared with 1,1,3,3-tetraethoxypropane.

2.8.3. Protein oxidation measurements

Ten μL of each nanoemulsion were diluted in 2 mL of 10 mM phosphate buffer (pH 7) and then placed in a 4 mL quartz spectrofluorometer cell for analysis using a fluorescence spectrophotometer (Agilent, Santa Clara, USA). The excitation wavelength was 290 nm based on preliminary experiments, which showed that the oxidation of the protein decreased the fluorescence intensity, but did not change the maximum emission wavelength. Emission spectra of tryptophan were recorded in a wavelength range from 300 to 400 nm at a scanning speed of 5 nm/s.

2.9. Statistical analysis

All experiments were carried out in triplicate. Statistical analyses were performed utilizing a software package (SPSS 17.0, SPSS Inc., Chicago, IL, USA). Data are reported as means \pm standard deviations, and the mean values of lipid oxidation were compared using Duncan's multiple-range tests to identify significant differences ($p < 0.05$).

3. Results and discussion

3.1. Effect of pectin concentration on the properties of nanoemulsions

To investigate the effect of adding LMP on the properties of CAS stabilized nanoemulsions at neutral pH, 2.0 wt% CAS solution was mixed with different concentrations of pectin to obtain nanoemulsions, and pH was then adjusted to 7.0. Fig. 1A depicts the particle size distribution and polydispersity index (PDI) of nanoemulsions. All nanoemulsions exhibited submicron size ranging from 273 nm to 324 nm with monomodal size distribution and the lowest diameter was obtained for pectin free nanoemulsions. The addition of 0.05 and 0.10 wt% pectin has no obvious effect on the average diameter of the nanoemulsions. These results also confirm no adsorption of pectin on the surface of the oil droplets. In fact, the average hydrodynamic size of the formulated nanoemulsions measured by Dynamic Light Scattering was almost constant. Similar result tendency was observed in the case of wheat protein-coated emulsion after addition of pectin and xanthan gum [22]. However, as the pectin concentration increased from 0.1 to 0.5 wt%, the average size of nanoemulsions showed slight increase, which can be

attributed to a slight flocculation that occurred in the original samples. In fact, the excess of free pectin in the medium could reduce polysaccharide adsorption which promote the flocculation of nanoemulsions via depletion process. Under neutral pH, increased size was also observed for nanoemulsions stabilized by soybean lipophilic protein as the concentration of hypromellose was increased [28]. Another possible explanation is that some anionic polysaccharides are able to adsorb on the surface of protein coated droplets even at neutral pH. Qiu et al. [22] reported that xanthan gum appeared to be capable of adsorbing to protein-coated droplet surfaces at neutral pH, where both are strongly negatively charged.

Surprisingly, an opposite result was observed in the case of ovalbumin stabilized oil-in water emulsions after addition of xanthan gum [29]. These results showed that at pH 7, the average particle size of prepared emulsions gradually decreased as the concentration of xanthan gum increased in the medium. These apparently contradictory results may be related to the used emulsifier, the type of polysaccharide, the formulation, and the emulsion preparation method. Meanwhile, with the gradual increase of the pectin concentration in the formulation, the polydispersity (PdI) of the nanoemulsions increased slightly, but remains lower than 0.3, showing acceptable narrow size distribution.

Typically, the stability of emulsions can be reflected by the surface potential. The larger the absolute value of the ζ -potential, the more stable the corresponding emulsion system. As shown in Fig. 1B, the ζ -potential of CAS stabilized nanoemulsions for different pectin concentrations exhibited relatively high absolute value (~ 42 mV). As can be observed, there is no significant effect of LMP concentration on the ζ -potential of the CAS-coated droplets. At pH values above the isoelectric point (pI) of the adsorbed protein, pectin molecules ($\text{pK}_a \sim 3.5$) and CAS-coated droplets are both negatively charged. Therefore, due to the relatively strong electrostatic repulsions between the negatively charged droplets and the negatively charged pectin molecules, the adsorption of pectin at pH 7 will be negligible or even there will have no adsorption at all. As a result, pectin is then mainly located in the aqueous phase of the emulsion rather on the droplets surface. Zang et al. [20] investigated the effect of different anionic polysaccharides on the rice bran protein hydrolysate-stabilized emulsions. They found that, at pH 7, adding pectin and Arabic gum did not significantly change the ζ -potential of rice brand protein-coated droplets, but the addition of xanthan gum and alginate showed slightly increases. This result was attributed to the high charge densities of alginate and xanthan gum compared to pectin and Arabic gum, affecting the charge characteristics of protein-coated droplets. Zhang et al. [21] developed oil in water emulsions using almond protein isolate / camellia saponin and they described that some of camellia saponin adsorbed to the almond protein-stabilized oil droplets despite the fact that both surfactant and protein were negatively charged. Moreover, steric repulsions could also participate in the maintenance of emulsion stability, and the magnitude of these repulsions was shown to be dependent on the properties of the polysaccharide [20]. Creaming index is another indicator related to the long-term stability of the emulsion. In absence of pectin or in presence of a small amount of this polyanionic biopolymer (≤ 0.1 wt%), CAS stabilized nanoemulsions were stable to creaming within 1 day (Fig. 1B). Indeed, even after 3 weeks of storage at room temperature, no obvious serum layer was detected in these nanoemulsions (data not shown), indicating that most of the droplets are small enough and the repulsions between them are sufficient to resist to creaming and did not aggregate during storage. However, when the concentration of pectin was increased to 0.25 and 0.50 wt%, the nanoemulsions were highly unstable to phase separation, which may be caused by depletion flocculation at neutral pH. The results of the microscopic structure (Fig. 1C) could support this conclusion. Interestingly, based on particle size measurements (Fig. 1A), the creaming of CAS-based emulsions arising from depletion flocculation is reversible, and the clusters of droplets could be disrupted by gentle stirring or dilution. This result was consistent with the study of Zang et al. [20]. The maximum creaming of

Table 1
The parameters of Herschel-Bulkely model for caseinate stabilized nanoemulsions containing different pectin concentrations at pH 7.

Pectin concentration (% w/w)	n	k (Pa.sn)	τ_0 (Pa)	R ²
0.00	0.937 ± 0.008	0.0016 ± 0.0001	0.0023 ± 0.0004	0.999
0.05	0.957 ± 0.009	0.0017 ± 0.0001	0.0001 ± 0.0050	0.999
0.10	0.876 ± 0.011	0.0025 ± 0.0001	0.0000 ± 0.0007	0.998
0.25	0.810 ± 0.009	0.0057 ± 0.0003	0.0000 ± 0.0011	0.998
0.50	0.841 ± 0.004	0.0043 ± 0.0001	0.0014 ± 0.0006	0.999

Value are means ± standard deviation of triplicates.

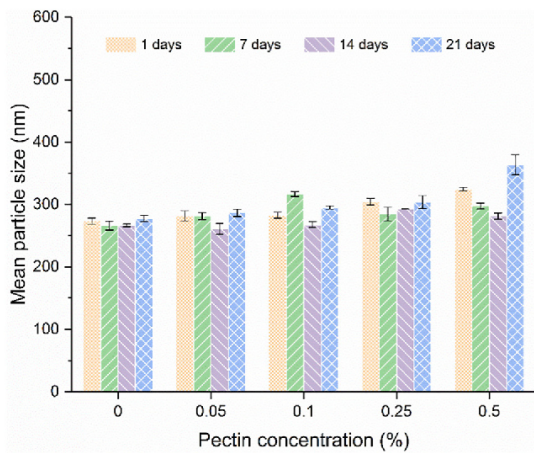


Fig. 2. Effect of pectin concentration on the ageing stability of caseinate stabilized nanoemulsions at pH 7.

protein-based emulsions at pH 7 was clearly observed at high concentration of anionic polysaccharides, however, creaming had no significant effect on the hydrodynamic particle size. The viscosity (Fig. 1 D) plays an important role in the taste and stability of food emulsions. The apparent viscosity decreased with increasing shear rate, which means that these nanoemulsions are pseudoplastic fluids [30]. Meanwhile, there was no significant difference between the CAS-stabilized nanoemulsions containing no pectin or containing low pectin concentrations (≤ 0.1 wt%), while at higher pectin concentration, a significant increase in viscosity was observed and the highest value was obtained for nanoemulsions containing 0.5 wt% LMP. This clearly showed the formation of flocculated droplets at higher pectin concentrations due to depletion flocculation, which was also supported by the creaming results (Fig. 1C). In fact, pectin is a non-adsorbing linear polysaccharide, and its aqueous solution had an excellent viscoelasticity. Besides, Table 1 exhibited the Herschel-Bulkely parameters of these nanoemulsions and the obtained flow data is fitted well with this model ($R^2 > 0.99$). The flow behavior index of all nanoemulsions was in a range of 0.810–0.957, which means that nanoemulsion containing no LMP or low concentrations of LMP exhibited a Newtonian behavior, whereas, at high concentrations of LMP, the nanoemulsions exhibited a shear-thinning behavior, clearly demonstrating the presence of flocculated oil droplets domains. Similar phenomena was found in nanoemulsions stabilized by whey proteins [9]. The yield stress (τ_0) is the instantaneous pressure required to initiate material flow, and the value obtained in these nanoemulsions is almost zero. The consistency coefficient (k) represents the viscosity behavior of a fluid and the results demonstrate that the k

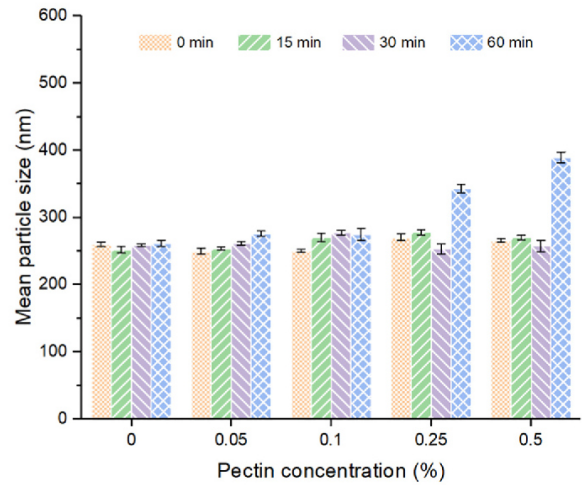


Fig. 3. Effect of heating time (100 °C) on caseinate stabilized nanoemulsions containing different concentrations of pectin at pH 7.

value of nanoemulsions increases gradually with increasing the pectin concentration.

3.2. Effect of pectin concentration on the ageing stability and environmental stress resistance of nanoemulsions

The mean droplet size of CAS-stabilized nanoemulsions containing different pectin concentrations stored at room temperature for 3 weeks were measured and the obtained results are reported in Fig. 2. From the particle size point of view, all nanoemulsions showed excellent storage stability and there was no significant change within three weeks. This could be attributed to CAS properties having relatively high negative charge at pH 7, which led to stronger electrostatic repulsions between oil droplets. Interestingly, a slight increased particle size was observed in the nanoemulsions containing 0.5 wt% LMP after 21 days storage. This result suggests that although flocculation caused by higher concentration of pectin in the nanoemulsions is reversible as mentioned in the previous section, the long-term storage effect may produce some

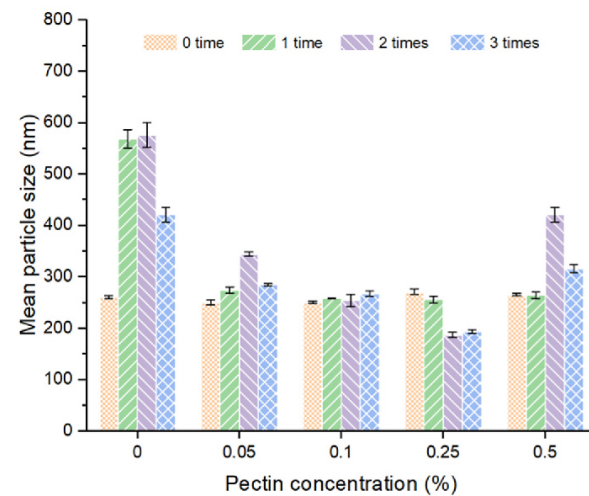


Fig. 4. Effect of the number of freeze-thaw cycles on caseinate stabilized nanoemulsions containing different concentrations of pectin at pH 7.

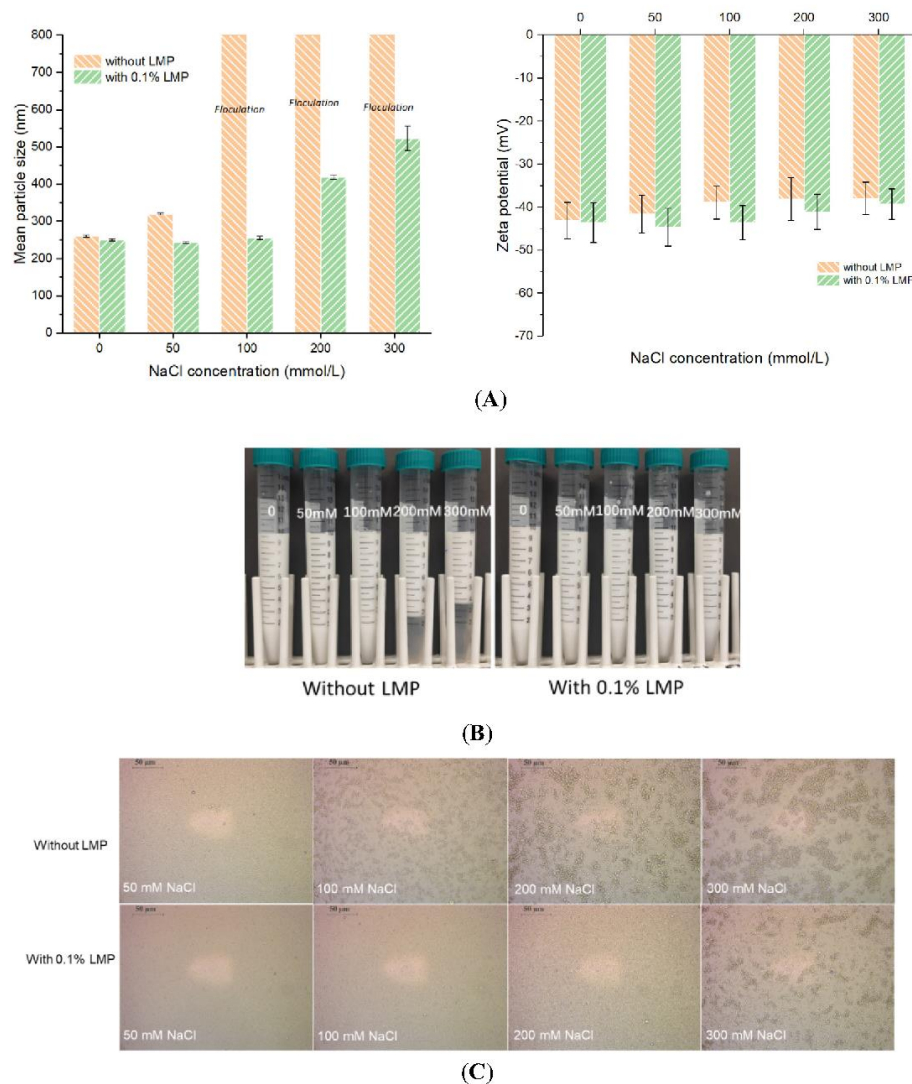


Fig. 5. Effect of ionic strength on the mean particle size and zeta potential (A), visual appearance (B) and microscopic structure (C) of caseinate stabilized nano-emulsions with 0.1 wt% or without pectin at pH 7.

irreversible growth of particle size.

To evaluate the effect of environmental stress on the properties of nanoemulsions, different heating times, freeze-thaw cycles, and salt concentrations were used to simulate conditions which might be experienced during manufacture, cooking or utilization. For each dispersion, droplet size distribution of the nanoemulsions was measured to evaluate their stability. Fig. 3 presented the effect of heating time (at 100 °C) on the stability of nanoemulsions containing different concentrations of LMP. All nanoemulsions appeared to be very stable to heat treatment and showed stable unimodal particle size distribution within 1 h of heating. This can be attributed to CAS as adsorbed layer which provides these nanoemulsions excellent thermal stability, because the structure and the conformation of caseinate is not significantly affected by thermal treatment [31]. The ζ -potential of nanoemulsions was also measured (data not shown) and was found to be not significantly affected by the thermal treatments, the surface charge was not significantly changed upon thermal treatments, demonstrating, that such

emulsions showed excellent stability against heating.

Food in emulsion forms may also undergo freezing and thawing treatments during the storage and consumption, so it is necessary to understand the stability of nanoemulsions during the freeze-thaw process. Fig. 4 presented the effect of freeze-thaw times on the average hydrodynamic size of nanoemulsions containing different concentrations of LMP. In the absence of LMP, there was a marked increase in the mean particle size after freeze-thaw cycles. Crystallization of either the lipid or water phase during freezing can explain this phenomenon. When a nanoemulsion is thawed, the droplets tend to aggregate, thereby resulting in an increase of hydrodynamic particle size [32]. However, in the presence of LMP, nanoemulsions were much more stable to droplet aggregation after three freeze-thaw cycles, especially the nanoemulsions containing 0.10 wt% and 0.25 wt% LMP. This result could be attributed to the ability of pectin to increase the amount of non-frozen aqueous phase in the nanoemulsions. A similar result was found in the case of nanoemulsions stabilized by multilayered biopolymers

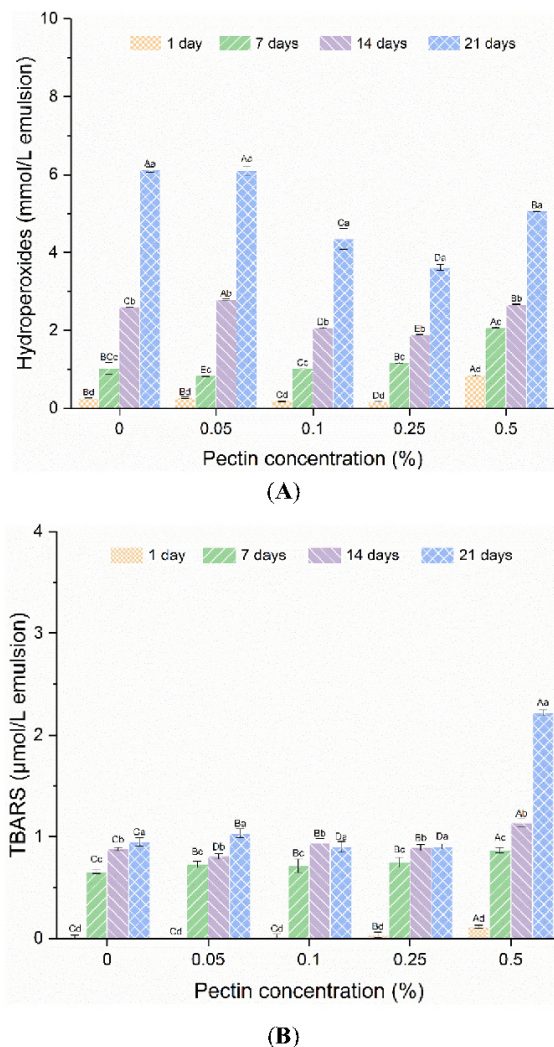


Fig. 6. Effect of pectin concentration on lipid oxidation of nanoemulsions during storage at 45 °C for 21 days. Lipid oxidation was monitored by measuring hydroperoxides (A) and TBARS (B). Samples with different uppercase superscripts (A–E) differ significantly ($p < 0.05$) when different pectin concentrations are compared at the same oxidation time; Samples with different lowercase superscripts (a–d) differ significantly ($p < 0.05$) when different oxidation times are compared at the same pectin concentration.

(β -Lactoglobulin- γ -carrageenan-gelatin) [33]. Meanwhile, some large individual oil droplets were observed in nanoemulsions after thawing treatment, which indicated that the lipid may leak from the droplet (because there were no large droplets in the untreated nanoemulsions). This phenomenon may explain the decreased size observed in nanoemulsions containing 0.25% pectin after 2 freeze-thaw cycles. A decreased droplet size after freeze-thaw treatments was also observed in lecithin and modified starch-based nanoemulsions [34]. In addition, some large irregularly shaped aggregates appeared in the nanoemulsions after dilution, especially for pectin free nanoemulsions, which may be caused by the massive aggregation of CAS during freezing and thawing. Thus, the presence of free pectin could prevent the aggregation of caseinate coated droplets to a certain extent during the freezing process and then participate on the dissociation of aggregates during the

thawing step due to the repulsive forces between CAS and LMP.

Adding edible salt to improve the taste of emulsion-based food products is a common requirement in the diet, and so it is essential to understand the effect of salts on the performance and stability of emulsions. Nanoemulsions containing 0.1 wt% pectin were selected in this section because they are highly stable to creaming and flocculation (Fig. 1C). The effect of different NaCl concentrations on the mean particle diameter, zeta potential, visual appearance and microscopic image of nanoemulsions containing or not 0.1 wt% pectin was examined (Fig. 5). The nanoemulsions containing no pectin were colloidal stable since no droplet aggregation (Fig. 5A) and creaming (Fig. 5B) were observed in the absence of salt but showed significantly increased mean particle size and phase separation in the presence of ionic force above 100 mM NaCl. The microscopic images (Fig. 5C) of nanoemulsions without LMP also showed a droplet aggregation phenomena. It was well established that at neutral pH, salt has the ability to promote the flocculation of droplets stabilized by protein based emulsifiers, which can be attributed to electrostatic screening and ion binding [35]. The zeta potential measurements (Fig. 5A) showed that the addition of NaCl did not markedly change the magnitude of the droplet charge, but a slight decrease (from -43.1 to -37.9 mV) could be observed in the free pectin nanoemulsion. It is interesting to notice that, in the presence of pectin, the nanoemulsions exhibited better salty tolerance, but when the salinity was higher than 200 mM NaCl, the particle size of the nanoemulsions increased significantly. Through visual appearance and microscopic images, no phase separation (Fig. 5B) and obvious aggregation (Fig. 5C) occurred in the nanoemulsion containing 0.1 wt% pectin in the investigated range of salt concentrations, except for 300 mM NaCl (some clusters were observed). This result indicates that even if both CAS and LMP are negatively charged at pH 7, LMP can still provide inhibition of aggregation. This may be attributed to the formation of gel-like network induced by free pectin in the aqueous continuous phase. Qiu et al. [22] also reported that adding xanthan gum can improve the properties of wheat protein-stabilized emulsions against high ionic strengths at pH 7, but the addition of pectin had no obvious effect. They attributed this phenomenon to the fact that xanthan gum has a higher linear charge density than pectin.

3.3. Effect of pectin addition on the oxidation of protein and emulsified lipid

The influence of pectin addition on the lipid oxidation of nanoemulsions was evaluated by monitoring the generation of primary (lipid hydroperoxides) and secondary (TBARS) reaction products for 3 weeks storage at 45 °C (Fig. 6). As expected, the lipid hydrogen peroxide and TBARS contents of all nanoemulsions gradually increased during storage, indicating that lipid oxidation was progressing. The results of primary reaction products (Fig. 6A) showed that, at neutral pH, the nanoemulsions containing pectin showed better ($p < 0.05$) antioxidant activity than nanoemulsions without pectin after 3 weeks, and the lowest ($p < 0.05$) lipid hydroperoxide content was measured in the case of nanoemulsions containing 0.25 wt% pectin. This may be related to several reasons. Firstly, it is reported that pectin have a certain antioxidant capacity and therefore the unadsorbed pectin molecules may react with free radical scavenging in the emulsion system [36,37]. Celus et al. [38] reported that the antioxidant capacity of pectin was mainly determined by the degree of methyl esterification (DM) and the LMP exhibited higher antioxidant activity than the HMP (High Methoxyl Pectin). Indeed, the high numbers of active hydroxyl and carboxyl groups on galacturonic acid (GalA) residues of pectin are essential for its antioxidant activities [39]. In addition, the antioxidant activity could be probably attributed to the non-pectic compounds, such as individual polyphenols and their conjugates in the extracted pectin [40]. Secondly, unadsorbed pectin may prevent water-soluble oxidants from reaching lipids by forming a weak gel-like network in the aqueous continuous phase [21]. The lipid oxidation was also reported to be affected by the

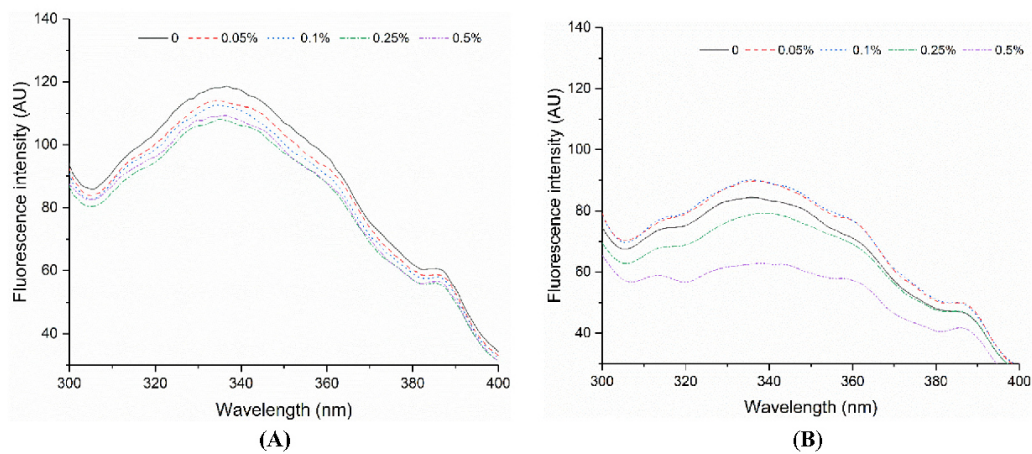


Fig. 7. Effect of pectin concentration on the intrinsic tryptophan fluorescence of nanoemulsions during storage at 45 °C for 0 (A) and 21 (B) days.

viscosity of emulsions [41]. In fact, the transfer of oxygen from the aqueous phase to lipid droplets could be retarded by higher apparent viscosity of nanoemulsions. The viscosity data (Fig. 1D) obtained in this study also support this hypothesis. However, the lowest lipid hydroperoxide content was obtained in nanoemulsions containing 0.25 wt% instead of 0.5 wt%. We hypothesized that flocculation might increase lipid oxidation since higher degree of droplet flocculation was observed for 0.5 wt% LMP. In fact, most droplets clump together and move upwards by gravity, and the aggregated droplets at the top of the emulsions are closer to the air oxygen, which could accelerate oxidation phenomena. In addition, previous studies showed that non-adsorbed proteins have the ability to bind cationic transition metal ions (pro-oxidants) and then inhibit their interactions with the encapsulated lipids [7,26]. In this regard, unadsorbed CAS and unadsorbed LMP in the negatively charged nanoemulsions at pH 7 may also interact with the cationic transition metals leading therefore to possible inhibition of oxidation process.

The TBARS measurements (Fig. 6B) showed that nanoemulsions without pectin have a similar ($p > 0.05$) trend compared to the nanoemulsions containing pectin, except the one containing 0.5 wt%. This indicated that, at neutral pH, the addition of different concentrations of pectin demonstrated a limited impact on the TBARS formation in caseinate-stabilized nanoemulsions. In addition, after 3 weeks of storage, a significantly increase of TBARS value was observed in the nanoemulsions containing 0.5 wt% pectin. After three weeks of storage at 45 °C, the depletion flocculation induced by the high concentration of unadsorbed pectin may explain the observed phenomenon.

In food systems, proteins are crucial targets of lipid co-oxidation. It was reported that lipid oxidation products such as free radicals, hydroperoxides and carbonyl compounds can greatly destroy proteins [42]. In this regard, we monitored the loss of intrinsic tryptophan fluorescence of CAS in the nanoemulsion systems for 3 weeks storage at 45 °C. The fluorescence spectra of nanoemulsions after 0 day and 21 days of storage are shown in Fig. 7A and B, respectively. The maximum fluorescence emission was observed at a wavelength of around 336 nm for all nanoemulsions. In the beginning (0 day), nanoemulsions without pectin exhibited the highest fluorescence intensity and the intensity value decreased as the pectin concentration increased. Similar phenomenon was found in almond protein stabilized emulsions [21]. This may be attributed to free pectin in the continuous phase of nanoemulsions and these unadsorbed pectin molecules may affect the exposure of tryptophan residues. Consistent with other studies [26,28], during the storage process, the intrinsic fluorescence intensity of tryptophan in all nanoemulsions decreased after 21 days (Fig. 7B), which

can be attributed to the oxidative degradation of tryptophan leading to changes in the spherical structure of caseinate. The nanoemulsions containing 0.05 wt% and 0.10 wt% pectin showed better ability to inhibit protein oxidation than pectin free nanoemulsions after 3 weeks. However, in the case of nanoemulsions containing higher pectin concentration (0.5 wt%), the tryptophan fluorescence intensity decreased significantly. This observation further supports that under neutral conditions, an appropriate pectin concentration can contribute to the oxidation stability of CAS-stabilized nanoemulsions.

In summary, even if both caseinate and pectin are both negatively charged at neutral pH, the addition of LMP can still improve the performance of CAS stabilized nanoemulsions, especially against high salt concentrations and freeze-thaw cycles, and appreciably enhance the antioxidant ability of nanoemulsions. The caseinate stabilized nanoemulsions containing 0.10 wt% and 0.25 wt% were the more stable formulations in this study.

4. Conclusion

The effect of pectin on the physical and oxidation stability of caseinate-stabilized nanoemulsions under neutral pH was investigated as a function of several parameters and conditions. It emerges from this systematic study that the presence of pectin could improve the physical (especially against high salt concentrations and freeze-thaw cycles) and chemical stability of caseinate-stabilized nanoemulsions, depending on its concentration. Nanoemulsions containing 0.10 wt% and 0.25 wt% are considered as the optimal formulation which exhibited the ability to inhibit lipid and protein oxidation more effectively than caseinate alone. There are at least two possible mechanisms for the antioxidant properties of pectin in nanoemulsions: i) the non-adsorbed pectin could have the ability to scavenge free radical and chelate metals; ii) the non-adsorbed pectin can reduce droplet mobility by forming a weak gel-like network that prevents water-soluble pro-oxidants reaching the lipids. In addition, a higher concentration of pectin (0.5 wt%) can promote the occurrence of depletion flocculation of nanoemulsions, resulting in phase separation, more secondary lipid oxidation products, and more tryptophan loss. This research could be interesting for the formulation of beverage emulsions with improved physical and chemical properties at neutral pH.

CRedit authorship contribution statement

The paper was coauthored by Wei Liao, Abdelhamid Elaissari, Sami Ghnimi, Emilie Dumas, and Adem Gharsallaoui.

All authors have participated in (a) conception and design, or analysis and interpretation of the data; (b) drafting the article or revising it critically for important intellectual content; and (c) approval of the final version.

This manuscript has not been submitted to, nor is under review at, another journal or other publishing venue.

Declaration of competing interest

The authors have no affiliation with any organization with a direct or indirect financial interest in the subject matter discussed in the manuscript.

References

- [1] M.-J. Teng, Y.-S. Wei, T.-G. Hu, Y. Zhang, K. Feng, et al., Citric acid cross-linked zein microcapsule as an efficient intestine-specific oral delivery system for lipophilic bioactive compound, *J. Food Eng.* 281 (2020) 109993.
- [2] C. Aphibantammakitt, K. Kasemwong, Chapter 15—nanocapsulation in agricultural applications, in: W.J. Lau, K. Faungnawakij, K. Piyachomkwan, U. R. Ruktanonchai (Eds.), *Handbook of Nanotechnology Applications*, Elsevier, 2021, pp. 359–382.
- [3] M. Katsouli, V. Polychniatou, C. Tzia, Optimization of water in olive oil nano-emulsions composition with bioactive compounds by response surface methodology, *LWT Food Sci. Technol.* 89 (2018) 740–748.
- [4] D.J. McClements, J. Rao, Food-grade nanoemulsions: formulation, fabrication, properties, performance, biological fate, and potential toxicity, *Crit. Rev. Food Sci. Nutr.* 51 (4) (2011) 285–330.
- [5] T. Li, D. Teng, R. Mao, Y. Hao, X. Wang, et al., Recent progress in preparation and agricultural application of microcapsules, *J. Biomed. Mater. Res. A* 107 (10) (2019) 2371–2385.
- [6] Y. Cai, X. Deng, T. Liu, M. Zhao, Q. Zhao, et al., Effect of xanthan gum on walnut protein/xanthan gum mixtures, interfacial adsorption, and emulsion properties, *Food Hydrocoll.* 79 (2018) 391–398.
- [7] C.E. Gumus, E.A. Decker, D.J. McClements, Impact of legume protein type and location on lipid oxidation in fish oil-in-water emulsions: lentil, pea, and faba bean proteins, *Food Res. Int.* 100 (2017) 175–185.
- [8] C.C. Berton-Carabin, A. Schröder, A. Rovailino-Cordova, K. Schroën, L. Sagis, Protein and lipid oxidation affect the viscoelasticity of whey protein layers at the oil–water interface, *Eur. J. Lipid Sci. Technol.* 118 (11) (2016) 1630–1643.
- [9] S. Khalloufi, M. Alexander, H. Douglas Goff, M. Corredig, Physicochemical properties of whey protein isolate stabilized oil-in-water emulsions when mixed with flaxseed gum at neutral pH, *Food Res. Int.* 41 (10) (2008) 964–972.
- [10] M. Hu, D.J. McClements, E.A. Decker, Lipid oxidation in corn oil-in-water emulsions stabilized by casein, whey protein isolate, and soy protein isolate, *J. Agric. Food Chem.* 51 (6) (2003) 1696–1700.
- [11] Q. Li, J. Zheng, G. Ge, M. Zhao, W. Sun, Impact of heating treatments on physical stability and lipid-protein co-oxidation in oil-in-water emulsion prepared with soy protein isolates, *Food Hydrocoll.* 100 (2020), 105167.
- [12] F. Zhang, X. Cai, L. Ding, S. Wang, Effect of pH, ionic strength, chitosan deacetylation on the stability and rheological properties of O/W emulsions formulated with chitosan/casein complexes, *Food Hydrocoll.* 111 (2021), 106211.
- [13] J. Wang, Y. Su, F. Jia, H. Jin, Characterization of casein hydrolysates derived from enzymatic hydrolysis, *Chem. Cent. J.* 7 (1) (2013) 1–8.
- [14] D.G. Dalgleish, M. Stinivasan, H. Singh, Surface properties of oil-in-water emulsion droplets containing casein and Tween 60, *J. Agric. Food Chem.* 43 (9) (1995) 2351–2355.
- [15] H. Singh, A. Sarkar, Behaviour of protein-stabilised emulsions under various physiological conditions, *Adv. Colloid Interf. Sci.* 165 (1) (2011) 47–57.
- [16] A. Villiere, M. Viau, I. Bronnec, N. Moreau, C. Genot, Oxidative stability of bovine serum albumin and sodium caseinate-stabilized emulsions depends on metal availability, *J. Agric. Food Chem.* 53 (5) (2005) 1514–1520.
- [17] M. Estévez, P. Kylli, E. Puolanne, R. Kivikari, M. Heinonen, Fluorescence spectroscopy as a novel approach for the assessment of myofibrillar protein oxidation in oil-in-water emulsions, *Meat Sci.* 80 (4) (2008) 1290–1296.
- [18] M. Obando, A. Papastergiadis, S. Li, B. De Meulenaer, Impact of lipid and protein co-oxidation on digestibility of dairy proteins in oil-in-water (O/W) emulsions, *J. Agric. Food Chem.* 63 (44) (2015) 9820–9830.
- [19] J. Surh, E.A. Decker, D.J. McClements, Influence of pH and pectin type on properties and stability of sodium-caseinate stabilized oil-in-water emulsions, *Food Hydrocoll.* 20 (5) (2006) 607–618.
- [20] X. Zang, J. Wang, G. Yu, J. Cheng, Addition of anionic polysaccharides to improve the stability of rice bran protein hydrolysate-stabilized emulsions, *LWT Food Sci. Technol.* 111 (2019) 573–581.
- [21] S. Zhang, L. Tian, J. Yi, Z. Zhu, E.A. Decker, et al., Mixed plant-based emulsifiers inhibit the oxidation of proteins and lipids in walnut oil-in-water emulsions: almond protein isolate-camellia saponin, *Food Hydrocoll.* 109 (2020), 106136.
- [22] C. Qiu, M. Zhao, D.J. McClements, Improving the stability of wheat protein-stabilized emulsions: effect of pectin and xanthan gum addition, *Food Hydrocoll.* 43 (2015) 377–387.
- [23] J. Wang, E. Dumas, A. Gharsallaoui, Low methoxyl pectin/sodium caseinate complexing behavior studied by isothermal titration calorimetry, *Food Hydrocoll.* 88 (2019) 163–169.
- [24] P.G. Chang, R. Gupta, Y.P. Timilsena, B. Adhikari, Optimisation of the complex coacervation between casein and protein isolate and chitosan, *J. Food Eng.* 191 (2016) 58–66.
- [25] W.W. Mwangi, K.-W. Ho, B.-T. Tey, E.-S. Chan, Effects of environmental factors on the physical stability of pickering-emulsions stabilized by chitosan particles, *Food Hydrocoll.* 60 (2016) 543–550.
- [26] Z. Zhu, C. Zhao, J. Yi, N. Liu, Y. Cao, et al., Impact of interfacial composition on lipid and protein co-oxidation in oil-in-water emulsions containing mixed emulsifiers, *J. Agric. Food Chem.* 66 (17) (2018) 4458–4468.
- [27] T. Beveridge, S.J. Toma, S. Nakai, Determination of SH- and SS-groups in some food proteins using Ellman's reagent, *J. Food Sci.* 39 (1) (1974) 49–51.
- [28] Y. Li, M. Zhong, F. Xie, Y. Sun, S. Zhang, et al., The effect of pH on the stabilization and digestive characteristics of soybean lipophilic protein oil-in-water emulsions with hypromellose, *Food Chem.* 309 (2020), 125579.
- [29] N. Xiao, W. He, Y. Zhao, Y. Yao, M. Xu, et al., Effect of pH and xanthan gum on emulsifying property of ovalbumin stabilized oil-in water emulsions, *LWT Food Sci. Technol.* 147 (2021), 111621.
- [30] L. He, H. Peng, X. Wei, B. Li, J. Tian, Preparation and characterization of emulsions stabilized with defatted sesame meal, *Food Sci. Technol. Res.* 26 (5) (2020) 655–663.
- [31] M. Srinivasan, H. Singh, P.A. Munro, Formation and stability of sodium caseinate emulsions: influence of retorting (121 C for 15 min) before or after emulsification, *Food Hydrocoll.* 16 (2) (2002) 153–160.
- [32] S. Liu, C. Sun, Y. Xue, Y. Gao, Impact of pH, freeze–thaw and thermal sterilization on physicochemical stability of walnut beverage emulsion, *Food Chem.* 196 (2016) 475–485.
- [33] Y.S. Gu, Eric A. Decker, D. Julian McClements, Application of multi-component biopolymer layers to improve the freeze–thaw stability of oil-in-water emulsions: β -Lactoglobulin– α -carrageenan–gelatin, *J. Food Eng.* 80 (4) (2007) 1246–1254.
- [34] F. Donsi, Y. Wang, Q. Huang, Freeze–thaw stability of lecithin and modified starch-based nanoemulsions, *Food Hydrocoll.* 25 (5) (2011) 1327–1336.
- [35] D.J. McClements, Protein-stabilized emulsions, *Curr. Opin. Colloid Interface Sci.* 9 (5) (2004) 305–313.
- [36] M. Celus, C. Kyomugasho, J. Keenen, A.M. Van Loey, T. Grauwet, et al., Simultaneous use of low methylesterified citrus pectin and EDTA as antioxidants in linseed/sunflower oil-in-water emulsions, *Food Hydrocoll.* 100 (2020), 105386.
- [37] M. Kumar, J. Potkule, M. Tomar, S. Punia, Surinder Singh, et al., Jackfruit seed slimy sheath, a novel source of pectin: Studies on antioxidant activity, functional group, and structural morphology, *Carbohydr. Polym. Technol. Appl.* 2 (2021), 100054.
- [38] M. Celus, L. Salvia-Trujillo, C. Kyomugasho, I. Maes, A.M. Van Loey, et al., Structurally modified pectin for targeted lipid antioxidant capacity in linseed/sunflower oil-in-water emulsions, *Food Chem.* 241 (2018) 86–96.
- [39] J. Cui, C. Zhao, L. Feng, Y. Han, H. Du, et al., Pectins from fruits: relationships between extraction methods, structural characteristics, and functional properties, *Trends Food Sci. Technol.* 110 (2021) 39–54.
- [40] S. Ahn, K. Halake, J. Lee, Antioxidant and ion-induced gelation functions of pectins enabled by polyphenol conjugation, *Int. J. Biol. Macromol.* 101 (2017) 776–782.
- [41] A. Pernin, V. Bosc, P. Soto, E. Le Roux, M.-N. Maillard, Lipid oxidation in oil-in-water emulsions rich in omega-3: effect of aqueous phase viscosity, emulsifiers, and antioxidants, *Eur. J. Lipid Sci. Technol.* 121 (9) (2019) 1800462.
- [42] R.J. Elias, S.S. Kellerby, E.A. Decker, Antioxidant activity of proteins and peptides, *Crit. Rev. Food Sci. Nutr.* 48 (5) (2008) 430–441.

Chapter V

Pectin-sodium caseinate based nanoemulsions: effect of pH and ratio on oil-water interfacial behavior and colloidal stability

Submitted to: Journal of Food Engineering

Summary of Chapter V

Generally, emulsions prepared from protein-polysaccharide complexes exhibit enhanced physical stability than that prepared by protein only. The interfacial properties of emulsions, such as interfacial tension, interfacial elasticity, and viscosity, can be used to assess and compare the interfacial composition of protein or protein-polysaccharide based emulsions. In this study, the effects of pH and low methoxyl pectin (LMP) concentration on the adsorption kinetics and interfacial dilatational rheology of sodium CAS/LMP complexes were investigated using a pendant drop tensiometer. The colloidal stability (microstructure, ζ -potential, particle size, and viscosity) of nanoemulsions was assessed by adjusting the pH from 7.0 to 3.0. Interfacial measurements suggested that pH and LMP concentration had limited effects on the equilibrium interfacial tension of CAS/LMP at the O/W interfaces, but an increased viscoelasticity modulus was observed at pH 5.0. Size and ζ -potential results suggested that LMP adsorbed to CAS-coated droplets at pH 3.0 and pH 5.0, but not at pH 7. Relatively higher concentrations of LMP can significantly inhibit the aggregation and creaming of CAS-coated nanoemulsions at pH 5.0. This research could support future applications of CAS-stabilized emulsions over a wide pH range.

Abstract

Emulsions prepared from protein-polysaccharide complexes generally exhibit enhanced stability compared to protein-stabilized emulsions. In this study, the effects of pH and low methoxyl pectin (LMP) concentration on the adsorption kinetics and interfacial dilatational rheology of sodium caseinate (CAS)/LMP complexes were investigated using a pendant drop tensiometer. In addition, oil-in-water (O/W) nanoemulsions were prepared by CAS/LMP with different ratios at pH 7.0. The colloidal stability (microstructure, ζ -potential, particle size, and viscosity) of nanoemulsions was assessed by decreasing the pH from 7.0 to 5.0 and 3.0. Interfacial measurements suggested that pH and LMP concentration had limited effects on the equilibrium interfacial tension of CAS/LMP at the O/W, but an increased viscoelasticity modulus was observed at pH 5.0 when LMP used. Size and ζ -potential results suggested that LMP adsorbed to CAS-coated droplet at pH 3.0 and pH 5.0, but not at pH 7. The corresponding isoelectric point (pI) for charge neutralization in CAS/LMP based nanoemulsions was shifted to lower pH. Relatively higher concentrations of LMP can inhibit the aggregation and creaming of CAS-coated nanoemulsions at pH 5.0. This work could facilitate the use of protein/polysaccharide complexes to stabilize emulsions for the application over a wide range of pH values.

Keywords: Sodium caseinate; Pectin; Complexes; Emulsion stability; Interfacial behavior.

1. Introduction

Over the past few years, many efforts have been devoted to incorporating bioactive compounds into food formulations to provide products with additional health benefits such as antioxidant, anti-cancer, anti-allergic, anti-inflammatory (Chung & McClements, 2014). However, certain bioactive compounds with great health benefits, such as carotenoids, phytosterols, vitamins, and essential oils, are lipophilic components that are difficult to introduce in food products or have limited effect when used directly (Teng et al., 2020). In fact, there are several issues, such as low water solubility, chemically unstable, and prone to oxidative degradation, should be overcome for further applying these fat-soluble active compounds in food industries (Liao et al., 2021). Currently, the development of systems based on oil-in-water (O/W) emulsions is able to address these deficiencies of lipophilic compounds. Meanwhile, for safety reasons, the encapsulated wall material for food emulsions needs to be carefully selected, usually edible, and inexpensive (Teng et al., 2020). Consequently, there has been a great interest in replacing synthetic emulsifiers with natural emulsifiers in recent years due to their wider consumer acceptance of food products.

Proteins and polysaccharides, as natural biopolymers with macromolecular structure, have been widely used in the food industry because of their great effect on the structure, texture, and stability of food. Particularly, different sources of proteins such as walnut protein (Cai et al., 2018), legume protein (Gumus et al., 2017), whey protein (Berton-Carabin et al., 2016; Khalloufi et al., 2008), soy protein (Hu et al., 2003; Li et al., 2020), casein protein (F. Zhang, Cai, et al., 2021), etc., have been well studied as natural emulsifiers for encapsulation systems due to their healthy and nutritional properties, their availability, good amphiphilic properties, and low production cost. Among them, casein from milk is the most common natural commercial emulsifier in the food industry, and is generally produced and sold in the form of sodium caseinate (CAS) in food industries (Wang et al., 2013). The casein molecule in solution adopts a flexible disordered configuration with almost no ordered secondary structure. It can

effectively adsorb by reducing the oil-water interfacial tension and forming a thicker interfacial film during the emulsification process (Dalglish et al., 1995; Singh & Sarkar, 2011). It was reported that CAS-based emulsions could meet current industrial requirements for food emulsion stability, but under certain conditions, their instability still limits their further applications (Liang & Luo, 2020). For example, CAS stabilized emulsions are generally not stable in certain environmental conditions, such as a pH value close to its isoelectric point (pI) (Dickinson & Golding, 1997), high ionic strengths (Srinivasan et al., 2000), and high storage temperatures (Karthik & Anandharamakrishnan, 2016). In this consideration, many researchers have focused on improving the adaptability of emulsions to environmental conditions by using a combination of emulsifiers rather than a single emulsifier. For instance, proteins and other oppositely charged biopolymers like polysaccharides have been successfully used to prepare nanoemulsions with enhanced stability (Surh et al., 2006; Zhang et al., 2020). Indeed, the ability of polysaccharides to improve the stability of protein-stabilized emulsions mainly depends on the nature of the polysaccharides (such as charge and structure) and the environmental conditions, especially the solution pH (Zang et al., 2019). For example, when the pH is below or above its pI, CAS-coated droplets carry negative or positive charges (Wang et al., 2019) and then they could attract the polysaccharide in the continuous phase, thereby forming a thicker layer at O/W interface. In this context, the addition of guar gum could promote the formation of a network and then improves the creaming stability of CAS-based emulsions at a pH near its pI (Neiryneck et al., 2007), Locust bean gum improved the stability of CAS-based emulsions against acidification and freeze thaw (Farshchi et al., 2013), Sodium alginate improves the stability of CAS-based emulsions to high ionic strength (up to 300 mM of NaCl) (Pallandre et al., 2007); pH emulsification range of casein could be effectively expanded as the non-covalent chitosan and casein complexes formed by electrostatic attraction between casein and chitosan (Zhang, Cai, et al., 2021). Zang et al. (2019) investigated the effect of different anionic polysaccharides on the rice bran protein -

stabilized emulsions and they found that the environmental stresses (salt, pH) of emulsions were significantly improved.

The interfacial properties of emulsions, such as interfacial tension, interfacial elasticity, and viscosity, have been used as key parameters to determine the physical stability of protein-stabilized emulsions in foods (Ruiz-Álvarez et al., 2022). In fact, environmental conditions such as pH can greatly affect the structural properties of proteins or protein-polysaccharide complexes, which in turn affect the interfacial and functional properties of protein-coated droplets. In this regard, the interfacial properties and molecular interactions of the oil-water interface may be used to evaluate or predict the stability of emulsions. However, the exact relationship between the interfacial properties of CAS/LMP solutions at the oil-water interface and the stability of CAS/LMP based emulsions is still unknown. In the current study, we first focused on the formation of complex coacervates as function of pH (3.0 to 7.0). The effect of CAS/LMP ratio and pH on the OD₆₀₀ was investigated, then a combination of dynamic interfacial tension and dilatational rheological tests were performed to determine the oil-water interfacial interactions between CAS and LMP at 3 different pH values (3.0, 5.0 and 7.0). Finally, CAS and LMP were used to prepare nanoemulsions at pH 7.0 and then their pH was adjusted from 7.0 to 3.0. The effects of LMP concentration and pH on particle size distribution, zeta potential (ζ -potential), creaming behavior, and microstructure of CAS-based nanoemulsions were compared and the correlation between the pH-dependent interfacial behavior and the macroscopic emulsion properties was discussed.

2. Materials and methods

2.1. Materials

The powder of sodium caseinate (CAS) with 93.20% protein content (determined by the Kjeldahl method, N=6.38) was purchased from Fisher Scientific (UK). The powder of low methoxyl pectin (LMP, esterification degree from 22% to 28% and acetylation degree from 20% to 23%) with 81.21% carbohydrate content was obtained

from Cargill (Baupte, France). Corn oil, imidazole, acetic acid, sodium azide, sodium hydroxide, and hydrochloric acid were purchased from Sigma-Aldrich Chimie (St Quentin Fallavier, France). The water used in all preparation was deionized water.

2.2. Sample preparation

Imidazole-acetate buffer solutions (5 mM) containing 0.04 wt.% sodium azide (to avoid microbial growth, (Chang et al., 2016)) was prepared by dispersing weighed amounts of imidazole and acetic acid into deionized water. Biopolymer stock solutions were prepared by slow dispersing separately 2.0 wt.% CAS and 2.0 wt.% of LMP into 5 mM imidazole-acetate buffer (pH 7.0) and stirring overnight to ensure complete hydration. The pH of the two stock solutions was then adjusted to 7.0 by adding HCl (1 M) or NaOH (1 M). Biopolymer mixtures containing different CAS/LMP ratios (1:0, 1:0.05, 1:0.1, 1:0.25, 1:0.5, w/w) were prepared by mixing the stock solutions with imidazole-acetate buffer at pH 7.0 under stirring, and then stored at room temperature for 24 h prior to analysis.

2.3. Preparation of CAS/LMP mixtures and turbidity measurement

Biopolymer mixtures were diluted with buffer (CAS was kept constant, 0.5 wt.%) and then their pH was adjusted in the range of 7.0 to 3.0 using dropwise addition of 1 M HCl or NaOH. The resulting suspensions for each pH were mixed for 1 min using a vortex mixer. Turbidity measurements were carried out as a function of the CAS/LMP ratio with a UV/Vis spectrophotometer (Jenway 3705, Villepinte, France). The pH of all suspensions was reconfirmed prior to measurement. The absorbance was carried out at 600 nm at room temperature (25 °C) using plastic cuvettes (1 cm path length). Thereafter, tested cuvettes were filled with the different samples and stored at room temperature for exactly 20 min. Digital photos were taken using a 16-megapixel camera.

2.4. Interfacial properties of CAS-LMP complexes

To compare the adsorption process at the oil-water interface, the above-prepared biopolymer mixtures at pH 3.0, 5.0, and 7.0 were selected and then diluted (CAS was kept constant, 0.01 wt.%) with the corresponding pH buffers. Corn oil (density=0.92

g/cm³) was used as oil phase which filled slowly with 250 µL SGE syringe (TRAJAN, Melbourne, Australia). The O/W interfacial properties were measured by a Tracker automatic droplet tensiometer equipped with an oscillating drop accessor (Civrioux d'Azergue, France) at room temperature. Before measurement, syringes and cuvettes should be carefully cleaned and rinsed several times with deionized water to avoid the presence of other surfactants. The surface tension of the last wash deionized water was in the range of 69 and 72 mN/m, determined by a pendant droplet type, indicating the used syringe cleaning.

According to the density of the oil phase, the rising drop method was selected. An initial droplet with a volume of 10 µL was generated at the vertical needle. A connected digital camera records droplet profiles every 0.02 s. The interfacial tension value was calculated from the Laplace equation (Castellani et al., 2010). Interfacial tension was studied over a period for at least 3 hours to achieve the adsorption at the oil-water interface. The dynamic dilatational rheological properties were carried out by performing a sinusoidal interfacial compression and expansion (five cycles), operated at 10% amplitude and frequency of 0.1 Hz, which was tested to be within the linear viscoelastic regime. The elastic dilatational modulus were calculated by the first harmonic of the Fourier transform of the oscillating interfacial tension signal (Bagley & Torvik, 1983).

2.5. Stability of CAS or CAS/LMP based nanoemulsions

2.5.1. Preparation of O/W nanoemulsions

Biopolymer mixtures containing different CAS/LMP ratios (1:0, 1:0.05, 1:0.1, 1:0.25, 1:0.5, w/w) at pH 7.0, respectively, were used as continuous phases. Oil-in-water coarse emulsions were formulated by mixing 10 wt.% corn oil and 90 wt.% emulsifier aqueous solution by high-speed homogenization (IKA, Staufen, Germany) under 13,500 rpm for 5 minutes. The resultant pre-emulsions (10 wt.% corn oil, 1 wt.% protein and 0~0.5 wt.% LMP) were further passed through a microfluidizer (Microfluidics LM20, Microfluidics Corp., Newton, MA, USA) 5 times at 5×10^7 Pa

to obtain nano-sized emulsions. The pH of the nanoemulsions was then slowly adjusted to 7.0, 6.0, 5.0, 4.0, 3.0, separately, using a HCl solution (0.1 M). All nanoemulsions were then stirred for 30 min and stored in 100 mL sealed glass bottles at room temperature in the dark for 24 h prior to analysis.

Meanwhile, clear flocs and phase separation can be observed in several nanoemulsions when their pH was adjusted to 5 and 3. Previous research has shown that these flocs can be redispersed by mechanical disruption (Ding et al., 2021; Guzey & McClements, 2006). In this regard, unstable nanoemulsions at pH 5 and pH 3 were selected for sonication for 30 s at a frequency of 50 kHz, an amplitude of 50%, and a duty cycle of 0.5 s (UP400S, Hielscher, Germany). The treated nanoemulsions were then stored for further analysis: particle size and microscopical analysis.

2.5.2. Particle size measurement

Mean particle size (nm) and size distribution were determined by dynamic light scattering using a Zetasizer Nano-ZS90 (Malvern Instruments, Worcestershire, UK) at fixed angle of 90°. To eliminate multiple scattering effects, nanoemulsions were diluted to a droplet concentration around 0.1 wt.% by corresponding pH buffers. After 90 s of equilibrium, each sample was analyzed three times.

The emulsions were then stirred for 30 min with or without subsequent ultrasound treatment for 30 s at a frequency of 20 kHz, amplitude of 40%, and duty cycle of 0.5 s (Model 500, Sonic Dismembrator, Fisher Scientific, Pittsburgh, PA). Emulsions were then stored at ambient temperature for 24 h before being analyzed.

2.5.3. Zeta potential (ζ) measurement

The ζ potential is measured by determining the direction and velocity of particle movement in the applied electric field. To avoid multiple scattering effects, the nanoemulsions were diluted to a concentration of around 0.05wt.% with corresponding pH buffers. Diluted samples were transferred to the cell of cuvettes for electrophoretic mobility measurement (Malvern Instruments, Worcestershire, UK). All measurements were performed three times and the ζ -potential values were calculated by the software

as the average of three individual measurements.

2.5.4. Creaming stability measurement

The creaming index can provide indirect information about the extent of droplet flocculation and aggregation in emulsion systems. Thus, the creaming stability of nanoemulsions as a function of pH was studied. Firstly, 10 mL of each pre-homogeneous nanoemulsion were transferred into a cylindrical test tube (inner diameter 1 cm, height 10 cm), tightly sealed with a rubber cap, and then stored at room temperature for further analysis. During storage, nanoemulsions were divided into an optically thin "cream" layer on top and a clear (or turbid) "serum" layer on the bottom due to instability mechanisms and gravity. After 24 hour at room temperature, the total height of the emulsions (HE) and the height of the serum layer (HS) were measured as described by [Mwangi et al. \(2016\)](#). The creaming index (CI) was calculated as follows (Eq. (1)):

$$CI(\%) = \frac{HS}{HE} * 100\% \quad (1)$$

2.5.5. Viscosity measurements

The apparent viscosity of nanoemulsions was measured by a dynamic shear rheometer (Anton-Paar MCR 302, Graz, Austria) with a 40 mm parallel stainless-steel plate. The nanoemulsions were transferred to the platform, and the gap between the plate and the platform was adjusted to 1 mm. After equilibrating for 5 minutes at 25 °C, the measurement of interfacial viscosity was carried out by performing in the shear rate ranging from 0.1 to 100 s⁻¹.

2.5.6. Microscopical analysis

Emulsions were gently agitated in a glass test tube before analysis to ensure that they were homogenous. A drop of emulsion was placed on a microscope slide and then covered with a cover slip. The microstructure of the emulsion was then visualized at room temperature using conventional optical microscopy (DM2000, Wetzlar, Germany).

2.6. Statistical analysis

All experiments were carried out at least three times with freshly prepared samples. Data are reported as means \pm standard deviations, and the mean values were compared using Duncan's multiple-range tests to identify significant differences ($p < 0.05$).

3. Results and discussion

3.1. Turbidity kinetic of the CAS/LMP coacervates

As described in our previous study (Wang et al., 2019), the net charge of CAS varied from negative at pH 7.0 to positive at pH 3, reaching a point of zero charge around pH 4.6 (isoelectric point, pI), and LMP is a polyanionic polymer for which the number of deprotonated carboxyl groups increases as the pH increased. Thus, the solution pH would play an important role determining the electrostatic attractions which are the main driving force in the formation of complexes between CAS and LMP.

The effect of the ratio on the pH-induced turbidity kinetics of the CAS/LMP complexes was assessed by turbidity measurements (Fig. 1). As expected, in the range of pH 7.0 to 6.0, all sample solutions are absolutely transparent, which can be attributed the fact that both biopolymers are negatively charged hindering their complexation. As the pH was lowered to pH 5.5 or pH 5.0, the turbidity of pure CAS or mixtures containing a small amount (1:0.05, w/w) of LMP increased significantly and both reached a maximum OD₆₀₀ at pH 5.0. The increase in turbidity values indicated that more size and number of CAS/LMP aggregates formed during acidification followed by dissolution (Schmitt et al., 1999). Meanwhile, clear insoluble aggregates were observed in the pure CAS solution at pH 5.0. This is the fact that the electrostatic repulsion was insufficient to prevent aggregation between casein molecules when the pH is near the pI. Interestingly, a small amount of LMP (≥ 0.05 wt.%) can inhibit the formation of insoluble aggregates at pH 5.0, and the OD₆₀₀ value of the mixtures at pH 5.0 decreased with increasing the LMP content. The reason is that there are some attractive interactions between casein molecules and LMPs, which, like soluble interpolymer complexes, are fully stabilized due to their high residual charge. Indeed, CAS has negligible charges near its Ip (pH 4.6) that are theoretically not able to form

complexes with polysaccharide chains. However, when pH is near the pI, some casein molecules moieties are still positively charged and they may interact with negatively charged polysaccharides to form soluble complexes that avoid casein aggregation. A similar result was reported for complexation between caseinate and gum tragacanth (Gorji et al., 2014).

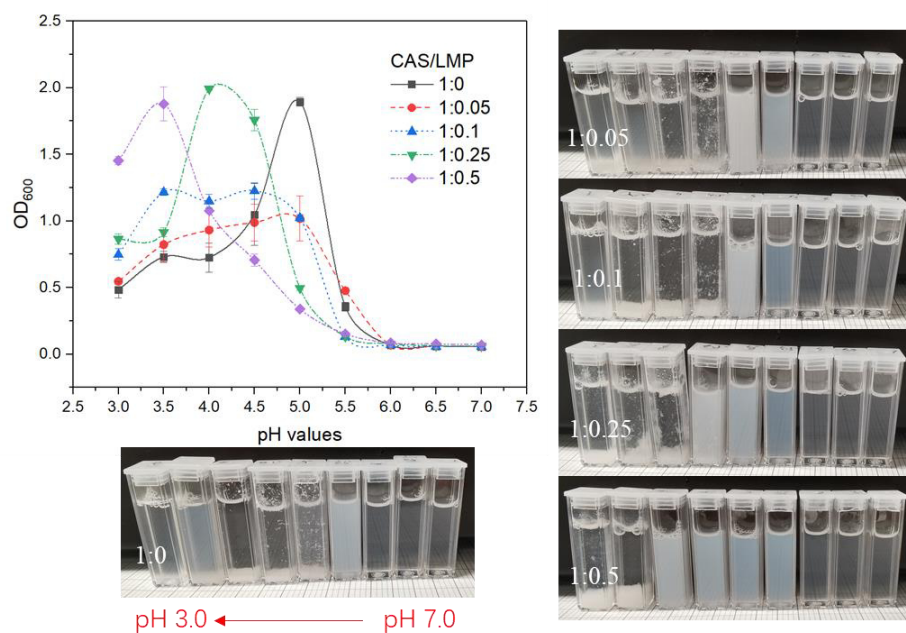


Fig. 1. OD₆₀₀ values and photographs of CAS or CAS/LMP suspensions at different pHs (3.0–7.0) and different CAS/LMP ratios (0 ~0.5, w/w). For all ratios, CAS was kept constant (0.5 wt.%) and LMP was changed from 0 (1:0) to 0.25 wt.% (1:0.5).

With continued acidification, the OD₆₀₀ values of the remaining mixed biopolymers gradually increased and reached a maximum OD₆₀₀ value, accompanied by the appearance of insoluble complexes. This is because the electrostatic repulsion between the two biopolymers is gradually decreasing and the soluble complexes may come closer and bind to a greater extent, resulting in a larger and tighter cohesive network. Among them, obvious insoluble complexes were not observed in mixtures containing higher LMP (1:0.5, w/w) until the pH dropped to 3.5. The electrostatic interactions between CAS and LMP with opposite charges were increased by further acidification (pH 5.0 to pH 3.0), which is evidenced by the transition from a transparent state to a

cloudy state with perspectives of insoluble complexes, similarly observed at gelatin/pectin and lysosome/pectin (Souza et al., 2018; Xiong et al., 2021). This result suggests that as the LMP content increases, the corresponding pH value of insoluble complexes present in the CAS/LMP mixtures can be shifted to lower pH values. This phenomenon can be further explored in emulsion-based products for extending its pH application range. Additionally, a large decline of turbidity was observed for each sample after reaching the maximum OD₆₀₀ values. It is a fact that further acidification will produce more positive charges on the casein molecules and will also lead to an increase in the solubility of the protein, thereby reducing the turbidity of the system.

3.2. Dynamic interfacial pressure and Dilatational rheological properties

The interfacial composition and structure of mixed layers at O/W interfaces is commonly involved in the stability of food emulsions, which mainly determined by two mechanistic phenomena-competitive adsorption from mixed solution and cooperative adsorption into multilayers (Dickinson, 2011).

The transient interfacial tension during the protein adsorption phase ($t = 10\ 800\ \text{s}$) of the O/W interface for CAS or CAS/LMP complexes at different pH values was shown in Fig. 2 A-C. During the formation of the O/W layer, the hydrophobic groups in the continuous phase emulsifier gradually adsorbed to the surface of the oil droplets, and then rearrange to become the interfacial layer. In all cases, the values of interfacial tension decreased with time. Surprisingly, it was shown that LMP concentrations have no obvious effects on the equilibrium interfacial tension in these three pH values. Equilibrium interfacial tensions were very close for the 5 ratios of LMP in each pH, with equilibrium values of approximately 14.0, 14.0 and 15.5 mN/m for pH 7.0, 5.0 and 3.0, respectively. This indicated that at these three tested pH values, the equilibrium O/W interfacial tension is dominated by casein rather than by LMP. Similar results were found in the study of sodium caseinate/xanthan gum (Liu et al., 2012) and sodium caseinate/high acyl gellan gum complexes in the pH range of 4.0 to 7.0 (Farooq et al., 2022). The reason for this is probably due to the flexible structure of casein proteins

and its excellent emulsifying ability (Dickinson, 1999). It should be noted that CAS and several CAS/LMP complexes are not very soluble at pH 3.0-5.0 (Fig. 1), but they can still effectively reduce interfacial tension by the small amount of soluble protein or soluble CAS/LMP complexes or insoluble proteins that did not sediment yet in the time frame of the experiment. This result was similar to the results of soy/whey protein isolate complexes at the oil-water interface (Zhang, Qi, et al., 2021). Their results indicated that the effect of pH values on protein-based equilibrium O/W interfacial tension is limited (21.0-22.5 mN/m) in the pH range of 2.0 to 11.0, although that pH approaches their isoelectric point. Lam and Nickerson (2014) reported the interfacial tension of β -lactoglobulin at pH 3.0 (~ 17.8 mN/m) and at pH 5.0 (~ 18.6 mN/m), even that β -lactoglobulin showed a very low solubility at pH 5. On the contrary, C. Chang et al. (2015) investigated the adsorption kinetics of four different proteins (pea, soy, lentil and canola protein isolates). They found that, at pH 7.0, proteins were more effective in reducing the interfacial tension than at pH 5.0 and pH 3.0 regardless of their differences in physicochemical properties, which was attributed to the hydrophobicity that was generally lower and surface charge that was relatively high at pH 7.0. Tian et al. (2021) reported that 7S pea protein at pH 3 and 8 can quickly adsorb onto the interfaces and form interfacial layers with higher interfacial pressure than that at pH 5. Ducel et al. (2005) found that the interfacial adsorption processes of pea globulin/gum Arabic complexes at the oil-water interface appear to strongly depend on the changes of pH and gum Arabic concentration.

On the other hand, CAS or CAS/LMP complexes showed relatively lower initial interfacial tension (~20 mN/m) value at pH 7.0 than that at pH 5.0 (~25 mN/m) and pH 3.0 (~27 mN/m) although all samples have overall similar equilibrated interfacial tension values. This phenomenon suggested that the biopolymers in solution at pH 7 have rapid initial adsorption at the interface, indicating the 0.01wt.% CAS or CAS/LMP mixtures at pH 7.0 should contain free proteins. In fact, both CAS and LMP show negative charges at pH 7.0, so the presence of LMP does not affect the adsorption of

CAS at the O/W interface. As a result, CAS can rapidly reach the interface during initial adsorption. A similar result was observed in the study of pea protein and steviol glycosides at O/W interface (Yang et al., 2022). Another interesting result was observed: at pH 5 and pH 3, CAS and CAS/LMP exhibited obvious different absorption curves at the initial period (0 ~ 2000 s). For example, at 1000 s, the mixtures with high content of LMP showed lower tension than pure CAS (Fig. 2B), and the higher the LMP content in the mixture, the lower value is the interface tension at 1000 s. A commonly used model to describe the properties of protein at the interfaces is divided into four stages: protein migration to the interface; adsorption; conformational reorganization (unfolding); and finally structural consolidation (Dickinson, 2011). The rate of mass transport to the interface is generally determined by protein solubility in the bulk aqueous solution. As we know, the solubility of CAS is very low when the solution pH is near its pI. Therefore, it is hypothesized that the rapid decrease of interfacial pressure at the initial stage with high content of LMP may be attributed to the formation of soluble CAS/LMP complexes at pH 5 (Fig. 2B). The simultaneous adsorption of soluble CAS/LMP complexes and remaining casein molecules at the interface may occur, and these soluble CAS/LMP complexes can reach the interface more rapidly due to their faster diffusion rate, thus resulting in the lower interfacial tension than others during initial adsorption. Moreover, opposite results were observed at pH 3 (Fig. 2C): the interfacial tension of mixtures containing high LMP (ratio>1:0.25) decreased more slowly than pure CAS or mixtures containing lower LMP. This can be explained by the fact that the interactions between the protein and the polysaccharide and the insoluble complexes formed may reduce the availability of the hydrophobic binding sites on the CAS, leading to a lower surface activity at the very beginning stage (Liu et al., 2011).

The dynamic expansion properties of the O/W interfacial adsorption layers formed by CAS or CAS/LMP mixtures at pH 3.0, 5.0 and 7.0 were further determined (Fig. 2 D-F). In all cases, the value of the elastic modulus gradually increased with time due to protein adsorption and the development of intermolecular interactions at the O/W

interface (Liu et al., 2016). Taking pure CAS as an example, the elastic module at pH 5 and pH 3 (~15 mN/m) were much higher than that at pH 7 (~10 mN/m), indicating the stronger intramolecular protein interactions that took place at pH 5 and pH 3. This is in agreement with the result observed for soybean protein isolate and oxidized bacterial cellulose (Zhang, Lei, et al., 2021). Dagleish (1993) demonstrated that the decrease in pH was associated with a significant increase in the coverage of the casein molecule on the oil droplet surface. The tail extension (the part of the lowest local density of hydrophobic residues) of casein molecules at O/W interface is diminished as pH was reduced from 7 to 5.5 (Dickinson, 1999). It can be assumed that the approach of hydrophobic residues to the oil-water interface may induce interactions between protein molecules. As expected, the elastic curves of CAS and CAS/LMP at pH 7 showed similar trend because CAS and LMP all carried negative charge. Interestingly, mixtures containing higher LMP contents exhibited higher equilibrium elastic modulus at pH 5 (Fig. 2E), and the modulus value increased with increasing LMP. The results suggested that the addition of LMP could be related to forming densely packed layers with in-plane protein-polysaccharides interactions at the O/W interface. Our findings were consistent with the caseinate/high acyl gellan gum (HG) complexes at the O/W interface: the viscoelastic films with higher moduli could be formed in CAS/HG mixed systems at pH 5.5 (Liu et al., 2016). However, the mixture containing LMP at pH 3 (Fig. 2F) did not contribute to the construction of interfacial layers, and even slightly inhibit the adsorption of CAS when the mixtures contained a relatively high content of LMP. This may be due to the formation of insoluble protein-polysaccharide complexes, which then lose their ability to adsorb on the O/W interface to some extent.

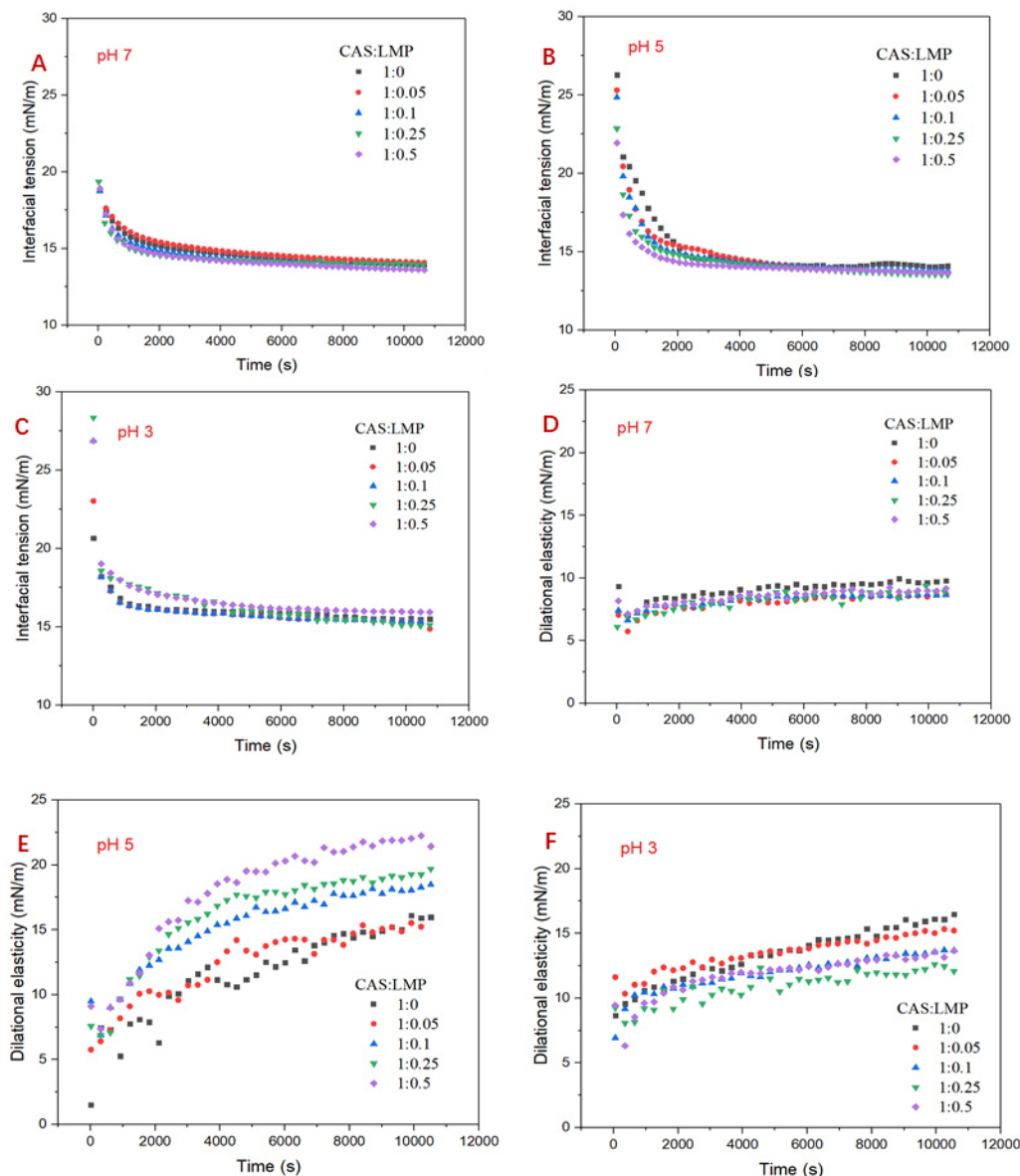


Fig. 2. (A-C) Interfacial tension over adsorption (10 800 s) at O/W interface for CAS or CAS/LMP at different pH values; (D-F) Surface dilatational elasticity over adsorption (10 800 s) at O/W interface for CAS or CAS/LMP at different pH values. For all ratios, CAS was kept constant (0.01 wt.%).

3.3. CAS or CAS/LMP based nanoemulsions

3.3.1. Zeta potential of nanoemulsions: biopolymer interaction analysis

The zeta potential and particle size of nanoemulsions stabilized by different ratios of CAS/LMP (1:0, 1:0.05, 1:0.1, 1:0.25, and 1:0.5, w/w) under pH reduction (7.0 to 3.0) was evaluated. Typically, the pH value can affect the stability of the emulsion by directly affecting the charge distribution in droplets.

The larger the absolute value of the ζ -potential, the more stable the corresponding emulsion system. As shown in Fig.3, the ζ -potential of all nanoemulsions was lower than -30 mV at pH 7, which could be considered as stable in these conditions (Lieberman et al., 2020). It can be assumed that LMP was probably not adsorbed to the droplet surfaces at pH 7 because of the relatively strong electrostatic repulsion between the negatively charged droplets and negatively charged pectin molecules. With the decrease of pH value, the absolute value of zeta potential of the nanoemulsions gradually decreases until it reaches the "0" point, then becomes positive, and continues to increase. This is the fact that further acidification will generate more positive charges on the casein molecule and further reduce the number of deprotonated carboxyl groups in the LMP (Wang et al., 2019). The net droplet charge of nanoemulsions not containing was close to zero somewhere between pH 4 and 5, which was close to the pI of CAS. At pH 5.0, the ζ -potential of the CAS-coated droplets was around -8.5 mV in the absence of LMP, which can be attributed to the fact that the pH was slightly above the pI of casein. However, the ζ -potential of the nanoemulsions containing LMP (≥ 0.1 wt.%) at pH 5 became more negative (< -20 mV), which suggested that anionic LMP might adsorb to the surfaces of the anionic CAS-coated droplets. Indeed, there was an electrostatic attraction between anionic carboxylate groups on the pectin molecules and cationic patches on the adsorbed protein molecules at pH 5.0 (Gu et al., 2004; Wang et al., 2019).

As shown in Fig. 3, with increasing the content of LMP in nanoemulsions, the corresponding isoelectric point (pI) for complete charge neutralization in CAS/LMP based nanoemulsions was shifted to lower pH values. For instance, the ζ -potential of the nanoemulsions containing 0.25 and 0.5 wt.% LMP became neutral until the pH dropped to 3.0. From the potential analysis of the emulsions, this phenomenon can be

further explored in emulsion-based products for extending their pH application range.

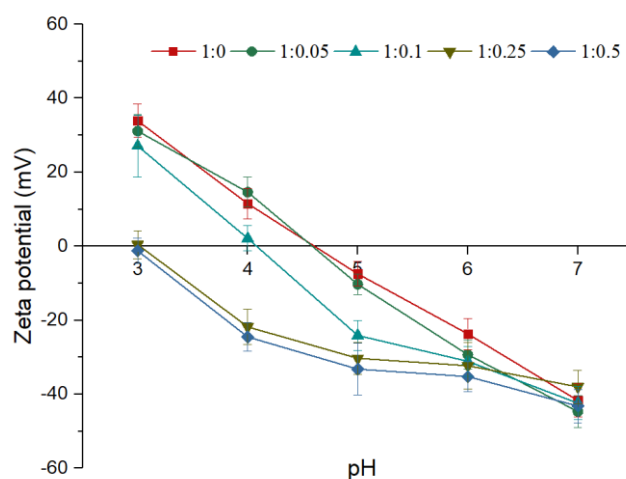


Fig. 3. ζ -potential of CAS or CAS/LMP based nanoemulsions at different pHs (3.0–7.0). For all ratios, CAS was kept constant (1.0 wt%) and LMP was changed from 0 (1:0) to 0.5 wt% (1:0.5).

3.3.2. Viscosity of nanoemulsions

[Fig. 4](#) presented the apparent viscosity of nanoemulsions at three pH values and 5 CAS/LMP ratios as a function of shear rate ($0.1 \leq \dot{\gamma} \leq 100 \text{ s}^{-1}$) at room temperature. As the shear rate increases, the viscosity of nanoemulsions tends to decrease, which means that these nanoemulsions are pseudoplastic fluids ([He et al., 2020](#)).

At pH 7, all nanoemulsions showed relatively lower apparent viscosity than pH 5 and pH 3 and exhibited relatively weak shear thinning behavior ([Fig.4 A](#)). The viscosity of CAS/LMP emulsions increased gradually with the addition of LMP from 0.05 wt.% to 0.5 wt.%. In fact, pectin is a non-adsorbing linear polysaccharide, and its aqueous solution had an excellent viscoelasticity. As a result, the viscosity increase can be attributed to the fact that free LMP molecules in the aqueous phase could increase the interparticle drag, thereby slowing down the flow of emulsion droplets and increasing the viscosity of the whole system. In addition, higher content of free pectin ($\geq 0.25 \text{ wt.}\%$) in the aqueous phase may promote depletion flocculation and these flocs further increased the viscosity of emulsions.

At pH 5, very high apparent shear viscosities ([Fig. 4B](#)) were observed in nanoemulsions without LMP or with 0.05 wt.% LMP, and both samples exhibited

strong shear thinning behavior. These results suggested that there was a high degree of droplet flocculation at pH 5, which was also supported by the surface charge (Fig. 3): relatively low surface potential (~ -10 mV) was insufficient to prevent aggregation between droplets and then increase the viscosity of nanoemulsions. Meanwhile, with the increase of LMP in nanoemulsions, the viscosity decreased significantly, especially when LMP was higher than 0.25 wt.%, indicating that the addition of LMP could inhibit the droplet flocculation at pH 5. The reason for this behavior can be attributed to the adsorption of pectin molecules to the droplet surface allowing to an increase of the repulsive forces between droplets, thereby preventing extensive droplet flocculation. The increased high elastic modulus at O/W interfaces (Fig. 2E) could support this phenomenon.

At pH 3, the lowest viscosity was observed in nanoemulsion not containing LMP, and the viscosity of the nanoemulsions increased as the LMP content increased from 0 to 0.5 wt.%, which was similar to the trend at pH 7. However, all the nanoemulsions at pH 3 showed higher viscosity values than those at pH 7, especially those containing high content of LMP. In fact, in nanoemulsions not containing LMP, flocculation occurs when the pH of the emulsion was adjusted from 7 to 3, as the pI of caseinate must be passed. Very high apparent viscosities and extensive shear thinning at high content of LMP nanoemulsions (≥ 0.25 wt%) can be attributed to charge neutralization and bridging flocculation of the positively charged CAS-stabilized droplets by the negatively charged LMP molecules. Therefore, LMP molecules may have adsorbed to the surface of multiple droplets, causing them to link together, depending on the pectin concentration. The surface potential (Fig. 3) close to “0” for nanoemulsions containing 0.25 and 0.5 wt.% also confirms this phenomenon. Similar studies also reported that anionic polysaccharides cause bridging flocculation of protein emulsions at acidic pH (Ding et al., 2021; Griffin & Khouryieh, 2020).

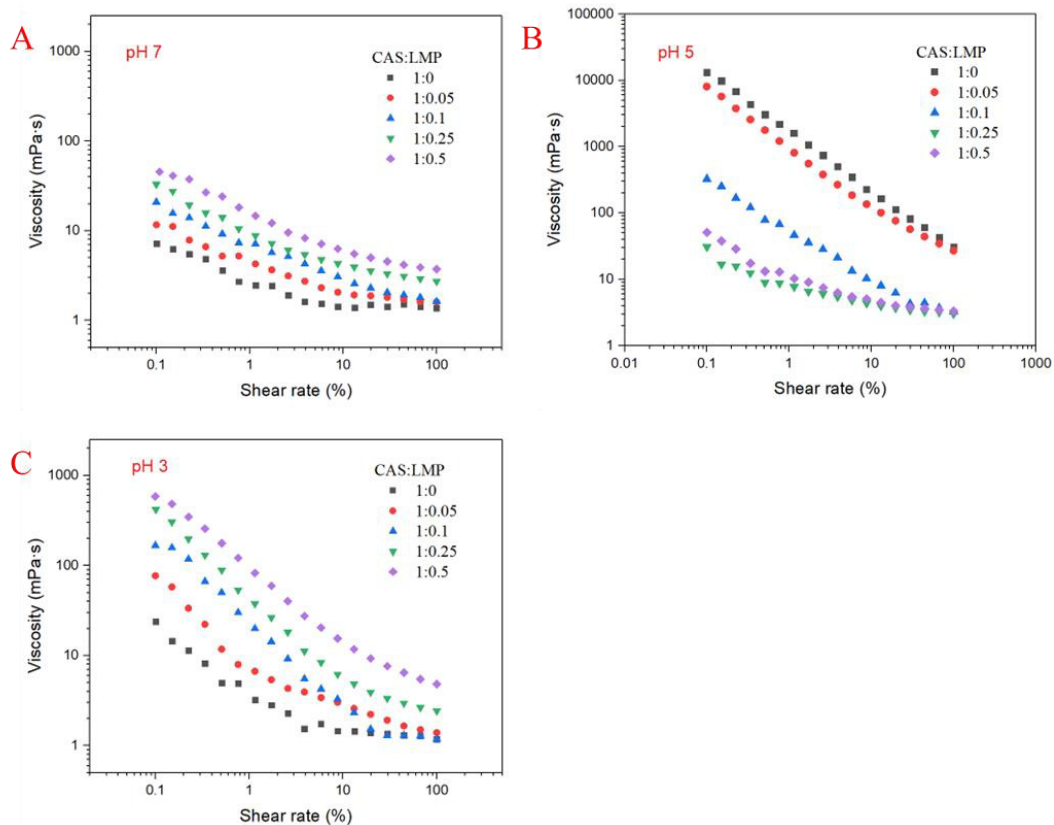


Fig. 4. Viscosity of CAS or CAS/LMP based nanoemulsions at (A) pH 7.0, (B) pH 5.0 and (C) pH 3.0. For all ratios, CAS was kept constant (1.0 wt%) and LMP was changed from 0 (1:0) to 0.5 wt% (1:0.5).

3.3.3. Stability of nanoemulsions: particle size, creaming and microstructure

During production, processing and storage, food products are exposed to a variety of environmental factors, especially changes in pH, which can have a significant impact on food. Therefore, it is very necessary to study the micro and macro changes of emulsion stability with pH changes. In this section, dynamic light scattering (DLS) (Fig. 5A), creaming index (Fig. 5B), and optical microscopy (Fig. 6) will be used to evaluate the mean particle size and droplet aggregation of diluted CAS or CAS/LMP-stabilized nanoemulsions under pH reduction (7.0 to 3.0).

At pH 7 or pH 6, nanoemulsions exhibited nanoscale sizes in the range of 250 to 300 nm with monomodal size distribution (Fig. 5A). These results demonstrate that caseinate is an effective emulsifier at mild pH, capable of producing emulsions with the vast majority of droplets having nanoscale diameters. As expected, at pH 7, LMP

concentrations has no obvious effect on the average diameter of the nanoemulsions, suggesting no adsorption of LMP on the surface of the oil droplets. For creaming stability (Fig. 5B), the free pectin or low content LMP (≤ 0.1 wt.%) CAS-stabilized emulsions were stable to creaming after 24 h storage at pH 7 and 6. However, when the concentration of LMP was increased to 0.25 and 0.5 wt.%, the nanoemulsions were highly unstable to phase separation, which may be caused by depletion flocculation at neutral pH. In the microstructural results, particle aggregation at pH 7 was clearly observed at high concentrations of LMP (Fig. 6 A). This also means that the creaming of CAS-based nanoemulsions caused by depletion flocculation is reversible because there is no significant increase in droplet size. A similar result was found in the study of anionic polysaccharides and rice bran protein based emulsions (Zang et al., 2019).

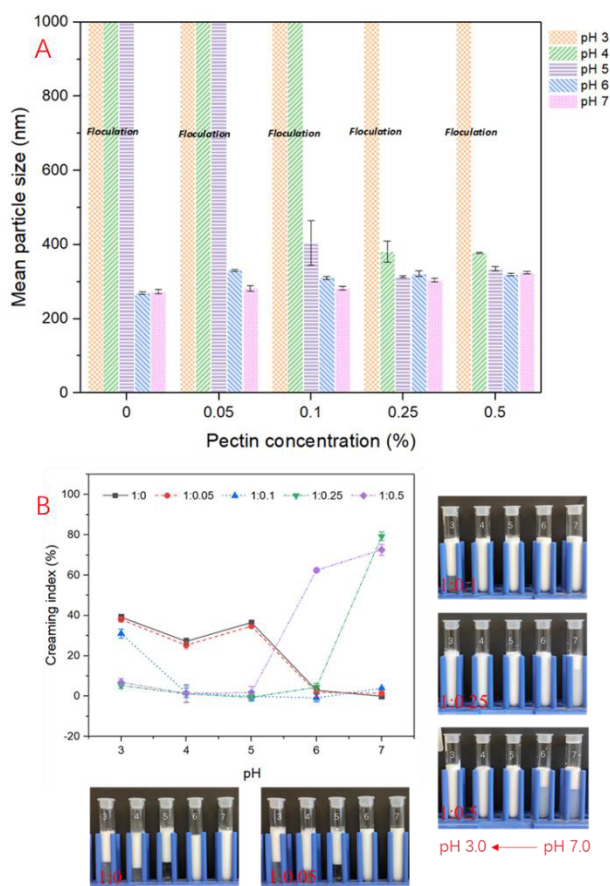


Fig. 5. (A) Mean particle size, (B) creaming index and photographs of CAS or CAS/LMP based nanoemulsions at different pHs (3.0–7.0). For all ratios, CAS was kept constant (1.0 wt%) and LMP was changed from 0 (1:0) to 0.5 wt% (1:0.5).

At pH 5.0, the mean particle size (Fig. 5A) of free LMP emulsion and emulsion containing 0.05 wt.% LMP was outside the measurement range of DLS and these emulsions rapidly separated into an opaque droplet-rich ‘cream’ layer at the top and a transparent droplet-free ‘serum’ layer within one hour (Fig. 5B). In fact, the electrostatic repulsions (Fig. 3) between droplets is not sufficient to prevent aggregation when the pH is close to the pI of the adsorbed CAS molecules. As a result, most of the droplets clump together and move upwards rapidly due to gravity. Remarkably, the nanoemulsions containing LMP (≥ 0.1 wt.%) exhibited stable nanoscale hydrodynamic size (Fig. 5A) and good creaming stability (Fig. 5B) at pH 5. Meanwhile, LMP (≥ 0.25 wt.%) greatly inhibited the amount of droplet aggregation observed in the microstructure of CAS stabilized nanoemulsions (Fig. 6B). This can be probably attributed to the fact that negatively charged LMP molecules can adsorb to positively charged patches of CAS on the droplet surface, thereby increasing the overall negative charge on the droplet, which was also supported by the result of interfacial moduli at pH 5 (Fig. 2E). Meanwhile, the thickness of the interfacial layer could be also strengthened by the adsorption of LMP, thereby increasing the steric repulsion between the droplets (Surh et al., 2006). Several other studies have also indicated that the mixed use of anionic polysaccharides with proteins can improve the stability of emulsions to aggregation (Surh et al., 2006; Zang et al., 2019; Zhang, Lei, et al., 2021).

As the pH continued to decrease, only the nanoemulsions containing 0.25 and 0.5 wt.% LMP exhibited nanoscale diameters (~ 400 nm) at pH 4, indicating that the pH stability of CAS-based emulsions was significantly improved. Taking the nanoemulsion containing 0.5 wt.% LMP as an example, the average particle size increased from 324 to 378 nm when the pH was decreased from 7.0 to 4.0. In fact, when the pH decreases, the repulsive forces gradually turn into attractive forces, and the droplet surface is stabilized by the non-covalent complexes of LMP/CAS, resulting in larger size droplets. This result was similar to the previous report about casein and chitosan (Zhang, Cai, et al., 2021). Optical microscopy measurements showed extensive droplet flocculation at

pH 3 in all nanoemulsions with or without pectin (Fig. 6C). This can be explained mainly by three reasons: (i) flocs formed when the pH of emulsions was reduced from 7.0 to 3.0 (passing through the pI); (ii) charge neutralization - LMP adsorption reduces the magnitude of the zeta potential, thereby reducing electrostatic repulsions between droplets; (iii) bridging flocculation — a single LMP molecule may have adsorbed to the surface of multiple droplets, causing them to link together (Guzey & McClements, 2006). Notably, the CAS/LMP blend (especially when LMP content ≥ 0.25 wt.%) also significantly enhanced the emulsion stability of the nanoemulsions in the acidic pH range (3.0 – 5.0). Additionally, the results of creaming and microscopic observation are inconsistent in some cases. For example, clear particle aggregation was observed in the microstructure (Fig. 6C) of nanoemulsion containing 0.5 wt.% LMP, but no obvious phase separation occurred in the macroscopic structure (Fig. 5B). This phenomenon could be explained by two reasons: (i) the formation of a network of strongly aggregated emulsion droplets that were held together by LMP molecules, thereby affecting the viscosity of the continuous phase and inhibiting the upward movement of the aggregates; (ii) the concentration of the nanoemulsion is relatively high, so the boundary between the "cream" layer and the "serum" layer is hardly visible. In conclusion, through the effective use of LMP/CAS complexes, the pH application range of CAS-based emulsions can be broadened.

3.3.4. Effect of ultrasonication on droplet aggregation

As described in previous studies (Ding et al., 2021; Guzey & McClements, 2006), bridging flocculation-induced aggregation during the preparation of multilayer systems can be disrupted and redispersed by mechanical forces, such as homogenization, blending or high intensity ultrasound. In this section, the aggregation of droplets formed at pH 5 and pH 3 was evaluated by sonication to test whether the flocs could be redispersed.

Our results showed that high content (≥ 0.25 wt.%) of LMP promotes depleted flocculation at pH 7.0 (Fig. 6A), but their corresponding size (Fig. 5A) still showed

nanoparticle size. This suggested that depleted flocculation is reversible which could be disrupted by gentle stirring or dilution. At pH 5, clear flocs were observed on free LMP nanoemulsions and nanoemulsions containing small amounts of LMP (≤ 0.1 wt.%); however, these three samples still showed massive aggregation of droplets after sonication (data not shown), and their hydrodynamic size was beyond the range of DLS measurements, which can be attributed to insufficient electrostatic repulsions to avoid agglomeration of CAS when the pH is close to the pI. At pH 3, sonication resulted in a significant reduction in droplet aggregation and a significant reduction in particle size for emulsions with relatively low LMP content (≤ 0.1 wt.%) (Fig. 6D). The mean particle size of the free LMP emulsions or those containing 0.05 and 0.1 wt.% were 681.2, 747.5 and 795.0 nm, respectively. This flocculation probably occurred as the emulsion passed the isoelectric point as the pH was adjusted from 7 to 3. One possible explanation for this phenomenon is that once the flocs are broken down, the relatively strong electrostatic repulsions between casein-stabilized droplets are sufficient to keep them stable. However, at pH 3, sonication was unable to disrupt flocs in emulsions with relatively high LMP pectin content (≥ 0.25 wt.%), probably because pectin promotes bridging between positively charged droplets flocculation. Even if these flocs are redispersed, the net charge of the system remains low. These results indicate that the ability of sonication to effectively reduce the degree of emulsion droplet aggregation is dependent on pH and pectin concentration.

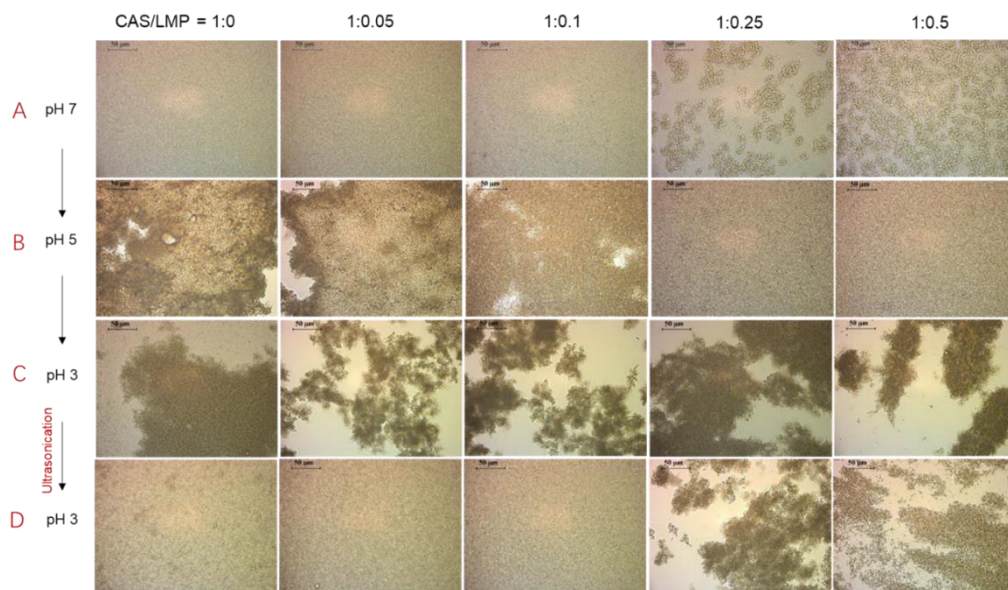


Fig. 6. Photomicrographs of CAS or CAS/LMP based nanoemulsions at (A) pH 7, (B) pH 5 and (C) pH 3. (D) Photomicrographs of CAS or CAS/LMP based nanoemulsions at pH 3 after ultrasonication. For all ratios, CAS was kept constant (1.0 wt%) and LMP was changed from 0 (1:0) to 0.5 wt% (1:0.5).

4. Conclusion

This study investigated the effect of pH on the dilatational rheological properties of CAS/LMP at O/W interface and colloidal stability of CAS/LMP nanoemulsions. The pH and LMP concentration had limited effects on the equilibrium interfacial tension of CAS/LMP at the O/W interface, but had a significant effect on the adsorption process in the initial stage. Further analysis indicated that the dilatational viscoelasticity modulus at pH 5 was significantly affected by the combination of CAS and LMP. Meanwhile, higher content of LMP can inhibit the aggregation and creaming of CAS-coated emulsions at pH 5, and improve the stability of nanoemulsions at acidic pH conditions. At pH 7, reversible aggregation was observed in nanoemulsions containing LMP (≥ 0.25 wt.%) while at pH 3, irreversible aggregation was observed in all nanoemulsions. When the LMP was lower than 0.1 wt.%, sonication treatment can disrupt the flocculation to a certain extent and redisperse the nanoscale droplets. This research could support future applications of CAS-stabilized emulsions over a wide pH range.

References

- Bagley, R. L., & Torvik, P. J. (1983). A theoretical basis for the application of fractional calculus to viscoelasticity. *Journal of Rheology*, 27(3), 201–210.
- Berton-Carabin, C. C., Schröder, A., Rovalino-Cordova, A., Schroën, K., & Sagis, L. (2016). Protein and lipid oxidation affect the viscoelasticity of whey protein layers at the oil–water interface. *European Journal of Lipid Science and Technology*, 118(11), 1630–1643.
- Cai, Y., Deng, X., Liu, T., Zhao, M., Zhao, Q., & Chen, S. (2018). Effect of xanthan gum on walnut protein/xanthan gum mixtures, interfacial adsorption, and emulsion properties. *Food Hydrocolloids*, 79, 391–398.
- Castellani, O., Al-Assaf, S., Axelos, M., Phillips, G. O., & Anton, M. (2010). Hydrocolloids with emulsifying capacity. Part 2–Adsorption properties at the n-hexadecane–Water interface. *Food Hydrocolloids*, 24(2–3), 121–130.
- Chang, C., Tu, S., Ghosh, S., & Nickerson, M. T. (2015). Effect of pH on the interrelationships between the physicochemical, interfacial and emulsifying properties for pea, soy, lentil and canola protein isolates. *Food Research International*, 77, 360–367.
- Chang, P. G., Gupta, R., Timilsena, Y. P., & Adhikari, B. (2016). Optimisation of the complex coacervation between canola protein isolate and chitosan. *Journal of Food Engineering*, 191, 58–66.
- Chung, C., & McClements, D. J. (2014). Structure–function relationships in food emulsions: Improving food quality and sensory perception. *Food Structure*, 1(2), 106–126.
- Dalgleish, D. G. (1993). The sizes and conformations of the proteins in adsorbed layers of individual caseins on latices and in oil-in-water emulsions. *Colloids and Surfaces B: Biointerfaces*, 1(1), 1–8.
- Dalgleish, D. G., Srinivasan, M., & Singh, H. (1995). Surface properties of oil-in-water emulsion droplets containing casein and Tween 60. *Journal of Agricultural and Food Chemistry*, 43(9), 2351–2355.
- Dickinson, E. (1999). Caseins in emulsions: Interfacial properties and interactions. *International Dairy Journal*, 9(3), 305–312.
- Dickinson, E. (2011). Mixed biopolymers at interfaces: Competitive adsorption and multilayer structures. *Food Hydrocolloids*, 25(8), 1966–1983.
- Dickinson, E., & Golding, M. (1997). Depletion flocculation of emulsions containing unadsorbed sodium caseinate. *Food Hydrocolloids*, 11(1), 13–18.
- Ding, M., Liu, L., Zhang, T., Tao, N., Wang, X., & Zhong, J. (2021). Effect of interfacial layer number on the storage stability and in vitro digestion of fish oil-loaded multilayer emulsions consisting of gelatin particle and polysaccharides. *Food Chemistry*, 336, 127686.
- Ducel, V., Richard, J., Popineau, Y., & Boury, F. (2005). Rheological Interfacial Properties of Plant Protein–Arabic Gum Coacervates at the Oil–Water Interface. *Biomacromolecules*, 6(2), 790–796.

- Farooq, S., Ahmad, M. I., & Abdullah. (2022). Interfacial rheology of sodium caseinate/high acyl gellan gum complexes: Stabilizing oil-in-water emulsions. *Current Research in Food Science*, 5, 234–242.
- Farshchi, A., Ettelaie, R., & Holmes, M. (2013). Influence of pH value and locust bean gum concentration on the stability of sodium caseinate-stabilized emulsions. *Food Hydrocolloids*, 32(2), 402–411.
- Gorji, S. G., Gorji, E. G., & Mohammadifar, M. A. (2014). Characterisation of gum tragacanth (*Astragalus gossypinus*)/sodium caseinate complex coacervation as a function of pH in an aqueous medium. *Food Colloids 2012: Creation and Breakdown of Structure*, 34, 161–168.
- Griffin, K., & Houryieh, H. (2020). Influence of electrostatic interactions on the formation and stability of multilayer fish oil-in-water emulsions stabilized by whey protein-xanthan-locust bean complexes. *Journal of Food Engineering*, 277, 109893.
- Gumus, C. E., Decker, E. A., & McClements, D. J. (2017). Impact of legume protein type and location on lipid oxidation in fish oil-in-water emulsions: Lentil, pea, and faba bean proteins. *Food Research International*, 100, 175–185.
- Guzey, D., & McClements, D. J. (2006). Formation, stability and properties of multilayer emulsions for application in the food industry. *In Honor of Professor Nissim Garti's 60th Birthday*, 128–130, 227–248.
- He, L., Peng, H., Wei, X., Li, B., & Tian, J. (2020). Preparation and Characterization of Emulsions Stabilized with Defatted Sesame Meal. *Food Science and Technology Research*, 26(5), 655–663.
- Hu, M., McClements, D. J., & Decker, E. A. (2003). Lipid oxidation in corn oil-in-water emulsions stabilized by casein, whey protein isolate, and soy protein isolate. *Journal of Agricultural and Food Chemistry*, 51(6), 1696–1700.
- Karthik, P., & Anandharamakrishnan, C. (2016). Enhancing omega-3 fatty acids nanoemulsion stability and in-vitro digestibility through emulsifiers. *Journal of Food Engineering*, 187, 92–105.
- Khalloufi, S., Alexander, M., Douglas Goff, H., & Corredig, M. (2008). Physicochemical properties of whey protein isolate stabilized oil-in-water emulsions when mixed with flaxseed gum at neutral pH. *Food Research International*, 41(10), 964–972.
- Lam, R. S., & Nickerson, M. T. (2014). The effect of pH and heat pre-treatments on the physicochemical and emulsifying properties of β -lactoglobulin. *Food Biophysics*, 9(1), 20–28.
- Li, Q., Zheng, J., Ge, G., Zhao, M., & Sun, W. (2020). Impact of heating treatments on physical stability and lipid-protein co-oxidation in oil-in-water emulsion prepared with soy protein isolates. *Food Hydrocolloids*, 100, 105167.
- Liang, L. I., & Luo, Y. (2020). Casein and pectin: Structures, interactions, and applications. *Trends in Food Science & Technology*, 97, 391–403.
- Liao, W., Gharsallaoui, A., Dumas, E., Ghnimi, S., & Elaissari, A. (2021). Effect of

- carrier oil on the properties of sodium caseinate stabilized O/W nanoemulsions containing Trans-cinnamaldehyde. *LWT*, *146*, 111655.
- Lieberman, H., Rieger, M., & Banker, G. S. (2020). *Pharmaceutical dosage forms: Disperse systems*. CRC Press.
- Liu, L., Zhao, Q., Liu, T., Long, Z., Kong, J., & Zhao, M. (2012). Sodium caseinate/xanthan gum interactions in aqueous solution: Effect on protein adsorption at the oil–water interface. *Food Hydrocolloids*, *27*(2), 339–346.
- Liu, L., Zhao, Q., Liu, T., & Zhao, M. (2011). Dynamic surface pressure and dilatational viscoelasticity of sodium caseinate/xanthan gum mixtures at the oil–water interface. *Food Hydrocolloids*, *25*(5), 921–927.
- Liu, L., Zhao, Q., Zhou, S., & Zhao, M. (2016). Modulating interfacial dilatational properties by electrostatic sodium caseinate and carboxymethylcellulose interactions. *Food Hydrocolloids*, *56*, 303–310.
- Mwangi, W. W., Ho, K.-W., Tey, B.-T., & Chan, E.-S. (2016). Effects of environmental factors on the physical stability of pickering-emulsions stabilized by chitosan particles. *Food Hydrocolloids*, *60*, 543–550.
- Neiryneck, N., Dewettinck, K., & Van der Meeren, P. (2007). Influence of pH and biopolymer ratio on sodium caseinate—Guar gum interactions in aqueous solutions and in O/W emulsions. *Food Hydrocolloids*, *21*(5–6), 862–869.
- Pallandre, S., Decker, E. A., & McClements, D. J. (2007). Improvement of stability of oil-in-water emulsions containing caseinate-coated droplets by addition of sodium alginate. *Journal of Food Science*, *72*(9), E518–E524.
- Ruiz-Álvarez, J. M., del Castillo-Santaella, T., Maldonado-Valderrama, J., Guadix, A., Guadix, E. M., & García-Moreno, P. J. (2022). PH influences the interfacial properties of blue whiting (*M. poutassou*) and whey protein hydrolysates determining the physical stability of fish oil-in-water emulsions. *Food Hydrocolloids*, *122*, 107075.
- Schmitt, C., Sanchez, C., Thomas, F., & Hardy, J. (1999). Complex coacervation between β -lactoglobulin and acacia gum in aqueous medium. *Food Hydrocolloids*, *13*(6), 483–496.
- Singh, H., & Sarkar, A. (2011). Behaviour of protein-stabilised emulsions under various physiological conditions. *Advances in Colloid and Interface Science*, *165*(1), 47–57.
- Souza, C. J., da Costa, A. R., Souza, C. F., Tosin, F. F. S., & Garcia-Rojas, E. E. (2018). Complex coacervation between lysozyme and pectin: Effect of pH, salt, and biopolymer ratio. *International Journal of Biological Macromolecules*, *107*, 1253–1260.
- Srinivasan, M., Singh, H., & Munro, P. A. (2000). The effect of sodium chloride on the formation and stability of sodium caseinate emulsions. *Food Hydrocolloids*, *14*(5), 497–507.
- Surh, J., Decker, E. A., & McClements, D. J. (2006). Influence of pH and pectin type on properties and stability of sodium-caseinate stabilized oil-in-water emulsions.

- Food Hydrocolloids*, 20(5), 607–618.
- Teng, M.-J., Wei, Y.-S., Hu, T.-G., Zhang, Y., Feng, K., Zong, M.-H., & Wu, H. (2020). Citric acid cross-linked zein microcapsule as an efficient intestine-specific oral delivery system for lipophilic bioactive compound. *Journal of Food Engineering*, 281, 109993.
- Tian, Y., Taha, A., Zhang, P., Zhang, Z., Hu, H., & Pan, S. (2021). Effects of protein concentration, pH, and NaCl concentration on the physicochemical, interfacial, and emulsifying properties of β -conglycinin. *Food Hydrocolloids*, 118, 106784.
- Wang, J., Dumas, E., & Gharsallaoui, A. (2019). Low Methoxyl pectin / sodium caseinate complexing behavior studied by isothermal titration calorimetry. *Food Hydrocolloids*, 88, 163–169.
- Wang, J., Su, Y., Jia, F., & Jin, H. (2013). Characterization of casein hydrolysates derived from enzymatic hydrolysis. *Chemistry Central Journal*, 7(1), 1–8.
- Xiong, W., Li, Y., Ren, C., Li, J., Li, B., & Geng, F. (2021). Thermodynamic parameters of gelatin-pectin complex coacervation. *Food Hydrocolloids*, 120, 106958.
- Yang, Y., Zhang, J., Liu, Y., Wu, L., Li, Q., Xu, M., Wan, Z., Ngai, T., & Yang, X. (2022). PH-dependent micellar properties of edible biosurfactant steviol glycosides and their oil-water interfacial interactions with soy proteins. *Food Hydrocolloids*, 126, 107476.
- Zang, X., Wang, J., Yu, G., & Cheng, J. (2019). Addition of anionic polysaccharides to improve the stability of rice bran protein hydrolysate-stabilized emulsions. *LWT*, 111, 573–581.
- Zhang, F., Cai, X., Ding, L., & Wang, S. (2021). Effect of pH, ionic strength, chitosan deacetylation on the stability and rheological properties of O/W emulsions formulated with chitosan/casein complexes. *Food Hydrocolloids*, 111, 106211.
- Zhang, S., Tian, L., Yi, J., Zhu, Z., Decker, E. A., & McClements, D. J. (2020). Mixed plant-based emulsifiers inhibit the oxidation of proteins and lipids in walnut oil-in-water emulsions: Almond protein isolate-camellia saponin. *Food Hydrocolloids*, 109, 106136.
- Zhang, X., Lei, Y., Luo, X., Wang, Y., Li, Y., Li, B., & Liu, S. (2021). Impact of pH on the interaction between soybean protein isolate and oxidized bacterial cellulose at oil-water interface: Dilatational rheological and emulsifying properties. *Food Hydrocolloids*, 115, 106609.
- Zhang, X., Qi, B., Xie, F., Hu, M., Sun, Y., Han, L., Li, L., Zhang, S., & Li, Y. (2021). Emulsion stability and dilatational rheological properties of soy/whey protein isolate complexes at the oil-water interface: Influence of pH. *Food Hydrocolloids*, 113, 106391.

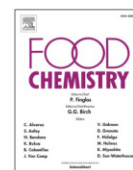
Chapter VI

Effect of trans-Cinnamaldehyde or citral on sodium caseinate: Interfacial rheology and fluorescence quenching properties

Published in: Food Chemistry

Summary of Chapter VI

Essential oils are known to be fragile and are often encapsulated in order to protect them from environmental stresses. Thus, it should be interesting to verify whether the nanoencapsulation systems could have an effect on the structural and physicochemical properties of the entrapped active molecules. The first objective of this study was to investigate the effect of natural aldehydes (Trans-Cinnamaldehyde (TCA) and citral) on the interfacial and oscillatory dilatational properties of CAS stabilized oil droplets. Meanwhile, fluorescence quenching was used to explore the binding properties among selected aldehydes and CAS under different temperatures and different concentrations of aldehydes. Small amounts of TCA or citral in the oil phase were shown to decrease the oil/water interfacial tension. In addition, the fluorescence quenching test showed that TCA has a more obvious quenching effect on CAS than citral. Further kinetic analysis suggests that TCA has strong affinity for CAS and this bonding process is spontaneous. In summary, these natural aldehydes, could be useful ingredients to improve the functionalities of food protein-based products.



Effect of *trans*-cinnamaldehyde or citral on sodium caseinate: Interfacial rheology and fluorescence quenching properties

Wei Liao^a, Abdelhamid Elaissari^b, Emilie Dumas^a, Adem Gharsallaoui^{a,*}

^a Univ. Lyon, University Claude Bernard Lyon 1, CNRS, LAGEPP UMR 5007, 43 Bd 11 Novembre 1918, 69622 Villeurbanne, France

^b Univ Lyon, University Claude Bernard Lyon 1, CNRS, ISA-UMR 5280, 69622 Villeurbanne, France

ARTICLE INFO

Keywords:

Sodium caseinate
Trans-Cinnamaldehyde
 Citral
 Interfacial properties
 Fluorescence quenching

ABSTRACT

The interactions between sodium caseinate (CAS) and two natural aldehydes (*trans*-cinnamaldehyde (TC) and citral) were studied by evaluating oil/water (O/W) interfacial and fluorescence quenching properties. A small amount of TC in the oily phase resulted in lower O/W interfacial tension (9.12 mN/m). Particularly, the use of TC developed a stronger interface with higher elastic moduli (~16.21 mN/m). This was supported by the fluorescence measurements: the quenching effect of TC on CAS was more pronounced than that of citral. Kinetic analysis indicated that both dynamic and static quenching occurs. The large binding constant ($1.78 \times 10^5 \text{ M}^{-1}$) at 25 °C suggests that TC has strong affinity for CAS. Meanwhile, this binding process seemed to be spontaneous and driven by hydrogen bond formation with unfavorable conformational changes. This work would provide guidance for using the binding properties of natural aldehydes to enhance the interfacial properties of proteins.

1. Introduction

Many food products are based on emulsions systems (oil-in-water (O/W) and water-in-oil (W/O)) (Castellani et al., 2010) which require the use of emulsifying agents to stabilize the interfaces between different phases. Nowadays, food industries prefer to use more natural emulsifiers like proteins rather than chemical synthetic emulsifiers (Felix et al., 2019), since these proteins can provide extra nutritional added values and are more accepted by consumers. Some proteins such as soy, pea, bovine serum albumin, and dairy proteins have been reported as emulsifiers with good characteristics (Sha et al., 2021; Tang & Shen, 2015; Wang et al., 2020). During the absorption process, protein molecules general unfold and expose hydrophobic residues which may physically or chemically interact with other functional compounds, thereby altering their functional performance (Dickinson, 1999). Protein emulsifiers can be modified to tailor their solubility, hydrophobicity, dispersibility, and surface charge by using some enzymes or crosslinking agents (Gerrard et al., 2003; H. Wang et al., 2022). Gerrard et al. (2003) studied the crosslinking of wheat proteins with glutaraldehyde, formaldehyde and glyceraldehyde by Maillard reaction and they found that the interaction between them could be harnessed by food processors to manipulate the texture of foods. H. Wang et al. (2022) revealed the mechanism of interactions between aldehydes and

myofibril proteins and provides guidance for controlling the flavor of meat. However, these treatments may introduce new groups which is limited for food uses due to possible toxicity effects or the absence of GRAS (Generally Recognized as Safe) status. For this reason, more natural compounds for protein functionalization should be sought and investigated.

It has been reported that the interactions between rice protein isolate and ferulic acid in O/W emulsions can be used to improve the oxidative stability (Jia et al., 2019); the interaction between glycosylated protein and tannic acid can be used to improve the thermal, salt ion, and storage stabilities of Pickering emulsions (Chen et al., 2021) and the interactions between cinnamaldehyde and whey proteins can be applied in O/W emulsions against the effects of different pH values and high ionic concentrations. Aldehydes have a crucial role in flavor development of food products (Banerjee & Chattopadhyay, 2019) and certain aldehydes are able to interact with various functional residues of amino groups, like ε-amino groups of lysine, the sulfhydryl group of cysteine, the imidazole ring of histidine and the phenol group of tyrosine, etc (Habeeb & Hiramoto, 1968). Among these, natural-based compounds include some aromatic aldehydes such as cinnamaldehyde, salicylaldehyde, syringaldehyde, vanillin, and anisaldehyde, which have been introduced in food and pharmaceutical industries (Banerjee & Chattopadhyay, 2019; Boeve & Joye, 2020). These aromatic aldehydes have gained

* Corresponding author.

E-mail address: adem.gharsallaoui@univ-lyon1.fr (A. Gharsallaoui).

<https://doi.org/10.1016/j.foodchem.2022.134044>

Received 31 March 2022; Received in revised form 22 August 2022; Accepted 25 August 2022

Available online 27 August 2022

0308-8146/© 2022 Elsevier Ltd. All rights reserved.

considerable attention due to their various health benefits like anti-inflammatory, antioxidant, antimicrobial, and anticancer properties (Banerjee & Chattopadhyay, 2019). *Trans*-cinnamaldehyde (3-phenyl-2-propenal, TC, FEMA 2286) is a major component of volatile cinnamon essential oil (Shen et al., 2015). It showed broad-spectrum antimicrobial activity against bacteria, yeast, and molds (Shen et al., 2015). Citral (3,7-dimethyl-2, 6-octadienal, FEMA 2303) is the main component of citrus fruit's peel oil which is widely applied as a flavoring additive in foods and beverages. As these two active compounds have extremely low solubility in water, it is difficult to prepare food formulations containing these natural aldehydes in solubilized form. There are two main approaches to overcome this insolubility issue: (i) mixing them with carrier oils and then producing oil in water systems by using some food emulsifiers since these aldehydes have a good solubility in oil; (ii) associating them with food molecules to form systems that allow them to be delivered, especially since several reports have shown that certain aldehydes are able to bind to proteins (Asghari et al., 2017; Felix et al., 2019). Several studies reported that aldehydes can bind to amino acid residues of proteins by irreversible covalent binding (Habeb & Hiramoto, 1968), hydrophobic interactions (Wang & Arntfield, 2015), or hydrogen bonds (Tan & Siebert, 2008), which depend on the specific chemistry and structure of the interacting molecules. Meanwhile, the binding between aldehydes and proteins could be also used in oil-in-water interfaces to adjust the physical stability (Chen et al., 2017; Chen et al., 2018) and the interfacial properties (Felix et al., 2017). However, the number of reports about the mechanisms of interaction between aromatic aldehydes and proteins, and the use of interaction mechanisms in emulsion design is still scarce.

Sodium caseinate (CAS) is a heterogeneous protein and usually consists of four different polypeptide chains: α (s1)- and α (s2)-caseins, β -casein, and κ -casein, which have good amphiphilic properties (Dickinson, 1999). CAS can endow food with certain functionalities, such as water solubility, emulsification, foamability and encapsulation ability. It is considered a good carrier for bioactive ingredients, as they are an integral part of many people's diets. Additionally, CAS can adsorb at O/W interfaces and have the ability to rapidly reduce the interfacial tension during the emulsification process. Eventually, a densely packed interface might be formed with viscoelastic behavior. The characteristics of the interfaces are essential for understanding the stability of O/W emulsion systems. Our hypothesis is that caseinate and natural aldehydes would interact and this interaction could provide better interfacial properties at O/W interface. This hypothesis will be verified by studying the interfacial properties and fluorescence quenching properties between CAS and both aldehydes (TC and citral). Therefore, the first objective of this work was to investigate the effect of aldehydes on the interfacial and oscillatory dilatational properties of CAS coated droplets. The second objective was to study the binding forces responsible for the interactions between the selected aldehydes and CAS. Hence, fluorescence quenching measurements were carried out in different temperatures and different concentrations of aldehydes. In fact, understanding the binding properties between natural aldehydes and dairy proteins would contribute to formulate dairy-based products with more health benefits and functional properties.

2. Material and methods

2.1. Materials

Trans-cinnamaldehyde (TC, 99 %) and citral (99 %) were purchased from Sigma-Aldrich (St Quentin Fallavier, France). Sodium caseinate (CAS) was purchased from Fisher Scientific (United Kingdom) and its protein content measured by the Kjeldahl method was 93.20 % (nitrogen conversion factor $N = 6.38$). A medium chain triacylglycerol oil (MCT) was purchased from Gattefossé (Saint-Priest, France). Analytical grade imidazole ($C_3H_4N_2$), sodium azide, pure ethanol, acetic acid, sodium hydroxide (NaOH), and hydrochloric acid (HCl), were purchased from

Sigma-Aldrich Chimie (St Quentin Fallavier, France). All the solutions were prepared in deionized water.

2.2. Interfacial properties

2.2.1. Sample preparation

The aqueous phase for interfacial measurements was prepared by dispersing CAS powder (0.01 wt%) into 100 mL of buffer solution (5 mmol/L acetic acid-imidazole, 0.05 wt% sodium azide, pH 7.0). The protein solution was stirred at room temperature until it was completely dissolved. Oily phases were prepared by mixing TC or citral (5 wt%) with MCT under stirring until they were completely homogeneous. Pure MCT was used as control.

2.2.2. Droplet tension measurement

The O/W interfacial properties were measured by a Tracker automatic droplet tensiometer equipped with an oscillating drop accessory (Teclis Scientific, Civrieux d'Azergue, France) at room temperature. Before measurement, the syringe and cuvette were carefully cleaned to avoid the presence of surface-active agents by rinsing it several times with deionized water. The surface tension of the last wash water was in the range of 69 and 72 mN/m, determined by a pendant droplet tensiometer, demonstrating the used syringe cleaning. The droplet profile was recorded every 0.02 s by a connected digital camera. The values of interfacial tension were calculated by the Laplace equation (Castellani et al., 2010). According to the density of the oily phase, the rising drop method were chosen. Three different oil compositions (MCT, TC/MCT, citral/MCT) were studied. An initial droplet with a volume of 10 μ L and a surface area of ~ 20 mm² was generated at the vertical needle, which was connected to an automatic syringe. The specific low absorbance glass cuvette (8 mL) was filled with the aqueous phase containing 0.01 wt% CAS. Interfacial tension was performed over a period of 10 800 s to monitor the protein adsorption kinetics. The oscillatory dilatational measurements (five cycles) were carried out at 10 % amplitude and at a frequency of 0.1 Hz, which was tested to be within the linear viscoelastic regime. Further dilatational analysis was carried out during the protein adsorption phase, every 100 s.

2.3. Binding properties

2.3.1. Sample preparation

The CAS stock solution (0.048 wt%, 20 μ mol/L) was prepared by dispersing CAS powder into 100 mL of pH 7.0 acetic acid-imidazole buffer solution (5 mM). The protein solution was stirred at room temperature until it was completely dissolved. Stock solutions (160 μ mol/L) of TC and citral were prepared by dissolving, respectively, 2 μ L and 2.8 μ L, into 100 mL of 10 % ethanol pH 7.0 buffer. Stirring was continued until all of aldehydes were dissolved. Samples for ultraviolet fluorescence quenching test were prepared by mixing required volume of the stock solution of CAS (20 μ mol/L), aldehydes, and pH 7.0 buffer to a final volume of 4 mL. Therefore, samples for fluorescence experiments had a fixed concentration of CAS (10 μ mol/L) and various concentrations of TC or citral (0, 5, 10, 20, 30, 40, 50, 60, and 80 μ mol/L). Meanwhile, the highest resulting concentration of ethanol in each sample was 5 wt%. Preliminary results showed that ethanol at this concentration does not affect the fluorescence intensity of the protein.

2.3.2. Ultraviolet (UV) spectroscopy

To study the interactions between each aldehyde and CAS, changes in absorption of CAS in the absence and the presence of various concentrations of each aldehyde was determined by an UV spectrophotometer (Jenway 3705, Villepinte, France) at room temperature and at a wavelength range of 230–350 nm. Before each measurement, quartz cuvettes (1 cm path length) were filled with the different samples and kept in the dark for 30 min. Sample blank was buffer alone and pure TC and citral (40 μ mol/L in buffer) were used as controls.

2.3.3. Intrinsic fluorescence

Intrinsic fluorescence intensity of CAS was carried out in the absence and in the presence of various concentrations of TC or citral at room temperature by a multimode microplate reader equipped with a temperature-controlled 96-wells microplate (Thermo Scientific™ Varioskan). The excitation wavelength was set at 280 nm and the emission spectrum was recorded in the wavelength range of 298–550 nm with an excitation and emission slit width of 5 nm. Different samples were placed in the wells in the order of increasing the concentration of aldehydes molar ratio range from 0 to 80 $\mu\text{mol/L}$. The measurements were performed at 25, 30, 35, and 40 °C, separately. Before each measurement, the mixtures of CAS and aldehydes were incubated at room temperature in the dark for 30 min. The fluorescence intensity of acetate-imidazole buffer was used as sample blank and pure TC and citral (40 $\mu\text{mol/L}$ in buffer) were used as controls.

2.4. Statistical analysis

All measurements were performed at least in triplicate. The results were then reported as averages and standard deviations of these measurements. Statistical analysis was performed by one-way ANOVA using SPSS software (IBM, version 19.0, USA).

3. Results and discussion

3.1. Impact of aldehydes on the interfacial behavior of CAS

The drop tensiometer has been used for the characterization of biopolymer interfaces since it can provide dynamic information at the O/W interface. During the formation of O/W interfacial membranes, hydrophobic groups of CAS molecules will gradually adsorb to the surface of the oil droplets and, after subsequent rearrangements, form an interfacial layer. Fig. 1A showed the plot of interfacial tension as a function of time ($t < 10\,800$ s) during protein adsorption at the surface of oily droplets with different compositions. In all three cases, the values of interfacial tension decreased with time, at least during the initial adsorption period, which is related to different stages of protein adsorption (from protein diffusion to protein penetration, unfolding, and rearrangement) (Felix et al., 2017). Pure MCT shows that the equilibrium interfacial tension was relatively high (about 13.56 mN/m), and when mixed with 5 wt% TC or citral, the equilibrium interfacial tension was significantly reduced to 9.12 and 11.27 mN/m, respectively. A similar result was observed for cinnamaldehyde and whey protein (Felix et al., 2019). One possible explanation is that these two aldehydes are able to interact with proteins, leading to additional rearrangements

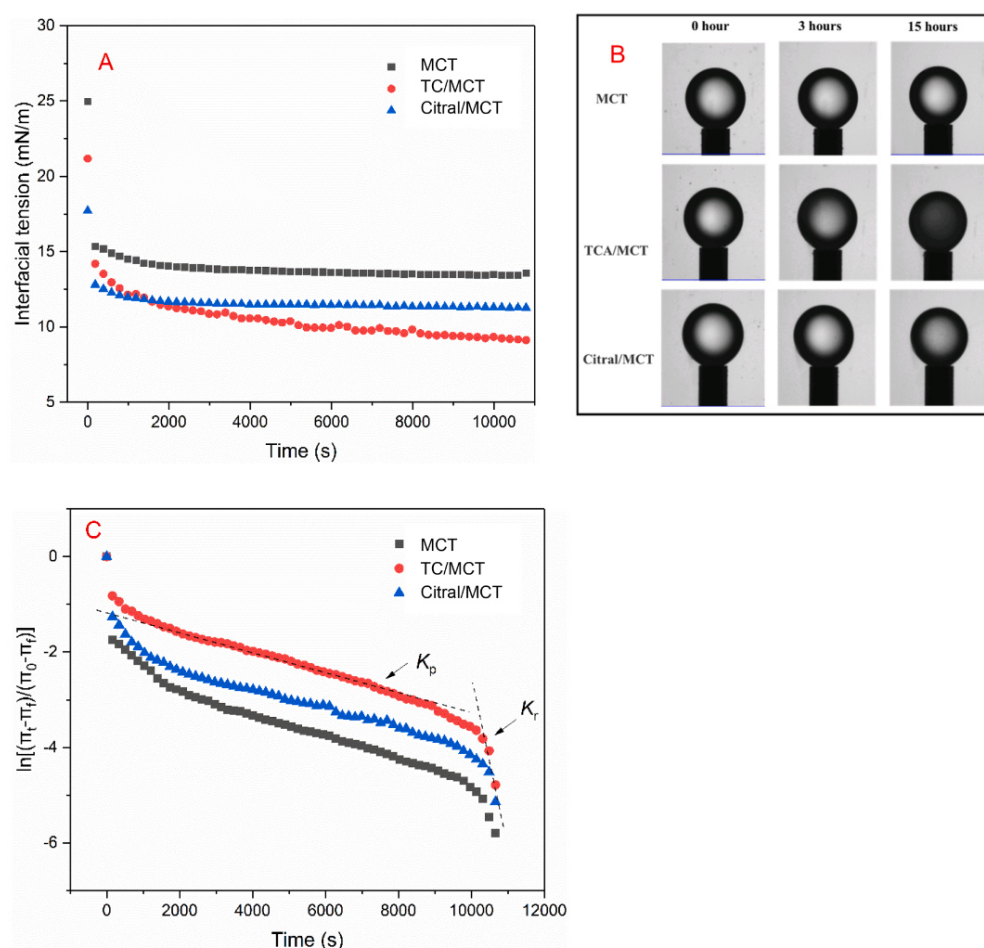


Fig. 1. (A) Interfacial tension over protein adsorption at O/W interface with or without TC or citral for 0.01% CAS solution at pH 7; (B) Visual images of oil droplets during measurement at different times and (C) The profile of the molecular penetration and configurational rearrangement steps over protein adsorption at the O/W interface with and without TC or citral for 0.01% CAS solution. K_p and K_r represents the first-order rate constants of penetration and rearrangement, respectively;

of CAS in the O/W interfaces, thereby resulting in a more densely packed structure, with lower interfacial tension (Dickinson, 1999). Interestingly, the image of oil droplets during measurement was recorded after 0, 3 and 15 h as shown in Fig. 1B. After 3 or 15 h of protein adsorption, the pictures of oil droplet containing TC were more turbid than the others. This phenomenon can further support the hypothesis according to which TC may have chemically reacted with the adsorbed CAS due to the presence of an aldehyde group in TC molecules, thereby changing the structure and adsorbed CAS.

The change in interfacial tension with absorption time can be fitted by the equation of Ward and Tordai (equation (1)) (Ward & Tordai, 1946):

$$\pi = 2C_0K_B T \left(\frac{Dt}{3.14} \right)^{1/2} \quad (1)$$

where C_0 is the concentration of continuous phase, K_B is the Boltzmann constant, T is the absolute temperature, D is the diffusion coefficient and t is the adsorption time. The initial process of adsorption was assumed to be mainly controlled by the protein diffusion (Graham & Phillips, 1979). The plot of interfacial tension as a function of $t^{1/2}$ was linear, and the diffusion rate (K_{diff}) can be calculated by the slope of this plot as shown in Table 1. The K_{diff} values for these three samples were in the range of 0.081 to 0.122 mN/m/s^{1/2}, which were similar to the result obtained for soy protein/whey protein isolate complexes (0.070 to 0.111 mN/m/s^{1/2} at pH range of 6 to 8) (Zhang et al., 2021, Zhang et al., 2021) and soy protein isolate/soy hull polysaccharides complexes (0.059 to 0.108 mN/m/s^{1/2}) (Wang et al., 2020) at the oil-water interface, but much lower than the results of ovalbumin/carboxymethylcellulose complexes (0.279 to 0.285 mN/m/s^{1/2}) (Xiong et al., 2018). This may be due to differences in the type and concentration of emulsifiers. Generally, high concentrations of protein emulsifiers result in high K_{diff} value. In the current study, the highest K_{diff} rate was observed in the case of TC/MCT oily phase, while there no obvious difference observed in the other two oily phases at the same CAS solution. These results suggested that for CAS stabilized interfaces, introducing citral into the oily phase has only a marginal effect on the protein diffusion. In addition, a small amount of TC into the oily phase can significantly improve the dispersibility and diffusion properties of CAS at the O/W interfaces. Several studies have indicated that TC have the ability to interact with proteins, resulting in the formation of larger protein species and additional rearrangements in the O/W interface (Chen et al., 2017, 2018). After the initial diffusion stage, the adsorption kinetics become visibly slow which could be caused by the energy barrier during adsorption and rearrangement (Graham & Phillips, 1979). Moreover, the rate of penetration and rearrangement of adsorbed proteins at O/W interfaces can be analyzed by the following first-order equation (Perez et al., 2009):

$$\ln \left[\frac{\pi_i - \pi_f}{\pi_0 - \pi_f} \right] = -K_i t \quad (2)$$

where π_0 , π_f and π_i are the interfacial tension at the initial, final, and at any time, respectively, t is the adsorption time, and K_i is the first-order rate constant. Fig. 1C displayed a typical fitting curve of $\ln[(\pi_f - \pi_i)/(\pi_f - \pi_0)]$ as a function of time. All of these curves include two linear regions that represent, respectively, the first-order rate constant of penetration (K_p) and the molecular reorganization (K_r) one at the O/W interface. As shown in Table 1, the relative highest K_p value was found in the pure MCT and TC/MCT oily phases, which suggested that TC only have the ability to promote the adsorption rate at the initial steps of protein absorption. Similar K_p values (Table 1) were found in pure MCT and TC/MCT oily phases, which indicates that TC does not have the ability to promote protein adsorption during the protein penetration process at the O/W interface. This could be probably attributed to the fact that TC is able to interact with adsorbed CAS molecular entanglement by forming a network structure, and then hindered the protein penetration at the interfacial layer. However, a relatively low K_p value was found in citral/MCT oil and the lower R-value was obtained by a linear fit. This result may be due to the low density of citral (0.888 g/L). The low density of the mixed oily phase gradually changed the shape of droplets during the protein adsorption. On the other hand, the highest K_r value was found in the pure MCT oily phase. A possible interpretation would be that as TC and citral were introduced into the oily phase, then the polarity of the oily phase increased (Liao et al., 2021). This decrease of the hydrophobicity of the oil phases would somehow reduce the ability to "attract" emulsifiers.

3.2. Dilatational viscoelastic properties

Measuring the viscoelastic properties of the layers adsorbed at the O/W interfaces is an effective way to evaluate the performance of emulsion systems (Chen et al., 2019). The dilatational modulus were calculated by the first harmonic of the Fourier transform of the oscillating interfacial tension signal (Bagley & Torvik, 1983). The dilatational elastic modulus (E'), dilatational viscosity modulus (E''), and loss angle tangent ($\tan\theta = E''/E'$) of three different oily phases are shown in Fig. 2. For all these samples, the dilatational elastic modulus of samples was significantly higher than the viscosity modulus, indicating that the O/W interfacial layer formed by CAS mainly exhibited an elastic behavior. After 3 h absorption, the highest E' (16.21 mN/m) was observed for the oily phase containing TC and the lowest E' (7.79 mN/m) was obtained for pure MCT as oily phase. In all cases, the value of elastic modulus gradually increased as a function of time due to the protein adsorption and the interactions between protein molecules, while the viscous modulus was almost constant. At the initial process of protein adsorption, the growth of elastic modulus was obvious and rapid and then it became gradually flattened. This tendency has been previously reported for other proteins, such as soy protein (Wang et al., 2020), bovine serum albumin (Tang & Shen, 2015), and pea protein (Sha et al., 2021). The effect of protein adsorption film on relative viscoelasticity can be well reflected by the change of $\tan \delta$ with time (Fig. 2B). For example, if the film is purely elastic, the $\tan \delta$ is zero. The presence of TC resulted in a shift of the $\tan \delta$ profiles towards a lower value, indicating the improvement of the relative viscoelasticity of the adsorbed films. In short, the results confirmed that the addition of both aldehydes, especially TC, can increase the elastic modulus which resulted in a stronger protein network. These findings suggested that the interactions between proteins and aldehydes had an important effect on the protein adsorption at the O/W interface.

3.3. Ultraviolet spectroscopy

UV spectroscopy is one of the generally used techniques for the highlighting of the binding mode of small molecules to proteins, by measuring the changes in absorption and shift in the wavelength (Sudha et al., 2016). The effect of various TC and citral concentrations (0–80 $\mu\text{mol/L}$) on the CAS solution (10 $\mu\text{mol/L}$) was shown in Fig. 3. Pure TC and citral (40 $\mu\text{mol/L}$ in buffer) were used as controls. Fig. 3A showed that the mixture of CAS and TC exhibited a maximum absorbance in the range of 280–290 nm and a distinct red shift was observed. Meanwhile,

Table 1

Apparent diffusion rate (K_{diff}), constants of penetration and structural rearrangement at the interface (K_p and K_r), and interfacial pressure at the end of adsorption (π_{10800}) for different oily phases in 0.01% CAS solution.

Samples	K_{diff} (mN/m/s ^{1/2})	$K_p \times 10^4$	$K_r \times 10^4$	π_{10800} (mN/m)
MCT	-0.090 ± 0.016	-2.151 ± 0.005	-8.543 ± 0.005	13.56 ± 0.18
TC/MCT	-0.122 ± 0.006	-2.178 ± 0.001	-7.046 ± 0.009	9.12 ± 0.04
Citral/MCT	-0.081 ± 0.010	-1.820 ± 0.002	-5.626 ± 0.002	11.27 ± 0.13

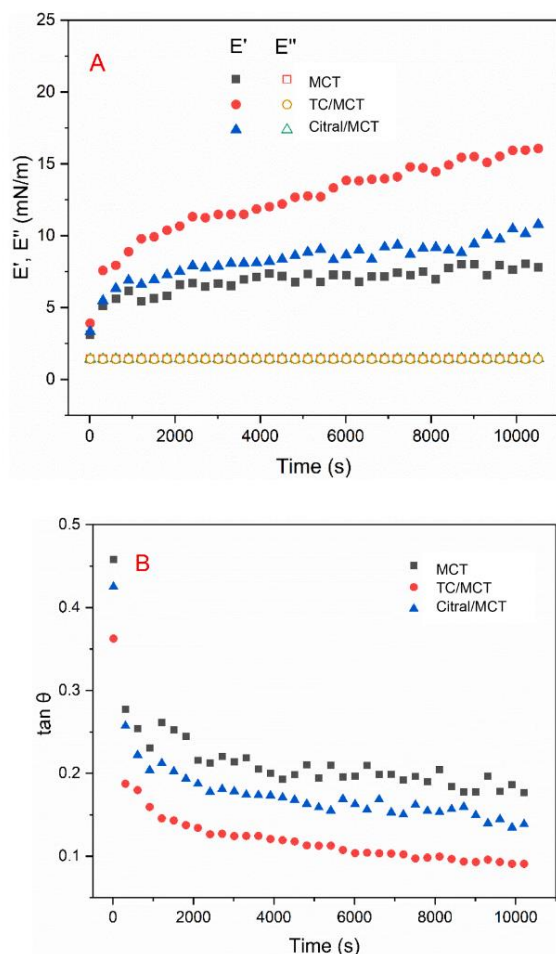


Fig. 2. Interfacial elastic and viscous moduli (E' and E''), respectively over protein adsorption at O/W interface with and without TC or citral for 0.01% CAS solution and (B) Time evolution of tangent of phase angle over protein adsorption at O/W interface with and without TC or citral for 0.01% CAS solution.

the intensity of the maximum absorbance was significantly improved with increasing TC concentration, indicating that there were interactions between TC and CAS. Moreover, the adsorption peak at 280 nm of the mixture suggested that high concentrated TC may cause the tryptophan, tyrosine and phenylalanine residues become more accessible and therefore causes conformational changes in the protein (Sudha et al., 2016). As shown in Fig. 3B, pure citral exhibited a maximum absorbance around 245 nm and the mixture of CAS and TC exhibited a similar maximum intensity around 280 nm, which suggesting there is no obvious interaction between CAS and citral.

3.4. Fluorescence spectra

The fluorescence spectra of CAS with the various concentrations of TC and citral at 25 °C are shown in Fig. 4. The CAS solution in the presence and in the absence of aldehydes possessed different fluorescence intensities which indicated the changes of environmental conditions. As reported by another study (Acharya et al., 2013), pure CAS solution exhibited an obvious emission band around 350 nm when the excitation band was 280 nm, since the intrinsic fluorescence of CAS is

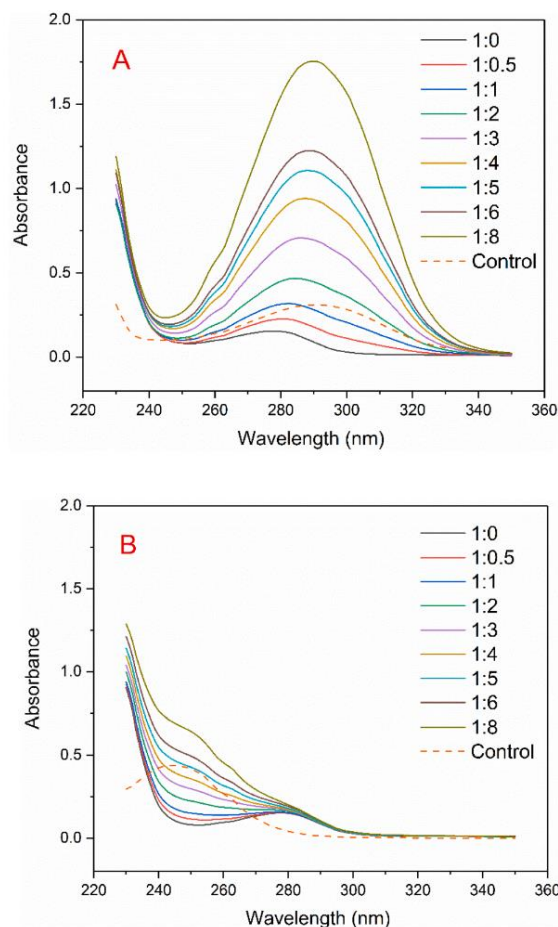


Fig. 3. Absorption spectra of 10 $\mu\text{mol/L}$ CAS solution in the presence of increasing TC (A) or citral (B) concentrations (0–80 $\mu\text{mol/L}$, legend: CAS/TC or CAS/Citral = 1:0 to 1:8) at 25 °C.

almost only due to tryptophan (Acharya et al., 2013). Therefore, the change of the intrinsic fluorescence intensity of CAS is mainly due to the change in the environment of tryptophan residues when small molecules such as aldehydes are added to the CAS solution. After mixing with TC (Fig. 4A), the fluorescence intensity of the maximum emission band decreased, which further indicated the occurrence of fluorescence quenching and the formation of complexes by TC binding to aromatic residues of CAS. This fluorescence quenching has been supported by many previous studies (Rabbani et al., 2018; Soltanabadi et al., 2018; H. Wang et al., 2022). With the subsequent increase in TC concentration, the maximum intensity further decreases with a gradual red shift, which may be caused by the presence of binding sites near the fluorophores in the protein (Soltanabadi et al., 2018). However, as shown in Fig. 4B, the fluorescence intensity of CAS and citral only shows a very weak quenching phenomenon, which suggested that CAS molecules could not provide a suitable environmental structure to bind citral molecules.

Fluorescence quenching of a fluorophore is caused by multiple molecular interactions, including the collisions between a fluorophore and a quencher (dynamic quenching) and the formation of non-fluorescent ground-state complexes. Both dynamic and static quenching can be analyzed by the Stern–Volmer equation (Lakowicz, 2013). The quenching of CAS induced by TC can be dynamic, due to a collision between the fluorophore (CAS) and quencher (TC), or static, due to the

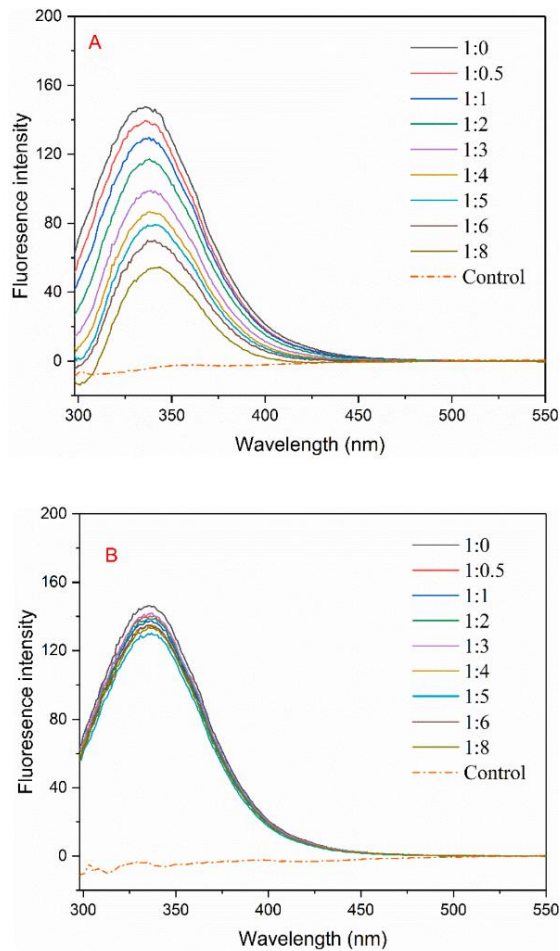


Fig. 4. Fluorescence spectra of 10 $\mu\text{mol/L}$ CAS solution at an excitation wavelength of 280 nm in the presence of increasing TC (A) or citral (B) concentrations (0–80 $\mu\text{mol/L}$. legend: CAS/TC or CAS/Citral = 1:0 to 1:8) at 25 $^{\circ}\text{C}$.

formation of a ground-state complex between the fluorophore and the quencher and can be further analyzed by the Stern-Volmer equation (3).

$$\frac{F_0}{F} = 1 + k_q \tau_0 [Q] = 1 + K_{SV} \quad (3)$$

where F_0 and F are respectively the fluorescence intensities at 280 nm excitation wavelength before and after mixing with the quencher; k_q is the bimolecular quenching constant, τ_0 is the average lifetime of the fluorophore in the absence of quencher; $[Q]$ is the concentration of the quencher (10^{-5} mol/L), and K_{SV} is the Stern-Volmer quenching constant which can be calculated by linear regression of a plot of F_0/F against $[Q]$.

The curve of F_0/F as a function of quencher concentration $[Q]$ at different temperatures was shown as Fig. 5A. It is worth to note that, at high TC concentrations, an upward deviation from linearity can be observed for different temperature measurements, which could suggest that both dynamic and static quenching may occur in the fluorescence quenching mechanism. However, this equation is still not enough to distinguish the dynamic quenching from static one (Acharya et al., 2013). An effective way to distinguish between dynamic quenching and static quenching can be to observe their bonding performance at different temperatures (Afrin et al., 2014). The temperature can increase the quencher diffusion constant, which is usually accompanied by an

increase in collisional quenching (Rabbani et al., 2018). For static quenching, the temperature has different effects (Acharya et al., 2013). Typically, this process will result in a decrease in the binding constant of the fluorophore quencher, and if the complexation reaction is exothermic, it will result in a decrease in the quenching of the static quencher (Rabbani et al., 2017). The modified Stern-Volmer equation (4) (Lakowicz, 2013) can be used when both static and dynamic quenching occur.

$$\frac{F_0}{F_0 - F} = \frac{1}{f} + \frac{1}{f} \frac{1}{K_{SV} [Q]} \quad (4)$$

where f is the available binding sites. When f is 1, the equation become the simple quenching process (equation (3)). The curve of $F_0/(F_0 - F)$ as a function of quencher concentration $[Q]^{-1}$ at different temperatures was shown as Fig. 5B. At 25 $^{\circ}\text{C}$, the quenching of CAS by TC, K_{SV} is $2.25 \times 10^{-4} \text{ M}^{-1}$. The fraction of the binding sites available for complexation was 1.63 higher than 1.0, which was probably attributed the occurrence of both dynamic and static quenching simultaneously. In addition, more binding sites could also be related to CAS which is a mixture of different casein proteins, such as α_{s1} , α_{s2} , β and κ -casein and there caseins differ in the number of tryptophan residues and their location in the hydrophobic regions (Yazdi & Corredig, 2012).

The fluorescence lifetime of tryptophan has been reported around 3 ns (Lakowicz, 2013). The K_q , calculated by the equation (3), is $7.5 \times 10^{12} \text{ M}^{-1} \text{ s}^{-1}$ per second at 25 $^{\circ}\text{C}$, which is highly greater than the maximum dynamic quenching constant ($\sim 10 \times 10^{10} \text{ M}^{-1} \text{ s}^{-1}$). This indicates that there was a specific complex formation between CAS and TC. It is worth noting that this quenching constant may be underestimated because in Stern-Volmer model, the total quencher concentration is used instead of the free quencher concentration, as critically discussed by van de Weert (2010). For further analysis of static quenching interactions, the binding constant and binding sites can be calculated by the following modified Stern-Volmer equation (5).

$$\log \left[\frac{F_0 - F}{F} \right] = \log K + n \log [Q] \quad (5)$$

where K is the binding constant and n the binding sites. Fig. 5C exhibited the curves of $\log [(F_0 - F)/F]$ against $\log [TC]$ for the quenching of CAS intrinsic fluorescence by TC. Table 2 displayed the quenching parameter K (binding constant) and n (binding sites) at different temperatures. The linear correlation coefficients obtained by fitting at different temperatures are all higher than 0.99 (Table 2), indicating that the Stern-Volmer equation is suitable for analyzing the interactions between CAS and TC. The large values of K were obtained at 25 and 30 $^{\circ}\text{C}$ which could indicate that the binding of TC to CAS is highly favorable. As increasing the temperature, the binding constants gradually decreased which suggested that the complexation becomes weak at high temperatures (Khatun & Rabbani, 2019). Similar results were also found in the study of resveratrol and whey proteins by fluorescence spectroscopy (Hemar et al., 2011). Meanwhile, plots were linear by modified Stern-Volmer equation, and the obtained slopes yielded binding stoichiometries (n) suggesting that CAS interacted with TC at a molar ratio of one-to-one at all temperatures in this study (Rabbani et al., 2018).

To a better understanding of the thermodynamic of the interactions between CAS and TC, Van't Hoff equation (6) was followed to calculate the change of enthalpy ΔH and entropy ΔS .

$$\ln K = -\frac{\Delta H}{RT} + \frac{\Delta S}{R} \quad (6)$$

where K is binding constant, R is the gas constant ($8.314 \text{ Jmol}^{-1} \text{ K}^{-1}$) and T is the absolute temperature (K). Thereby, thermodynamic parameters ΔH and ΔS can be calculated by the slope and intercept of the curve of $\ln K$ as a function of $1/T$. Fig. 5D showed the current Vant's Hoff fitting curve (correlation coefficient = 0.975) and it gives $\Delta H = -55.76 \text{ kJmol}^{-1}$, $\Delta S = -86.05 \text{ Jmol}^{-1}$. The free energy change (ΔG) can be then

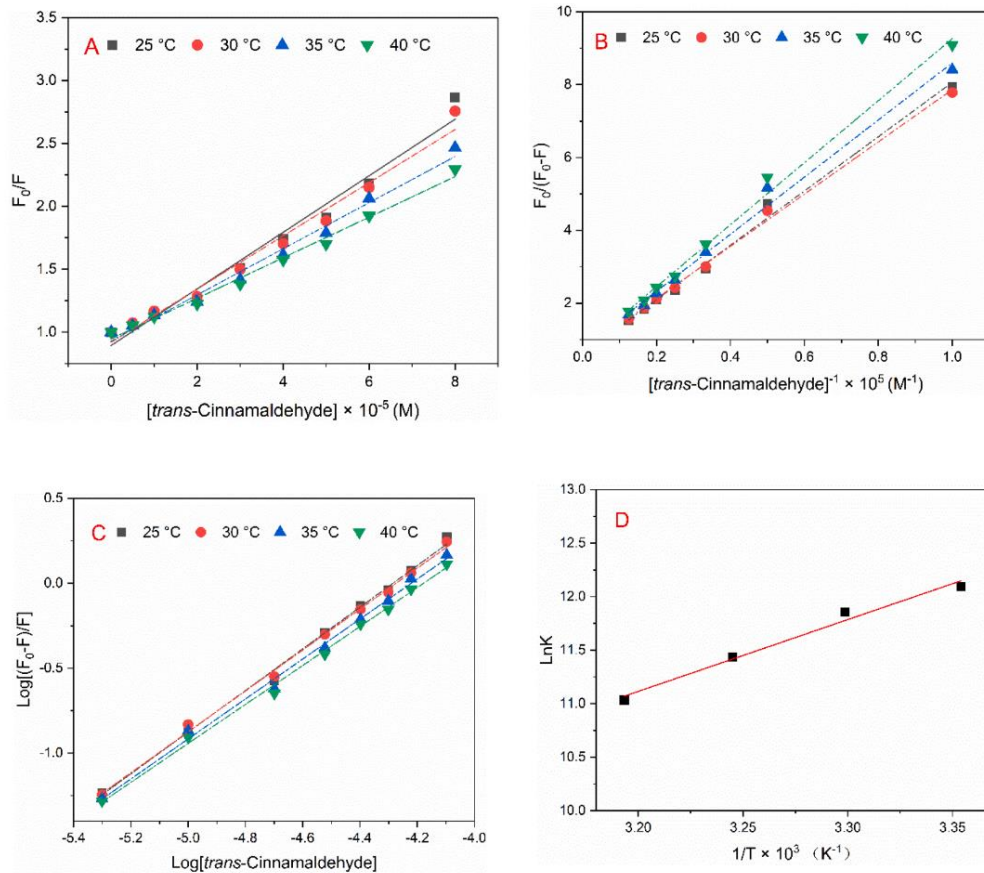


Fig. 5. (A) Stern–Volmer plot of F_0/F as a function of the concentration of TC at different temperatures; (B) Plot of $(F_0/(F_0-F))$ as a function of the reciprocal of TC concentration at different temperatures; (C) Plot of $\text{Log}[(F_0 - F)/F]$ as a function of log of the concentration of TC at different temperatures. F_0 and F represent the fluorescence intensity in the absence and the presence of TC, respectively; (D) The Van't Hoff plot of $\ln K$ as a function of $1/T$ (K) for the binding of TC to CAS molecules.

Table 2

Variation of binding constant K and the number of binding sites n as a function of temperature and thermodynamic parameters of binding calculated using Van't Hoff equation.

T (°C)	K	n	r^2	ΔH (kJ mol ⁻¹)	ΔS (J mol ⁻¹ K ⁻¹)	ΔG (kJ mol ⁻¹)
25	1.782×10^5	1.225	0.996	-55.76	-86.05	-30.11
30	1.406×10^5	1.204	0.997			-29.68
35	0.925×10^5	1.177	0.996			-29.25
40	0.618×10^5	1.147	0.997			-28.81

calculated from the equation (7) as follow:

$$\Delta G = \Delta H - T\Delta S \quad (7)$$

Table 2 summarizes the thermodynamic parameters of binding between CAS and TC. ΔG values at different temperatures are all negative, indicating that the binding process of TC and CAS is spontaneous and exothermic. The negative ΔH and ΔS values suggested that binding would be mainly driven by hydrogen bonds, which would promote a more ordered configuration of the solvent molecules around the

complexes (Aghili et al., 2016). This similar interaction was also found for other protein-small molecules combinations, such as zein proteins-resveratrol (Joye et al., 2015), crosslinked caseinate-quercetin, caseinate-kaempferol (Zhang et al., 2021, Zhang et al., 2021) and bovine serum albumin-theaflavin-3,3'-digallate (Yu et al., 2022). Moreover, the high absolute value of ΔH could indicate that a covalent bond may be formed between CAS and TC. Other complementary technologies are needed in the future to fully explore the exact type and strength of interactions between CAS and TC. Nevertheless, the present work showed that TC, a common flavoring in food, may be used as an interesting ingredient to improve the surface rheological properties of protein-based interfaces.

4. Conclusion

The interactions between two selected aldehydes and CAS were investigated in the current study. Both aldehydes, especially TC, have pronounced abilities to decrease the interfacial tension to 9.12 mN/m at O/W interface after 3 h adsorption. A small amount of TC introduced into the oily phase was shown to significantly improve the diffusion properties of CAS at the O/W interfaces. Compare with pure MCT (7.79 mN/m), dilatational measurements indicated that the use of TC into the oily phase resulted in the development of stronger and more elastic interfaces (16.21 mN/m). Furthermore, the fluorescence quenching test

proved that TC has a more obvious quenching effect on CAS than citral. The large binding constants ($1.78 \times 10^5 \text{ M}^{-1}$) was calculated by Stern-Volmer equation which suggest that TC has a strong affinity to CAS. The negative free energy change for the binding between TC and CAS indicated that complexation process is spontaneous. The negative enthalpy and negative entropy changes suggested that the binding is mainly driven by formation of hydrogen bonds. Entropy is unfavorable suggesting that there is a loss of conformational freedom associated with binding. In summary, the two studied natural aldehydes could be useful ingredients to enhance the interfacial properties of food protein-based products.

Declaration of Competing Interest

The authors declare that they have no known competing financial interests or personal relationships that could have appeared to influence the work reported in this paper.

Data availability

Data will be made available on request.

Acknowledgement

Wei Liao greatly thanks Chinese Scholarship Council for support.

References

- Acharya, D. P., Sanguansri, L., & Augustin, M. A. (2013). Binding of resveratrol with sodium caseinate in aqueous solutions. *Food Chemistry*, *141*(2), 1050–1054.
- Afrin, S., Rabbani, G., & Khan, R. H. (2014). Spectroscopic and calorimetric studies of interaction of methimazole with human serum albumin. *Journal of Luminescence*, *151*, 219–223.
- Aghili, Z., Taheri, S., Zeinabad, H. A., Pishkar, L., Saboury, A. A., Rahimi, A., & Falahati, M. (2016). Investigating the interaction of Fe nanoparticles with lysozyme by biophysical and molecular docking studies. *PLoS One*, *11*(10), e0164878.
- Asghari, G., Atri, M. S., Saboury, A. A., & Mohadjerani, M. (2017). Study of the interaction of cinnamaldehyde with alpha-lactalbumin: spectroscopic and molecular docking investigation. *Biomacromolecular Journal*, *3*(2), 123–132.
- Bagley, R. L., & Torvik, P. J. (1983). A theoretical basis for the application of fractional calculus to viscoelasticity. *Journal of Rheology*, *27*(3), 201–210.
- Banerjee, G., & Chattopadhyay, P. (2019). Vanillin biotechnology: The perspectives and future. *Journal of the Science of Food and Agriculture*, *99*(2), 499–506.
- Boeve, J., & Joye, I. J. (2020). Food grade strategies to increase stability of whey protein particles: Particle hardening through aldehyde treatment. *Food Hydrocolloids*, *100*, Article 105353. <https://doi.org/10.1016/j.foodhyd.2019.105353>
- Castellani, O., Al-Assaf, S., Axelos, M., Phillips, G. O., & Anton, M. (2010). Hydrocolloids with emulsifying capacity. Part 2-Adsorption properties at the n-hexadecane-Water interface. *Food Hydrocolloids*, *24*(2–3), 121–130.
- Chen, C., Shi, K., Qin, X., Zhang, H., Chen, H., Hayes, D. G., ... Liu, G. (2021). Effect of interactions between glycosylated protein and tannic acid on the physicochemical stability of Pickering emulsions. *LWT*, *152*, Article 112383.
- Chen, E., Gao, L., McClements, D. J., Liu, S., Li, B., & Li, Y. (2018). Enhancement of physicochemical properties of whey protein stabilized nanoemulsions by interfacial cross-linking using cinnamaldehyde. *Food Hydrocolloids*, *77*, 976–985.
- Chen, E., Wu, S., McClements, D. J., Li, B., & Li, Y. (2017). Influence of pH and cinnamaldehyde on the physical stability and lipolysis of whey protein isolate-stabilized emulsions. *Food Hydrocolloids*, *69*, 103–110.
- Chen, W., Liang, G., Li, X., He, Z., Zeng, M., Gao, D., ... Chen, J. (2019). Impact of soy proteins, hydrolysates and monoglycerides at the oil/water interface in emulsions on interfacial properties and emulsion stability. *Colloids and Surfaces B: Biointerfaces*, *177*, 550–558.
- Dickinson, E. (1999). Adsorbed protein layers at fluid interfaces: Interactions, structure and surface rheology. *Colloids and Surfaces B: Biointerfaces*, *15*(2), 161–176.
- Felix, M., Romero, A., & Guerrero, A. (2017). Viscoelastic properties, microstructure and stability of high-oleic O/W emulsions stabilised by crayfish protein concentrate and xanthan gum. *Food Hydrocolloids*, *64*, 9–17.
- Felix, M., Yang, J., Guerrero, A., & Sagis, L. M. C. (2019). Effect of cinnamaldehyde on interfacial rheological properties of proteins adsorbed at O/W interfaces. *Food Hydrocolloids*, *97*, Article 105235.
- Gerrard, J. A., Brown, P. K., & Fayle, S. E. (2003). Maillard crosslinking of food proteins III: The effects of glutaraldehyde, formaldehyde and glycerinaldehyde upon bread and croissants. *Food Chemistry*, *80*(1), 45–50. [https://doi.org/10.1016/S0308-8146\(02\)00233-9](https://doi.org/10.1016/S0308-8146(02)00233-9)
- Graham, D. E., & Phillips, M. C. (1979). Proteins at liquid interfaces: III. Molecular structures of adsorbed films. *Journal of Colloid and Interface Science*, *70*(3), 427–439.
- Habeeb, A., & Hiramoto, R. (1968). Reaction of proteins with glutaraldehyde. *Archives of Biochemistry and Biophysics*, *126*(1), 16–26.
- Hemar, Y., Gerbeaud, M., Oliver, C. M., & Augustin, M. A. (2011). Investigation into the interaction between resveratrol and whey proteins using fluorescence spectroscopy. *International Journal of Food Science & Technology*, *46*(10), 2137–2144.
- Jia, X., Zhao, M., Xia, N., Teng, J., Jia, C., Wei, B., ... Chen, D. (2019). Interaction between plant phenolics and rice protein improved oxidative stabilities of emulsion. *Journal of Cereal Science*, *89*, Article 102818.
- Joye, I. J., Davidov-Pardo, G., Ludescher, R. D., & McClements, D. J. (2015). Fluorescence quenching study of resveratrol binding to zein and gliadin: Towards a more rational approach to resveratrol encapsulation using water-insoluble proteins. *Food Chemistry*, *185*.
- Khatun, S., & Rabbani, G. (2019). A comparative biophysical and in-silico studies on the interactions of ticlopidine hydrochloride with two serum albumins. *The Journal of Chemical Thermodynamics*, *131*, 9–20.
- Lakowicz, J. R. (2013). *Principles of fluorescence spectroscopy*. Springer science & business media.
- Liao, W., Gharsallaoui, A., Dumas, E., Ghnimi, S., & Elaissari, A. (2021). Effect of carrier oil on the properties of sodium caseinate stabilized O/W nanoemulsions containing Trans-cinnamaldehyde. *LWT*, *146*, Article 111655.
- Perez, A. A., Carrara, C. R., Sánchez, C. C., Santiago, L. G., & Patino, J. M. R. (2009). Interfacial dynamic properties of whey protein concentrate/polysaccharide mixtures at neutral pH. *Food Hydrocolloids*, *23*(5), 1253–1262.
- Rabbani, G., Baig, M. H., Jan, A. T., Lee, E. J., Khan, M. V., Zaman, M., ... Choi, I. (2017). Binding of erucic acid with human serum albumin using a spectroscopic and molecular docking study. *International Journal of Biological Macromolecules*, *105*, 1572–1580.
- Rabbani, G., Lee, E. J., Ahmad, K., Baig, M. H., & Choi, I. (2018). Binding of tolperisone hydrochloride with human serum albumin: Effects on the conformation, thermodynamics, and activity of HSA. *Molecular Pharmaceutics*, *15*(4), 1445–1456.
- Sha, L., Koois, A. O., Wang, Q., True, A. D., & Xiong, Y. L. (2021). Interfacial dilatational and emulsifying properties of ultrasound-treated pea protein. *Food Chemistry*, *350*, Article 129271.
- Shen, S., Zhang, T., Yuan, Y., Lin, S., Xu, J., & Ye, H. (2015). Effects of cinnamaldehyde on Escherichia coli and Staphylococcus aureus membrane. *Food Control*, *47*, 196–202.
- Soltanabadi, O., Atri, M. S., & Bagheri, M. (2018). Spectroscopic analysis, docking and molecular dynamics simulation of the interaction of cinnamaldehyde with human serum albumin. *Journal of Inclusion Phenomena and Macroscopic Chemistry*, *91*(3), 189–197.
- Sudha, A., Srinivasan, P., Thamilarasan, V., & Sengottuvelan, N. (2016). Exploring the binding mechanism of 5-hydroxy-3', 4', 7-trimethoxyflavone with bovine serum albumin: Spectroscopic and computational approach. *Spectrochimica Acta Part A: Molecular and Biomolecular Spectroscopy*, *157*, 170–181.
- Tan, Y., & Siebert, K. J. (2008). Modeling bovine serum albumin binding of flavor compounds (alcohols, aldehydes, esters, and ketones) as a function of molecular properties. *Journal of Food Science*, *73*(1), S56–S63.
- Tang, C.-H., & Shen, L. (2015). Dynamic adsorption and dilatational properties of BSA at oil/water interface: Role of conformational flexibility. *Food Hydrocolloids*, *43*, 388–399.
- van de Weert, M. (2010). Fluorescence quenching to study protein-ligand binding: Common errors. *Journal of Fluorescence*, *20*(2), 625–629.
- Wang, H., Zhu, J., Zhang, H., Chen, Q., & Kong, B. (2022). Understanding interactions among aldehyde compounds and porcine myofibrillar proteins by spectroscopy and molecular dynamics simulations. *Journal of Molecular Liquids*, *349*, Article 118190. <https://doi.org/10.1016/j.molliq.2021.118190>
- Wang, K., & Arntfield, S. D. (2015). Binding of selected volatile flavour mixture to salt-extracted canola and pea proteins and effect of heat treatment on flavour binding. *Food Hydrocolloids*, *43*, 410–417.
- Wang, S., Yang, J., Shao, G., Qu, D., Zhao, H., Yang, L., ... Zhu, D. (2020). Soy protein isolated-soy hull polysaccharides stabilized O/W emulsion: Effect of polysaccharides concentration on the storage stability and interfacial rheological properties. *Food Hydrocolloids*, *101*, Article 105490.
- Ward, A. F. H., & Tordai, L. (1946). Time-dependence of boundary tensions of solutions I. The role of diffusion in time-effects. *The Journal of Chemical Physics*, *14*(7), 453–461.
- Xiong, W., Ren, C., Li, J., & Li, B. (2018). Characterization and interfacial rheological properties of nanoparticles prepared by heat treatment of ovalbumin-carboxymethylcellulose complexes. *Food Hydrocolloids*, *82*, 355–362.
- Yazdi, S. R., & Corredig, M. (2012). Heating of milk alters the binding of curcumin to casein micelles: A fluorescence spectroscopy study. *Food Chemistry*, *132*(3), 1143–1149.
- Yu, X., Cai, X., Li, S., Luo, L., Wang, J., Wang, M., & Zeng, L. (2022). Studies on the interactions of theaflavin-3,3'-digallate with bovine serum albumin: Multi-spectroscopic analysis and molecular docking. *Food Chemistry*, *366*, Article 130422.
- Zhang, X., Qi, B., Xie, F., Hu, M., Sun, Y., Han, L., ... Li, Y. (2021). Emulsion stability and dilatational rheological properties of soy/whey protein isolate complexes at the oil-water interface: Influence of pH. *Food Hydrocolloids*, *113*, Article 106391. <https://doi.org/10.1016/j.foodhyd.2020.106391>
- Zhang, Y.-J., Zhang, N., & Zhao, X.-H. (2021). The non-covalent interaction between two polyphenols and caseinate as affected by two types of enzymatic protein crosslinking. *Food Chemistry*, *364*, Article 130375.

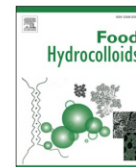
Chapter VII

The formation mechanism of multilayer emulsions studied by isothermal titration calorimetry and dynamic light scattering

Published in: Food Hydrocolloids

Summary of Chapter VII

Under certain conditions, emulsions containing oil droplets surrounded by multilayer interfaces are known to be resistant to environmental stresses than conventional oil-in-water emulsions. So far, few thermodynamic analyses have been performed on the preparation process of multi-layer emulsions. Thus, this study tries to demonstrate the basic mechanism for the preparation of multilayer emulsions by titrating primary emulsions into coating materials based on the results of isothermal titration calorimetry (ITC) and dynamic light scattering (DLS). In the first part, the thermodynamic parameters and surface charge obtained during the formation (titration and back-titration) of the multilayer emulsions were evaluated to understand the stabilization mechanism during the preparation process. Moreover, the multilayer emulsions prepared by titration and direct mixing methods were compared in terms of particle size distribution. Results indicated that stable multilayer emulsions could be formulated by titrating the primary emulsion into LMP instead of back-titrating. ITC titration confirmed that LMP does bind CAS-coated droplets through the electrostatic forces and it was a spontaneous exothermic process ($\Delta G < 0$, $\Delta H < 0$). DLS results indicated that slow titration can effectively avoid droplet aggregation. In conclusion, this study may help to obtain optimal coating conditions for the preparation of multilayer emulsions.



The formation mechanism of multilayer emulsions studied by isothermal titration calorimetry and dynamic light scattering

Wei Liao^a, Emilie Dumas^a, Abdelhamid Elaissari^b, Adem Gharsallaoui^{a,*}

^a Univ. Lyon, University Claude Bernard Lyon 1, CNRS, LAGEPP UMR 5007, 43 Bd 11 Novembre 1918, 69622, Villeurbanne, France

^b Univ Lyon, University Claude Bernard Lyon 1, CNRS, ISA-UMR 5280, 69622, Villeurbanne, France

ARTICLE INFO

Keywords:

Multilayer emulsions
Isothermal titration calorimetry
Dynamic light scattering
Electrostatic interactions
Bridging flocculation

ABSTRACT

The formation of multilayer interfaces in oil-in-water (O/W) systems has many advantages in delivering lipid-soluble active compounds. In this study, isothermal titration calorimetry (ITC) and dynamic light scattering (DLS) were used to investigate the formation mechanism of multilayer emulsions by mixing low methoxyl pectin (LMP) and sodium caseinate (CAS) stabilized O/W emulsion. Thermodynamic properties and ζ -potential curves were studied as a function of polymer ratio, suggesting that ITC could provide more accurate information about the polymer concentration effect. ITC titration confirmed that LMP binds CAS-coated droplets mainly through electrostatic forces, which was a spontaneous exothermic process ($\Delta G < 0$). Furthermore, stable multilayer emulsions were obtained by titrating CAS-stabilized droplets into LMP instead of back-titrating. Finally, the effects of mixing methods on the stability of multilayer emulsions were evaluated. The results suggest that titration rather than direct mixing can produce uniform and smaller-sized droplets and delay the onset of droplets aggregation.

1. Introduction

Oil in water (O/W) emulsion systems, produced by homogenizing oil and aqueous phases together in the presence of one or more emulsifiers, have been extensively applied in foods such as soft drinks, milk, mayonnaise, and vinaigrette, etc. (Guzey & McClements, 2006). Along with the food safety concerns, there is a growing interest trend in the food field to replace commercial synthetic emulsifiers with natural “label-friendly” ones. In this regard, several food protein-based emulsifiers, from different sources like milk, whey, eggs, legume, oilseed, and so on, have been extensively investigated as natural emulsifiers in recent years due to their amphiphilic character, polymeric structure, and electrical charge characteristics (Kim et al., 2020). Despite their favorable properties, protein-stabilized emulsions have been reported to be highly sensitive to environmental stresses such as pH, ionic strength, temperature, and oxygen (Bouyer et al., 2012). This instability of protein-based emulsions under these conditions will limit their further application in certain commercial products. In fact, the quality and stability of emulsions can be improved by combining protein emulsifiers with other natural polymers to form multilayered interfaces (Surh et al., 2006). For example, protein-coated droplets are either negatively or

positively charged when the pH is below or above their isoelectric point (pI) (Wang et al., 2019), and then they could attract the oppositely charged polysaccharides present in the continuous phase, thereby forming a thicker layer at O/W interface. Zhang et al. (2020) developed multilayer emulsions by addition of camellia saponin (CS) into almond protein isolate (API) based primary emulsions at pH 3. Compared to primary emulsions with single-layer interfaces, droplets with multi-layered interfaces show improved inhibit lipid and protein oxidation during storage. Emulsions with multilayered interfaces were also found to have better stability against environmental stresses, such as pH extremes, high ionic strengths, thermal processing, and freezing (Ogawa et al., 2003, 2004).

The basic method for the preparation of multilayer interfaces is to add oppositely charged polymers to a “primary” emulsion prepared by conventional homogenization techniques (Ogawa et al., 2003). As a result, a “secondary” emulsion with a two-layer interface could be formulated due to electrostatic attraction. This process can be repeated several times to produce three or more-layer emulsions with desired functional properties. Previous studies (Guzey & McClements, 2006; McClements, 2012) demonstrated that adsorption layers can be deposited around droplets in two different ways: a one-step or two-step mixing

* Corresponding author.

E-mail address: adem.gharsallaoui@univ-lyon1.fr (A. Gharsallaoui).

<https://doi.org/10.1016/j.foodhyd.2022.108275>

Received 29 August 2022; Received in revised form 14 October 2022; Accepted 26 October 2022

Available online 3 November 2022

0268-005X/© 2022 Elsevier Ltd. All rights reserved.

procedure, depending on the charge-pH properties of the used biopolymer. In the one-step mixing method, a solution containing oppositely charged biopolymers is directly mixed with a primary emulsion containing charged droplets. This approach tends to promote the tendency of droplets to flocculate or coalesce during the process, and the aggregation is generally irreversible (Guzey & McClements, 2006; Surh et al., 2006). In the two-step method, the solution containing the charged biopolymer is mixed with the primary emulsion at a pH where there is no strong electrostatic attraction between them. The pH of the mixture is then adjusted to a pH where the droplets and the unadsorbed polymer have opposite charges, so that the polymer can be adsorbed to the droplet surface. This method is usually preferred for the production of multilayered interfaces at laboratory scale, since the second layer of biopolymer is more uniformly distributed throughout the aqueous phase prior to adsorption (Liu et al., 2022; Mundo et al., 2021; Shi et al., 2021). Nonetheless, the two-step approach has several drawbacks: (i) Irreversible aggregation occurs when the pH is adjusted to pass the isoelectric point (pI) of protein emulsifiers; (ii) not suitable for the preparation of emulsions with more than two layers; (iii) relatively complex process is not suitable for industrial mass production. For this reason, the one-step approach was selected in our study and further optimized to avoid droplet aggregation for preparing stable multilayer emulsions.

To minimize droplet aggregation in the one step method, it is necessary to ensure that enough biopolymers for coatings is present in the system to surround the entire surface of the added oil droplets. Otherwise, bridging flocculation may occur, as one polyelectrolyte may adsorb to the surface of multiple droplets, causing them to link together (McClements, 2012). Even with sufficient free polyelectrolyte concentration in the aqueous phase, droplet aggregation cannot be completely avoided because particle-particle collisions are sometimes faster than the adsorption of biopolymers to the surface of the primary coating droplets. One strategy to avoid the droplet aggregation during the process of forming multilayer emulsions is to control the ratio of mixing by titrating primary emulsions into coating solutions (Zeeb et al., 2015). Therefore, the concentration and mixing methods of biopolymers must be carefully designed to avoid extensive droplet aggregation and massive free polyelectrolyte remaining in the aqueous phase after the coating step.

The saturation concentration for a multilayer system has been mostly characterized by dynamic light scattering (DLS), which provides the saturation condition by identifying the ζ -potential plateau (Okubo & Suda, 2003). Indeed, the saturation concentration is only the theoretical concentration for the preparation of multilayer emulsions. Even when the system reaches the ζ -potential plateau, it is impossible to speculate whether the multilayer system is stable, since extensive aggregation of droplets may occur. The ζ -potential can only represent the overall potential of the system. Therefore, other methods are needed to study the preparation mechanism of multilayer emulsions and understand the occurrence of droplet flocculation. In this study, we used isothermal titration calorimetry (ITC) and conventional DLS to investigate the interaction and thermodynamic characteristics between sodium caseinate (CAS) stabilized emulsion and low methoxyl pectin (LMP) during the preparation of multilayer emulsions. In the first part, the thermodynamic parameters and surface charge during the formation (titration and back-titration) of the multilayer emulsion were evaluated to understand the stabilization mechanism of the multilayer emulsion during the preparation. Meanwhile, the advantages of ITC and DLS in measuring the system are described and compared. In the second part, the multilayer emulsions prepared by titration and direct mixing methods were compared in terms of particle size distribution, zeta potential (ζ -potential), creaming behavior, microstructure, and fluorescence intensity. This research could provide more information for the rational design of multilayer emulsions.

2. Materials and methods

2.1. Materials

The powder of CAS with 93.20% protein content (determined by the Kjeldahl method, N = 6.38) was purchased from Fisher Scientific (UK). The powder of LMP (esterification degree from 22% to 28% and acetylation degree from 20% to 23%) with 81.21% carbohydrate content was obtained from Cargill (Baupte, France). A medium chain triacylglycerol oil (MCT) was purchased from Gattefossé (Saint-Priest, France). Imidazole, acetic acid, sodium azide, sodium hydroxide, and hydrochloric acid were purchased from Sigma-Aldrich Chimie (St Quentin Fallavier, France). The water used in all preparations was deionized water.

2.2. Sample preparation

Imidazole-acetate buffer solutions (5 mM) containing 0.04 wt% sodium azide (to avoid microbial growth (Chang, Gupta, et al., 2016)) was prepared by dispersing weighed amounts of imidazole and acetic acid into deionized water. Biopolymer stock solutions were prepared by slowly dispersing 0.53 wt% CAS and 0.50 wt% LMP separately into 5 mM imidazole-acetate buffer and stirring overnight to ensure complete hydration. The pH of both stock solutions was then adjusted to 3.0 by adding HCl (1 M) 24 h prior their use. Based on our previous study (Wang et al., 2019), CAS showed positive charge and LMP showed negative charge at pH 3.0. This pH environment could provide appropriate environment for forming multilayer interfaces by electrostatic interactions between them.

2.3. Preparation of primary emulsions and multilayer emulsions

Oil-in-water coarse emulsions were prepared by mixing 5.0 g MCT oil and 95 g emulsifier aqueous solution (0.53 wt% CAS stock solution at pH 3.0) by high-speed homogenization (IKA, Staufen, Germany) under 13,500 rpm for 5 min. The resultant pre-emulsions were then passed through a microfluidizer (Microfluidics LM20, Microfluidics Corp., Newton, MA, USA) 5 times at 5×10^7 Pa to obtain nanoemulsions (Liao et al., 2021). The obtained nanoemulsions (containing 0.5 wt% CAS) were then adjusted to pH 3.0 and considered as "primary emulsions".

Multilayer emulsions were prepared by titrating the primary emulsions into LMP stock solution (0.5 wt%) at a rate of 2.5 mL/min by using an automated procedure with the TitroLine 5000 (TitroLine 5000, Xylem Analytics GmbH, Weilheim in Oberbayern, Germany). During the titration, the samples were kept under agitation and different ratios of primary emulsion/LMP were collected for subsequent analysis. To investigate the effect of LMP on the formulation of multilayer emulsions when the coating material was insufficient, back-titration was also performed on the same ratio of CAS-based emulsion/LMP. Meanwhile, direct mixing was performed by slowly pouring different volumes of primary emulsions in same ratios (w/w) into the LMP stock solution under stirring to compare the effects of different mixing methods on the multilayer emulsions.

2.4. Isothermal titration calorimetry (ITC)

The energetics of the interactions between primary emulsions and LMP was measured using an isothermal titration calorimeter with a viewing and printing software (VP-ITC) (MicroCal, Malvern Instruments, Northampton, MA) in a reaction cell volume of 1.4214 mL. LMP and CAS-based emulsions were diluted to the desired concentration (0.05 or 0.50 wt%) with the same buffer (5 mM imidazole-acetate buffer, pH 3.0). All solutions were degassed under stirring for 5–10 min before being loaded. The pH of each solution was checked again before measuring to ensure the same values in the cell and in the syringe. The calorimetric cell was filled with LMP solution (0.5 wt%) and the

electric injector was filled with CAS-based emulsion (0.05 wt%), equilibrated at 25 °C. The titration was performed by adding an initial 2 μ L injection and 28 consecutive 10 μ L injections while continuously stirring the mixture at 307 rpm. Each injection lasted 20 s with a 200 s interval between consecutive injections. Back-titration was also performed by placing the CAS-based emulsion (0.5 wt%) into the cell and the LMP solution (0.05 wt%) into the syringe, separately. Controlled titrations were performed by injecting the primary emulsion or LMP solution into imidazole-acetate buffer to obtain the heat of dilution, so corrected data were obtained by subtracting the heat of dilution data from the raw data. Data analysis was carried out by Origin 7.0 software. The Gibbs free energy is calculated by the equation $\Delta G = \Delta H - T\Delta S$. Measurements were performed in triplicate and results are reported as mean and standard deviation.

2.5. Intrinsic fluorescence

Intrinsic fluorescence intensity of multilayer emulsions with different ratios of CAS-based emulsion/LMP was carried out at room temperature by a multimode microplate reader equipped with a temperature-controlled 96-wells microplate (Thermo Scientific™ Varioskan). The excitation wavelength was set at 280 nm and the emission spectrum was recorded in the wavelength range of 298–550 nm with an excitation and emission slit width of 5 nm. The multilayer emulsions formulated by titration in different ratios was diluted with 5 mM imidazole acetate buffer (pH 3.0) to a final concentration of 0.05 wt% CAS. The diluted samples were then evenly transferred to 96-well plates for analysis, with 6 measurements per sample. The fluorescence intensity of acetate-imidazole buffer and pure LMP solution were used as a blank and a control, separately.

2.6. Zeta potential (ζ potential)

The ζ potential was performed by electrophoretic mobility (Zetasizer Nano-ZS90, Malvern Instruments, Worcestershire, UK) under room temperature. To avoid multiple scattering effects, each sample was diluted to a concentration of around 0.05 wt% with the same buffer (5 mM imidazole-acetate buffer, pH 3) (Liao et al., 2022). Diluted samples were transferred to disposable cells for electrophoretic mobility measurement. All measurements were performed three times and the ζ -potential values were calculated by the software as the average of three individual measurements.

2.7. Mean particle size

Mean particle size (nm), polydispersity index (Pdl) and size distribution were determined by dynamic light scattering using a Zetasizer Nano-ZS90 (Malvern Instruments, Worcestershire, UK) under room temperature. To eliminate multiple scattering effects, each sample was diluted to a droplet concentration around 0.1 wt% with corresponding pH buffers (Liao et al., 2022). After 90 s of equilibrium, each sample was analyzed three times.

2.8. Microscopic observations

Before analysis, each sample was gently stirred in glass tubes to ensure they were homogeneous. A drop of the emulsion was placed on a microscope slide and covered with a coverslip. The microstructure of samples was then visualized at room temperature using an Evos bright-field microscope (EVOS M5000, Thermo-Invitrogen, USA).

2.9. Statistical analysis

All experiments were carried out at least three times with freshly prepared samples. Data are reported as means \pm standard deviations.

3. Results and discussions

3.1. Formation mechanism of multilayer emulsions

3.1.1. Zeta potential analysis

The appropriate concentration of the biopolymer coating around the primary emulsion droplets can usually be assessed by measuring the zeta potential (Okubo & Suda, 2003). It has been reported that the ζ -potential of colloidal systems varies with the continuous addition of adsorbable polymers, and the plateau of the ζ -potential as a function of ratio is related to the surface saturation of the polymer coating (Chang, Gupta, et al., 2016).

Fig. 1 showed the ζ -potential of multilayer emulsions prepared by titration and back-titration as function of CAS/LMP or LMP/CAS ratio. The ζ -potential of pure LMP solution (Fig. 1A) at pH 3.0 is negative (−17.0 mV) which is attributed to the ionization of its carboxyl groups. When the ratio of CAS-based emulsion/LMP was increased, the ζ -potential initially remain stable until the ratio reached 0.5, then became increasingly less negative, with a point of zero charge in the ratio range around 1.25–1.50, and finally reached a plateau for higher ratio (3.0) (ζ -potential close to that of primary emulsion). This is the fact that the

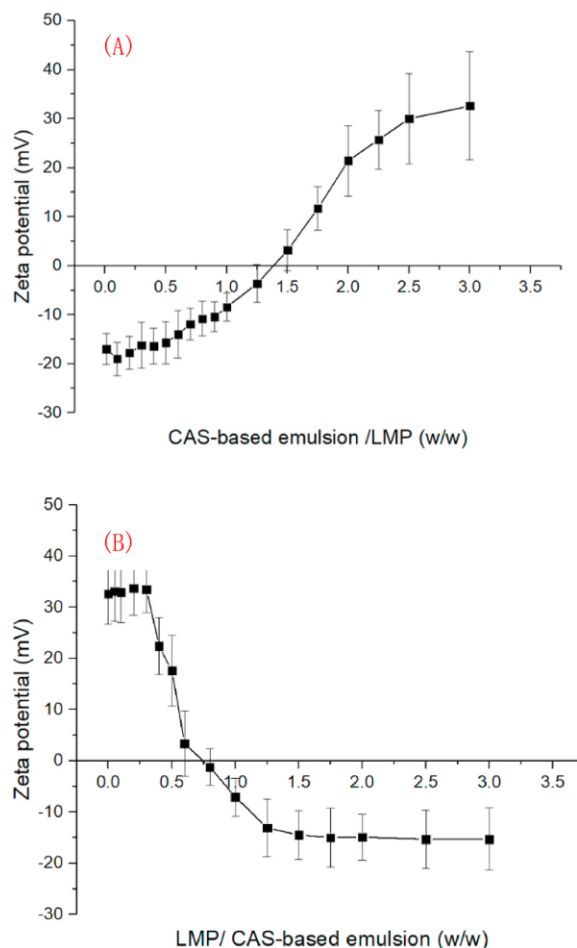


Fig. 1. ζ -potential of multilayer emulsions at pH 3.0 as a function of biopolymer ratio: (A) titrating the primary emulsion into LMP solution or (B) titrating LMP solution into the primary emulsion (Primary emulsion: 0.5 wt% CAS; LMP solution: 0.5 wt%).

primary emulsion exhibited positive charge at pH 3.0 because the protonation of the basic side chain (NH_3^+) of the casein molecules. As a result, LMP molecules can be adsorbed on the droplet surface by electrostatic force, and then the overall negative charge of the system gradually increases until there are not enough LMPs in the system to cover the newly dropped droplet. As shown in Fig. 1B, the ζ -potential of the primary emulsion is positive (+32.6 mV) and this value could be considered enough to ensure high intermolecular repulsions. When the LMP concentration was increased, the ζ -potential initially remains stable until the ratio reaches 0.3, then becomes increasingly less positive, with a point of zero charge in the ratio range around 0.6–0.8, and finally reached a plateau at a ratio of 1.5 (Fig. 1B). According to previous reports (Chang, Gupta, et al., 2016; Liu et al., 2019), the plateau of ζ -potential indicates that the lipid droplet surface is saturated with coating polysaccharides at this level. It should be mentioned that during the experiment, the titration of the primary emulsion into the LMP solution resulted in a stable multilayer emulsion, while titration in the opposite direction (LMP solution into the primary emulsion) showed obvious flocs and these flocs did not disappear with the continuous addition of LMP (Data not shown). Based on our results, the forward titration reached a plateau at ratio 3.0 (Fig. 1A), which corresponds exactly to a ratio of 0.3 (Fig. 1B) for titration of the primary emulsion into the LMP solution. After the ratio 0.3, the absolute value of the zeta potential begins to decrease, indicating that the droplet saturation potentials corresponding to the titrated and back-titrated samples are consistent. Therefore, this finding suggests that the zeta potential can represent the overall distribution of particles in solution but cannot reflect whether the multilayer emulsion formulation is stable during preparation (the occurrence of particle aggregation).

Meanwhile, to find the exact concentration of coating polymer at

which the multilayer emulsions reach the plateau, a large number of samples in different ratios should be prepared to measure for ζ -potential measurements, which are considered very complex and time-consuming processes. In this regard, we employed ITC to measure thermodynamic parameters to gain a deeper understanding of the stoichiometry of layer-by-layer interactions and to analyze the energetics of multilayered interfaces processes.

3.1.2. ITC analysis

ITC have been widely used to investigate molecular interactions in biological systems (Jafari et al., 2007; Wang et al., 2019), but there are few reports on the use of this technique for studying the interactions between droplets and molecules (Fotticchia et al., 2014). Hence, ITC was used to obtain more information about the evolution of deposition around the primary emulsion, such as the equilibrium adsorption constant, enthalpy of adsorption, and adsorption stoichiometry. CAS-based emulsions and LMP solutions at pH 3.0 were chosen to perform ITC tests at 25 °C because CAS-coated droplets showed positive charge and LMP molecules showed negative charges at pH 3.0 (Wang et al., 2019). In this study, heat flow versus time curves (the upper of Fig. 2) were obtained by gradually injecting 0.5 wt% primary emulsion or 0.5 wt% LMP solution into a reaction cell containing 0.05 g/L LMP solution or 0.05 wt% primary emulsion at 25 °C. The enthalpy changes (the lower of Fig. 2) as a function of mass ratio were obtained by the software. Since both CAS and LMP are high molecular weight polymers, mass units were used instead of molecular weight unit in this study. In addition, the mass fraction of the emulsion samples was replaced by the mass fraction of CAS.

The ITC measurements (Fig. 2A) showed that the titrating process was exothermic with a stepwise change in the exothermic value for each

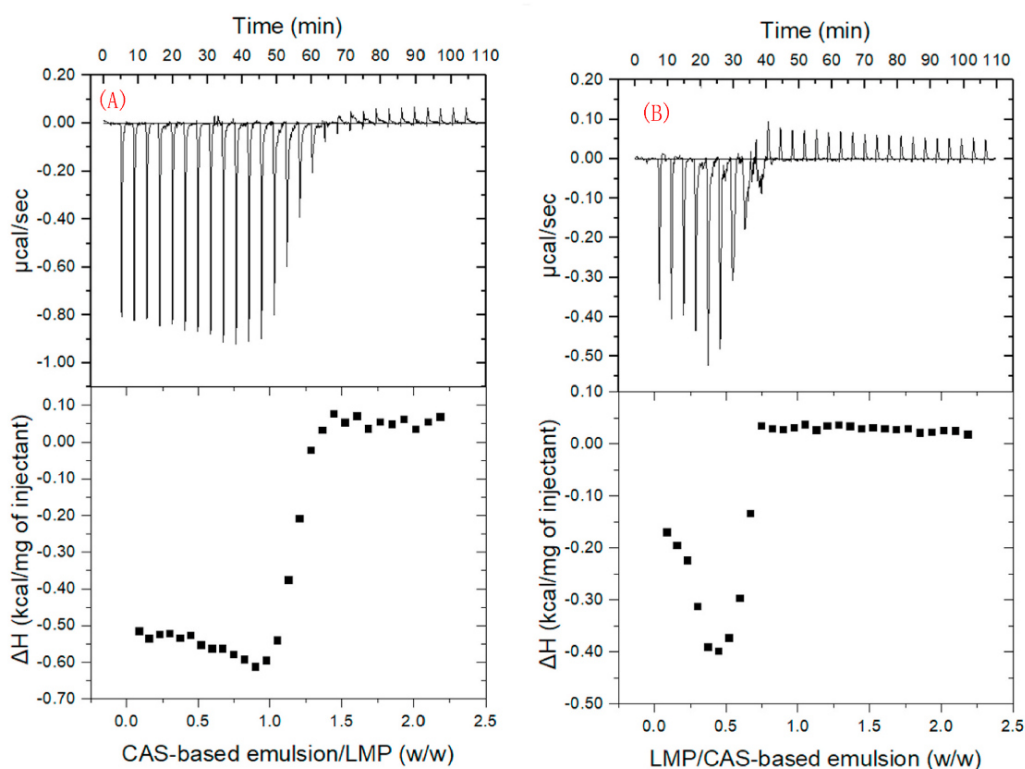


Fig. 2. ITC titration graphs (Upper) and enthalpy change (Lower) of (A) CAS-based emulsion/LMP and (B) LMP/CAS-based emulsion at pH 3.0. The calorimetric cell and the syringe were respectively filled with 0.05 wt% CAS-based emulsion and 0.5 wt% LMP solution or 0.05 wt% LMP and 0.5 wt% CAS-based emulsion.

injection. When the ratio of primary emulsion/LMP is lower than 1.0, the values of heat released per injection are very close, which indicates that the injected CAS-coated droplets have a more stable interaction with the LMP molecules in the reaction cell at this stage. This phase also corresponds to that when the absolute value potential of zeta (Fig. 1A) gradually approaching the "0" point from larger values (-17.0 mV to -8.42 mV), implying that emulsions may go from stable to relatively unstable from this point (Ratio 1.0). This was probably attributed to the fact that, at the initial stage, excess negatively charged LMP molecules in the cell can quickly adsorb on the surface of the positively charged emulsion droplets due to electrostatic interactions. Our previous study (Wang et al., 2019) reported the interactions between CAS and LMP when used at the same content. Interestingly, the heat released by the interaction between CAS and LMP decreases with regularity from the beginning. This difference may stem from differences in binding between molecules and between molecules and droplets. The CAS-encapsulated droplets prepared in this study have nanoscale diameters with an average particle size of about 300 nm, so the CAS molecules adsorbed on the surface of the oil droplets have a more ordered structure in the system than free casein molecules in the aqueous phase. As a result, each casein-coated droplet entering the cell has enough LMP molecules to cover the droplet surface through electrostatic attraction rather than disordered droplet aggregation, thereby releasing a relatively stable heat per injection at the initial stage. For ITC measurements between CAS and LMP solutions, complexes were formed during each injection and these complexes were confirmed to be insoluble at pH 3.0 (Wang et al., 2019). Therefore, it can be hypothesized that the casein molecules may rapidly form disordered network fibers after entering the reaction cell, and the degree of network structure is more extensive, and the heat released is higher. When the ratio was above 1.0, the heat released per injection stated to decrease regularly (Fig. 2A). This may be attributed to the gradual depletion of LMP chains in the reaction cell. Above the ratio of 1.4, the enthalpy becomes slightly positive and remains stable, indicating that none of the LMP molecules in the cell can interact with the newly added droplet. This also means that almost all LMP molecules in the cell are adsorbed onto CAS-based O/W interface at this ratio. However, the result of zeta potential (Fig. 1A) showed that the plateau was obtained when the ratio of CAS-based emulsion/LMP was around 3.0, which was not consistent with ITC results. Our previous study (Wang et al., 2019) reported a similar phenomenon by investigating the complex formation between CAS and LMP. The enthalpy of the thermodynamic curve (by ITC) reaches a plateau (Value "0") at a ratio of 1.0, while the zeta potential of the sample with the same ratio was positive ($\sim +20$ mV). Potticchia et al. (2014) also reported similar results by titration of chitosan or poly-L-lysine into egg lecithin based emulsions. These contradictory results seem to indicate that the potential change in the system may not be accompanied by intermolecular interactions or that the endothermic and exothermic systems have reached a thermodynamic equilibrium. In addition, the measurement of zeta potential is highly sensitive to environmental conditions and may not represent the real environment in the system well (Potticchia et al., 2014). For instance, sample should be diluted before measurements the ζ -potential and the dilution may influence the authenticity of the system. However, more characterization tools are needed to further elucidate the relationship between zeta potential changes and thermodynamic changes in emulsion systems.

Fig. 2A showed that the enthalpy change (ΔH) in the titration was -534.4 kcal/g. Table S1 (see supplemental file) summarized the Gibbs free energy (ΔG , -8957.8 kcal/g) and entropy (ΔS) which were calculated by fitting the curve of "one set of sites". The negative ΔG indicated that the interaction between the primary emulsion and LMP was a spontaneous reaction. Similar exothermic sequences were also found in ovalbumin/chitosan (Xiong et al., 2016) and soy proteins/gum Arabic (Dong et al., 2015). This result supports the generally accepted view that adsorption is primarily driven by electrostatic interactions (Burgos-Díaz et al., 2016; Potticchia et al., 2014). In fact, it was found that $\Delta H < 0$ and

$\Delta S > 0$, indicating that electrostatic interactions play a major role in the binding between CAS-based emulsion and LMP. Indeed, the interactions that occur during the preparation of multilayer emulsions is more complex than just an electrostatic mechanism. It may also include hydrophobic interactions, *van-der-Waals* forces, and hydrogen bonding. However, we cannot say whether these forces are present, because ITC measures the sum of all events that occur in the reaction cell. Furthermore, comparing to the ΔG value (-8134.5 kcal/g (Table S1, Supplementary material) obtained from studying the interactions between CAS and LMP (Wang et al., 2019), it was found that the absolute value of ΔG is higher in this study. This could be attributed to the fact that the adsorbed caseinate molecules ($+32.6$ mV) exhibited stronger surface charge than free caseinate molecules ($+20$ mV) in the continuous phase at pH 3.0 (Wang et al., 2018).

ITC measurements by titrating LMP solution into primary emulsions were also performed to understand the heat flow (Fig. 2B) in the presence of insufficient polysaccharides. Instead of decreasing regularly, the heat released of each injection increased in the initial phase and the maximum heating was obtained at ratio 0.3. Several possibilities may explain this behavior: (i) insoluble flocs were clearly observed by titration of LMP into the primary emulsion at the initial stage, and these flocs did not disappear with the continuous addition of LMP (Data not shown). This can be attributed to the bridging flocculation caused by negatively charged pectin molecules and positively charged droplets. The bridging flocculation process may be accompanied by more complex reactions than electrostatic adsorption, such as some endothermic effects (unfavorable conformational changes, hydrophobic interactions, etc. (Bou-Abdallah & Terpstra, 2012)) and, (ii) when the pH of stock solution was adjusted to 3.0 by HCl, some ions remained in the solution may inhibit binding interactions (Xiong et al., 2017) due to the formation of an ionic screen that prevents the interactions between the two biopolymers. Interestingly, the ratio 0.3 also corresponds to the starting decrease of ζ -potential (Fig. 1B), suggesting that the overall droplet surface charge in this system changed. Beyond this ratio, the heat released after each injection started to decrease regularly and reaches the "0" point at ratio 0.7. However, Fig. 1B showed that the ζ -potential reached a plateau until the ratio 1.5, while ITC data indicated that there was no obvious heat changed at ratios higher than 0.7. This finding suggested that the continued decrease in potential caused by the addition of LMP is probably not accompanied by a significant thermal change.

3.1.3. Schematic representation of the formation of multilayer emulsions by titration

Based on the above results, a schematic diagram was established to summarize the main events occurring as a function of the ratio in titration and back-titration systems (Fig. 3). For the primary emulsion titration by LMP solution, stable multilayer emulsions are successfully formed at the initial stage, which were stable to droplet flocculation. This is because each injection contains enough LMP chains to completely cover oil droplets and gives them a negative surface charge, thereby avoiding droplet aggregation due to electrostatic repulsions. Theoretically, as the LMP in the system is gradually depleted, the injected droplets will interact with other LMP-coated droplets, causing large droplets to aggregate. In general, bridging flocculation tends to occur earlier (before the biopolymer in the continuous phase is completely depleted), which are mainly dependent on the mixing methods (mixing (Liu et al., 2019) or titration (Zeeb et al., 2015)) and biopolymer properties (e.g., charge density, molecular weight, and conformation (Gharsallaoui et al., 2010)). For back-titration, bridging flocculation occurs at the initial stage, as the injected negatively charged LMP molecules will adsorb to the surface of multiple droplets and link them together. Although negatively charged pectin continued to be added to the system, making the surface of the entire system negatively charged (Fig. 1B), the flocs that had produced did not disappear. This finding is consistent with some other reports (Liu et al., 2019; Surh et al., 2006).

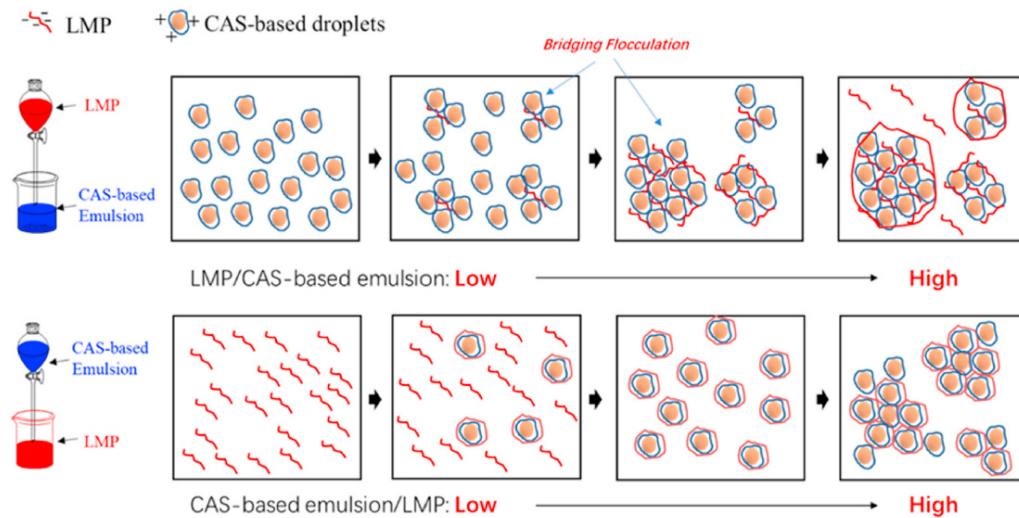


Fig. 3. Schematic representation of the formation of multilayer emulsions by titration based on CAS-coated emulsion and LMP at pH 3.0.

Clusters of droplets held together by protein bridges is generally not reversible, which can be disrupted only by strong shear forces (e.g. a second-stage of homogenization) (Dickinson, 2019). For instance, Liu et al. (2016) mixed primary emulsions and lactoferrin and then used a blender and a high pressure homogenizer to redisperse droplets to obtain stable multilayer emulsions. However, Fotticchia et al. (2014) indicated that stable multilayer emulsions can be prepared by titrating chitosan or poly-L-lysine into the primary emulsion, although bridging flocculation occurs at the initial stage of titration. Tang et al. (2021) successfully prepared multilayer emulsions by direct mixing relatively high content of sodium alginate with chitosan based picking emulsions. These differences may originate from the properties of the different used biopolymers (e.g., charge density, molecular weight, and conformation), the primary layer thickness of emulsion droplets, as well as the solution conditions (e.g., pH, ionic strength, temperature, and stirring) (Burgos-Díaz et al., 2016).

3.1.4. Analysis of fluorescence intensity

Several studies have reported (Acharya et al., 2013; Qiu et al., 2015) that CAS or CAS-based droplets exhibited an obvious emission band around 330 nm when the excitation band was 280 nm due to the presence of tryptophan. When the protein conformation is changed, the local molecular environment of tryptophan and phenylalanine groups will be changed, resulting in changes in the endogenous fluorescence spectrum. For this reason, measurements of tryptophan fluorescence spectroscopy during the formation of CAS-LMP based multilayer emulsions could be used to study CAS conformational changes. Wang et al. (2022) added proteases to soybean protein-based emulsions and investigated the structure or aggregation state of protein-coated droplets after protease treatment by observing typical intrinsic fluorescence emission curves.

Fig. 4A shows the fluorescence spectra of multilayer emulsions prepared by titrating the primary emulsion into LMP solution with different ratios and while maintaining the same CAS content. All emulsion samples showed strong fluorescence emission upon excitation at 280 nm, with a peak near 330 nm. Interestingly, when the ratio ≤ 0.6 , there was no obvious shift in the maximum emission wavelength of LMP-CAS based emulsion. However, when the ratio was above 0.6, the wavelength corresponding to the maximum fluorescence showed a slight red shift compared to the primary emulsion. It has been reported that the red or blue shift in the emission band of CAS is usually related to changes in the tryptophan environment (Li et al., 2019). Therefore, no shift was

observed at ratio ≤ 0.6 which suggest that binding of LMP and CAS-coated droplets in this stage did not change the tryptophan environment.

The quenching of the fluorescence intensity has been reported as an indicator of the interactions between the components in the solution (Wang et al., 2015). Therefore, the conformation and stability of LMP and protein-based emulsion systems can be inferred in part from the test results. The maximum fluorescence intensities of these emulsions prepared by titration as a function of ratio are plotted in Fig. 4B. In the ratio range of 0–0.6, titration-prepared samples showed similar maximum fluorescence intensities; however, when the ratio was greater than 0.6, the maximum intensity of samples decreased obviously with the increase of the ratio until it reached 1.75. The decrease in fluorescence intensity indicated that part of the tryptophan residues of CAS adsorbed on the surface of droplets were buried in the interior of the large particles, which may be caused by the partial aggregation of the droplets. Similar behavior was reported for soy protein isolate/pectin interactions (Li et al., 2021). In this study, the authors explained that the decrease in fluorescence intensity was due to the formation of complexes. As the ratio increased from 1.75 to 2.5, the maximum fluorescence intensity of these samples increased. This can be attributed to the presence of some individual CAS-coated droplets in the system due to the relatively high CAS-based emulsion/LMP ratio.

3.2. Effect of titration or mixing on the properties of multilayer emulsions: analysis of droplet size and flocculation

It should be noted that many papers demonstrated the successful preparation of multilayer emulsions by adding primary emulsions to other coating materials (Burgos-Díaz et al., 2016; Liu et al., 2019; Shi et al., 2021). However, there are no details on how to define “add”. In fact, there are many ways of addition, such as slow/quick addition, titration or direct pouring, etc. and these different ways of addition seem to have a significant effect on droplet aggregation during the preparation of multilayer emulsions. In this section, the direct mixing and titration under stirring were used to prepare multilayer emulsions with different ratios of CAS-based emulsion/LMP. Then, dynamic light scattering (DLS) (Fig. 5A–D), creaming index (Fig. 6A), and optical microscopy (Fig. 6 B) will be presented to evaluate the surface charge, mean particle size and droplet aggregation of these emulsions.

Fig. 5A exhibited the zeta potential of emulsions in both preparation

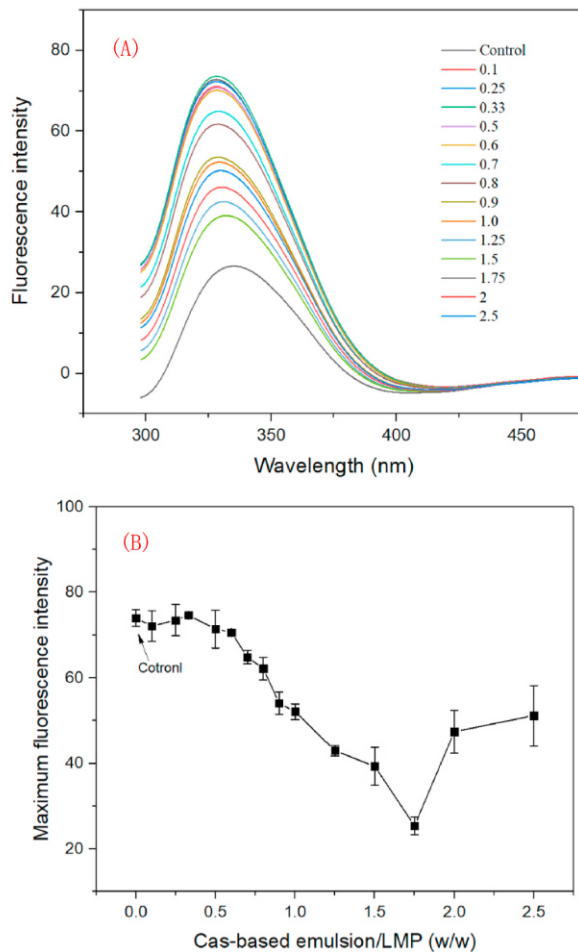


Fig. 4. (A) Fluorescence spectra and (B) maximum intensity of multilayer emulsions as a function of ratio by titrating the primary emulsion into LMP solution. The excitation wavelength was set to 280 nm and the emission slit width was 5 nm (The final concentration of each sample was 0.05 wt% CAS).

methods. Interestingly, the multilayer emulsions in both methods showed similar trends in surface charge as a function of ratio, although distinct flocs were observed earlier in the emulsions prepared by direct mixing. This might be the limitation of the microelectrophoresis mobility method: samples need to be highly diluted and this process may have changed the surface charge of the system (Hu et al., 2017; Salvia-Trujillo et al., 2013). For example, droplet aggregation in highly concentrated emulsions may be partially redispersed to some extent after dilution and agitation. Primary emulsions exhibited nanoscale diameter (~ 300 nm, Fig. 5B) with relatively lower polydispersity index (PDI) values (Fig. 5C). As the ratio increases, all emulsions showed increased droplet size and PDI values, which can be attributed to the fact that negatively charged LMP molecules adsorbed on the surface of CAS-coated droplets or droplet aggregates. A similar result was found in a study of chitosan/pectin-stabilized multilayer emulsions (Liu et al., 2019). It is worth noting that the particle size and PDI values of samples prepared by mixing method are higher than those prepared by titration one. Until the ratio reached 0.8, the titration-prepared multilayer emulsions still exhibited nanoscale average droplet diameter (~ 600 nm) based on DLS analysis. However, when the ratio was higher than 0.5, the size of samples prepared by mixing method was outside the

measurement range of DLS. This could be probably attributed to the fact that directly mixing provides more droplets in the same time than titration, and consequently droplet-droplet collisions may occur more rapidly than polyelectrolyte molecules adsorption to the droplet surfaces, thereby causing larger droplets (Guzey & McClements, 2006). However, during the titration process, a small number of droplets added each time can be quickly encapsulated by the polyelectrolyte at a lower concentration ratio. As a result, once the surface charge reached a certain value, there will be a strong electrostatic repulsions between the surfaces and similarly charged polyelectrolytes in the aqueous phase, which limits further adsorption of the polyelectrolyte molecules, thereby reducing the probability of droplet-droplet collision and retarding the occurrence of particle aggregation. This result was also confirmed by the droplet size distribution measurement. The titration-prepared samples did not show distinct peaks in the larger size range until the ratio reached 0.5, while even for a ratio of only 0.1 (Fig. 5D), distinct peaks in the larger size range were detected in the sample formed by mixing (Fig. 5E). This result proved that droplet flocculation is readily to occur in the direct mixing method, indicating that different adding methods have a significant effect on the droplet flocculation during the formulation of multilayer emulsions.

Fig. 6A showed the visual appearance of multilayer emulsions prepared by directly mixing and titration methods. As expected, those prepared by mixing showed a cream layer when the ratio increased. Even at a ratio of 0.1, a phase separation can be observed where an opaque cream layer at the top and a strongly turbid droplet-depleted layer at the bottom, which was consistent with result of particle size (Fig. 5E). This behavior can be attributed to bridging flocculation promotion leading to an increase in particle size, which facilitates gravitational separation (Grundy et al., 2018). However, when the ratio was increased to 0.5, there was a slight creaming at the bottom of the emulsion prepared by mixing, which may be due to an increase in viscosity (polymer entanglement or viscoelastic network formation) (Grundy et al., 2018). As a result, the increased viscosity restricts the upward movement of the aggregated droplets. Notably, the multilayer emulsion prepared by titration showed much better stable creaming stability than that prepared by mixing, since no obvious phase separation occurred until the ratio reached 1.0. This could be attributed to relatively low PDI value (Fig. 5C) in these emulsions.

For further analysis, the microstructure of the primary emulsion (control) and several selected multilayer emulsions prepared by titration at different ratios (0.5:1; 0.8:1; 1:1; 1.5:1; 2:1) were observed by optic microscopy. These samples represent different states of droplets during the preparation of multilayer emulsions. Compared to the primary emulsion, the multilayer emulsion also exhibits a very homogeneous microstructure in the ratios ≤ 0.5 , which supports the results of the size measurements. As the ratio increased, droplet aggregation was clearly observed at higher chitosan concentrations, especially when the ratio was higher than 1.0. This is because there are not enough LMP molecules in the system to coat the droplets, and then two or more droplets share a polysaccharide chain to form aggregates. Remarkably, both extensive droplet aggregation and significantly increased droplet size (Fig. 5B) occurred around the ratio 1.0, which corresponds to the ratio where the heat released by titration began to decrease (Fig. 2A). These findings suggest that ITC could provide accurate information on when flocculation occurs, leading to optimal conditions for the preparation of O/W multilayer emulsions. Nevertheless, the long-term stability of emulsions is still an important indicator that we cannot ignore, and we will explore the physical stability under different conditions of multilayer emulsions in a future work.

4. Conclusion

This study tried to explain the mechanism of the formation of multilayer emulsions by titrating primary emulsions into coating materials. According to the obtained results, ITC measurements by titration

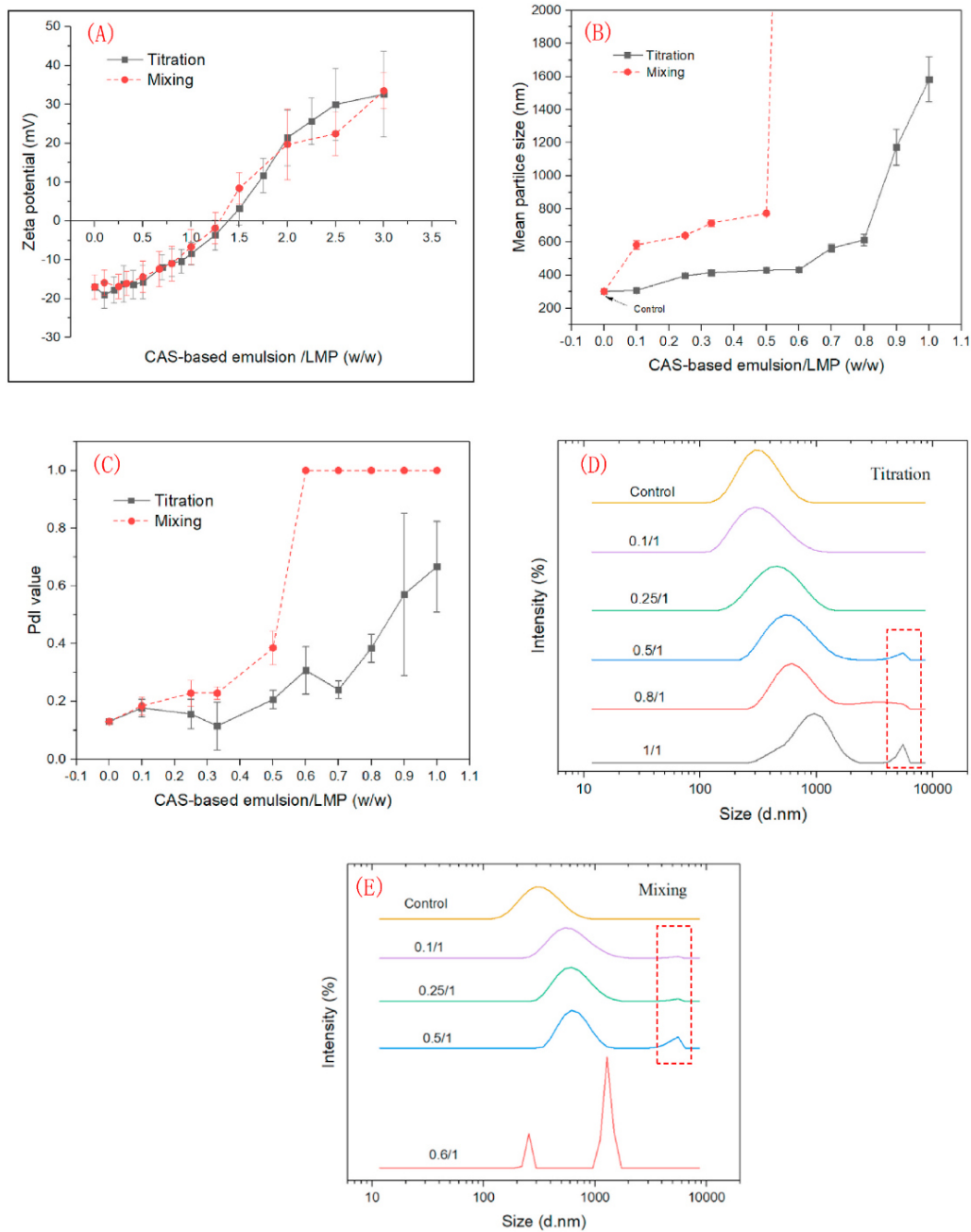


Fig. 5. (A) ζ -potential, (B) Mean particle size, and (C) Polydispersity index as a function of ratio by titrating or mixing directly CAS-based emulsion and LMP; The particle size distributions as a function of ratio prepared by (D) titration or (E) mixing. (Primary emulsion: 0.5 wt% CAS; LMP solution: 0.5 wt%).

of the primary emulsion into the coating material allow the acquisition of thermodynamic characteristics of the studied system, and are fast, accurate and informative compared to the information obtained from zeta potential measurements. ITC titration confirmed that LMP does bind CAS-coated droplets mainly through the electrostatic forces and this absorption was a spontaneous exothermic process ($\Delta G < 0$, $\Delta H < 0$). Titration of the primary emulsion into the LMP solution resulted in a stable multilayer emulsion, while titration in the opposite direction

showed obvious flocs due to bridging flocculation. Meanwhile, uniform and smaller-sized droplets can be prepared by titrating the primary emulsion into LMP solution rather than mixing them directly, which can be attributed to the fact that slow addition can effectively avoid the aggregation of droplets. Based on emulsion stability and microscopy observations, ITC appears to have the ability to define when flocculation begins, thus providing optimal conditions for the preparation of O/W multilayer emulsions. In this way, the remaining coating materials in the

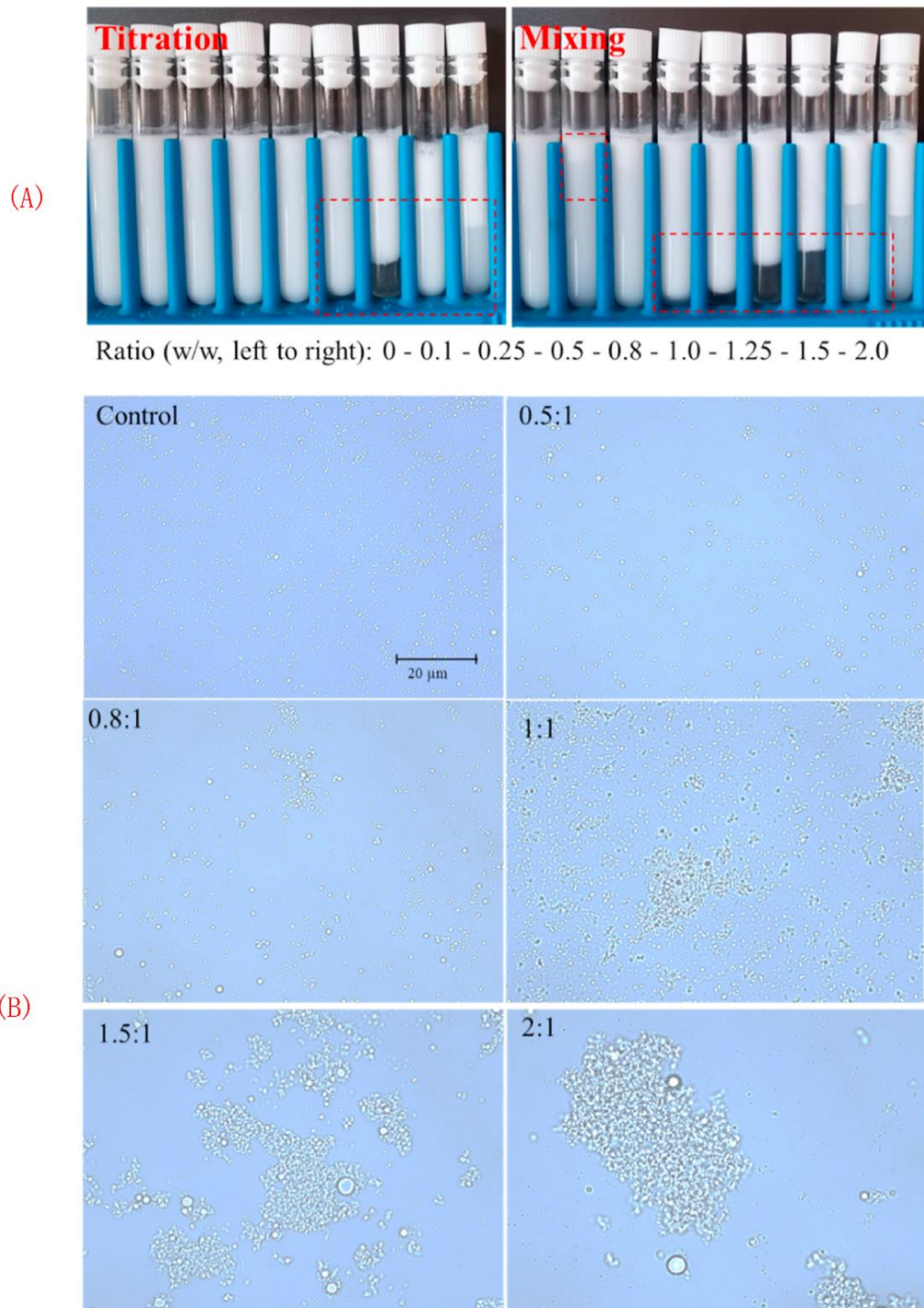


Fig. 6. (A) Visual appearance of multilayer emulsions prepared by titration or mixing as a function of ratio; and (B) Photomicrographs of multilayer emulsions prepared by titration. The scale bar is 20 μm in length.

continuous phase of the prepared double-layer emulsion can be reduced, so as to further prepare emulsions with three or four interfaces ..., thus providing more possibilities for O/W food emulsion products.

Credit author Statement

- o All authors have participated in (a) conception and design, or analysis and interpretation of the data; (b) drafting the article or revising it critically for important intellectual content; and (c) approval of the final version.
- o This manuscript has not been submitted to, nor is under review at, another journal or other publishing venue.
- o The authors have no affiliation with any organization with a direct or indirect financial interest in the subject matter discussed in the manuscript.

Declaration of competing interest

The authors declare no conflicts of interest that pertain to this manuscript.

Data availability

Data will be made available on request.

Acknowledgements

Wei Liao greatly thanks Chinese Scholarship Council for support.

Appendix A. Supplementary data

Supplementary data to this article can be found online at <https://doi.org/10.1016/j.foodhyd.2022.108275>.

References

- Acharya, D. P., Sanguansri, L., & Augustin, M. A. (2013). Binding of resveratrol with sodium caseinate in aqueous solutions. *Food Chemistry*, 141(2), 1050–1054.
- Bou-Abdallah, F., & Terpstra, T. R. (2012). The thermodynamic and binding properties of the transferrins as studied by isothermal titration calorimetry. *Biochimica et Biophysica Acta (BBA) - General Subjects*, 1820(3), 318–325.
- Bouyer, E., Mekhloufi, G., Rosilio, V., Grossiord, J.-L., & Agnely, F. (2012). Proteins, polysaccharides, and their complexes used as stabilizers for emulsions: Alternatives to synthetic surfactants in the pharmaceutical field? *International Journal of Pharmaceutics*, 436(1), 359–378. <https://doi.org/10.1016/j.ijpharm.2012.06.052>
- Burgos-Díaz, C., Wandersleben, T., Marqués, A. M., & Rubilar, M. (2016). Multilayer emulsions stabilized by vegetable proteins and polysaccharides. *Current Opinion in Colloid & Interface Science*, 25, 51–57. <https://doi.org/10.1016/j.cocis.2016.06.014>
- Chang, P. G., Gupta, R., Timilsena, Y. P., & Adhikari, B. (2016). Optimisation of the complex coacervation between canola protein isolate and chitosan. *Journal of Food Engineering*, 191, 58–66.
- Chang, Y., Hu, Y., & McClements, D. J. (2016). Competitive adsorption and displacement of anionic polysaccharides (fucoidan and gum Arabic) on the surface of protein-coated lipid droplets. *Food Hydrocolloids*, 52, 820–826. <https://doi.org/10.1016/j.foodhyd.2015.08.023>
- Dickinson, E. (2019). Strategies to control and inhibit the flocculation of protein-stabilized oil-in-water emulsions. *Food Hydrocolloids*, 96, 209–223.
- Dong, D., Li, X., Hua, Y., Chen, Y., Kong, X., Zhang, C., & Wang, Q. (2015). Mutual titration of soy proteins and gum Arabic and the complexing behavior studied by isothermal titration calorimetry, turbidity and ternary phase boundaries. *Food Hydrocolloids*, 46, 28–36.
- Fotticchia, I., Fotticchia, T., Mattia, C. A., Netti, P. A., Vecchione, R., & Giancola, C. (2014). Thermodynamic signature of secondary nano-emulsion formation by isothermal titration calorimetry. *Langmuir*, 30(48), 14427–14433. <https://doi.org/10.1021/la503558w>
- Gharsallaoui, A., Saurel, R., Chamblin, O., Cases, E., Voilley, A., & Cayot, P. (2010). Utilisation of pectin coating to enhance spray-dry stability of pea protein-stabilised oil-in-water emulsions. *Food Chemistry*, 122(2), 447–454.
- Grundy, M. M. L., McClements, D. J., Ballance, S., & Wilde, P. J. (2018). Influence of oat components on lipid digestion using an in vitro model: Impact of viscosity and depletion flocculation mechanism. *Food Hydrocolloids*, 83, 253–264. <https://doi.org/10.1016/j.foodhyd.2018.05.018>
- Guzey, D., & McClements, D. J. (2006). Formation, stability and properties of multilayer emulsions for application in the food industry. *Honor of Professor Nissim Garti's 60th Birthday*, 128–130, 227–248. <https://doi.org/10.1016/j.cis.2006.11.021>
- Hu, Y.-T., Ting, Y., Hu, J.-Y., & Hsieh, S.-C. (2017). Techniques and methods to study functional characteristics of emulsion systems. *Dietary Natural Compounds*, 25(1), 16–26. <https://doi.org/10.1016/j.jida.2016.10.021>
- Jafari, S. M., He, Y., & Bhandari, B. (2007). Production of sub-micron emulsions by ultrasound and microfluidization techniques. *Journal of Food Engineering*, 82(4), 478–488. <https://doi.org/10.1016/j.jfoodeng.2007.03.007>
- Kim, W., Wang, Y., & Selomulya, C. (2020). Dairy and plant proteins as natural food emulsifiers. *Trends in Food Science & Technology*, 105, 261–272. <https://doi.org/10.1016/j.tifs.2020.09.012>
- Liao, W., Elaissari, A., Ghnimi, S., Dumas, E., & Gharsallaoui, A. (2022). Effect of pectin on the properties of nanoemulsions stabilized by sodium caseinate at neutral pH. *International Journal of Biological Macromolecules*, 209, 1858–1866. <https://doi.org/10.1016/j.ijbiomac.2022.04.160>
- Liao, W., Gharsallaoui, A., Dumas, E., Ghnimi, S., & Elaissari, A. (2021). Effect of carrier oil on the properties of sodium caseinate stabilized O/W nanoemulsions containing Trans-cinnamaldehyde. *Lebensmittel-Wissenschaft und -Technologie*, 146, Article 111655. <https://doi.org/10.1016/j.lwt.2021.111655>
- Liu, G., Hu, M., Du, X., Qi, B., Lu, K., Zhou, S., Xie, F., & Li, Y. (2022). Study on the interaction between succinylated soy protein isolate and chitosan and its utilization in the development of oil in water bilayer emulsions. *Food Hydrocolloids*, 124, Article 107309. <https://doi.org/10.1016/j.foodhyd.2021.107309>
- Liu, C., Tan, Y., Xu, Y., McClements, D. J., & Wang, D. (2019). Formation, characterization, and application of chitosan/pectin-stabilized multilayer emulsions as astaxanthin delivery systems. *International Journal of Biological Macromolecules*, 140, 985–997. <https://doi.org/10.1016/j.ijbiomac.2019.08.071>
- Liu, F., Wang, D., Sun, C., McClements, D. J., & Gao, Y. (2016). Utilization of interfacial engineering to improve physicochemical stability of β -carotene emulsions: Multilayer coatings formed using protein and protein-polyphenol conjugates. *Food Chemistry*, 205, 129–139. <https://doi.org/10.1016/j.foodchem.2016.02.155>
- Li, F., Wang, H., & Mei, X. (2021). Preparation and characterization of phytosterol-loaded microcapsules based on the complex coacervation. *Journal of Food Engineering*, 311, Article 110728. <https://doi.org/10.1016/j.jfoodeng.2021.110728>
- Li, X., Wu, G., Qi, X., Zhang, H., Wang, L., & Qian, H. (2019). Physicochemical properties of stable multilayer nanoemulsion prepared via the spontaneously-ordered adsorption of short and long chains. *Food Chemistry*, 274, 620–628. <https://doi.org/10.1016/j.foodchem.2018.09.002>
- McClements, D. J. (2012). Advances in fabrication of emulsions with enhanced functionality using structural design principles. *Current Opinion in Colloid & Interface Science*, 17(5), 235–245. <https://doi.org/10.1016/j.cocis.2012.06.002>
- Mundo, J. L. M., Zhou, H., Tan, Y., Liu, J., & McClements, D. J. (2021). Enhancing emulsion functionality using multilayer technology: Coating lipid droplets with saponin-polypeptide-polysaccharide layers by electrostatic deposition. *Food Research International*, 140, Article 109864. <https://doi.org/10.1016/j.foodres.2020.109864>
- Ogawa, S., Decker, E. A., & McClements, D. J. (2003). Production and characterization of O/W emulsions containing cationic droplets stabilized by lecithin–chitosan membranes. *Journal of Agricultural and Food Chemistry*, 51(9), 2806–2812.
- Ogawa, S., Decker, E. A., & McClements, D. J. (2004). Production and characterization of o/w emulsions containing droplets stabilized by lecithin–chitosan–pectin multilayered membranes. *Journal of Agricultural and Food Chemistry*, 52(11), 3595–3600.
- Okubo, T., & Suda, M. (2003). Multilayered adsorption of macrocations and macroanions on colloidal spheres as studied by dynamic light scattering measurements. *Colloid and Polymer Science*, 281(8), 782–787.
- Qiu, C., Zhao, M., Decker, E. A., & McClements, D. J. (2015). Influence of protein type on oxidation and digestibility of fish oil-in-water emulsions: Gladin, caseinate, and whey protein. *Food Chemistry*, 175, 249–257. <https://doi.org/10.1016/j.foodchem.2014.11.112>
- Salvia-Trujillo, L., Qian, C., Martín-Belloso, O., & McClements, D. J. (2013). Influence of particle size on lipid digestion and β -carotene bioaccessibility in emulsions and nanoemulsions. *Food Chemistry*, 141(2), 1472–1480. <https://doi.org/10.1016/j.foodchem.2013.03.050>
- Shi, F., Tian, X., McClements, D. J., Chang, Y., Shen, J., & Xue, C. (2021). Influence of molecular weight of an anionic marine polysaccharide (sulfated fucan) on the stability and digestibility of multilayer emulsions: Establishment of structure-function relationships. *Food Hydrocolloids*, 113, Article 106418. <https://doi.org/10.1016/j.foodhyd.2020.106418>
- Surh, J., Decker, E. A., & McClements, D. J. (2006). Influence of pH and pectin type on properties and stability of sodium-caseinate stabilized oil-in-water emulsions. *Food Hydrocolloids*, 20(5), 607–618. <https://doi.org/10.1016/j.foodhyd.2005.07.004>
- Tang, Y., Gao, C., Zhang, Y., & Tang, X. (2021). The microstructure and physicochemical stability of Pickering emulsions stabilized by chitosan particles coating with sodium alginate: Influence of the ratio between chitosan and sodium alginate. *International Journal of Biological Macromolecules*, 183, 1402–1409. <https://doi.org/10.1016/j.ijbiomac.2021.05.098>
- Wang, J., Dumas, E., & Gharsallaoui, A. (2019). Low Methoxyl pectin/sodium caseinate complexing behavior studied by isothermal titration calorimetry. *Food Hydrocolloids*, 88, 163–169. <https://doi.org/10.1016/j.foodhyd.2018.10.006>
- Wang, X., Liu, F., Liu, L., Wei, Z., Yuan, F., & Gao, Y. (2015). Physicochemical characterisation of β -carotene emulsion stabilised by covalent complexes of α -lactalbumin with (–)-epigallocatechin gallate or chlorogenic acid. *Food Chemistry*, 173, 564–568.
- Wang, S., Liu, X., Zhao, G., Li, Y., Yang, L., Zhu, L., & Liu, H. (2022). Protease-induced soy protein isolate (SPI) characteristics and structure evolution on the oil-water interface of emulsion. *Journal of Food Engineering*, 317, Article 110849. <https://doi.org/10.1016/j.jfoodeng.2021.110849>

- Wang, J., Souihi, S., Amara, C. B., Dumas, E., & Gharsallaoui, A. (2018). Influence of low methoxyl pectin on the physicochemical properties of sodium caseinate-stabilized emulsions. *Journal of Food Process Engineering*, *41*(8), Article e12906.
- Xiong, W., Ren, C., Jin, W., Tian, J., Wang, Y., Shah, B. R., Li, J., & Li, B. (2016). Ovalbumin-chitosan complex coacervation: Phase behavior, thermodynamic and rheological properties. *Food Hydrocolloids*, *61*, 895–902.
- Xiong, W., Ren, C., Tian, M., Yang, X., Li, J., & Li, B. (2017). Complex coacervation of ovalbumin-carboxymethylcellulose assessed by isothermal titration calorimeter and rheology: Effect of ionic strength and charge density of polysaccharide. *Food Hydrocolloids*, *73*, 41–50.
- Zeeb, B., Lopez-Pena, C. L., Weiss, J., & McClements, D. J. (2015). Controlling lipid digestion using enzyme-induced crosslinking of biopolymer interfacial layers in multilayer emulsions. *Food Hydrocolloids*, *46*, 125–133.
- Zhang, S., Tian, L., Yi, J., Zhu, Z., Decker, E. A., & McClements, D. J. (2020). Mixed plant-based emulsifiers inhibit the oxidation of proteins and lipids in walnut oil-in-water emulsions: Almond protein isolate-camellia saponin. *Food Hydrocolloids*, *109*, Article 106136. <https://doi.org/10.1016/j.foodhyd.2020.106136>

**GENERAL DISCUSSION,
CONCLUSION AND
PERSPECTIVES**

Many foods are perishable and require food preservatives from preparation to consumption to prevent spoilage and pathogenic bacteria. Due to the increasing safety requirements, efforts have been devoted to designing novel food preservatives with food-grade molecules and biopolymers, which are generally considered safer and more reliable. One of the potential strategies is the encapsulation of essential oils (EOs) with food-grade emulsifiers, especially proteins, to formulate O/W emulsion systems. Therefore, it will be very important to formulate nanoemulsions with long-term stability and good antibacterial activity by incorporating different natural or food-grade biopolymers. Besides, it is important to investigate the putative interactions between selected biopolymers and antimicrobial components and to identify the interactions that govern emulsion stability.

This thesis aims to develop novel food preservatives formulated from natural compounds and food-grade biopolymers. In the first part, nanoemulsions were successfully prepared by high-speed homogenization and high-pressure homogenization in the different combinations of emulsifiers (CAS or lecithin) and EOs (TCA and citral). Nanoemulsions containing TCA exhibited higher antimicrobial activities against two common Gram-negative (*Escherichia coli*) and Gram-positive (*Listeria innocua*) bacteria than that containing citral whatever the used emulsifier. These nanoemulsions were then incorporated into low methoxyl pectin (LMP) films and the obtained results showed that films containing TCA droplets coated by CAS had a larger inhibition zone than the ones stabilized by lecithin whatever the EO used. These results could be attributed to the combination of several phenomena such as (i) evaporation of free EOs during the formation of biopolymer films, (ii) diffusion of EOs through the interfacial membrane containing the emulsifier, (iii) diffusion of EOs through the pectin matrix, (iv) film structure, and (v) interactions between pectin, emulsifier, EO molecules, and the bacterial membranes. Thus, the antimicrobial activity of nanoemulsions and nanoemulsion-based films was the highest when the combination of TCA and CAS was used. Furthermore, nanosized emulsions prepared by TCA and

CAS were more stable than micro-sized ones in our systems, but no significant differences were observed concerning their antibacterial activity. These results highlight the potential advantages of emulsions as delivery systems of EOs as preservatives, but more factors should be considered in our future studies to evaluate the effect of the type, chemical structure, and physical properties of EOs on their antibacterial activities.

One of the main challenges to overcome when formulating essential oil-loaded emulsions is that the oil phase contains components that are soluble in water, which promotes droplet growth through Ostwald ripening, thereby accelerating emulsification and phase separation. To overcome Ostwald ripening, we compared the ability of two different carrier oils to improve the properties of emulsions containing TCA and stabilized by CAS. The effects of different contents of two different oils (MCT and LCT) on the physical stability and antibacterial activity of nanoemulsions were investigated. The analyses revealed that stable CAS-coated nanoemulsions are difficult to formulate using pure TCA. However, nanoemulsions containing TCA mixed with a carrier oil could keep stable for a relatively long period (more than one month at room temperature), especially when LCT is used as carrier oil. This stability improvement can be attributed to a reduction of TCA diffusion in the aqueous phase and an inhibition of Ostwald ripening. Antibacterial effect measurement revealed that, compared to nanoemulsions containing pure TCA, the activity of nanoemulsions containing mixtures of TCA and carrier oils exhibited better antibacterial activity against *E. coli* and *L. innocua*. The incorporation of carrier oils into nanoemulsion-based systems containing TCA is a promising technique that can extend the shelf life of perishable foods.

After optimizing the preparation, the next step was to further improve the stability of nanoemulsions under certain conditions (high ionic concentration, freeze-thaw cycle, accelerated oxidation). In this regard, the effect of pectin on the physical and oxidation stability of CAS-stabilized nanoemulsions under neutral pH was investigated as a

function of several parameters and conditions. It emerges that the presence of LMP could improve the physical (especially against high salt concentrations and freeze-thaw cycles) and chemical stability of CAS-stabilized nanoemulsions, depending on its concentration. Particularly, nanoemulsions containing 0.10 wt% and 0.25 wt% are considered as the optimal formulation which exhibited the ability to inhibit lipid and protein oxidation more effectively than CAS alone. There are at least two possible mechanisms to explain the antioxidant properties of pectin in nanoemulsions: (i) the non-adsorbed pectin could have the ability to scavenge free radical and chelate metals; and (ii) the non- adsorbed pectin can reduce droplet mobility by forming a weak gel-like network that prevents water-soluble pro-oxidants reaching the lipids. In addition, a higher concentration of pectin (0.5 wt%) can promote the occurrence of depletion flocculation of nanoemulsions, resulting in phase separation, more secondary lipid oxidation products, and more tryptophan loss.

Environmental conditions, especially pH, have been reported to greatly affect the structural properties of proteins or protein-polysaccharide-based emulsion systems. To further understand the stability of CAS-LMP-based nanoemulsions under different pH conditions, the effect of pH on the interfacial rheology of CAS/LMP at the O/W interfaces was systemically investigated. Meanwhile, the colloidal stability (microstructure, ζ -potential, particle size, and viscosity) of CAS-LMP-based nanoemulsions was studied by adjusting the pH from 7.0 to 3.0. Interfacial measurements suggested that pH and LMP concentration had limited effects on the equilibrium interfacial tension of CAS/LMP at the O/W interface. The studied pH conditions showed that CAS can effectively reduce the O/W interfacial tension to an equilibrium value of about 14.0 ~ 15.5 mN/m, but an increase in viscoelastic modulus was observed at pH 5.0 with increasing LMP content. Size and ζ -potential results suggested that LMP adsorbed to CAS-coated droplet at pH 3.0 and pH 5.0, but not at pH 7.0. The corresponding isoelectric point (pI) for charge neutralization in CAS/LMP based nanoemulsions was shifted to lower pH values. Notably, nanoemulsions

containing LMP can significantly inhibit the aggregation and creaming of CAS-coated droplets at pH 5 compared to the nanoemulsions without LMP.

After the characterization of the physical properties of prepared nanoemulsions, the interactions between the different components of the emulsions systems were also investigated. In this part, the interactions between the two used natural aldehydes (TCA and citral) and CAS were evaluated at the O/W interface. First of all, both aldehydes, especially TCA, have pronounced abilities to decrease the interfacial tension at O/W interfaces during adsorption process. Small amounts of TCA introduced into oil phase were shown to significantly improve the dispersibility and diffusion properties of CAS at the O/W interfaces. Dilatational measurements showed that the use of TCA into the oily phase resulted in stronger and more elastic interfaces. The fluorescence quenching test proved that TCA has more obvious quenching effect on CAS than citral. The large binding constants ($1.78 \times 10^5 \text{ M}^{-1}$) were calculated by Stern-Volmer equation and suggested that TCA has a strong affinity with CAS. The negative enthalpy and negative entropy change suggested that the binding is mainly driven by formation of hydrogen bonds, which is spontaneous. Entropy was unfavorable suggesting that there is a loss of conformational freedom associated with binding.

In the final step of this thesis, we tried to explain the mechanism of the formation of multilayer emulsions by titrating primary emulsions into coating materials by isothermal titration calorimetry (ITC) and dynamic light scattering (DLS). Stable multilayered interfaces could be formed by titrating primary emulsion (CAS-based droplets) into LMP solution, rather than the titration in the opposite direction. ITC titration confirmed that LMP does bind CAS-coated droplets through electrostatic forces and it was a spontaneous exothermic process ($\Delta G < 0$, $\Delta H < 0$). In addition, more uniform and smaller-sized droplets could be obtained by titrating the primary emulsion into LMP solution rather than mixing them directly, which can be attributed to the fact that slow addition can effectively avoid the aggregation of droplets. Compared to DLS, ITC measurements allowed to obtain thermodynamic properties of the studied systems

and it appears to have the ability to define when flocculation begins, thereby providing optimal conditions for the preparation of O/W multilayer emulsions. In brief, ITC measurements by titration of the primary emulsion into the coating material allow the acquisition of thermodynamic characteristics of the studied system, which are fast, accurate and informative compared to the information obtained from zeta potential measurements.

In conclusion, encapsulation systems containing EOs as preservatives and based on food-grade emulsifiers (proteins and polysaccharides) were successfully prepared. The physicochemical stability of these emulsions during storage and under certain applied conditions were systematically investigated. Meanwhile, the molecular interactions between the different components in the emulsions were illustrated from the point of view of oil-water interfaces and fluorescence quenching. In summary, these results are expected to provide more information for using natural active biomolecules to manufacture food antibacterial agents with stable multifunctional bioactivity.

Concerning the perspectives of this work, there are some aspects that could be explored in future works:

- 1) Our results showed the potential advantages of emulsions as delivery systems of EOs as preservatives, but more factors should be considered in future studies to evaluate the effect of the type, chemical structure, and physical properties of EOs on their antibacterial activities.
- 2) It would be interesting to measure the release kinetics of EOs from emulsions and films and to follow their diffusion in different environments, like food/drug matrices, simulated gastrointestinal tract (GIT) system, or food packaging...
- 3) The interactions between emulsion droplets and target bacteria, the effective concentration of the encapsulated molecules and the resistance phenomena of the bacteria are also worth studying.
- 4) The multilayered nanoemulsions are worth to convert into powders by

evaporating water by spray-drying or freeze-drying. The resulting powders can be characterized in terms of activity, density, flow, size, stability, and re-dispersion properties for further applications.